THE UNIVERSITY OF CHICAGO

SWALLOWING BIOMECHANICS OF THE *MACACA MULATTA* HYOLINGUAL APPARATUS

A DISSERTATION SUBMITTED TO

THE FACULTY OF THE DIVISION OF THE BIOLOGICAL SCIENCES

AND THE PRITZKER SCHOOL OF MEDICINE

IN CANDIDACY FOR THE DEGREE OF

DOCTOR OF PHILOSOPHY

GRADUATE PROGRAM IN INTEGRATIVE BIOLOGY

BY

COURTNEY PETERSON ORSBON

CHICAGO, ILLINOIS

JUNE 2018

For my favorite monkeys: Chewbacca, Hestia, James Brown, Kiki, Maia, and David.

TABLE OF CONTENTS

ACKNOWLEDGEMENTS

These last five years have been incredible, challenging, and transformative, and I cannot wait to apply what I have learned to the adventures to come in the clinic and the lab. But first, I need to look back in gratitude to the people who have so generously helped make this dissertation possible.

My advisor, Prof. Callum Ross, fostered my dreams of becoming an anatomist and scientist into reality. He made me feel at home in his lab well before I was a graduate student, and he has been unwaveringly committed to supporting my research financially, physically, and intellectually. His impact on my professional and personal development is profound, and I am immensely grateful to count myself among his students.

Support from my dissertation committee—Profs. Nicho Hatsopoulos, Stephanie Palmer, Rebecca German, and Nicholas Gidmark—has been invaluable as this dissertation became more focused. Nicho was extremely generous in allowing use of his lab space for animal training and care. He provided animals for essential pilot studies during the earlier stages of this dissertation research. Stephanie gave me much-needed encouragement to make my research understandable to a general audience. Her reminders to be able to explain my research to family members will stay with me always, and I will carry this advice to my interactions with patients as well. Thanks to her knack at finding clarity in a subject matter that can often seem quite murky, Rebecca helped me to contextualize my interest in tongue biomechanics within dysphagia research so that I could better communicate the clinical significance of my findings. Nick helped me to collect half of the data for this dissertation and was an incredible teacher of all things XROMM and

muscle physiology. In my third year, he provided invaluable mentorship that helped me to become a more independent experimentalist in the lab.

Several faculty members who were not formally on my committee have nonetheless shaped my graduate school experience. Prof. Michael LaBarbera has been a key figure in my graduate school experience from the day he told me that I was accepted into the program through his time as the Director for Graduate Studies, and I always looked forward to the insights that he would bring to tongue biomechanics from his invertebrate biology perspective. Prof. Zhe-Xi Luo was immensely supportive of my learning how to use the PaleoCT scanner, allowing me to use it at no cost while I was learning how to optimize my scanning parameters and how to stain specimens. I have always enjoyed our musings over mammalian hyoids. Prof. Mark Westneat introduced me to the wider world of anatomy and biomechanics outside of my primate comfort zone by having me TA his comparative anatomy course, which was more like a playground for a young anatomist.

The current, former, and proxy members of the Ross Lab—Dr. Jim O'Reilly, Prof. Jose Iriarte-Diaz, Prof. David Reed, Dr. Laura Porro, Dr. Richard Madden, Dr. Regan Dunn, Prof. Ali Nabavizadeh, Prof. Kazutaka Takahashi, Prof. Fritzie Arce-McShane, Dr. Yuki Nakamura, Dr. Naru Shiraishi, Prof. Felippe Prado, Dr. Michael Granatosky, Dr. Myra Laird, Dr. Yasheshvini Ram, Kelsey Stilson, Katie Whitlow, JD Laurence-Chasen, and Aileen Tartanian, and Carrie Balcer—have made graduate school feel like home. I have never met such an enthusiastic group of curious people who could geek out so readily about biology and anatomy. I will miss the practical jokes, the dark jokes, the dirty jokes, and everything in between. I am grateful to have another two years on campus that I might be able to squeeze out a little bit more time with those that are still in Chicago. Special mention goes to a some of these individuals for their help in this

dissertation research. David unhesitatingly welcomed me into his lab earlier in graduate school for some histology work and was a very patient teacher for a student who asked a lot of questions. Rick helped me to do some passive tissue manipulations towards the end of this dissertation that were a tremendous help in solidifying some of my arguments. Taka was a great teacher on neurophysiological experimental design, kept me sane through many months of experiments, and helped me collect data from and provided most of the care for Monkey He. Ali's artistic style and passion for scientific illustration influenced my own illustrations in this dissertation. Michael, Myra, Vini, Kelsey, and Katie all helped me at some point with monkey work—Michael and Myra deserve special mention because they collected the data for Monkey Ch and cared for the animal. Carrie ensured that our animals (including the graduate students) were trained and the lab was stocked and provided support in animal care. Several undergraduates also helped me with either my dissertation work or other projects in the lab: Elise Lemp, Katie Green, Tiffany Chen, Max Site, Mihir Karve, Joshua Meymir, Oran Avivi, and Nikki Kijak.

Other labs have also been practically or intellectually supportive. The Hale Lab—Prof. Melina Hale, Dr. Brett Aiello, Hilary Katz, Adam Hardy, and Katie Henderson—generously supplied me with deionized water for staining specimens and loaned wet lab equipment. My interactions with the Alemseged Lab—Prof. Zeresenay Alemseged, Dr. Andrew Du, Dr. Amanda Smith, and Kelsi Hurdle—along with Michael and Myra brought more regular conversations about primatology and anthropology into my graduate school experience in my fourth year and motivated me to apply for an NSF grant under the biological anthropology program. It was quite refreshing to debate about material I had studied in undergraduate after having gained a broader comparative perspective, and I thoroughly enjoyed Andrew's journal club. Prof. Robert Martin

and Dr. Lu Yao were excellent collaborators on a primatology side project using diceCT. From the Luo Lab, April Isch Neander was my CT scanning guru and resident Maya wizard.

Several other students and faculty in the cluster—members of my cohort, the current and former members of the Anatomy Cremasters softball team, the Darwin's Revenge broomball team, TG attendees, and Fish Group—were either socially or intellectually supportive along the way. Dr. Aaron Olsen had a particular influence on this dissertation—an avid programmer, he helped me to get started coding in R and encouraged me to process kinematic data myself. Although it was certainly the more difficult route, learning how to process my own kinematic data ultimately made me more flexible with my data analyses and gave me better command over my data. Aside from his programming prowess, it was a joy to teach anatomy with him.

I owe an immense debt to those at Brown University who developed the XROMM workflow and much of the open-source code for bringing 2D images to life. In particular, Prof. Beth Brainerd spearheaded XROMM and supported us as we brought the UChicago XROMM facility online. I am particularly grateful for the opportunity to attend the Short Course in 2014, and to Prof. Thomas Roberts and the American Association of Anatomists for funding another trip to Brown in 2015, where I learned how to use XMALab and saw my first muscle physiology experiments. Dr. Ben Knörlein was always swift to respond to questions about XMALab, and he helped me find a stellar computer workstation that greatly expedited XROMM data processing. Dr. Ariel Camp was instrumental in helping me to model tongue, oral cavity volume, and hyoid range of motion—not only did she introduce me to alpha shapes and share her code with me, but she also wrote some Maya scripts so that I could produce some jaw-dropping visualizations for talks. Moreover, she was very helpful in introducing me to the basics of fluoromicrometry and offered pointers about implanting markers in soft tissue when I was getting start. In a similar

vein, fellow hyoid enthusiast Prof. Nicolai Konow taught me how to implant drilled tantalum beads, which improved the precision of hyoid kinematics compared to our pilot animals. Nicolai has also provided a lot of encouragement throughout graduate school, happily introducing me to concepts like architectural gearing as well as to Prof. Manny Azizi himself, and I greatly enjoyed scheming about hyoid and feeding biomechanics at SICB.

Many others have enriched my graduate experience. I have greatly enjoyed an intellectual resonance with Prof. François Gould, and I deeply appreciate the personal and professional support he has shown me. Prof. Diane Kelly has been a joy to geek out with about hydrostatic structures and escape rooms. Prof. Casey Holliday has been supportive throughout graduate school since we first met at the XROMM short-course, and he gave me my first experience chairing a conference symposium at AAA in 2017. Casey was also a member of the Austin Working Group, led by Prof. Paul Gignac, which helped to refine my staining techniques so that the iodine could fully penetrate specimens as large as rhesus macaques, which was essential to my methodology. A special thanks goes to Prof. Bhart-Anjan Bhullar for funding this trip to Austin, and for mentoring me on iodine staining and comparative anatomy in general.

Many people provided essential support outside of the science itself. The administrative staff in OBA—Norma del Real, Stephanie Zandy, Cindy King, and Josh Berg—have all helped to make sure that the gears keep turning while we scientists think and write. Norma in particular was very helpful in preparing my successful NSF grant application. The members of primate care team at the Animal Resource Center—Dr. Marek Niekrasz, Dr. Allison Ostdiek, Jennifer McGrath, Alyssa Brown, Joanne Hernandez, Dr. Nicole Pach, and Dr. Darya Multsyn—provided phenomenal care for our animals and were immensely supportive when their biology went astray. This research would not have been possible without them.

As time goes on, the consequences of initial trajectory become that much more apparent. Prof. Chris Wall was instrumental in setting me on the track that I am on today. She gave me the opportunity to teach anatomy as an undergraduate, an experience that cemented my desire to become an anatomist. I am grateful for her mentorship and general interest in my career and well-being over the years. Further still, Mrs. Helen Sheely, my high school anatomy and biology teacher, had a foundational influence on me. Not many teachers would stay after school to allow a student to do extra dissections, and it was in those hours and with her encouragement that my passion for anatomy was born.

I have had the pleasure of having two families throughout this dissertation. I greatly enjoyed trips out West with Tony, Susan, Ben, and Nancy Orsbon that slaked my wanderlust and set my head straight by getting me out of the lab for a while. Holidays with Sarah, Jake, Wyatt, Melissa et al. were always a joy.

My parents, Peggy and Terry Peterson, have lovingly endured my detour from medical school, and I am immensely grateful for the sacrifices they have made so that I could have the opportunities that led met to where I am today. I am also grateful for the formative trips we've been on, including sojourns in Boothbay Harbor and a trek to see the 2017 solar eclipse—these memories are invaluable to me. Although being Chicago has meant seeing them less, I have enjoyed getting closer to my sisters, Tori and Katheryn, particularly as Tori has inundated my phone with pictures of her kids shouting "SCIENCE!" with joy.

To my husband, David Allison Orsbon: You are my everything. Your drive for excellence inspires me when I want to give up. Your tenderness refuels me when I am running on empty. Your silliness makes me laugh when I take things too seriously. I wish that words could express what your love, support, and encouragement have meant to me over the years.

LIST OF TABLES

LIST OF FIGURES

ABSTRACT

Swallowing is essential to vertebrate life, yet its biomechanical basis is poorly understood compared to other behaviors such as chewing, suction feeding, reaching, and locomotion. Human swallowing biomechanics is of clinical interest for treating dysphagia, or difficulty swallowing, with neuromuscular rehabilitation. Swallowing is also of anthropological interest because purported adaptations for speech also allow food and air to mingle near an open larynx, which some argue renders humans maladapted to swallowing. However, this hypothesis has not been thoroughly tested and in fact is refuted by several studies of human feeding physiology. This dissertation uses a macaque (*Macaca mulatta*) model system to determine the biomechanical basis of two important movements involved in bolus propulsion and airway protection—tongue base retraction and hyoid superoanterior excursion—and examines how changes in hyolingual and craniofacial morphology over the course of human evolution and ontogeny affect hyolingual biomechanics. Tongue base retraction was caused by neither extrinsic lingual muscle shortening nor hydrostatic deformation. Kinematic evidence suggests that suprahyoid muscles cause tongue base retraction by regionally changing tongue volume, which is consistent with a hydraulic linkage between the suprahyoid muscles and the tongue. These suprahyoid muscles are not only active and shortening during tongue base retraction, but they also rotate as they move the hyoid. This rotation either amplifies or reduces hyoid velocity depending on the geometry of the muscle and the direction of rotation. In this way, suprahyoid muscles are functionally analogous to pennate muscles, which also exhibit fiber rotation and gearing. A computational model of hyoid range of motion demonstrates that hyoid descent—which is commonly assumed to be detrimental to swallowing—may actually help to maintain swallowing performance as the

human face has shortened in recent evolutionary history, especially if tongue volume must be preserved to maintain a hydraulic linkage between the tongue and hyoid. Moreover, because mandibular morphology affects suprahyoid muscle length, selective pressure to maintain swallowing performance may have resulted in the emergence of humanity's characteristic vertical mandibular symphysis and then chin. However, geometric constraints require human suprahyoid muscles to shorten relatively more when the hyoid is descended, which may leave humans vulnerable to dysphagia not because the human airway allows for more mixing of food and air near the larynx but rather because of fundamental constraints on vertebrate skeletal muscle biomechanics. Given that muscles from the cranium, mandible, pharynx, soft palate, larynx, sternum, and scapula all converge on this nexus of the neck, the mammalian hyolingual apparatus may have an underappreciated role in shaping the structures from which it is so elegantly suspended.

CHAPTER ONE: AN INTRODUCTION TO SWALLOWING

WHY SWALLOWING?

Swallowing is essential to vertebrate life—to survive, a vertebrate must transport food and, in terrestrial tetrapods, liquids from the oral cavity to the esophagus. Although swallowing poses little trouble for organisms without lungs, Darwin's (1859) note regarding "the strange fact that every particle of food and drink which we swallow has to pass over the orifice of the trachea, with some risk of falling into the lungs" highlights the paradox of swallowing in air-breathing vertebrates: its importance for sustaining life is equally matched by its capacity to end life if it goes awry. Despite this danger, the reader will swallow hundreds of times while reading this dissertation, after a sip of coffee, during a meal, or even without being aware of having done so.

Hopefully, whatever is swallowed does so without "falling into the lungs". Safe swallows successfully direct food and liquid into the esophagus thanks to finely tuned sensorimotor integration by the central nervous system. Although a swallow can be reflexively evoked by stimulating the mucosa around the larynx (Doty and Bosma 1956), brainstem motor neurons controlling the swallowing muscles change their firing patterns, or modulate, in response to either variable sensory information about different types of foods and liquids, or increased motor drive from the cortex (Dodds et al. 1988; Chi-Fishman and Sonies 2002; Kajii et al. 2002; German et al. 2009; Steele et al. 2011; Humbert et al. 2012; Steele et al. 2012). Safe swallowing involves learning to coordinate respiration with swallowing after transitioning from the airless womb—where aspiration of sterile amniotic fluid is of little consequence—to independent

breathing while juggling swallowing and sucking during feeding sessions (Selley et al. 1989; Smith et al. 1989; McFarland and Lund 1995; Crompton et al. 1997; German et al. 1998; Klahn and Perlman 1999; Martin-Harris et al. 2003; Gewolb and Vice 2006; K. Matsuo et al. 2008; Matsuo and Palmer 2015; Ballester et al. 2018). The ability to modulate the swallow may be gained most swiftly during a critical period of development (Illingworth and Lister 1964; Mason et al. 2005), but adults retain the ability to adapt to new stimuli (Humbert et al. 2012; Humbert et al. 2013). Given these characteristics, safe swallowing is arguably a learned behavior—one is not born knowing how to safely swallow foods ordinarily consumed by adults, let alone pills.

Learning to modulate the many muscles involved in swallowing over the course of weaning is complicated by how these structures morph over the course of human ontogeny. Human infants are born with similar craniofacial and oropharyngeal anatomy compared to other nonhuman primates (Negus 1949; Crelin 1969; Falk 1973; Laitman et al. 2014; Lieberman et al. 2001), but these structures grow in ways that are hypothesized to make them maladapted to swallowing as a consequence of selection for traits that are adapted to speech (Negus 1949; Dantas et al. 1990; Lieberman et al. 1992; Lieberman et al. 2001). Specifically, the tongue, hyoid (the bone at the base of the tongue), and larynx (i.e., the voice box, which originally functioned as a valve for airway protection during swallowing, Negus 1949) descend away from the hard palate and further into the neck (Lieberman et al. 2001) (Figure 1.1). This configuration leads to separation of the epiglottis and soft palate, which has been argued to be beneficial for producing unambiguous vowels in speech but dangerous for the airway because it allows greater mixing of air and food in the pouch at the base of the tongue called the vallecula (Negus et al. 1949; Lieberman et al. 1969; Laitman et al. 1977; Stevens 1989; Lieberman et al. 1992; Lieberman 2012). This purported propensity for dysphagia—unsafe or difficult swallowing—comes at no

small cost to patients, whose quality of life can be impaired (García-Peris et al. 2007; Chen et al. 2009), as well as to the healthcare system, where at least 3 % of inpatients carry a diagnosis of dysphagia at an annual cost of up to $7.1 billion in inpatient care alone (Patel et al. 2018).

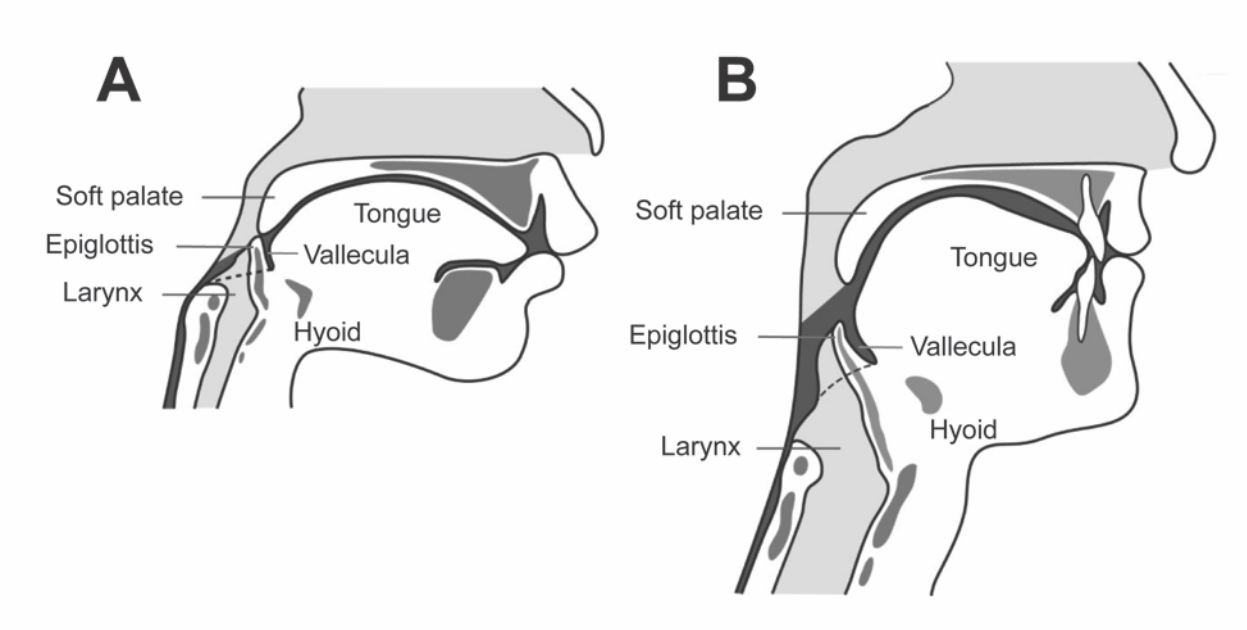

Figure 1.1: Hyolingual and laryngeal descent in Homo sapiens. A) Human infant. B) Human adult. Modified from Matsuo and Palmer 2008.

Treatment for movement disorders such as dysphagia frequently[1] comes not in the form of a pharmaceutical but rather neuromuscular rehabilitation—that is, the most promising cure for dysphagia is learning, or rather, relearning how to swallow safely (Humbert and German 2013). However, many dysphagia therapies are still in their infancy, and the dysphagia research community is going through its own learning process of determining which muscles need to be targeted by therapists and how these muscles should be rehabilitated to restore swallowing function as efficiently as possible (Burkhead et al. 2007; Huckabee and Macrae 2014; Martino

[1] Less frequently, the cause of a movement disorder is a physiological process that can be targeted with pharmacological therapies or prevented with vaccines, e.g., those that target the neuromuscular junction: myasthenia gravis, tetanus, botulism, etc.

and McCulloch 2016). The muscles of the tongue and hyoid, or the hyolingual apparatus, have been of particular interest because tongue movements propel the bolus for most of the swallow (McConnel 1988; Palmer et al. 1992), and hyoid displacement probably underlies a number of mechanisms that protect the larynx during the swallow (Cook et al. 1989; Jacob et al. 1989; Kahrilas et al. 1991; Logemann et al. 1992; Inamoto et al. 2011; Seo et al. 2014; Pearson et al. 2016). Establishing the biomechanical basis of these movements could resolve ambiguities about the etiology of many forms of dysphagia and choices regarding the most effective treatments for the underlying cause of a patient's dysphagia.

Despite the importance of understanding how muscles produce a safe swallow and how swallowing performance depends on morphology, we know relatively little about the basic biomechanics of swallowing compared to other behaviors that ultimately culminate in swallowing, including: chewing, which prepares the bolus for swallowing; ingestion, which relocates food from the environment into the oral cavity for chewing and can involve either limb-, tongue-, or jaw-based prehension or, in the case of some aquatic vertebrates, suction; and locomotion, which moves the organism closer to food so that it can be ingested. (Alternatively, locomotion can also prevent the organism from becoming food). This gap in knowledge arises from practical and theoretical challenges. First, the structures involved in swallowing are difficult to visualize and measure. While limb and jaw kinematics can be observed using light cameras, the skin obscures the inner workings of tongue and throat. Therefore, highly specialized—and not widely available—imaging equipment is necessary to visualize the swallowing structures with sufficient spatiotemporal resolution to definitively test hypotheses about swallowing biomechanics. Moreover, some of these approaches are sufficiently invasive that human subject research would be unethical. Second, limb and jaw biomechanics rest on a

theoretical framework of lever mechanics, which allows biomechanical outputs such as force and velocity to be estimated from morphology (Smith and Savage 1956; Smith and Savage 1959). However, as will be discussed below, most of the structures involved in swallowing have no such levers, and the relationship between morphology and performance is less mathematically straightforward.

Given the difficulty of studying human swallowing biomechanics *in vivo*, a model organism with similar morphology and swallowing physiology stands to accelerate dysphagia rehabilitation by testing current mechanistic hypotheses and using these results to guide the development of new therapies to be tested with human patients. Such a model organism could also be used to establish a validated biomechanical framework for testing more general hypotheses about hyolingual form:function relationships, which would have extensive applicability in the fields of evolutionary biology and anthropology. Although masticatory adaptations have been studied extensively in primates and other mammals, whether swallowing performance has exerted similar selective pressure on craniofacial form and function is relatively unexplored. A better understanding of how craniofacial shape is related to swallowing may also help resolve long-standing uncertainty about some relationships between primate craniofacial form and function (DuBrul and Sicher 1954; Daegling 1993; Dobson and Trinkaus 2002; Groening et al. 2011; Daegling 2012; Ross and Iriarte-Diaz 2014).

The rhesus macaque (*Macaca mulatta*) is a suitable candidate for such a model. Despite slight morphological differences in the swallowing structures, macaque swallowing physiology is similar to humans (Hiiemae et al. 1981; Franks, Crompton, and German 1984; Franks et al. 1985; Palmer et al. 1992; Hiiemae, Hayenga, and Reese 1995; Matsuo and Palmer 2010; Nakamura et al. 2017). Although hominoids (e.g., chimpanzees, bonobos, gorillas, gibbons)

would arguably be better models because their laryngeal anatomy is more similar to humans than macaques (Nishimura 2003), the Great Ape Protection and Cost Savings Act of 2012 prohibits the use of great apes for this line of research. Moreover, rhesus macaques are a well-established model system for human neurobiology, including orofacial motor control (Huang et al. 1989; Murray et al. 1991; Lin et al. 1994; Martin et al. 1997; Martin et al. 1999; Yao et al. 2002; Sessle et al. 2005; B. J. Sessle et al. 2007; Arce-McShane et al. 2014; Arce-McShane et al. 2016). Therefore, the research presented in this dissertation could be expanded to examine how sensorimotor integration leads to biomechanical modulation. Overall, the use of rhesus macaques as a model for human swallowing biomechanics represents the best compromise among physiological similarity, phylogenetic relatedness, practical availability, and experimental rigor.

This dissertation uses the rhesus macaque model system to test hypotheses about the underlying biomechanics of the hyolingual apparatus during swallowing and establishes a biomechanical framework that quantifies the relationship between hyolingual morphology and swallowing performance. Contrary to previous assertions that humans are maladapted to swallowing because air and food can mix in the oropharynx, I argue that functional trade-offs have left humans vulnerable to dysphagia because human muscles need to shorten relatively more than those of other primates in order to achieve a safe swallow. This dissertation ultimately proposes that selection to maintain swallowing performance underlies the recent emergence of other quintessentially human morphological traits, including the chin.

Before discussing the specific aims of this dissertation, however, a brief review of the anatomy and physiology of swallowing is warranted.

HYOLINGUAL ANATOMY

Although the human hyolingual apparatus has changed shape over the course of human evolution, it is fundamentally similar to that of a macaque. This section reviews the anatomy of the hyolingual apparatus and highlights differences between humans and macaques.

The tongue

The primate tongue is composed of two sets of muscles. One set, the intrinsic muscles, are located entirely within the tongue (Figure 1.2). The superior and paired inferior longitudinal muscles are oriented parallel to the long axis of the tongue and are located at the periphery of the tongue. The vertical and transverse muscles are arranged in alternating sheets and form the core of the tongue. This fiber arrangement appears to be conserved among studied anthropoid primates, although humans have a more rounded tongue shape as a result of hyoid descent (Sokoloff and Deacon 1992; Takemoto 2001; Takemoto 2008). These intrinsic muscles are hypothesized to function as a muscular hydrostat, in which fiber shortening produces movement by capitalizing on the incompressibility of the water within the muscle fibers—decreases in fiber length must be accommodated by bulging, which increases fiber width and depth (Kier and Smith 1985; Smith and Kier 1989). For example, tongue protrusion is hypothesized to result from a combination of transverse and vertical fiber shortening, which decreases tongue diameter and increases tongue length (Vitaly J. Napadow et al. 1999).

The other set of muscles, the extrinsic muscles, originates from the cranium, mandible, hyoid, and soft palate. Styloglossus originates from the stylomandibular ligament in macaques and the styloid process in humans and inserts into the posterolateral tongue (Hartman and Straus 1933; Standring 2015). Genioglossus originates from the mandibular symphysis and fans out in

the midsagittal plane to insert into the tongue midline, interdigitating with the transverse and vertical fibers in the core of the tongue. Hyoglossus originates from the hyoid body and greater horns and inserts into the posterolateral tongue deep to styloglossus. Palatoglossus originates in the lateral part of the soft palate and inserts into the posterolateral tongue, merging with styloglossus. These extrinsic muscles are thought to produce tongue movement by moving the entire tongue as well as by deforming the tongue locally. For example, genioglossus shortening is thought to produce a midline furrow in the tongue (Abd-El-Malek 1955; Stone and Lundberg 1996).

Several terms have been used to describe the different parts of the tongue surface. The oral tongue is the anterior two-thirds of the tongue anterior to the circumvallate papillae. The pharyngeal tongue is the posterior one-third of the tongue posterior to the circumvallate papillae (Standring 2016) and is synonymous with the tongue base or base of tongue referred to in the clinical literature (e.g., Logemann and Bytell 1979; Logemann et al. 1998; Pauloski et al. 2000; Veis et al. 2000; Lazarus et al. 2002). The term "tongue base" is used throughout this dissertation. The tongue base is not to be confused with the tongue root, which is the inferior aspect of the tongue, where it is attached to the hyoid and mandible, and is spatially related to mylohyoid and geniohyoid (Standring 2016).

The hyoid and hyoid muscles

The primate hyoid is composed of several parts—a body, or basihyoid, a pair of lesser horns, and a pair of greater horns (Figure 1.2). The macaque basihyoid is more dorsoventrally elongate and shield-shaped than the human basihyoid, and it has a concavity accommodating a laryngeal air sac, which is commonly found in anthropoid primates but which

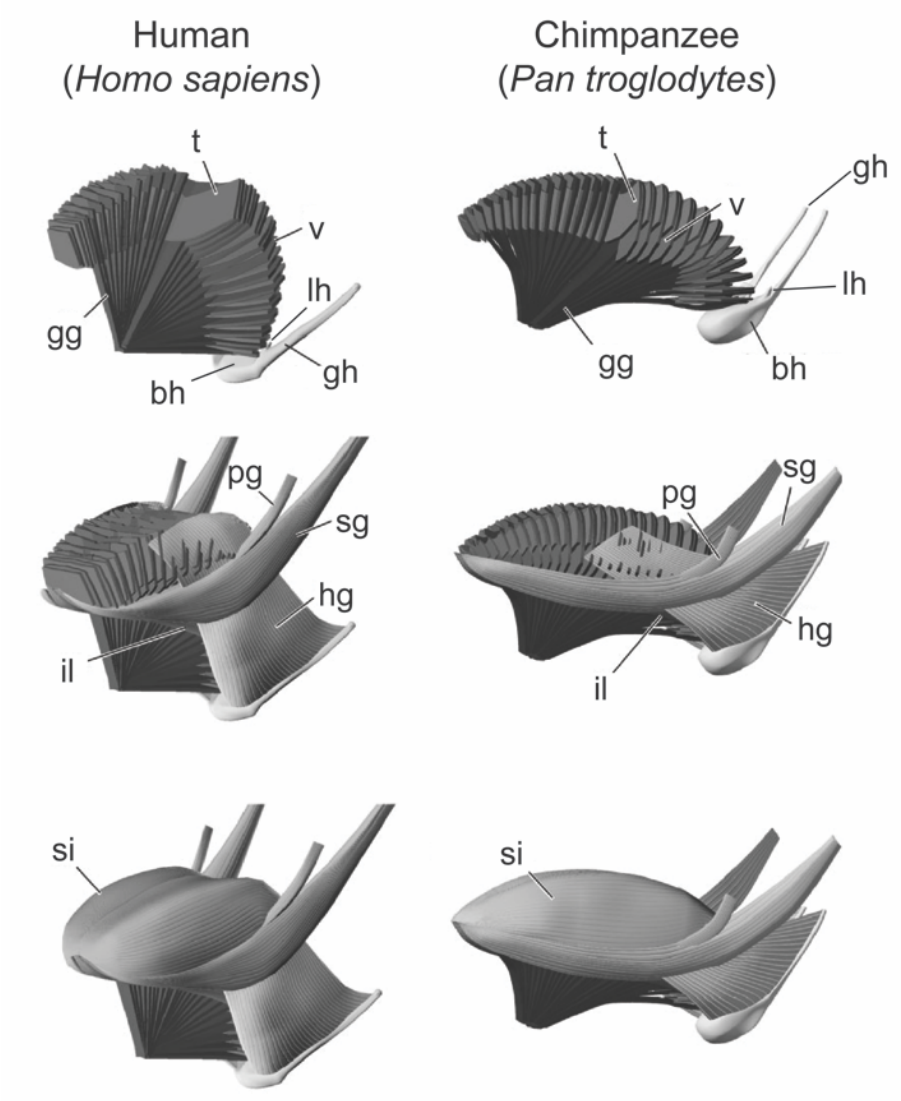

Figure 1.2: The anatomy of the human and chimpanzee tongue. Anatomy proceeds from deep to superficial as one reads from top to bottom. Abbreviations: bh, basihyoid; gg, genioglossus; gh, greater horn; hg, hyoglossus; il, inferior longitudinal fibers; lh, lesser horn; pg, palatoglossus; sg, styloglossus; t, transverse fibers; v, vertical fibers. Modified from Takomoto 2008.

has been lost since the human lineage diverged with that of chimpanzees[2] (Figure 1.3) (Hartman and Straus 1933). Additionally, the macaque lesser horns are longer than a human's, and the macaque's greater and lesser horns are spanned by a small muscle, ceratohyoid (Sprague 1944).

[2] The hominid hyoid fossil record is poor, but a juvenile australopithecine basihyoid had a concavity consistent with an air sac, whereas a Neanderthal basihyoid did not (Arensburg et al. 1989; Alemseged et al. 2006).

Unlike many other mammals, the primate hyoid is not normally connected to the cranium by a chain of ossicles, but rather 'floats', suspended from the cranium, mandible, thyroid cartilage, pharynx, sternum, and scapula by a muscular sling (Hartman and Straus 1933; Sprague 1943; Standring 2015). Muscles originating superior to the hyoid are broadly categorized as suprahyoid muscles, while muscles originating inferior to the hyoid are termed infrahyoid muscles.

The suprahyoid muscles probably produce most hyoid movements during swallowing. Geniohyoid originates from the mandibular symphysis and inserts on the basihyoid. Mylohyoid originates on the lingual surface of the mandibular corpus along the mylohyoid line, and its posterior fibers insert into the basihyoid whereas its more anterior fibers insert into a midline raphe. Stylohyoid originates from the styloid area in macaques and the styloid process in humans and inserts into the inferior pole of the basihyoid in macaques and at the junction between the basihyoid and greater horn in humans (Hartman and Straus 1933; Standring 2015). Although neither belly of the digastric directly inserts into the hyoid, the digastric tendon is attached to the hyoid by a membrane in macaques and a fascial sling in humans and is therefore frequently considered a suprahyoid muscle (Hilloowala 1975; Standring 2015). The posterior belly originates from the mastoid process of the basicranium in macaques and the mastoid notch in humans, and the anterior belly originates from the inferior border of the mandible for approximately half of the mandible's length, whereas in humans this belly inserts inferior to the mandibular symphysis in the digastric fossa (Hartman and Straus 1933; Standring 2015).

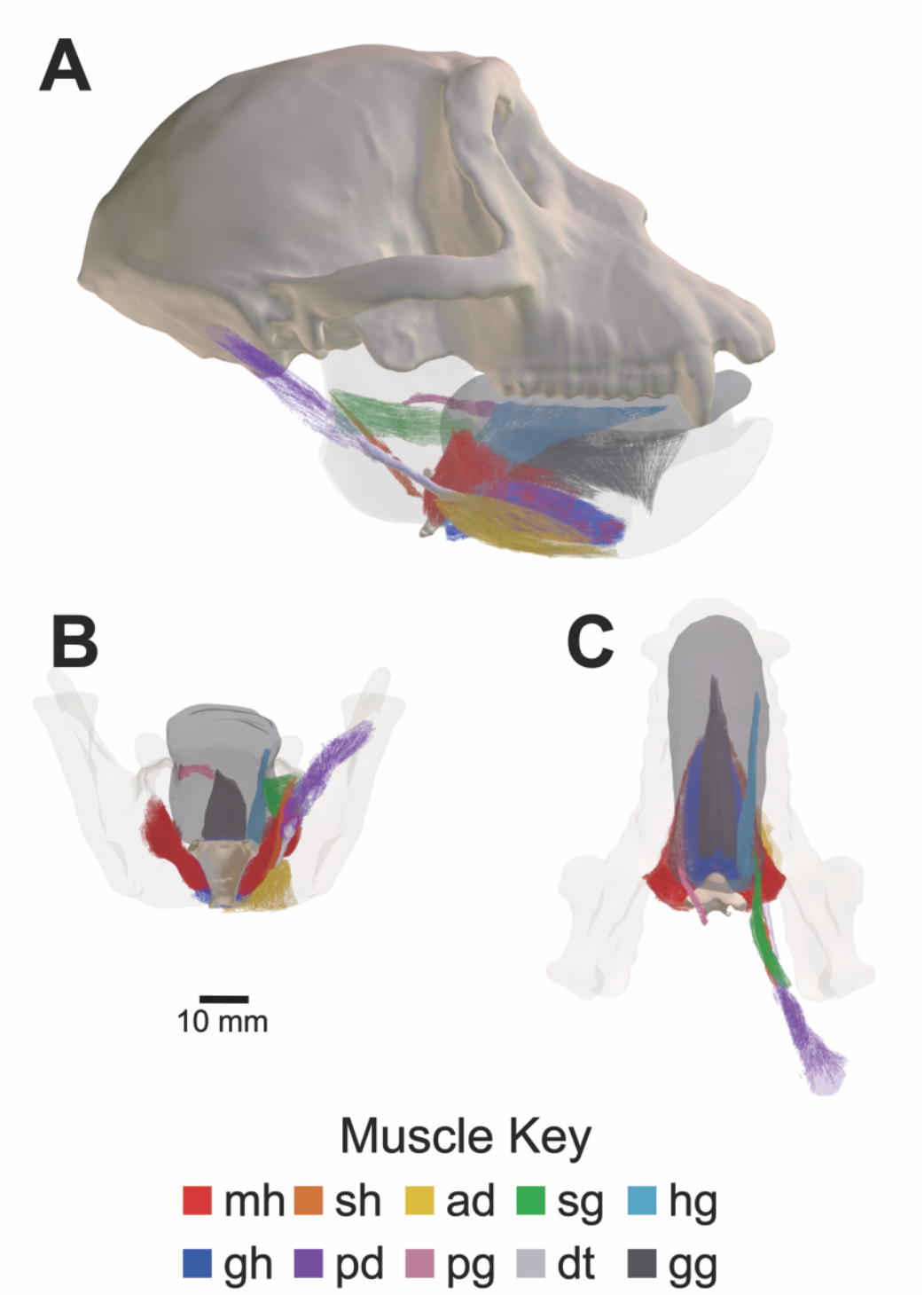

Figure 1.3: Hyolingual anatomy of the rhesus macaque (*Macaca mulatta*). Reconstructed using diffusible iodine-based contrast-enhanced computed tomography (diceCT). The concavity in the basihyoid (tan) accommodates the laryngeal air sac. Modified from Orsbon et al. 2018. Abbreviations: ad, anterior digastric; dt, digastric tendon; gg, genioglossus; gh, geniohyoid; hg, hyloglossus; mh, mylohyoid; pd, posterior digastric; pg, palatoglossus. Only the basihyoid is shown.

HYOLINGUAL PHYSIOLOGY DURING SWALLOWING

During a mammalian feeding sequence, the tongue transports food from the ingestion point, usually lips and anterior dentition, to the post-canine dentition, a process called stage I transport (Franks et la. 1984; Franks et al. 1985; Hiiemae and Crompton 1985; German et al. 1989). Alternatively, food can be placed directly on the post-canine teeth by the forelimbs or by utilizing wide gapes to break or slice off pieces of food. Once on the post-canine teeth, the tongue participates in mastication—rhythmic superoinferior and mediolateral movements of the mandible which mechanically digest the food with the teeth—by working with the buccinator muscles of the cheek to keep food on the tooth row. Meanwhile, the highly sensitive lingual epithelium gathers sensory information to determine whether a bolus is ready to be swallowed (Hiiemae and Crompton 1985; Trulsson and Essick 1997; Mu and Sanders 2000; Hiiemae and Palmer 2003). If it is ready, the tongue moves the bolus posteriorly during stage II transport for storage in the valleculae, which are bilateral pouches between the most posterior part of the tongue and the epiglottis (Figure 1.1). After one or several of such stage II transport cycles, a swallow commences, and the tongue base retracts against the posterior wall of the pharynx, moving the bolus from the valleculae, through the pharynx, past a closed laryngeal inlet, and into the esophagus. Once complete, the tongue relaxes and the larynx reopens as breathing resumes.

Because the movements of the tongue and hyoid are linked with those of the jaw as part of a "chain" in which the movements of one structure affects the movements of others (Hiiemae and Crompton 1985; Hiiemae and Palmer 2003), a basic understanding of jaw movements is also necessary. During chewing and swallowing sequences, mandibular movements increase gape through a combination of changes in pitch (i.e., rotation) and anterior translation at the temporomandibular joint (TMJ) because the mandible's center of rotation is

inferior to the TMJ (Wall 1999; Keefe et al. 2008; Terhune et al. 2011; Ross et al. 2012; Menegaz et al. 2015; Iriarte-Diaz et al. 2017). The mandible accelerates and decelerates during opening and closing, respectively; consequently, the gape cycle—defined as the period from maximum gape to maximum gape—is often partitioned into four phases based on the velocity of the mandible: fast close (FC), slow close (SC), slow open (SO), and fast open (FO) (Hiiemae et al. 1995; Reed and Ross 2010; Iriarte-Díaz et al. 2011; Ross et al. 2012; Nakamura et al. 2017). Humans and macaque monkeys also feature an intercuspal phase (IP), which overlaps with SC and SO, during which the molar cusps intersect and the mandible may cease to change in pitch (Figure 1.4) (Palmer et al. 1992; Hiiemae et al. 1995; Orsbon et al. 2018).

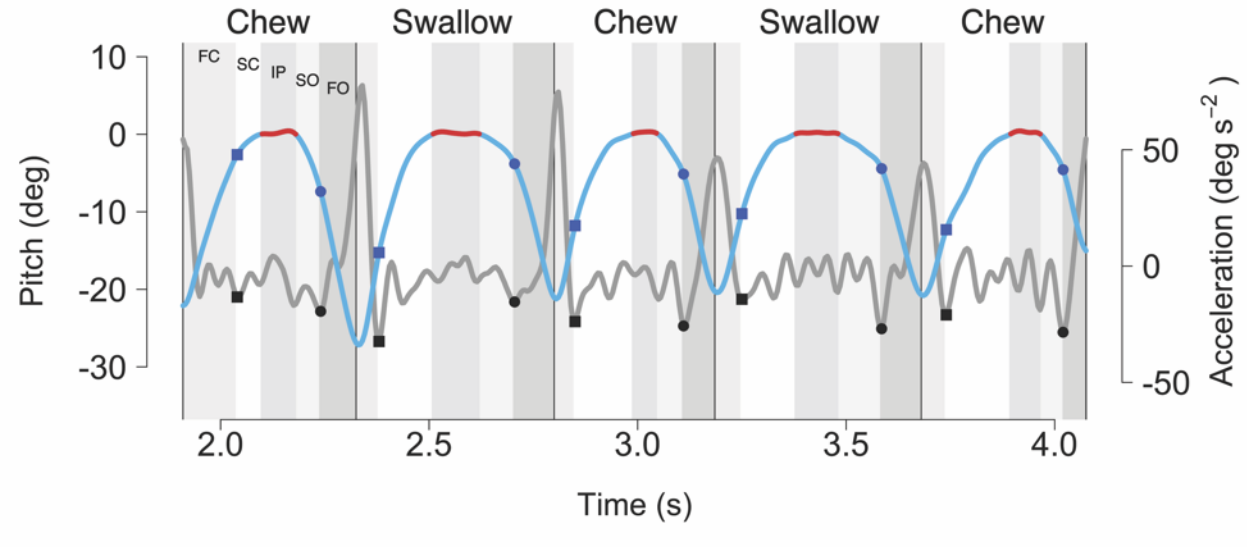

Figure 1.4: Mandibular kinematics and gape cycle phases. Although IP is shown here as a distinct phase, in reality SC continues into IP and SO begins before IP is complete. Cycles are separated by black lines. Different colored gray boxes indicate different phase cycles indicated in the first cycle (FC, fast close; SC, slow close; IP, intercuspal phase; SO, slow open; FO, fast open). Light blue lines indicate mandible pitch, gray lines indicate mandible acceleration. Squares indicate the lowest acceleration prior to the intercuspal phase and indicate the FC-SC transition. Circles indicate the lowest acceleration after the intercuspal phase and indicate the SO-FO transition. The inter-cuspal phase is indicated on the pitch trace in red. Reproduced from Orsbon et al. 2018.

Anatomical differences are thought to underlie differences between primates and other mammals in how bolus transport and swallowing relate to the mandibular cycle. In most studied nonprimate mammals, the bolus moves posteriorly as the hyolingual apparatus retracts during FO and FC, and ultimately masticated food accumulates in the valleculae (Figure 1.1) (Franks et al. 1985; Hiiemae and Crompton 1985). Ridges on the hard palate called palatal rugae prevent anterior movement of the bolus as the tongue then proceeds to protract during SO. During the swallow, the tongue base retracts during SO to transfer the bolus to the posterior oropharynx and laryngopharynx, after which the pharyngeal constrictors propel the bolus into the esophagus (Hiiemae and Crompton 1985). In contrast, humans and macaques have diminutive palatal rugae that cannot resist anterior movement of the bolus as the tongue protracts during SO (Franks et al.1984). Consequently, primates transfer the bolus to the oropharynx using a different mechanism: the anterior tongue contacts the hard palate as the hyolingual apparatus protracts during IP and early SO; then, the middle tongue maximally elevates during SO; finally, the hyoid and posterior tongue are maximally elevated shortly after the SO-FO transition (Nakamura et al. 2017). These movements create a wave of palatal contact travelling posteriorly, and the tongue "squeezes back" the bolus towards the valleculae (Figure 1.5) (Franks et al. 1984; Palmer et al. 1992). As a result, stage II transport occurs during SO in catarrhine primates instead of FO and FC as it does in nonprimate mammals (Hiiemae and Crompton 1985). Because humans and macaques store only small amounts of masticated food in their relatively small valleculae before the swallow, much of the masticated bolus is still in the oral cavity prior to swallowing (Franks et al. 1984; Palmer et al. 1992). When a macaque or human is ready to swallow, the tongue performs a similar squeeze-back mechanism that features greater hyoid excursion than a stage II transport, as well as tongue base retraction (Franks et al. 1984; Palmer et al. 1992). Unlike

nonprimate mammals, humans and macaques use the squeeze-back mechanism to swallow both food and liquids, whereas nonprimate mammals only use the squeeze-back mechanism to transport liquids from the oral cavity to the valleculae (Hiiemae et al. 1981; Franks et al. 1984; Franks et al. 1985; Hiiemae and Crompton 1985; Palmer et al. 1992b).

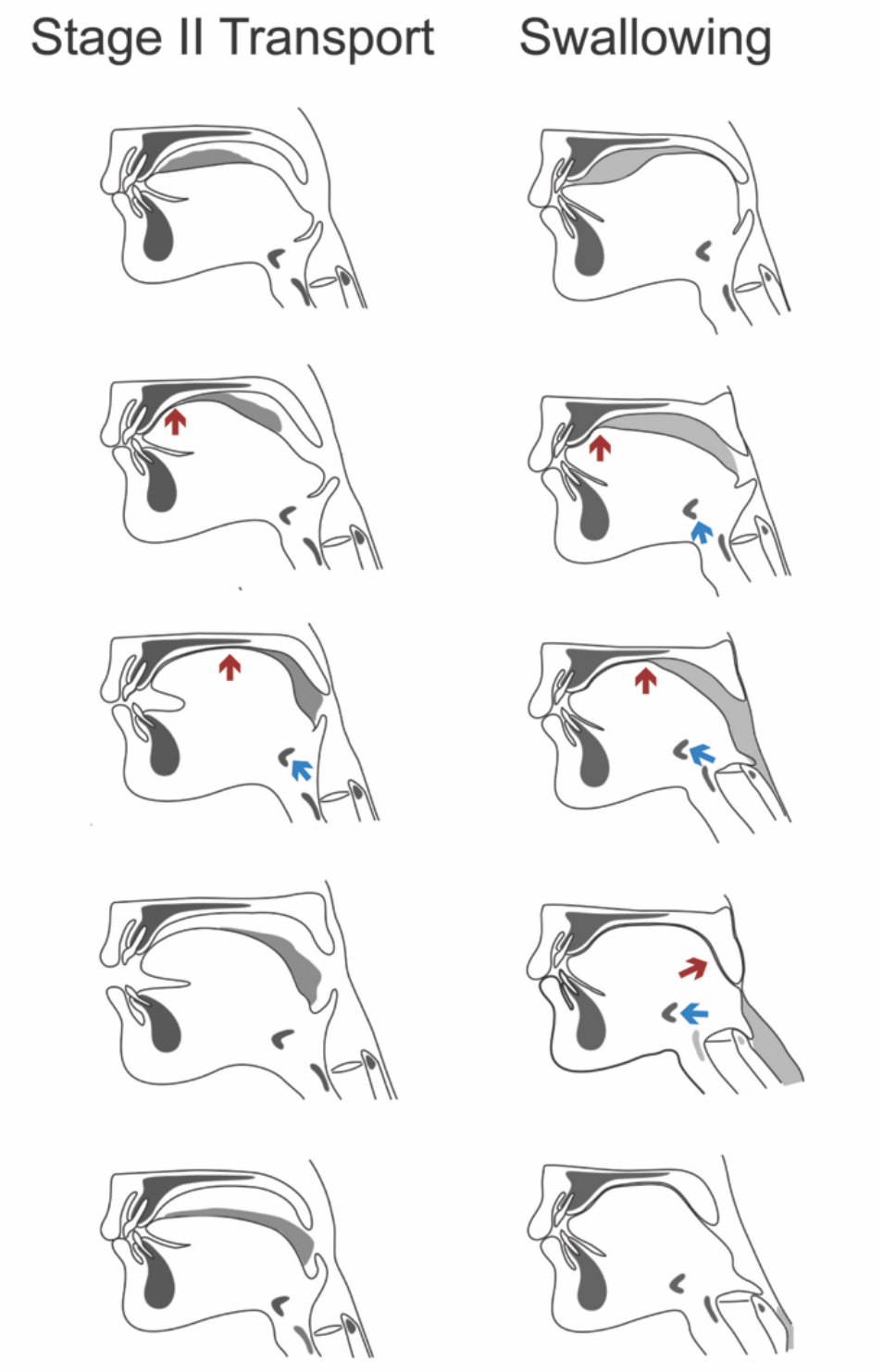

Figure 1.5: The squeeze-back mechanism during stage II transport and swallowing in a human. Red arrows indicate progression of point of contact between tongue and palate. Blue arrows indicate direction of hyoid movement. The hyoid displaces more in swallowing, particularly anteriorly. Modified from Matsuo and Palmer 2008.

WHY STUDY THE SQUEEZE-BACK MECHANISM?

The squeeze-back mechanism has two important functions for airway protection, both during and after the swallow. First, hyoid elevation and protraction pull the larynx superiorly and anteriorly to avoid contact with the oncoming bolus as tongue base retraction propels the bolus through the oropharynx and flips the epiglottis over the airway (McConnel 1988; Gassert and Pearson 2016). These movements function to prevent the bolus from entering the airway *during* the swallow. Second, as tongue base retraction propels the bolus toward the esophagus and clears the throat, or oropharynx, of any lingering residues (Dejaeger et al. 1997), hyoid protraction opens a sphincter guarding the entrance to the esophagus (Cook et al. 1989). This opening corresponds with increased pressures at the tongue base and laryngopharynx—likely facilitated by pharyngeal constrictor activity onset—which generates a pressure gradient that facilitates bolus transfer to the lower-pressure esophagus and prevents bolus stasis in the laryngopharynx (McConnel 1988; Dejaeger et al. 1997). These movements function to prevent the bolus or its remnants from entering the airway once breathing resumes *after* the swallow. Accordingly, patients with dysphagia frequently present with poor tongue base retraction (Logemann et al. 2006; Logemann et al. 2008; King et al. 2016) and/or poor hyoid displacement or velocity (Paik et al. 2008; Steele et al. 2011; Hoffman et al. 2013; Steele and Cichero 2014; Seo et al. 2016)

To rehabilitate tongue base retraction and hyoid excursion, a therapist needs to know what muscles need to be targeted. Current morphological and physiological data suggest that tongue base retraction is caused by shortening of the styloglossus, hyoglossus, and transverse intrinsic tongue muscles (Napadow et al. 1999; Gassert and Pearson 2016). Similarly, hyoid excursion is likely caused by geniohyoid, mylohyoid, and digastric shortening (Palmer et al. 1992; Pearson et al. 2011; Inokuchi et al. 2014; Inokuchi et al. 2016). However, as will be

discussed in Chapter 2, determining muscle functional morphology requires more than knowing the orientation of muscles and their activity patterns—to determine a muscle's function, muscle velocity and activity must be measured simultaneously to determine whether the muscle shortens, lengthens, or is isometric during a given behavior, and whether it actively produces force at that time (German et al. 2011). These different types of activity not only determine muscle function but also the types of exercises that would best restore those functions if they are lost (Thorstensson et al. 1976; Coyle et al. 1981; Gür et al. 2002; Stathopoulos and Ducchan 2006; Hubbard et al. 2009). Moreover, changes in hyoid posture over smaller time scales, such as during a single swallow, or over longer time scales, such as over human ontogeny or evolution, could affect these muscles' functions (German et al. 2011).

AIMS

The objective of this dissertation is to determine the biomechanical basis of the primate squeeze-back mechanism of swallowing and how craniofacial changes observed over human evolution and development affect swallowing performance. The specific aims are as follows:

Aim 1: Develop a workflow to measure in vivo hyolingual muscle kinematics and activity, and use these data to build a computational model of hyolingual biomechanics

The *in vivo* workflow integrates existing data acquisition workflows to simultaneously measure 3D mandibular and hyolingual kinematics with individual hyolingual muscle kinematics and activity. Specifically, the method integrates X-ray Reconstruction of Moving Morphology (XROMM, Brainerd et al. 2010) with diffusible iodine-based contrast enhanced computed tomography (diceCT, Mestcher 2009; Gignac et al. 2016) and electromyography (EMG, Loeb

and Gans 1986). Although XROMM and diceCT provide high temporospatial resolution, whether they provide sufficient precision to measure hyolingual velocity, and whether their integration significantly improves measurement accuracy, are unknown. This method is applied in the second and third aims.

The computational model uses custom-developed software in R (R Core Team, 2017) to predict hyolingual range of motion from muscle morphology and length change. This model is used to simulate the biomechanical consequences of changes in muscle morphology that are based on the human fossil record, comparative anatomy, and human ontogenetic changes. The model constrains maximum and minimum muscle length based the limits of muscle length change observed *in vivo*. This method is applied in the fourth aim.

Aim 2: Determine whether tongue base retraction is caused by intrinsic and/or extrinsic tongue muscle shortening.

Tongue retraction is hypothesized to be due to a combination of shortening of extrinsic (styloglossus, hyoglossus) and intrinsic (transverse lingual) muscles (Napadow et al. 1999; Gassert and Pearson 2016). However, a key assumption underlying tongue biomechanics—that the tongue is isovolumetric (Kier and Smith 1985; Smith and Kier 1989)—has not been tested in primates and is challenged by *in vivo* data from other mammalian species (Doran and Baggett 1970; Doran and Baggett 1971; Liu et al. 2008; Liu et al. 2009; Harper et al. 2013). Evidence of regional changes in volume would open the possibility that regional volume displacement by suprahyoid muscles may produce tongue base retraction through a hydraulic linkage. In such a linkage, hyoid excursion and mouth floor elevation decrease the volume available for the tongue within the oral cavity. Consequently, some tongue volume must be displaced posteriorly because

it cannot go superiorly due to the hard palate, anterolaterally because of the tooth row, or inferiorly as the mouth floor both raises and stiffens. In such a scenario, the hyoid effectively squeezes-back the tongue, analogous to how the tongue squeezes back the bolus during swallowing. However, if tongue retraction does not coincide with a decrease in the volume available for the tongue, then such a hypothesis is not supported.

Hypotheses

H_1: At least one extrinsic tongue retractor (i.e., hyoglossus, palatoglossus, and styloglossus) shortens as much as the tongue retracts during swallowing.

H_2: Posterior tongue width decreases as the tongue retracts.

H_3: The tongue does not shear outside of sagittal planes, i.e., the lateral tongue retracts as much as the tongue midline.

H_4: Posterior tongue volume remains constant throughout retraction.

H_5: Tongue retraction occurs as the volume bounded by the hard palate, tooth row, and mouth floor decreases.

Aim 3: Evaluate whether hyolingual muscles primarily function through active shortening during tongue base retraction specifically and swallowing in general.

If tongue base retraction is due to suprahyoid muscles producing hyoid excursion and mouth floor elevation, then these muscles must be active during tongue base retraction. Hyoid elevation and protraction during swallowing are frequently assumed to result primarily from suprahyoid muscle active shortening. Although hyolingual muscles are hypothesized to also behave isometrically and eccentrically (Thexton 1984), the potential functions of such activity

are unknown. Moreover, the geometric arrangement of hyolingual muscles allows hyoid movement to occur not only as a result of muscle shortening but also fiber rotation that, based on observations of pennate musculature, may enhance hyoid displacement and velocity at the expense of muscle force production (Azizi et al. 2008). As with isometric and eccentric activity, the functional implications of fiber rotation are unclear. Non-concentric activity and fiber rotation have important implications for understanding how force-velocity tradeoffs affect hyoid muscle performance during swallowing.

Hypotheses

H_1: Suprahyoid muscles are active during tongue base retraction

H_2: Hyolingual muscles are only active during muscle shortening

H_3: Muscle shortening is the sole cause of hyoid protraction and elevation

Aim 4: Examine the biomechanical consequences of craniofacial and hyolingual shape changes observed over human evolution and development

The short face and low tongue base, hyoid, and larynx of humans have been argued to be adapted for speech and maladapted for swallowing (Negus 1949; Lieberman et al. 1969; Lieberman et al. 1992). However, more recent studies cast doubt on both of these claims, including studies of the physical capacity for vowel production in nonhuman primates (Fitch et al. 2016; Boë et al. 2017), swallowing physiology (Palmer et al. 1992; Palmer 1998; Hiiemae and Palmer 1999; Matsuo and Palmer 2015), and choking epidemiology (Heimlich 1974; Mittleman and Wetli 1982; Vilke et al. 2004; Soroudi et al. 2007; Inamasu et al. 2010; Sakai et al. 2014). Aim 4 considers an alternative to this maladaptive vocal tract hypothesis; namely, that

the low position of the hyolingual apparatus and larynx is a product of spatial/functional constraints related to facial shortening and, more specifically, mandibular shortening. A low hyolingual apparatus may not be an adaptation for speech but rather may be necessary to maintain swallowing performance as the face becomes shorter and the cervical spine becomes more vertically oriented. This fourth aim is pursued using computational modeling based on *in vivo* data. Rather than applying these models to specific fossils in attempt to recreate an evolutionary sequence, I instead apply biomechanical principles ro examine how changes observed—or not observed—in the evolution of hominid craniofacial and vertebral morphology may have affected hyolingual biomechanics and performance.

Hypotheses

H_1: Hyoid descent is necessary and sufficient to maintain hyoid excursion when only mandibular length is shortened.

H_2: Hyoid descent is necessary and sufficient to maintain hyoid excursion when mandibular length is shortened in combination with the other characters mimicking a more humanoid morphology.

DISSERTATION OVERVIEW

The biomechanical basis of musculoskeletal functional morphology is presented in Chapter 2. This chapter reviews the many variables that determine the function of a given muscle and how the morphology and physiology of muscle produce trade-offs between muscle force and velocity. Particular attention is given to how experimental approaches integrating morphological and physiological lines of evidence have demonstrated the importance of using dynamic

approaches to study functional morphology. Of the many functional determinants discussed in Chapter 2, this dissertation is primarily concerned with relationships among muscle activity, morphology, hyoid movement, and tongue base retraction; therefore, the scope of the analyses presented here focus on electromyography; muscle length, velocity, and orientation; and hyolingual kinematics.

Chapter 3 addresses the first aim and details the methodologies employed in Chapters 4-6. The research presented in this dissertation is the first to simultaneously measure craniomandibular and hyolingual kinematics in three dimensions as well as hyolingual electromyography. Kinematic data were collected using X-ray Reconstruction of Moving Morphology (XROMM, Brainerd et al. 2010; Knörlein et al. 2016), and muscle length and orientation reconstructions were guided by integrating diffusible iodine-based contrast enhanced CT (diceCT, Metscher 2009; Gignac et al. 2016). This chapter also details data processing and statistical analyses for Chapters 4 and 5 and presents the development of the hyoid range of motion computational model used in Chapter 6.

Chapter 4 argues that hyoid excursion causes tongue base retraction through a mechanical coupling in which hyoid protraction and elevation displace tongue volume posteriorly. This coupling is consistent with the definition of a hydraulic linkage, in which volume is displaced in one region, generating force or displacement in a region remote from where force was originally applied. This chapter falsifies two alternative hypotheses, namely that tongue base retraction is due to either extrinsic or intrinsic lingual muscle shortening (Napadow et al. 1999; Gassert and Pearson 2016). Moreover, these data suggest that hyoglossus functions to protract and elevate the hyoid rather than to directly retract the tongue. These findings have implications for the motor control and rehabilitation of tongue base retraction. Mechanical coupling between the hyoid and

the tongue base would reduce the degrees of freedom involved in swallowing, which could simplify swallowing motor control. This coupling also would make several key aspects of swallowing—tongue base retraction, laryngeal elevation, and upper esophageal sphincter opening—dependent on suprahyoid muscle function, which suggests that suprahyoid muscles may have strong but underappreciated selective pressures to maintain their performance. Additionally, if tongue base retraction is caused by hyoid displacement, then therapies which target suprahyoid muscles may be more effective at rehabilitating tongue base retraction that those that do not.

Chapter 5 investigates the functional morphology of these suprahyoid muscles in pursuit of the third aim: how does their activity relate to tongue base retraction, what kinds of activity (i.e., concentric, isometric, and/or eccentric) do these muscles produce, and how does morphology affect these muscles' ability to generate force and displacement? Suprahyoid muscles were primarily concentrically active during tongue base retraction, while lingual muscles were primarily eccentrically active. Small amounts of active muscle stretch before shortening in some suprahyoid muscles suggest that infrahyoid muscles may contribute to swallowing performance. Because suprahyoid muscles reached peak activity during active shortening, muscle velocity and/or power may be more important determinants of swallowing performance than maximum force. Exercise regimes to maximize velocity and power differ from those that maximize force, and the former may be more effective at rehabilitating swallowing performance than the latter because they better match *in vivo* function (Thorstensson et al. 1976; Coyle et al. 1981; Gür et al. 2002; Stathopoulos and Ducchan 2006; Hubbard et al. 2009). Hyolingual morphology is also consistent with the importance of velocity over high force production in swallowing performance because several hyolingual muscles amplify hyoid velocity through fiber rotation, but this likely

comes at the expense of force production based on *in vitro* studies (Azizi et al. 2008; Holt et al. 2016). However, this chapter argues that fiber rotation can also reduce hyoid velocity and, under certain circumstances, may actually improve muscle force production.

Chapter 6 builds on Chapter 5 by using the data on muscle shortening and fiber rotation to examine how swallowing performance is affected by changes in hyolingual and craniomandibular morphology similar to those occurring during human ontogeny and evolution. As discussed above, hyolingual descent is thought to be detrimental to swallowing function because it allows mixing of air and food near the larynx. However, the biomechanical consequences of hyoid descent have not been studied quantitatively, and it is possible that hyoid descent helps to preserve swallowing function when the mandible—and therefore the geniohyoid and hyoglossus—is shortened. To test this hypothesis, I developed a computational model which, using hyoid excursion as a proxy, predicts swallowing performance based on parameters defining craniomandibular and hyoid shape, hyoid posture, and muscle physiology. When the mandible was shortened, sufficient swallowing performance could only be maintained through extreme muscle rotation, changes in mandibular symphysis shape, and/or increased muscle shortening. Hyoid descent imposed performance deficits when the mandible was shortened because muscle rotation decreased hyoid protraction. These deficits were nearly resolved by a vertical symphysis, which increases geniohyoid length, and by increasing the amount of muscle shortening. However, when other aspects of human morphology are included in the model—a dorsoventrally compressed hyoid, basicranial flexion, and digastric insertion on the hyoid—hyoid excursion is further restricted except when both hyoid descent and a vertical symphysis are present. Consequently, hyoid descent, a vertical symphysis, and increased muscle shortening are all necessary to achieve sufficient excursion. I argue that not only is hyoid descent potentially

adaptive for swallowing in the context of mandibular shortening—which challenges decades of assertions to the contrary—but also that swallowing performance can generate selective pressures which would favor a more vertically oriented symphysis. With this latter assertion, I argue that human symphyseal shape is a product of both masticatory and deglutitive functional requirements and offer the first quantitative analysis of comparative hyolingual biomechanics to support this claim.

Chapter 7 concludes this dissertation by discussing future directions for the work presented in Chapters 4-6 and further contextualizing the implications of this research. The hypothesized hydraulic linkage among the hyoid, suprahyoid muscles, and the tongue base, as well as the underlying shearing mechanisms argued to link them, can be further tested by increasing marker density in the posterior tongue, *post mortem* tissue manipulations, *in vivo* stimulation experiments isolating single nerves, and further *in vivo* material properties analyses. The functional morphology of suprahyoid muscles can be probed further by modeling *in vivo* force-length curves and assessing fiber type distribution to generate force-velocity curves. The computational model of range of motion can be further validated against *in vivo* data from other primates—including humans—and used to predict hyoid range of motion among fossil hominids, patient populations, and many species of mammals with spectacularly diverse hyolingual apparatuses.

If tongue base retraction, laryngeal inlet closure, and upper esophageal sphincter opening all depend on suprahyoid muscle shortening, then changes in the latter's morphology and function due to craniofacial modifications—whether evolutionary, ontogenetic, or pathological in origin—can profoundly affect swallowing performance and organismal fitness. These changes are deserving of much-needed attention in the ostensibly dualistic realms of clinical and

comparative research, each of which stands to benefit from the other's perspective on swallowing performance. My hope is that this dissertation will invigorate quantitative swallowing functional morphology research, not only to improve our knowledge of swallowing biomechanics, as lever mechanics did for craniomandibular and locomotor systems, but also to advance our understanding of how natural selection could have crafted such a curious contraption:

> I can, indeed, hardly doubt that all vertebrate animals having true lungs have descended by ordinary generation from an ancient prototype, of which we know nothing, furnished with a floating apparatus or swimbladder. We can thus…understand the strange fact that every particle of food and drink which we swallow has to pass over the orifice of the trachea, with some risk of falling into the lungs, notwithstanding the beautiful contrivance by which the glottis is closed. In the higher Vertebrata the branchiæ have wholly disappeared—the slits on the sides of the neck and the looplike course of the arteries still marking in the embryo their former position. But it is conceivable that the now utterly lost branchiæ might have been gradually worked in by natural selection for some quite distinct purpose (Darwin 1859).

CHAPTER TWO: REVIEW OF THE MORPHOLOGICAL AND PHYSIOLOGICAL DETERMINANTS OF MUSCLE FUNCTION

INTRODUCTION

Musculoskeletal output force, velocity, and displacement play essential roles in organismal performance during a variety of vertebrate behaviors, including feeding and locomotion. Decades of physiological and biomechanical research have revealed a fundamental constraint on musculoskeletal design[3] in vertebrates: the tradeoff between force and velocity due to the basic morphological and physiological properties of vertebrate muscle. The ways in which different lineages deal with this constraint are an important focus of evolutionary biomechanics and neuromechanics. Although the ways in which muscles interact with the skeleton to adjust output force and velocity are well-studied, comparatively little is known about force-velocity trade-offs in vertebrate musculoskeletal systems which lack levers, such as muscular hydrostats and the primate hyolingual apparatus.

This chapter has two aims. First, I review the morphological and physiological parameters that have been shown to affect muscle function in lever-based musculoskeletal systems and discuss how these parameters interact. Throughout this section, I comment on how these principles can or have been applied to the primate hyolingual apparatus. Second, I argue for the necessity of integrating morphological and physiological lines of evidence to determine muscle function. Newly developed, high resolution imaging technologies are advancing muscle

[3]Throughout this chapter, I define musculoskeletal design as the relationship among musculoskeletal morphology, physiology, and biomechanical performance—in short, form:function relationships (Ross et al. 2017). Because morphology and physiology interact to produce biomechanical performance, musculoskeletal design may be a product of adaptation by natural selection if the design increases fitness through improved performance.

functional morphology research through the seamless integration of these lines of evidence. I focus on two of these, which are both utilized in this dissertation: diffusible iodine-based contrast enhanced Computed Tomography (diceCT, Gignac et al. 2016) and X-Ray Reconstruction of Moving Morphology (XROMM, Brainerd et al. 2010).

THE PARAMETERS OF PERFORMANCE

Morphological Parameters

Active muscle force, with its inherent force-velocity tradeoffs, is determined in part by the morphology of proteins within muscle cells, or fibers. Muscle fibers are composed of myofibrils, which are themselves composed of repeating units of contraction called sarcomeres (Zatsiorsky and Prilutsky 2012). Within these sarcomeres are overlapping actin and myosin filaments, which can slide past each other as the sarcomere lengthens and shortens. These filaments form cross bridges with each other and rapidly develop force when the muscle is depolarized by motoneuron activity and calcium is released into the cytoplasm (Hill 1949; Spudich and Watt 1971). When sarcomeres are not changing in length (that is, when they are isometrically active), force is determined by the amount of overlap between actin and myosin filaments (Ramsey and Street 1941; Gordon et al. 1966). If fiber length is longer than the lengths at which there is optimal overlap, then force declines. If the fiber is shorter than the length of the actin filaments, then force declines as actin filaments from the opposite sides of the sarcomere begin to overlap with each other and interfere with myosin binding. When fiber length is shorter than the length of the myosin filament, the myosin filaments collide with the z-discs which separate the sarcomeres—giving vertebrate skeletal muscles its characteristic cross-striated appearance—and support the actin filaments. Although myosin length is conserved across

vertebrates, actin length varies among species, producing slightly different force-length curves for different species (Burkholder and Lieber 2001) (Figure 2.1). When sarcomeres are permitted to change length, fiber force decreases as fiber shortening velocity increases, and power (force x velocity) is maximal at approximately 33 % of maximum shortening velocity (Figure 2.2) (Gasser and Hill 1924; Stevens and Snodgrass 1932; Zatsiorsky and Prilutsky 2012). Unlike the force-length relationship and its morphological basis, the force-velocity curve is empirically determined.

The cross-striated structure of vertebrate sarcomeres fundamentally constrains the range of motion of vertebrate muscular hydrostats and hyolingual apparatuses (Kier and Smith 1985). Vertebrates have compensated for these fundamental limitations through a number of morphological modifications at the sarcomere and whole-muscle level. Chameleons, which are capable of ballistic tongue projection, have perforated z-discs in their hyolingual retractor muscles (Rice 1973). Such perforations extend this muscle's range of motion by allowing sarcomeres to 'supercontract', which prevents collision between the myosin filaments and the z-discs as the retractors pull the hyolingual apparatus back into the oral cavity after projection and shorten up to 16 % of their maximum length (Rice 1973). Rather than modify the sarcomere, plethodontid salamanders instead have extremely long fiber lengths, such that the hyolingual retractors are pleated when at rest (Lombard and Wake 1977). Similarly, long retractor lengths are seen in mammals with extreme tongue protrusion, including pangolins (*Manis*), giant anteaters (*Vermilingua*), the honey possum (*Tarsipes*) and echidnas (*Tachyglossus*) (Doran and Baggett 1971; Naples 1999).

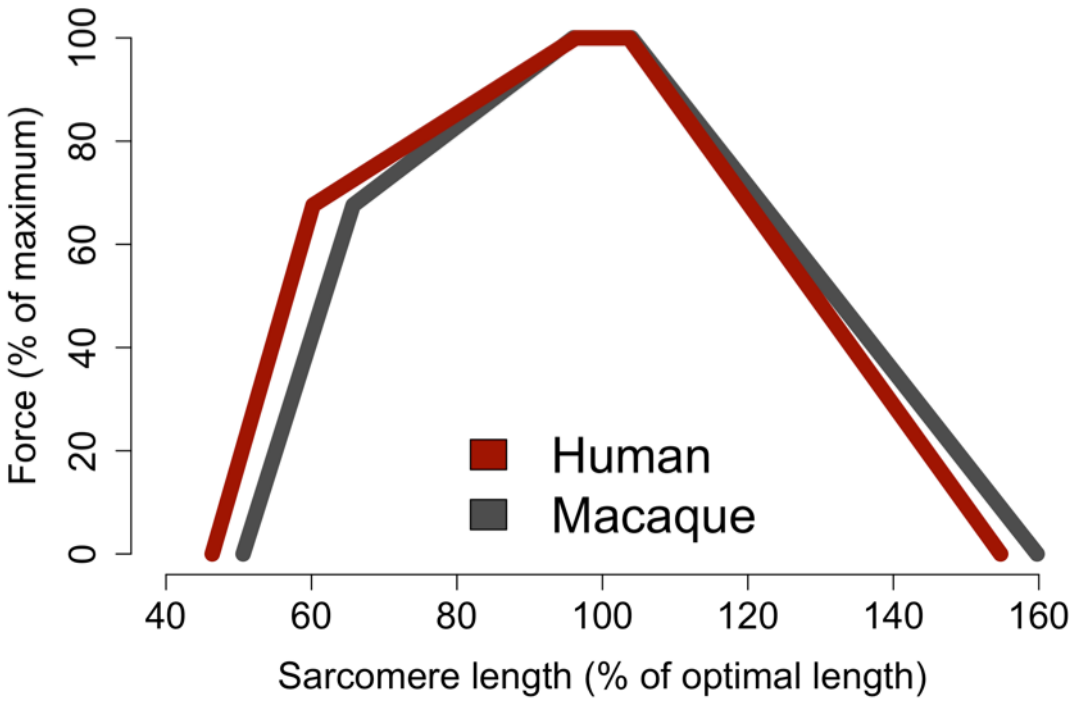

Figure 2.1: Force-length curves in humans and rhesus macaques. Red, human length-tension curve; gray, macaque length-tension curve. Curves are calculated from myofibril lengths reported in Walker and Schrodt 1974 and Winters et al. 2011 and equations in Gordon et al. 1966.

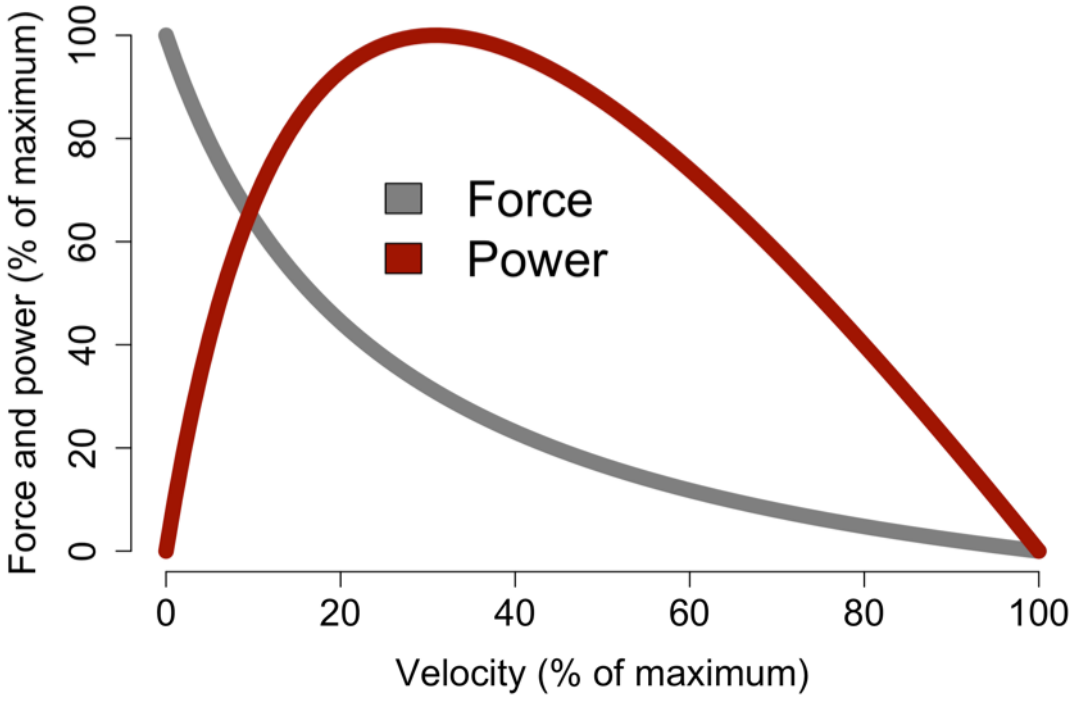

Figure 2.2: Force-velocity and power-velocity curve. Red, power-velocity curve; gray, force-velocity curve. Curves are calculated using a Hill-type model (Hill 1938; Zatsiorsky and Prilutsky 2012).

Muscle architecture (fiber pennation, fiber length, and tendon morphology) determines how these forces are combined and transformed at the whole muscle level (Gans and Bock 1965; Anapol and Barry 1996). At a whole-muscle lever, muscle force correlates with the number of sarcomeres in parallel (i.e., the cross-sectional area of muscle fibers) while muscle velocity correlates with the number of sarcomeres in series (i.e., the length of the muscle fibers). The cross-sectional area of muscle is frequently adjusted by fiber length and orientation, given that some muscles have shorter fibers oriented at an oblique angle to the long axis of the muscle, giving them a feather-like, or pennate, appearance. This physiological cross-sectional (PCSA) strongly correlates with maximum isometric muscle force (Powell et al. 1984) while fiber length, when normalized by sarcomere length, accurately predicts the range of motion over which the muscle can actively produce isometric force (Felder et al. 2005; Winters et al. 2011). For a given volume of whole skeletal muscle, architecture can vary along a spectrum favoring high velocity on one end and high force on the other (Gans and Bock 1965; Gans 1982; Gans and de Vree 1987). Long fibers arranged in parallel to the muscle's line of action place more sarcomeres in series and therefore combine larger displacements and shortening velocities with lower but more consistent force over a wider range of whole muscle length. In contrast, short fibers arranged at an angle to the line of action (i.e., pennate fibers) place more sarcomeres in parallel and consequently produce higher force over a more limited range of whole muscle length than parallel-fibered muscles.

Muscle attachment site location also impacts force-velocity tradeoffs. Mechanical advantage—the ratio of the muscle's moment arm from the center of rotation to that of the output and/or reaction forces—determines how the magnitude and direction of muscle force vectors change as bones move into different postures among individual movements, organismal designs,

or body sizes (Smith and Savage 1956; Smith and Savage 1959; Stern 1974; Biewener 1989; Lieber and Fridén 2000; German et al. 2011). Variation in attachment location relative to the center of rotation, i.e., in-lever length, not only affects output forces but also the magnitude of muscle displacement: longer in-levers require greater changes in muscle length for a given amount of joint rotation (Herring and Herring 1974; Lieber et al. 1997). Therefore, while joint moment increases with a longer in-lever, such gains come at the cost of a more limited range of joint motion over which the muscle can actively produce force.

These aspects of vertebrate musculoskeletal morphology impact functional system design in a variety of species. In the mammalian feeding system, the fundamental tradeoff between muscle force and displacement manifests as a tradeoff between bite force and gape (Herring and Herring 1974; Taylor and Vinyard 2004; Eng et al. 2009; Taylor et al. 2009; Perry et al. 2011; Hartstone-Rose et al. 2012; Hylander 2013; Taylor and Vinyard 2013). In the fish feeding system, variation in relative lengths of input and output lever arms maps onto variation in the relative importance of suction feeding (which requires high muscle shortening velocities) and biting (Westneat 2004). Elegant linkages in the jaws of teleost fish and birds further elaborate on the basic design of skeletal levers to amplify displacement, velocity, and joint moment (Westneat 1990; Westneat 2003; A. M. Olsen and Westneat 2016).

While some vertebrates show morphological specialization to optimize force or velocity, tradeoffs can also be negotiated by a medley of more generalized morphologies. To summarize the morphological contributions to muscle function described above, force and velocity can be affected by three different morphological parameters independent of fiber type: 1) the number of sarcomeres in a fiber, 2) muscle architecture, and 3) moment arm length (Lieber and Ward 2011; Kandel et al. 2012). Because multiple components can interact to produce different amounts of

force and velocity, musculoskeletal design is redundant, that is, different forms can function similarly (Lauder 1990; Lauder 1995; Wainwright et al. 2005). Therefore, understanding how muscle morphology relates to performance necessarily involves not only analysis of the muscle itself but its moment arm to determine how the two interact to produce output force and displacement. For example, a muscle producing less force inserting further away from an axis of rotation may produce a greater joint moment than a muscle producing more force but inserting closer to the axis of rotation due to the former's larger moment arm, e.g., the human tensor fascia latae versus the more massive gluteus maximus (Hoy et al. 1990; Lieber 2009). In contrast, a muscle with long fibers may have a smaller moment arm than a muscle with a similar line of action but with short fibers, as with the human extensor carpi radialis longus and brevis, respectively (Lieber et al. 1990; Lieber et al. 1997). Long moment arms are not necessarily accompanied by long fibers and vice versa (Maganaris et al. 2006), which limits the functional inferences that can be made from either muscular or skeletal morphology alone.

Additionally, many muscles themselves are redundant because joints frequently have more than one muscle capable of producing movement with a given degree of freedom. In humans, an average of 2.6 muscles controls each degree of freedom (Prilutsky and Zatsiorsky 2002), and examples of highly redundant movements include jaw elevation, knee extension, and ankle plantarflexion. Mechanical redundancy presents a motor control problem for the brain given the unlimited number of potential kinetic and kinematic solutions (Bernstein 1967; Zatsiorsky and Prilutsky 2012). However, redundancy may also offer a solution to a separate problem presented by the tradeoffs of muscle function: controlling force over a wide range of motion and velocities while decreasing overall muscle mass and its attendant maintenance costs (Lieber and Fridén 2000). Synergists—muscles capable of producing movement in the same

degree of freedom—often vary not only in architecture and moment arm length but also in fiber types (i.e., slow-twitch vs fast-twitch) that can either exacerbate or mitigate functional tradeoffs among the synergists (Spector et al. 1980; Wakeling et al. 2006; Wakeling et al. 2011; Rupert et al. 2015).

While many studies have highlighted how muscle architecture and mechanical advantage relate to performance tradeoffs, functional specialization for force or displacement/velocity is not a universal phenomenon among skeletal muscles. Muscles can produce both higher force and higher excursion and velocity through increased muscle mass (Organ et al. 2009; Taylor and Vinyard 2009; Terhune et al. 2015), although such increases may be accompanied by a decrease in moment arm length that limits potential gains in output force (Terhune et al. 2015). The presence of a "supermuscle" (*sensu* Lieber and Fridén 2000) rather than separate, specialized synergists may have specific functional implications that warrant further investigation.

In contrast to lever-based musculoskeletal structures, the geometric arrangement of hyolingual muscles has received comparatively little attention, particularly using experimental approaches. Compared to many limb muscles and the muscles of mastication, most primate hyolingual muscles have simple, fusiform architecture individually (Howell and Straus 1933; Pearson et al. 2011). However, because the primate hyoid is a floating bone and is therefore unconstrained by joint surfaces, the entire hyolingual apparatus could be conceptualized and studied as extremely complex pennate muscle capable of generating force along multiple axes. Such an approach has demonstrated that geniohyoid and mylohyoid are capable of generating the largest anteriorly and superiorly directed forces, respectively, but consideration of force alone does little to inform how the hyoid is actually moved by these muscles (Pearson et al. 2011;

German et al. 2011). The benefits of approaching the hyolingual apparatus as a complexly pennate muscle are discussed below and demonstrated in Chapters 5 and 6.

This section on the morphological parameters of muscle function concludes with a caveat. As noted by Taylor and Vinyard (2004), caution should be exercised when testing evolutionary hypotheses regarding musculoskeletal functional morphology with "natural experiments" among different species because muscle architecture is plastic and therefore not necessarily a direct product of a heritable genotype. First, muscles do not exhibit uniform responses to increased high force exercise: rabbit feeding musculature increases PCSA through gains in mass while fiber length and pennation remain constant (Taylor et al. 2006), whereas mouse forelimb muscles exhibited variable gains in mass while consistently increasing PCSA and decreasing fiber length (Rabey et al. 2015). Second, fiber length increases in response to increasing resting length, moment arm, eccentric loading behaviors, and high velocity exercise (Williams and Goldspink 1973; Koh and Herzog 1998; Butterfield et al. 2005; Rabey et al. 2015). Recent experimental evidence suggests that bony attachment site morphology is not responsive to changes in loading conditions over the course of several weeks (Zumwalt 2006; Rabey et al. 2015), and therefore one can assume that mechanical advantage is not plastic. In light of the evidence for muscle plasticity, physiological adaptation needs to be accounted for when making claims that a muscle's morphology is a product of adaptation by natural selection. Indeed, muscle plasticity likely plays a significant role in the evolution of musculoskeletal design. By altering force, range of motion and velocity, or both through changes in fiber morphology in response to organismal behavior, muscle plasticity can create the conditions in which natural selection may favor a different, less plastic mechanical advantage as new behaviors emerge (Anapol and Barry 1996).

Physiological Parameters

Morphological studies are necessary but not sufficient for studying musculoskeletal function because the nervous system can activate muscles to variable degrees and under various physiological conditions. The flexibility of the nervous system, termed the neurological "wildcard" by Lauder (1995), highlights the need for *in vivo* validation to establish that a given morphology consistently aligns with a given function. While *in vivo* studies are ideal, more controlled *in situ* and *in vitro* experiments serve a vital role in guiding *in vivo* research by highlighting the physiological principles that determine how the timing and magnitude of central nervous system output affects muscle force and velocity. This section is not a comprehensive review of the physiological determinants of function; rather, it focuses on how the timing of fiber activation relative to whole muscle length change and its associated proprioceptive feedback allows the nervous system to affect, and even amplify, musculoskeletal output to mitigate the tradeoffs and constraints between force and velocity. Specifically, I discuss the benefits of active muscle stretch—eccentric activation—and mechanisms that decouple fiber and whole muscle length.

Eccentric activity is commonly conceived as detrimental to performance due to its capacity to induce muscle damage under novel exercise conditions (Lieber et al. 1991; Lieber and Fridén 1993; Clarkson and Hubal 2002). However, controlled eccentric activity immediately prior to shortening, termed a stretch-shortening cycle (SSC) or countermovement, increases shortening force (Abbott and Aubert 1952; Cavagna et al. 1968; Cavagna and Citterio 1974; Gregor et al. 1988; Finni et al. 2000). An abundance of evidence suggests that elastic energy storage in tendons and titin—a large, calcium-dependent, spring-like protein spanning half of the sarcomere—underlies the enhanced and increased metabolic efficiency of force production

during SSCs and may actually protect the sarcomeres from damage during whole muscle stretch (Edman et al. 1978; Roberts et al. 1997; Biewener et al. 1998; Joumaa et al. 2008; Leonard et al. 2010a,b; Nishikawa et al. 2012; Joumaa and Herzog 2013; Azizi and Roberts 2014; Holt et al. 2014; Konow et al. 2015; Monroy et al. 2016; Powers et al. 2016; Pace et al. 2017). Indeed, Herzog et al. (2015; 2016) argue that titin should be considered a third myofilament alongside actin and myosin due to its substantial contributions to force production during active lengthening. Muscles of variable architecture exhibit SSCs during cyclic behaviors *in vivo* (Biewener 1998; Altringham and Ellerby 1999; Nelson and Jayne 2001; Soman et al.2005; Higham et al. 2008; Aiello et al. 2013), suggesting that SSCs may be a common mechanism of enhancing force production (Biewener 1998). Although titin offers a promising mechanistic explanation for increased performance associated with SSCs, the ultimate cause of enhanced power *in vivo* is still contested (Van Hooren and Zolotarjova 2017).

Muscle stretch may also facilitate performance due to changes in the length-tension curve associated with submaximal activation. Architecture-based arguments assume that the force-length relationship is independent of muscle activation level; however, *in situ* and *in vitro* studies show that optimal length increases as activation level decreases (Rack and Westbury 1969; Roszek et al. 1994; Holt and Azizi 2014; but see de Brito Fontana and Herzog 2016 for conflicting *in vivo* data). The effect of activation level on *in vivo* muscle force and velocity is poorly understood and may contribute to the difficulty of accurately modeling submaximal force production *in silico* (Perreault et al. 2003; Wakeling et al. 2012; Lee et al. 2013; Millard et al. 2013; Dick et al. 2017).

To relate submaximal activation to morphology and SSCs, the ability to stretch a muscle prior to shortening should improve performance because optimal length is longer during

submaximal activation. Similarly, the inability to stretch a submaximally activated muscle imposes a constraint that leads to suboptimal performance under certain circumstances. In the cane toad, a crouched posture and flexed knees prior to hopping does not allow the primary ankle plantarflexor, plantaris, to reach its optimal length for submaximal activation (Holt and Azizi 2016). Although it shortens at a velocity that optimizes power for the force that it does produce, plantaris nonetheless does not function optimally during submaximally active hops due to a morphological constraint: the inability to further stretch the muscle when the hindlimb is in its fully flexed position prior to the hop (Holt and Azizi 2016). Although the cane toad is not able to capitalize on stretch-shortening cycles to enhance force or velocity during hopping, other species of anurans utilize a separate method to enhance muscle power: tendon elasticity returns energy faster than it is stored to amplify power (Roberts et al. 2011; Astley and Roberts 2012; Astley and Roberts 2014). Elastic recoil also underlies ballistic tongue projection in salamanders and chameleons, another system in which countermovement prior to shortening is limited (Deban et al. 2007; Anderson and Deban 2010; Anderson 2016).

Tendon elasticity is one of two mechanisms bypassing architectural tradeoffs by decoupling fiber kinematics from whole muscle kinematics. While *in vitro* studies suggest that active whole muscle length-tension relationships can be modeled as scaled sarcomeres during isometric contraction regardless of architecture (Winters et al. 2011), such modeling does not account for the fact that in *in vivo* dynamic conditions fiber length can be decoupled from whole muscle length. Decoupling mechanisms include fiber rotation in pennate muscles and the aforementioned elastic tissue strain in muscles with internal or external tendons.

In vitro studies have demonstrated that increased fiber rotation leads to increases in the ratio of muscle belly velocity to fiber velocity (architectural gear ratio, AGR), and this ratio

increases with fiber pennation angle (Brainerd and Azizi 2005). A muscle's AGR is not fixed during either shortening or lengthening but rather is dependent on loading conditions and connective tissue properties (Azizi et al. 2008; Azizi and Roberts 2014; Holt et al. 2016), violating a fundamental assumption of architectural predictions of the effective range of motion in pennate muscles (Zajac 1989). However, fiber rotation offers little benefit to muscle power because muscle velocity increases at the expense of force.

In contrast, decoupling fiber length from whole muscle length through tendon strain can greatly amplify whole muscle power. Because tendons can return stored energy more quickly than the duration of the initial stretch, muscles with pennate architecture and long tendons may produce higher velocity and higher-powered movements than would be expected from their fiber architecture alone (Roberts et al. 1997; Aerts 1998; H. 2005; Soman et al. 2005; Deban et al. 2007; Anderson and Deban 2010; Astley and Roberts 2012; Astley and Roberts 2014; Sawicki et al. 2015; Roberts 2016). Moreover, estimates of fiber length from whole muscle length must assume that tendons are stiff; consequently, contributions of internal and external tendon strain are ignored, potentially neglecting significant contributions of elastic energy storage to performance or protecting sarcomeres from excessive stretch (Zajac 1989; Soman et al. 2005; Lieber 2009; Konow et al. 2015; Roberts 2016). Therefore, the morphology of the muscle fibers should be considered in tandem with the internal and external tendon morphology in functional arguments (Anapol and Barry 1996; Biewener 1998; Anapol and Gray 2003).

Whether either of these decoupling mechanisms are employed in the hyolingual apparatus is currently unknown. As discussed above, the hyolingual apparatus can be approached as a complexly pennate muscle, and gear ratios can be used to quantitatively determine whether suprahyoid muscle rotation amplifies hyoid kinematics. Because hyolingual muscles lack long

external tendons connecting them to bone, the force-enhancing properties of eccentric activity prior to shortening may be particularly important for swallowing performance if these muscles do indeed rotate and consequently produce less force along the hyoid's axis of movement. Chapter 5 examines whether gearing affects hyoid kinematics and whether such stretch-shortening cycles are utilized. Although the macaque hyoid is not suspended from the digastric tendon as it is in humans (Howell and Straus 1933; Standring 2015), the digastric tendon is the sole long, external tendon of the hyolingual apparatus. Therefore, tendon stretch and its relationship to digastric belly length and rotation are also examined. Moreover, because fiber geometry affects how much velocity is amplified by fiber rotation (Brainerd and Azizi 2005), Chapter 6 investigates whether changes in hyolingual posture affect hyoid kinematics.

Brief mention is warranted of other important morphological and physiological processes that affect muscle function but are beyond the scope of this review. Body size introduces another level of complexity to musculoskeletal functional morphology due to the negative allometry of force production to mass (e.g., Biewener 1989; Biewener 1990). The effects of scaling extend to not only the duration of vertebrate locomotor and feeding cycles—and therefore potentially to the relative velocity of muscle fibers—but also the timing of muscle activation in appendages large enough to utilize momentum for movement (Pennycuick 1975; Pontzer 2007; Hooper et al. 2009; Ross et al. 2009; Gintof et al. 2010; Hooper 2012; Ross et al. 2017). Cycle duration, musculoskeletal design, and the spring-like properties of muscle-tendon units may also function to reduce energy expenditure and fatigue (Taylor 1985; Cavagna et al. 1997; Marsh et al. 2004; Raichlen 2004; Modica and Kram 2005; Hunter and Smith 2007; Pontzer 2007; de Ruiter et al. 2013; Kilbourne and Hoffman 2013; Kilbourn and Hoffman 2015), and some organisms may be optimized for submaximal activations and endurance at longer fiber lengths rather than maximal

activations and power at “optimal” fiber lengths. Lastly, I have focused exclusively on motor output; however, sensory input (e.g., proprioception) is equally important for the performance of musculoskeletal structures (Dickinson et al. 2000; Nishikawa et al. 2007). Elements of biomechanical design correlate with sensory function and the morphology of peripheral sensory receptors, and integrating evidence of sensory “tuning” to a given function may be instrumental in supporting or falsifying functional hypotheses (Aiello et al. 2017). For example, the sensitivity of stretch-sensing spindle fibers may be higher in hyolingual muscles with smaller ranges of motion than those which stretch or shorten more.

INTEGRATIVE APPROACHES

Morphological and physiological studies have been instrumental to the advancement of our understanding of muscle function. However, for the reasons discussed above, morphology does not have a one-to-one correspondence with function, and the tightly controlled conditions of laboratory experiments are not necessarily reflective of how muscles are used during natural behavior (Gregor et al. 1988). Therefore, the strongest evidence to support or falsify adaptive hypotheses of musculoskeletal function derives from *in vivo* experimental studies (Lauder 1996; Ross et al. 2002). Although *in silico* modeling offers a promising alternative to costlier *in vivo* experiments, these models struggle to produce accurate results under dynamic, submaximal conditions (Perreault et al. 2003; Wakeling et al. 2012; Lee et al. 2013; Millard et al. 2013; Dick et al. 2017). *In silico* model parameters are commonly based on static length-tension curves and force-velocity curves derived from isometric and isotonic activity (Zajac 1989). However, submaximally active muscles have longer optimal fiber lengths (Rack and Westbury 1969; Roszek et al. 1994; Holt and Azizi 2014; Holt and Azizi 2016), and submaximal stretch-

shortening cycles allow organisms to produce forces greater than that predicted by a supramaximally stimulated isotonic force-velocity curve (Gregor et al. 1988). Thus, determining how morphology and physiology interact through *in vivo* study of natural behavior is necessary to improve our ability to both accurately model and understand muscle function. Specifically, whether and how variation in fiber type, activity patterns, history-dependence (e.g., SSCs), and decoupling mechanisms contribute to the difficulties of modeling muscle force is poorly understood. This section discusses additional dynamic processes that could underlie modeling inaccuracies—including moment arm and axis of rotation dynamics, synergist interactions, and muscle morphological heterogeneity—and methodological approaches that may resolve these issues by integrating morphological and physiological lines of evidence.

Dynamic interactions between morphology and physiology

Although a muscle's moment arm is primarily dependent on the distance of its attachment points from the center of rotation, mechanical advantage is also dependent on skeletal posture and the center of rotation (Biewener 1989; Herzog and Read 1993; Loren et al. 1996; Gonzalez et al. 1997; Kargo and Rome 2002; Iriarte-Diaz et al. 2017). Additionally, because organisms adopt different postures for different behaviors, e.g., human walking vs running, a given muscle's mechanical advantage can be dynamic not only within behaviors but among them as well (Biewener et al. 2004), which may contribute to changes in muscle function with changes in gait (Gregor et al. 1988; Arnold et al. 2013). Dynamic models of a variety of vertebrates have been useful in understanding how joint moments vary due to both moment arm length and fiber length (Kargo and Rome 2002; Hutchinson et al. 2005; Hutchinson et al. 2015; Charles et al. 2016a; Charles et al. 2016b) and highlight how 3D approaches are necessary for measuring joint

moments accurately when movements are complex, as in linkage systems (Olsen and Westneat 2016). Interactions between moment arm length, muscle length, and posture may be particularly important when considering the function of biarticular muscles.

However, a fundamental assumption in these *in silico* models is the location of the joint axis of rotation, which affects the length of a muscle's moment arm and therefore how much a muscle strains during a given behavior. In the feeding systems of many mammalian species the mandibular condyle translates anteroposterior during jaw opening and closing, meaning that the axis of rotation is located inferior to the temporomandibular joint (Wall 1999; Keefe et al. 2008; Terhune et al. 2011; Ross et al. 2012; Menegaz et al. 2015). Translation of the mandibular condyle during jaw opening and closing ameliorates the force-length tradeoff in the highly pennate masseter muscle by taking advantage of the longer fibered temporalis (Weijs et al. 1989; Iriarte-Diaz et al. 2017). In light of these *in vivo* data, accounting for the active (i.e., myofibrils) and passive (e.g., connective tissues) contributions to the location of the center of rotation is important to the accuracy of both moment arm and fiber length computations *in silico*.

As mentioned previously, specialization of synergists can facilitate the production of consistent force over a wide range of motions or velocities while decreasing overall muscle mass. In the case of the mandibular axis of rotation, joint kinematics allow the muscles of mastication to optimize force production within the constraints of their length-tension curves (Iriarte-Diaz et al. 2017). However, counterintuitive to the term 'synergist', high performance in one synergist may come at the expense of performance in the other. For example, the short, highly pennate, and predominantly slow-twitch fibers of the human soleus suggest that this muscle functions optimally at lower velocities, whereas the heads of the gastrocnemius have longer, less pennate, and predominantly fast-twitch fibers (Edgerton et al. 1975; Ward et al.

2009). The shortening velocity of soleus fibers during high-speed behaviors can exceed that of the maximum velocity of slow twitch fibers, thus rendering the soleus mechanically sub-optimal or even incompetent at high speeds (Wakeling et al. 2006). Although early studies are promising, it is unclear whether accuracy of *in silico* models is improved by incorporating fiber type, which warrants further investigation (Lee et al. 2013; Dick et al. 2017).

Morphological and functional heterogeneity can also be found *within* muscles in the form of variable activation patterns, fiber lengths, pennation, and fiber types. Muscles with simple morphology can thus be functionally subdivided to achieve more complex movements (Aiello et al. 2014). In muscles with regional disparity in fiber-type distribution, the orderly recruitment of smaller, slow-twitch fibers prior to larger, fast-twitch fibers in both locomotor and feeding musculature (Henneman et al. 1965; Milner-Brown et al. 1973; Goldberg and Derfler 1977; Yemm 1977; Clark et al. 1978; Mendell 2005; Ross et al. 2007; Ross et al. 2010) probably results in portions of muscles with different lengths, maximum velocities, forces, and moment arm lengths becoming active prior to others (Higham and Biewener 2011). As mentioned previously, high velocities produced by fast fibers may subsequently render the slow fibers mechanically incompetent at high activation levels, thus reducing force and power further beyond the losses incurred from the force-velocity relationship. Higham and Biewener (2011) offer a testable hypothesis that more homogenous muscles are more specialized in function while more heterogeneous muscles function similarly to specialized synergists by improving both motor control over a joint and mechanical performance over a wider range of postures and behaviors. Overall, morphological heterogeneity raises important questions about the definition of a muscle from a functional perspective and whether the central nervous system controls

different sections of a muscle independently or if peripheral specialization simplifies motor control while increasing functional complexity (Zatsiorsky and Prilutsky 2012).

Capturing muscle kinematics and kinetics

To determine how the various morphological and physiological parameters of musculoskeletal performance interact, one needs to relate muscle fiber activity to three-dimensional kinematics and kinetics of fibers (ideally from multiple regions of the same muscle), whole muscle-tendon units, and the skeleton (German et al. 2011). All of these kinematic variables can be measured simultaneously using the high-resolution methods discussed below. However, accurate measures and predictions of *in vivo* fiber and muscle kinetics remain elusive for certain kinds of muscles. Although the kinetics of muscles with long tendons can be obtained using buckle tendon force transducers (Barnes and Pinder 1974; Biewener 1992), fiber optic sensors (Finni et al. 1998), or tendon strain measurements (Dick et al. 2016), such methods cannot be applied to muscles with short or internal tendons. Strain gauges implanted on bone or near sites of bone attachment have been used to study the force production of muscles with short or no external tendons, such as the primate jaw elevators (e.g., Hylander and Crompton 1986; Hylander et al. 1987; Hylander and Johnson 1989; Hylander and Johnson 1993; Ross et al. 2007), avian pectoralis (Biewener et al. 1998; Soman et al. 2005), and testudine hindlimb musculature (Aiello et al. 2013). However, strain gauges cannot measure an individual muscle's force in isolation because their measurements are affected by activity in other muscles that attach to the same bone as well as joint and bite reaction forces. A recently developed probe capable of measuring thousands of sarcomeres *in vivo* (Young et al. 2017) offers a promising alternative to mechanical transducers and may help resolve the problems of modeling single muscle force from

sarcomere length during non-isometric and submaximal activity. However, multiple such probes will be necessary given that fiber and sarcomere strain are heterogeneous throughout the muscle (Ahn et al. 2003; Konow et al. 2010; Wentzel et al. 2011; Holman et al. 2012; Moo et al. 2016; O'Connor et al. 2016).

Muscle kinetics are frequently integrated with synchronized recordings of skeletal kinematics from high-speed cameras and kinetics from implants or external sensors. Systems such as Vicon (Vicon Motion Systems, Oxford UK) permit the study of rigid body kinematics, joint kinematics, instantaneous axis of rotation (which influences dynamic torque), and whole muscle length change (Reed and Ross 2010; Ross et al. 2012; Ross and Iriarte-Diaz 2014; Takahashi et al. 2017; Iriarte-Diaz et al. 2017). Although light-based motion capture technology can generate large data sets of multiple skeletal segments and allow assessment of the distribution of kinematic variance across species, individuals, and behaviors (Iriarte-Diaz et al. 2012; Ross et al. 2012; Iriarte-Diaz et al. 2017), it cannot provide data on internal kinematics of soft tissues such as individual fibers or structures obscured by skin (e.g., oropharyngeal structures). To measure these obscured-yet-essential kinematics, light-based motion capture must be combined with additional methods, such as invasive sonomicrometry (e.g., Roberts et al. 1997; Biewener et al. 1998; Konow et al. 2012), noninvasive ultrasound (e.g., Dick et al. 2016; Dick et al. 2017), or, the focus of this paper, biplanar x-ray imaging.

New approaches to functional morphology and biomechanics

In the last decade two technologies have been developed that hold particular promise for advancing integrative studies in functional morphology of musculoskeletal systems: diffusible

iodine-based contrast-enhanced computed tomography (diceCT) (Gignac et al. 2016; Metscher 2009) and X-ray Reconstruction of Moving Morphology (XROMM) (Brainerd et al. 2010).

DiceCT and other non-iodine staining methods make it possible to take morphological measurements of soft-tissue morphology using non-destructive methods and with unprecedented spatial resolution. Not only does diceCT have the potential to improve our ability to measure musculo-tendon morphology, but it also enables data collection from museum specimens that were previously inaccessible to destructive techniques. Applications of diceCT and other staining methods include the digital dissection of muscles too small or complex for traditional dissection (Metscher 2009; Jeffery et al. 2011; Cox and Jeffery 2011; Holliday et al. 2013; Cox and Faulkes 2014; Porro and Richards 2017), determining muscle orientation in models of bite force (Gignac and Erickson 2017; Sellers et al. 2017), reconstructing three-dimensional muscle architecture (Kupczik et al. 2015; Dickinson et al. 2018), and improving the accuracy of inverse dynamic modeling of joint moments (Charles et al. 2016a,b). One of diceCT's key strengths in muscle functional morphology is its potential to measure muscle architecture *in situ*, which may generate more accurate measures of joint moment if architecture varies along the length of the muscle's attachment site. Meanwhile, methods of digitally determining muscle architecture are promising and continue to improve (Kupczik et al. 2015; Dickinson et al. 2018).

X-ray Reconstruction of Moving Morphology (XROMM, Brainerd et al. 2010) and its corollary fluoromicrometry (FMM, Camp et al. 2016) capture internal musculoskeletal kinematics with high spatiotemporal resolution and can be integrated with workflows to estimate force output by individual muscles. XROMM measures the 3D rotation and translation of rigid tissues such as bone whereas FMM measures the 3D deformation of soft tissues. Studies using XROMM and FMM have made significant progress in the field of muscle functional

morphology, demonstrating that suction feeding in largemouth bass is powered primarily by axial rather than cranial musculature (Camp and Brainerd 2014; Camp et al. 2015; Camp and Brainerd 2015), the length-tension curve constrains the performance of structures that lack joints and the benefits of mechanical advantage, as in carp pharyngeal jaws (N. J. Gidmark et al. 2013), and tendon elasticity decouples fiber and joint kinematics to power frog hopping through a catapult-like mechanism (Astley and Roberts 2012; Astley and Roberts 2014).

Combining diceCT, XROMM, and EMG

Together, diceCT and XROMM promise to increase the depth of knowledge about musculoskeletal design in unprecedented ways. Given the many determinants of function discussed above, methods that discern how individual fibers and muscles each contribute to a given movement are necessary to fully understand how muscles function with the skeleton to produce force and movement. The remainder of this article describes how incorporation of diceCT into the XROMM workflow can enhance the study of muscle kinematics, particularly in musculoskeletal systems that are difficult to access for surgical implantation of muscle markers.

Previous studies have integrated XROMM and kinetic or EMG measurements in a limited number of muscles to relate muscle behavior to skeletal outputs by implanting individual muscles with tantalum beads or by reconstructing their attachments on bone from osteological landmarks (Astley and Roberts 2012; Gidmark and Konow 2013; Camp et al. 2015; Konow et al. 2015). In Chapter 3, I demonstrate how diceCT can be incorporated into XROMM and EMG workflows to study over a dozen muscles, many of which are difficult to access surgically for FMM. Moreover, because *in silico* studies have demonstrated that measures of joint moment are sensitive to the accuracy of muscle attachment site location (Hutchinson et al. 2015; Charles et

al. 2016b), I demonstrate the sensitivity of XROMM-based muscle kinematics to variation in attachment site location. I also demonstrate that these methods are precise enough to measure *in vivo* muscle fiber linear and angular velocity in my model system, the hyolingual apparatus of the rhesus macaque (*Macaca mulatta*).

The benefits of integrating XROMM, diceCT, and EMG are especially salient for investigations of vertebrate feeding systems. Jaw and hyolingual musculature are redundant, have variable architecture and, in many species, execute their functional promiscuity within the limited space sampled by the capture volume of XROMM. Moreover, the complex, three-dimensional orientations of feeding system muscles, as well as the three-dimensional movements and shape changes of the hyolingual apparatus (Kier and Smith 1985; Pearson et al. 2011; German et al. 2011) are obscured by the tissues of the head and neck. Therefore, skeletal, lingual, and muscle kinematics can currently only be studied simultaneously and with high spatiotemporal resolution using these radiography-based techniques, which have been successfully applied to feeding in several vertebrate species (Gidmark et al. 2013; Camp and Brainerd 2014; Gidmark et al. 2014; Camp and Brainerd 2015; Camp et al. 2015; Gidmark et al. 2015; Menegaz et al. 2015). Thus, the field of vertebrate feeding functional morphology stands to reap significant benefits from XROMM, FMM, diceCT, EMG, and their integration.

CHAPTER THREE: MATERIALS & METHODS

The *in vivo* workflow described below integrates existing data acquisition workflows to simultaneously measure 3D mandibular and hyolingual kinematics with individual hyolingual muscle kinematics and activity. Specifically, the method integrates X-ray Reconstruction of Moving Morphology (XROMM. Brainerd et al. 2010) with diffusible iodine-based contrast enhanced computed tomography (diceCT, Metscher 2009; Gignac et al. 2016) and chronic fine-wire electromyography (EMG, Loeb and Gans 1986). Here the method of integration is described, and results of accuracy and precision studies are presented to demonstrate the method's utility for studying hyolingual biomechanics. This method is used to acquire and process all *in vivo* data used in this dissertation. Chapter-specific analyses are included in separate sections.

The computational model is developed in R and predicts hyolingual range of motion from muscle morphology and length change. Specifically, these *in silico* experiments examine the biomechanical consequences of changes in muscle morphology that are based on changes observed in the human fossil record, comparative anatomy, and human ontogenetic changes. The model constrains maximum and minimum muscle length based the limits of muscle length change observed *in vivo*. This model is used in pursuit of the fourth aim.

INTEGRATING XROMM, DICECT, AND EMG

The marker-based XROMM workflow actually involves two data collection workflows (Brainerd et al. 2010); integration of XROMM with diceCT adds a third (Figure 3.1).

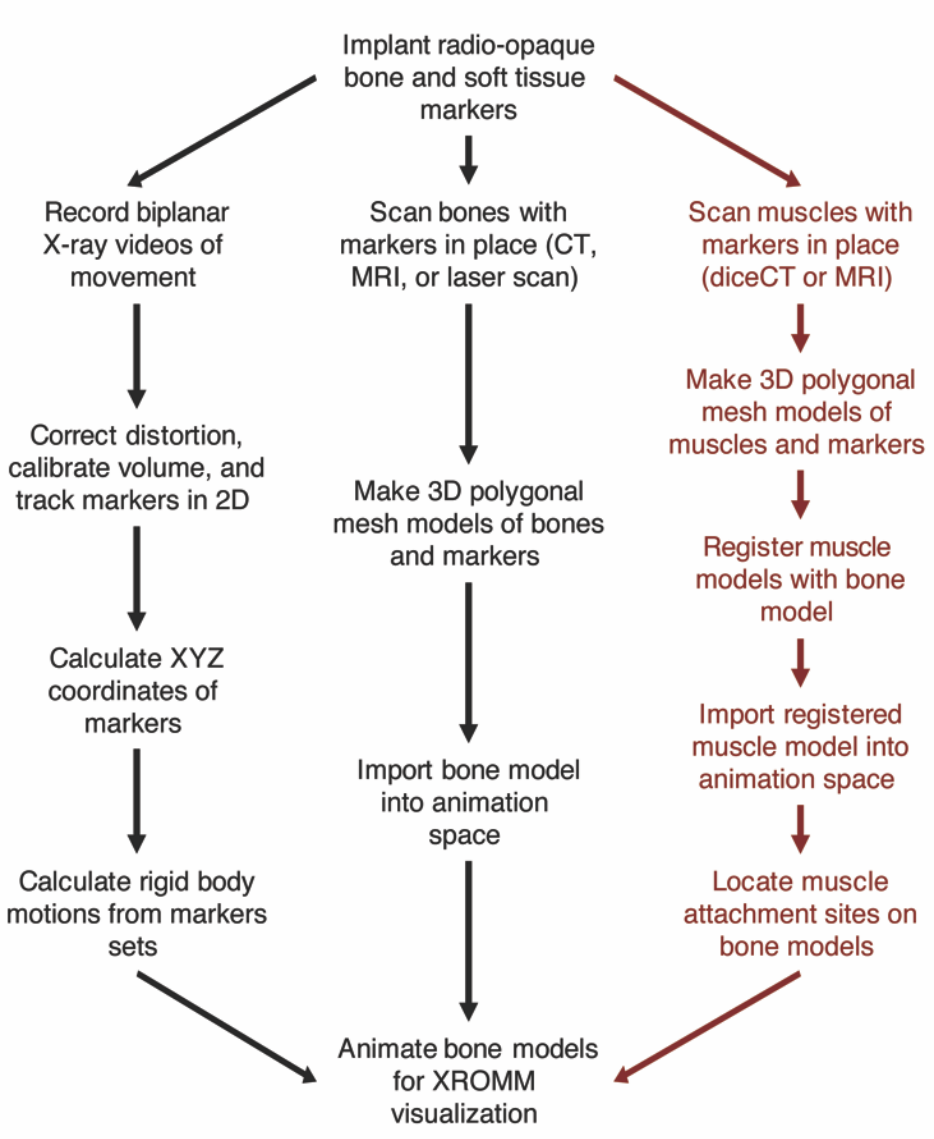

Figure 3.1: XROMM-diceCT workflow. The described method integrates XROMM (black, Brainerd et al. 2010) and diceCT (red, Gignac et al. 2016; Orsbon et al. 2018) workflows to determine the relationships among muscle, bone, and implanted markers. Figure modified from Brainerd et al. 2010 and reproduced from Orsbon et al. 2018.

Animal subjects

Four adult rhesus macaques (*Macaca mulatta*) were used in this study. The monkeys had been used previously in neurophysiological experiments involving neural array implantation in orofacial motor and sensory cortex (Monkey He, female, age 8, 7.46 kg), limb areas of

sensorimotor cortex (Monkey Ki, female, age 12, 7.55 kg), parietal and premotor cortex (Monkey JB, male, age 16, 8.48 kg), and prefrontal cortex (Monkey Ch, male, age 9, 8.83 kg).

The methods described were a part of an IACUC-approved protocol at the University of Chicago. The animals were housed at an on-campus, AAALAC-accredited animal facility attended to daily by veterinary and husbandry staff. The animals were trained to feed while sitting in an XROMM-compatible, acrylic primate chair. The animals were trained to be transferred to and from their cages by a pole-and-collar system.

On non-training days, animals were fed monkey biscuits and given daily enrichment along with *ad libitum* access to water. On training days, the animals were sometimes food and water delayed until after data collection to encourage them to eat during the session.

Surgical implantation

The animals were implanted with 1.0 mm tantalum markers in the cranium, mandible, hyoid body, and orofacial soft tissues. The surgical approach builds on that described by previous XROMM studies of the mammalian feeding system (Brainerd et al. 2010; Menegaz et al. 2015). Implanted EMG fine-wire electrodes in hyolingual muscles were viable for up to seven months.

Tantalum beads were inserted into the cranium and mandible by making an incision in the skin, clearing away a small area of periosteum, and drilling a 1-2 mm deep hole into the bone with a hand drill and a 1.0 mm drill bit, and then press-fitting a tantalum bead into the hole. Tantalum beads were inserted into the hyoid by locating two exposed portions of bone at the inferior pole of the hyoid body and inserting markers in a similar manner as in the cranium and mandible. A third marker was placed in the midline of the hyoid body after dividing the

mylohyoid raphe and gently blunt dissecting the fibers of geniohyoid to visualize the midline of the bone. A marker was then inserted as stated above. Following marker insertion, the cut ends of the mylohyoid raphe were sutured back together using 4-0 absorbable suture. Markers were inserted into soft tissues using a 16-gauge angiocatheter in the following manner: a needle introduced the catheter, the needle was withdrawn, a marker was placed into the catheter, a spinal needle stylus was used to hold the marker in the tissue as the catheter was removed by drawing it backwards over the stylus, and finally the stylus was removed while applying pressure to the insertion site. If necessary to achieve hemostasis, or to prevent the marker from falling out, the incision was sutured closed using 4-0 Vicryl suture.

Figure 3.2 shows the constellation of implanted markers in the tongue for all four animals. Seven markers were implanted under the dorsal tongue surface. Four of these were implanted under the lateral dorsal tongue surface: bilaterally at the junction of the palatoglossal arch with the tongue and at the lateral border of the tongue, and halfway between the posterior-most circumvallate papillae and the tip of the tongue. Three were implanted in the midline dorsal tongue surface: one in the tip of the tongue, one between the posterior-most circumvallate papillae, and one halfway between these two. Two additional midline markers were more deeply implanted, about 10-20 mm deep to the dorsal surface: one at the posterior-most circumvallate papillae, and another at half way to the tip of the tongue. This overall constellation of markers approximates a pyramidal shape when the tongue is at rest.

A marker was also implanted in the tongue base (i.e., the lingual side of the vallecula) in each animal, however in Monkey He this marker was extruded during healing. Monkey Ki's posterior deep tongue marker was found to be immediately adjacent to the basihyoid so that its kinematics closely mirrored those of the hyoid.

Insulated, medical-grade stranded stainless steel fine-wire electrodes (Cooner Wire, Chatsworth CA) were implanted for EMG recordings. A 27-pin connector (Omnetics Connector Corporation, Minneapolis MN) was housed in a custom-built, percutaneous, titanium housing that was rigidly fixed to the cranium using bone screws. The EMG connector allowed for recording from 13 muscles using four differential amplifiers (Model 1700, AM Systems, Sequim WA), and the 27th wire remained implanted under the skin as a ground wire. The wires were tunneled subcutaneously to the submandibular area and 1-2 mm of insulation was stripped. Electrodes were implanted into the muscle using an 18- or 20-gauge needle and were stimulated through the connector intraoperatively to confirm their location (single stimulation, train rate = 1 Hz, train duration = 300 ms, stim rate = 250 pulses per second, delay = 0.01 ms, duration = 0.2 ms, voltage = 5-10 V, Grass S48 Stimulator, AstroNova, Inc., West Warwick RI).

The animals were given intramuscular buprenorphine for two days and cephalosporin antibiotics for five to seven days following the surgery. We waited two weeks prior to collecting data to allow healing and the formation of scar tissue around the markers that fixes them in place relative to the surrounding tissue.

These procedures have been replicated six times and, by fluoroscopically observing the animals swallowing contrast-enhanced liquids mixed with fruit juice (240 mg/ml iohexol and 60% w/v barium sulfate), we were able to find no evidence of chronic swallowing pathology as a result of these procedures.

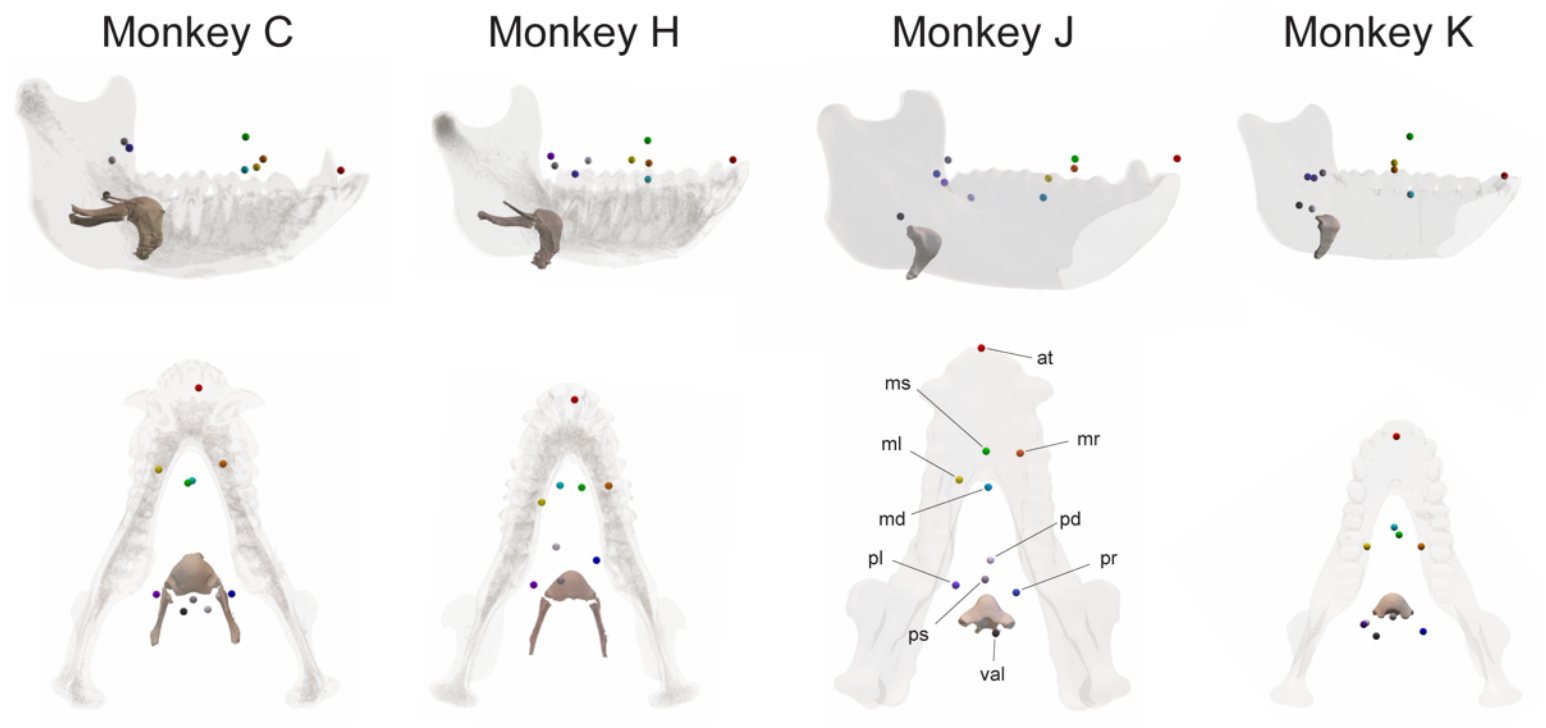

Figure 3.2: Tongue marker location in all four rhesus macaques. In addition to slight variation in marker implantation location, asymmetries are due to post-mortem deformation. Red, anterior tongue (at); orange, middle right (mr); yellow, middle left (ml); green, middle surface (ms); light blue, middle deep (md); dark blue, posterior right (pr); violet, posterior left (pl); gray, posterior surface (ps); white, posterior deep (pd); dark gray, vallecula

In vivo data collection and sacrifice

Kinematic and precision data presented here were collected in the University of Chicago's XROMM Facility (https://xromm.uchicago.edu/). This custom-designed facility features the high speed biplanar cineradiography equipment necessary for XROMM and FMM (Brainerd et al. 2010, Camp et al. 2016), differential amplifiers for EMG (AM Systems Model 1700) and a video processing unit (XCitex ProCapture VPU) that synchronizes the two data sources. Prior to data collection, the capture volume was spatially calibrated using undistortion grids and a calibration cube (Brainerd et al. 2010). The monkeys ate a variety of foods, including the red grapes with skin reported here, presented to them using tongs while they were seated in a primate chair situated in the XROMM capture volume. X-ray video data were collected at 90-100 kVp, 10-16 mA 200 Hz, and with a 2000-4000 ms shutter speed, balancing the need to minimize motion blur, data size, X-ray tube heat, and animal X-ray exposure. Electromyography data were amplified (gain: 100-10,000), bandpass filtered (high-pass: 1-10 Hz; low-pass: 1 kHz-5 kHz). Electromyography sampling rates were 2,000-10,000 Hz.

The animals were trained to transfer via pole-and-collar method from their home cage to a custom-designed polycarbonate primate chair that loosely restrained them by their necks. Two individuals (Monkey JB and Monkey Ki) frequently spun in the chair during data collection, making marker tracking throughout the entire sequence impossible for many markers and introducing motion artifacts to the EMG data. Therefore, the next two animals recruited for these experiments (Monkey Ch and Monkey He) were trained to feed while their heads were restrained via percutaneous head posts. In addition to facilitating marker tracking, head restraint reduced motion artifacts in the EMG data and, because fewer trials were needed to obtain useful data, reduced radiation exposure to the monkey and the experimenters.

Following a separate terminal experiment, the animals were perfused under deep anesthesia with 0.5 to 1.0 L of saline plus heparin sodium (10 IU/mL) followed by 1.0 to 2.0 L 10% formalin solution, infused under pressure through the left ventricular cannula, and sacrificed via exsanguination.

Generating XROMM bone models

After sacrifice, the head and neck were placed in a 20 L bath of 10% formalin solution for at least seven days to fix and decontaminate the tissue of zoonotic organisms. The stained and unstained carcasses were scanned in the PaleoCT at the University of Chicago, a General Electric Phoenix v|tome|x Microfocus CT (microCT) scanner. Scanning parameters for unstained and stained specimens can be found in Table 1. For each animal, tantalum markers and bone models were segmented to create polygonal mesh models using Amira 5.5.0 (FEI Company, Hillsboro OR) hosted on a visualization node of the Research Computing Center at the University of Chicago. Minimally smoothed outputs from Amira were used when locating landmarks for kinematic measurements. For 3D rendered figures, a shell was created using 3-matic Research v10.0 (Materialise, Leuven, Belgium). The shells were subsequently smoothed and metal implants and artifacts were removed using Autodesk ReMake 2016 (Autodesk, San Rafael CA).

DiceCT

After the precision experiment, the carcasses were placed in a 5 liter 20% weight/volume sucrose solution prewash to minimize tissue shrinkage during staining (Morhardt et al. 2016). Following the prewash the carcasses were placed in either a two liter (Monkey Ki) or three liter

(Monkey JB) 1.25% I_2 / 2.50% KI solution made by diluting a 5% I_2 / 10% KI stock solution with deionized water. Iodine binds with a higher affinity for skeletal muscle than its surrounding connective tissue and is thought to specifically stain the glycogen within muscle (Bock and Shear 1972; Lecker, Kumari, and Khan 1997; Gignac and Kley 2014). Short (five to ten minute) microCT scans were conducted every two to four weeks to evaluate staining progress. After at least two weeks in 1.25% I_2 / 2.50% KI solution, the carcasses were transferred to a 2% I_2 / 4% KI solution that was replenished every two to four weeks until staining of the center of the specimen was observed on the interval CT scans. After the iodine penetrated to the center of the specimen, the carcasses were placed in a deionized water bath for 2-4 days to even the contrast throughout the specimen before the final microCT scan.

Segmentation and registration

The diceCT data set was segmented using Amira 5.5.0. When segmenting, fascicles were defined as the high-density material (muscle fibers and endomysium) surrounded by lower density material (perimysium). Low-density tissues below a minimum gray-scale value threshold were excluded from the segmented volume. Because voxel width approximated the reported diameter of macaque styloglossus fibers (37.0-64.5 μm versus ca. 40-90 μm, respectively), no distinction could be made between fibers or between fibers and endomysium (Sokoloff et al. 2007). For the geniohyoid and posterior mylohyoid, the fascicles immediately adjacent to the bare ends of the EMG electrodes were segmented. For stylohyoid, palatoglossus, and the posterior digastric, the entire muscle was segmented. For hyoglossus, genioglossus, styloglossus, and anterior digastric, only the fascicles containing or most closely related to an implanted

marker were segmented. Additionally, the tantalum markers in the cranium, mandible, and hyoid were segmented for registration with the unstained bone model dataset.

When transforming the muscle models into the bone model coordinate systems, models of each bone's tantalum markers from each data set were registered using the AffineRegistration function in Amira. The unstained CT data set was set as the "Reference" and the stained CT data set was set as the "Model". The transformation matrix used to align the stained CT model with the unstained CT model was then applied to the stained CT muscle models, and the transformed muscle models were exported as .obj files. Because tissue deformation during iodine staining moved the hyoid and mandible relative to the cranium (Figure 3.3), separate models were made using bone-specific transformation matrices. Specifically, two models were generated for the posterior mylohyoid, geniohyoid, and stylohyoid. One model in the coordinate system of the bony attachment was created for each of the following muscles: styloglossus, hyoglossus, genioglossus, and anterior and posterior digastrics.

Tissue shrinkage has been observed in muscle following iodine staining (Vickerton et al. 2013) but to our knowledge the effects on bone morphology have not been quantified. The registered marker models were also exported as .obj files and imported into Autodesk Maya 2016 (Autodesk, San Rafael CA). The vAvg XROMM function of XROMM Maya Tools v2.1.8 was used to calculate their centroids. To quantify the error introduced by both skeletal tissue shrinkage and using either cranial or bone-specific registrations for muscle models, the mean inter-marker distance between homologous markers was calculated for each bone (Table 2). The average registration error of diceCT and unstained CT data sets using bone-specific transformation matrices was 0.08 mm (Table 3.1). These results indicate that the iodine staining protocol did not result in significant bone shrinkage. In contrast, staining deformed the sort

tissues and moved the bones relative to one another; as a result, applying the cranial registration transformation matrix to the mandible and the hyoid introduced an average alignment error of 2.15 mm. Therefore, applying bone-specific transformation matrices is more accurate than applying a single transformation matrix to all bones and muscle models.

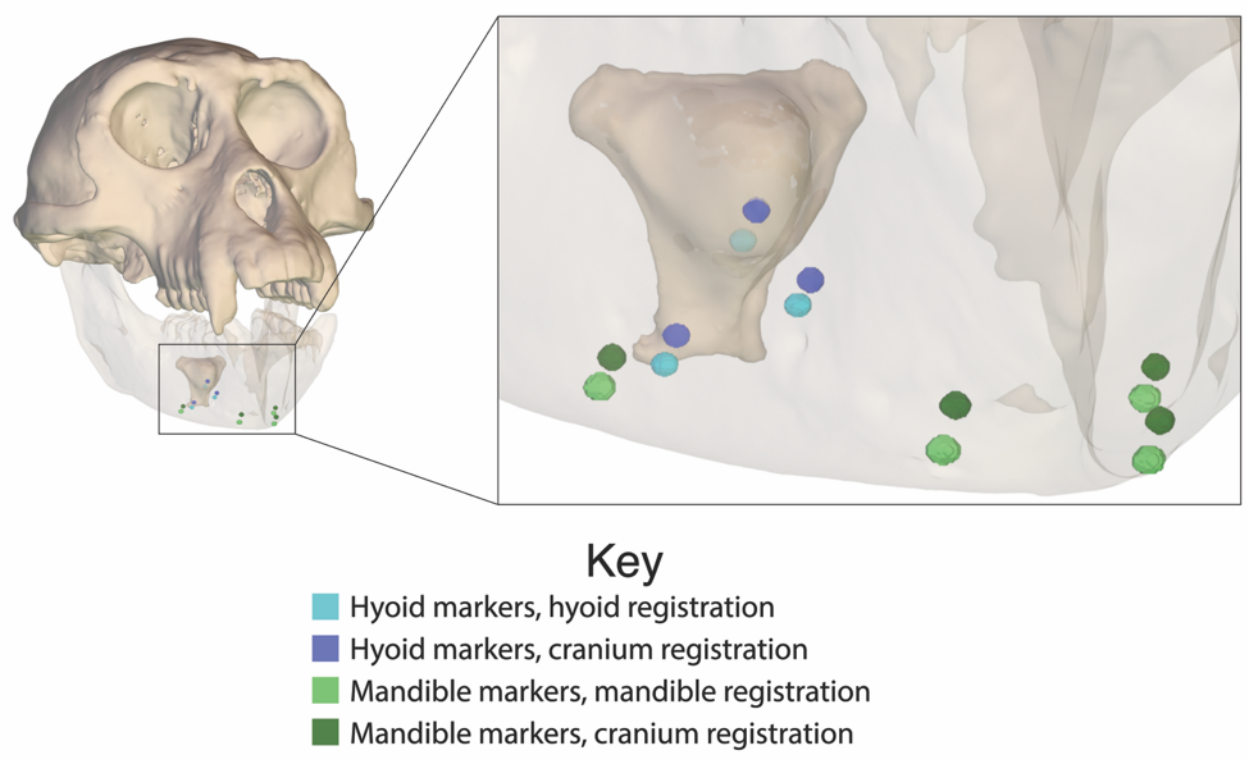

Figure 3.3: XROMM and diceCT bone model registration. Maya rendering of macaque cranium, mandible (translucent), basihyoid, and registered markers from the diceCT scan in anterolateral view. Registering by using the transformation matrix for the cranial markers for all bones instead of bone-specific transformation matrices introduces additional error. Markers from the original scan are not shown because they nearly completely overlap markers in lighter shades (Table 3.1). Reproduced from Orsbon et al. 2018.

Table 3.1: XROMM and diceCT bone model registration error

Bone	Mean Intermarker Distance (mm)			
	Registered using bone-specific matrix		Registered using cranial matrix	
	Monkey JB	Monkey Ki	Monkey JB	Monkey Ki
Cranium	0.07	0.07	—	—
Mandible	0.06	0.09	2.20	1.85
Hyoid	0.11	0.05	2.32	2.22
All Markers	0.08	0.07	2.26	2.03

Reproduced from Orsbon et al. 2018

Defining muscle attachment sites

After creating registered muscle models, the models were imported into Maya to determine the location of the fascicles' attachments on the bones (Figure 3.4). The vertices on the bone surrounding the muscle at its attachment point were selected. Some muscle fascicles did not directly insert into bone (e.g., if a fascicle inserted into a tendon that contrasts poorly with the surrounding tissue), prompting the development of a method to determine the attachment point of these muscles. Maya's modeling capabilities were used to create cylindrical polygons to bridge the gap. These cylinders were manually adjusted to have the approximately same diameter and orientation as the terminal end of the fascicle and extended to the bone where the connective tissue was assumed to attach. After creating a ring of identified vertices around the fascicle attachment site, the vAvg function of the XROMM Maya Tools was used to calculate the XYZ location of the attachment site centroid. For muscles that attach to bone a separate muscle model for each attachment site was generated using bone-specific transformation matrices.

Styloglossus required a specialized reconstruction because it inserts into soft tissue (the stylomandibular ligament) and not directly to the rigid cranium. The attachment sites of the ligament at the styloid area and mandible were segmented and ligament length was defined as the Euclidean distance between the two. A cylindrical polygon was used to simulate the stylomandibular ligament and another cylinder bridged the gap between the segmented styloglossus fascicles and the ligament. To define the styloglossus attachment site, an XYZ locator was manually placed at the intersection between the reconstructed ligament and the gap-filling cylinder. The distance from the reconstructed attachment site to the styloid process was normalized by ligament length to create a ratio defining how far along the stylomandibular

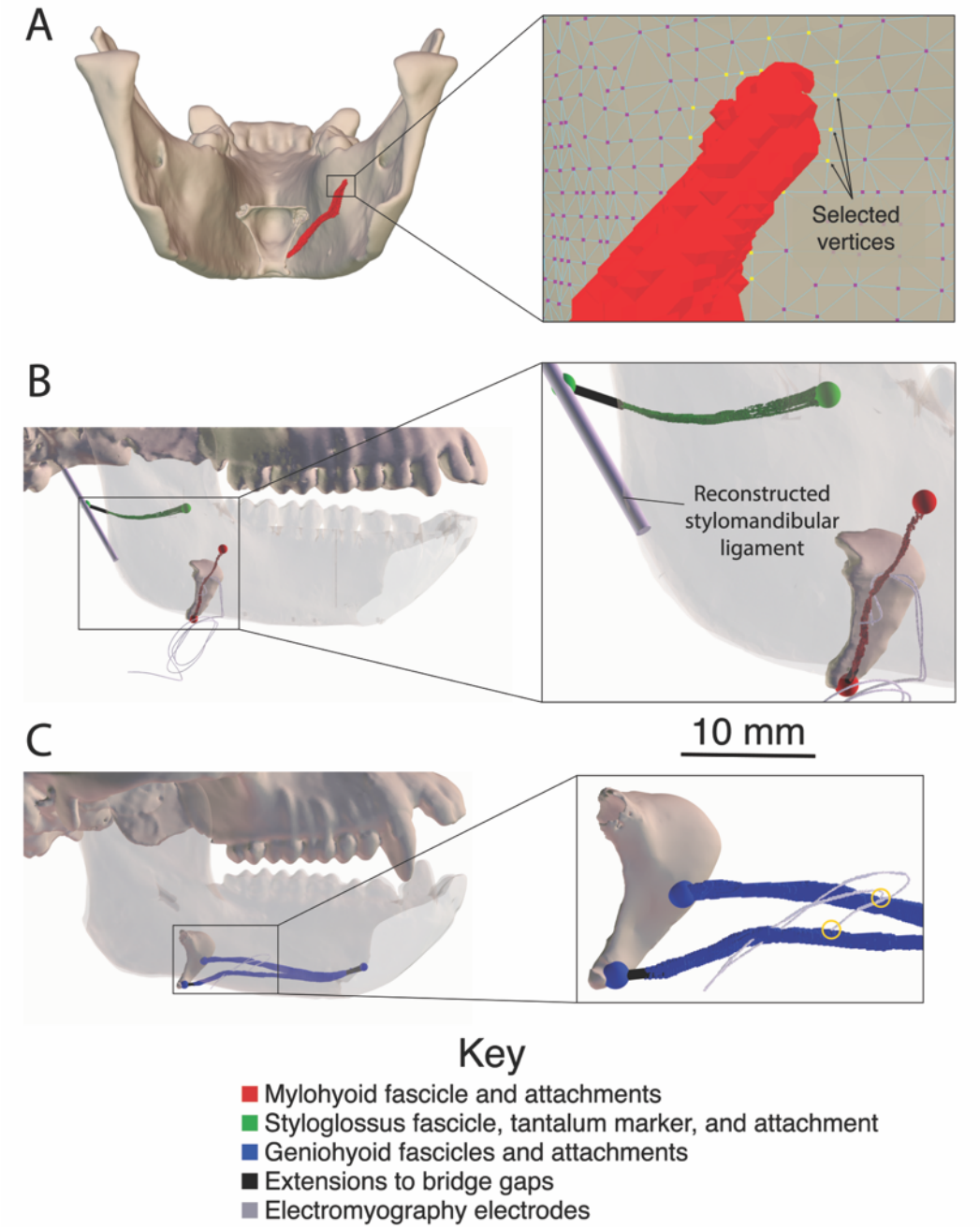

Figure 3.4: Reconstructed muscle fascicles and attachment sites. A) Rendered posterior view of the mandible, basihyoid, and mylohyoid fascicle. The inset focuses on the mylohyoid's mandibular attachment site in Maya's "vertex" mode. The model's vertices are purple, and the vertices surrounding the mylohyoid's attachment on the mandible have been selected (yellow) for calculation of the attachment site. Vertices are enhanced in size. B) Styloglossus (green) and mylohyoid (red) reconstructions. C) Geniohyoid reconstruction, demonstrating that the electrodes were more widely spaced in this muscle. Gold circles indicate where electrodes insert into the fascicles. The fascicles immediately surrounding the bare end of each electrode were segmented and modeled, and geniohyoid measurements were taken as the average of the results for the two groups of fascicles. Colored spheres are reconstructed attachment points, except for the anterior green sphere which was a digitized tantalum marker implanted in the styloglossus. Scale bar is for insets of B and C. Reproduced from Orsbon et al. 2018.

ligament the styloglossus inserted. The ligament was reconstructed as a vector with the tail at the styloid process and the head at the mandibular ligament. The instantaneous styloglossus attachment location was reconstructed as the XYZ coordinate of the head of the dot product of the stylomandibular ligament vector and the above ratio. This method assumes that strain is homogenous throughout the ligament and that the ligament neither curves around other structures or buckles.

All muscle measurements in this study were taken from the right side, except for palatoglossus because the markers in the right palatoglossus were extruded during healing.

Digitizing

The biplanar X-ray videos were saved as .avi files for storage and converted to .tiff stacks locally for digitization using ImageJ v1.51a (National Institutes of Health, Bethesda MD). All videos were undistorted, calibrated, and digitized using XMALab v1.4.0 (Knörlein et al. 2016), which generates both the XYZ coordinates of individual markers and rigid body transformations for markers assigned to the same bone. The XYZ coordinates and transformation matrices were filtered at 20 Hz after visually confirming in XMALab's built-in plotting features that this frequency did not over-smooth the data.

Defining coordinate systems

Two coordinate systems were created, one fixed to the cranium and another fixed to the mandible. The cranial coordinate system was aligned such that the XZ plane was parallel to the occlusal surface of the maxillary tooth row (positive X = anterior, positive Y = dorsal, positive Z = right, after Menegaz et al. 2015) and the origin was set on the posterior nasal spine. The

mandibular coordinate system was also aligned such that the XZ plane was parallel to the occlusal surface of the mandibular molars and the origin was set halfway between the mandibular condyles.

These coordinate systems can be created manually using the XROMM Maya Tools shelf (Brainerd et al. 2010) or computationally using the XYZ coordinates of the landmarks on the bones; this study used the latter method using custom-written scripts in R (R Core Team 2017). When computationally creating coordinate systems, the maxillary and mandibular molar tooth cusps, the posterior nasal spine, and the medial-most aspect of the mandibular condyles were digitized using the vAvg function of the XROMM Maya Tools. In macaques, the four cusps (hypocone, metacone, paracone, and protocone) on the three maxillary molars (M1, M2, M3) were used, and the four cusps (hypoconid, metaconid, entoconid, protoconid) on mandibular m1, m2, and m3 were used, in addition to the hypoconulid on the m3.

The *in vivo* movements of these landmarks in 3D space were reconstructed by applying rigid body transformation matrices exported from XMALab to the XYZ coordinates of the cusp landmarks to every frame. Two datasets were then created by subtracting the XYZ coordinates of the cranial and mandibular origin from the XYZ coordinates of the tooth cusps. The prcomp function of the stats package in R (R Core Team 2017) was used to run a principle components analysis (PCA) on the location of the tooth cusps that returns a rotation matrix to align the cusps along their principle axes of variation. The first, second, and third eigenvectors define anteroposterior, mediolateral, and superoinferior, respectively, as confirmed by plotting and visually inspecting the transformed data. The rotation matrix generated by the PCA is then applied to all of the markers in the cranial and mandibular datasets—including the originally tracked tantalum markers as well as the reconstructed bone, tooth, and muscle landmarks—to

create datasets describing marker location relative to the cranium and the mandible. Each dataset was then imported into Maya and animated to visually confirm that no mathematical errors had occurred.

Mandibular tooth cusps were used to calculate mandibular pitch (Z-axis rotation, mandible elevation and depression), yaw (Y-axis rotation, mandible transverse movement), and roll (X-axis rotation, mandible roll). The positions of the mandibular tooth cusps were first calculated within a cranial coordinate system, which was established by the plane of the maxillary tooth cusps. Because the principal components of the maxillary and mandibular tooth cusps are in the same anatomical directions, a rotation matrix that reorients the mandibular tooth cusp within a cranial coordinate system along their principal components also aligns them with the maxillary tooth cusps. The prcomp function of the R stats package was applied to these coordinates in each frame and the loading matrix was converted to Euler angles using a method described by Slabaugh (1999) using a modified version of the rotationMatrixtoEP function of the linkR package in R (v1.1.1, Olsen 2016; Olsen and Westneat 2016).

Reconstructing hyoid rigid body kinematics

Hyoid anteroposterior and superoinferior positions were measured as the value of the X and Y coordinate, respectively, of the tantalum marker implanted in the midline of the hyoid. Velocity in either direction was measured as the marker coordinate's time derivative using the splinefun function of the R stats package (R Core Team 2017).

Measuring the length of muscles attaching to the hyoid required reconstructing hyoid rigid body kinematics. Operating under the assumption that the markers are rigidly fixed to that bone, the XMALab algorithm that produces the rigid body transformation matrices minimizes

error among all markers within the same bone (Knörlein et al. 2016). However, the assumption of rigidity was violated in the hyoid of each animal because inter-marker distances were observed to vary regularly during feeding. Examining each animal *post mortem* revealed that markers had been extruded a small distance from the bone during healing. The standard deviation of *in vivo* hyoid inter-marker distances in Monkey Ki was comparable to that of the precision study; however, the same *in vivo* measurement in Monkey JB was nearly an order of magnitude larger than that of precision study (Table 3.2). Consequently, the reconstructed hyoid for Monkey JB was observed to be abnormally rotated around its anteroposterior axis in the *in vivo* XROMM data. This finding prompted the development of an alternative method of generating a transformation matrix. Because the middle hyoid marker was either within (Monkey JB) or immediately adjacent (Monkey Ki) to the hyoid bone, new rigid body transformation matrices were generated using the rotonto function of the Morpho package in R (v2.5.1, Schlager and Jefferis 2017) that generated zero error for the middle hyoid marker and minimized error for the other two markers. The alternative reconstruction resolved the abnormal rotation about the anteroposterior axis (Figure 3.5).

Table 3.2: Precision study and *in vivo* intermarker distance standard deviations

Bone	Intermarker distance SD (cm)			
	Monkey Ki		Monkey JB	
	Precision study	*In vivo*	Precision study	*In vivo*
Cranium	0.007	0.007	0.004	0.008
Mandible	0.010	0.006	0.003	0.005
Hyoid	0.005	0.010	0.003	0.049

Reproduced from Orsbon et al. 2018

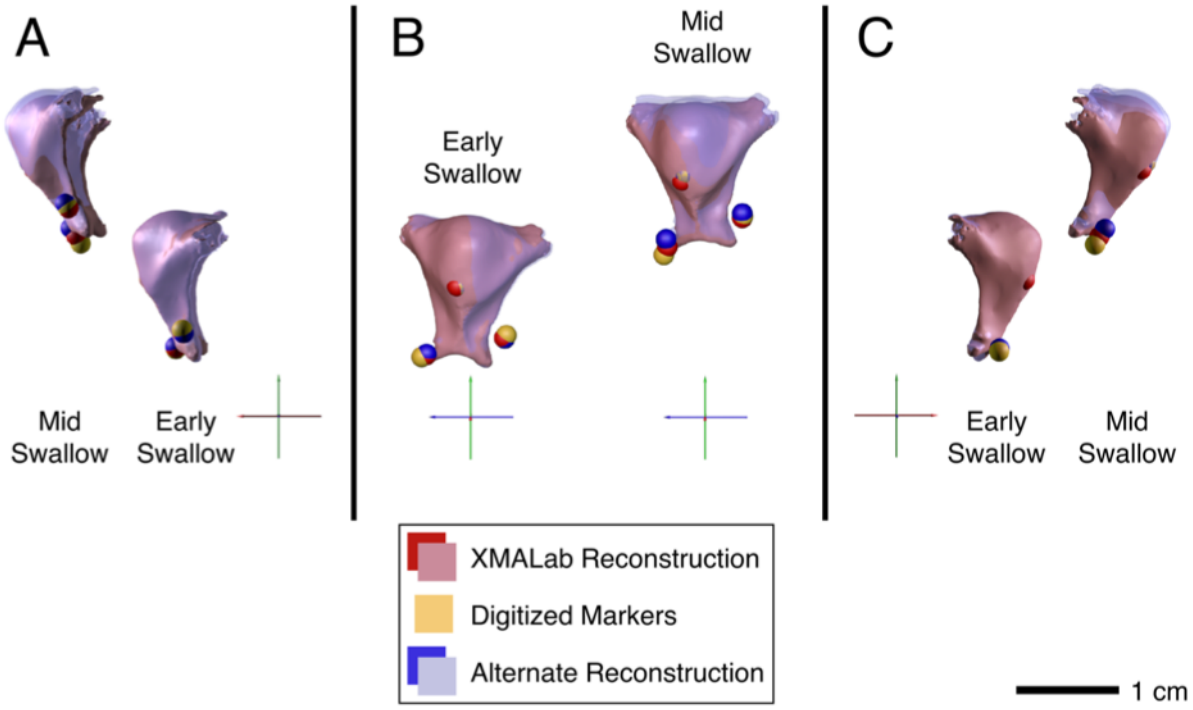

Figure 3.5: Alternative reconstruction of basihyoid rigid body kinematics. Monkey JB basihyoid reconstructions early in the swallow and in the middle of the swallow, at maximum excursion. Yellow markers are the originally tracked markers. Solid red hyoid and red spheres indicate the XMALab reconstruction, which is rotated slightly counterclockwise at mid-swallow due to inferior displacement of the right basihyoid marker relative to the other two. Translucent blue basihyoid and solid blue spheres indicate the alternate reconstruction. Arrows indicate orientation of the coordinate system: red, pointing anterior; green, pointing superior; blue, pointing right. A) Left lateral view of hyoid. B) Anterior view. C) Right lateral view.

Reconstruction of muscle length and orientation

Muscle length (d) was defined as the Euclidean distance between muscle attachment points, either from bone-to-bone (posterior mylohyoid, geniohyoid, stylohyoid), reconstructed attachment-to-marker (styloglossus), bone-to-marker (genioglossus, hyoglossus, anterior digastric, posterior digastric), or marker-to-marker (palatoglossus). Anterior mylohyoid length was not measured in this study. Muscle orientation was defined in each coordinate system by modeling the muscle as a vector of length d (E1).

$$d = \sqrt{(x_2 - x_1)^2 + (y_2 - y_1)^2 + (z_2 - z_1)^2} \quad \text{(E3.1)}$$

This method is limited in its ability to measure fascicle length in all muscles. The fascicles of genioglossus insert into a tendon at the mandibular symphysis and therefore whole muscle length was measured. The fibers of the anterior digastric are unipennate, permitting reconstruction of fiber length; however, the posterior belly is bipennate and only whole muscle belly lengths were calculated. Moreover, the accuracy of this method may suffer in muscles that exhibit curvature *post mortem*, including mylohyoid, styloglossus, and hyoglossus.

Muscle orientation was expressed using the relative magnitudes of the anteroposterior ($\hat{\imath}$), superoinferior ($\hat{\jmath}$), and mediolateral ($\hat{k}$) components of the vector within each coordinate system.

$$\hat{\imath} = x_2 - x_1 \quad \text{(E3.2)}$$

$$\hat{\jmath} = y_2 - y_1 \quad \text{(E3.3)}$$

$$\hat{k} = z_2 - z_1 \quad \text{(E3.4)}$$

The origin and insertion were ordered so that positive values were oriented anteriorly, superiorly, and right at rest to reflect the signs of the coordinate systems. Muscle angles were calculated in the coronal (ZY), sagittal (XY), and axial planes (XZ). Muscle linear and angular velocity were calculated by taking the first derivative of the data using the splinefun function of the R stats package (R Core Team 2017).

$$\theta_{axial} = \tan^{-1}\frac{\hat{\imath}}{\hat{k}} \quad \text{(E3.5)}$$

$$\theta_{coronal} = \tan^{-1}\frac{\hat{\jmath}}{\hat{k}} \quad \text{(E3.6)}$$

$$\theta_{sagittal} = \tan^{-1}\frac{\hat{\jmath}}{\hat{\imath}} \quad \text{(E3.7)}$$

The orientation of lines of action for each plane are demonstrated in Figure 3.6. In the axial plane, 0 degrees was right and 90 degrees was anterior. In the coronal plane, 0 degrees was

right and 90 degrees was superior. In the sagittal plane, 0 degrees was anterior and 90 degrees was superior.

Precision study

Precision experiments (following Menegaz et al. 2015) were conducted prior to specimen staining to evaluate whether the described methods are precise enough to measure *in vivo* muscle linear and angular displacement and velocity. In brief, the frozen specimen was waved within the capture volume while running each X-ray emitter at the same voltage and current that was used *in vivo* and using the same camera frame rate and shutter speed. Five hundred frames were digitized to generate XYZ coordinates and rigid body transformations using XMALab (Knörlein et al. 2016). To characterize typical *in vivo* digitizing, markers were digitized using a combination of manual and automated digitizing; the refinement functions of XMALab were not used. The precision measurements were therefore more conservative (less precise) than if more time were put into digitizing. Muscle and tendon length, angle, velocity, and orientation were reconstructed from data collected during the precision study described above and the landmark-based definition of the coordinate system. Because the specimens were frozen and therefore the markers could not move relative to one another, three standard deviations of the various *post mortem* kinematic measurements were used to define a 99.7% confidence interval for *in vivo* measurements. Muscle length and velocity were normalized by lengths observed *in vivo* by taking the average length reconstructed from 30-50 frames (150-250 ms) while structures of interest were not moving. Longer durations were not possible because the animals either frequently moved or were not still in postures that allowed digitization of the necessary markers.

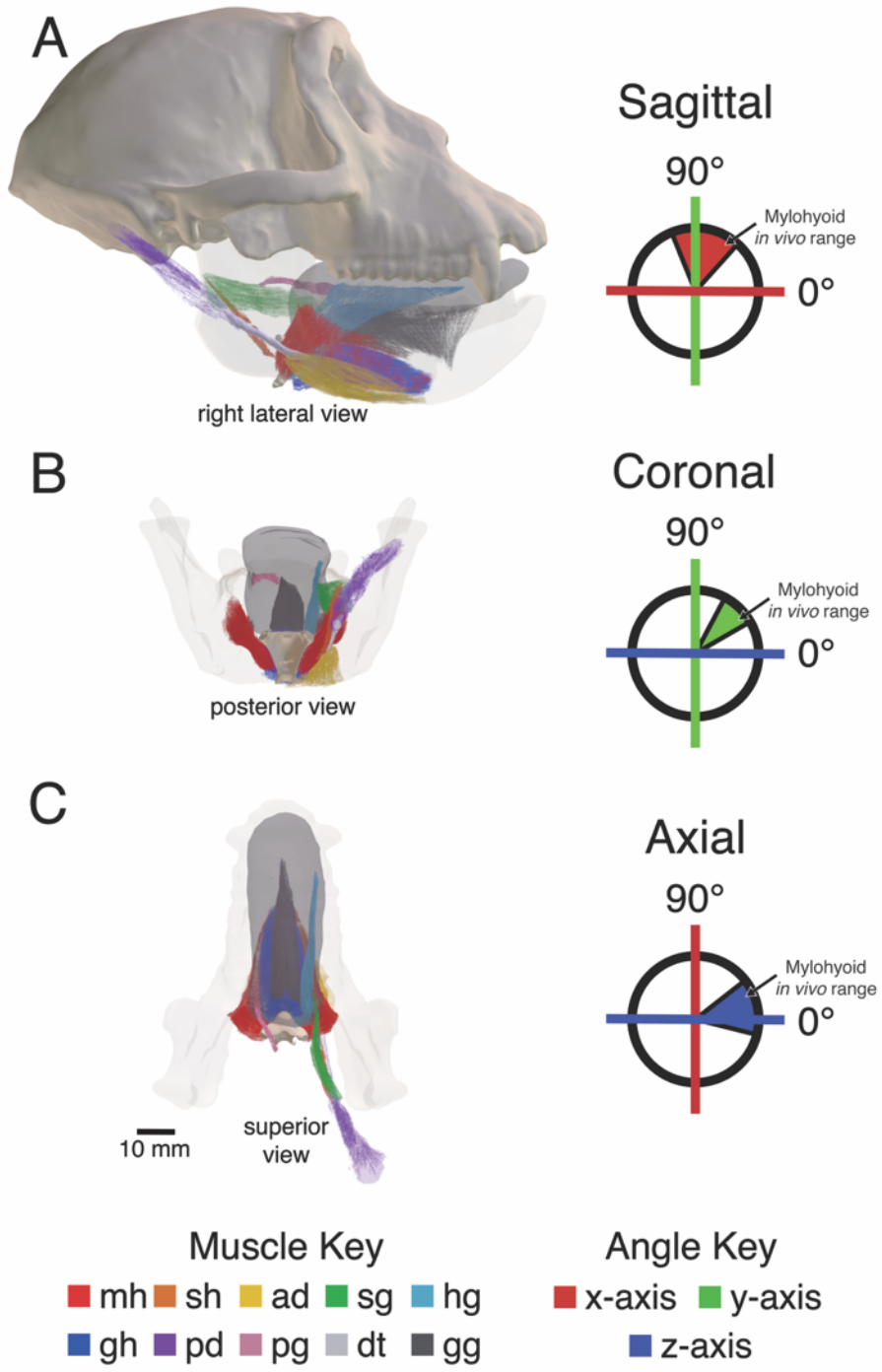

Figure 3.6: Muscle orientation in anatomical planes. (A) Sagittal plane, right view. On the crosshair, the anteroposterior axis is red and superoinfe- rior axis is green. Anterior is set at 0 and superior is set at 90. (B) Coronal plane, posterior view. On the crosshair, the mediolateral axis is blue and superoinferior axis is green. Right is set at 0 and superior is set at 90. (C) Axial plane, superior view. On the crosshair, the mediolateral axis is blue and anteroposterior axis is red. Right is set at 0, anterior is set at 90. Each crosshair's colored area indicates the posterior mylohyoid's in vivo range within a given plane in both cranial and mandibular coordinate systems. Abbreviations: ad, anterior digastric; gg, genioglossus; gh, geniohyoid; hg, hyoglossus; mh, mylohyoid; pd, posterior digastric; pg, palatoglossus; sg, styloglossus; sh, stylohyoid. Reproduced from Orsbon et al. 2018.

Table 3.3: Precision compared to *in vivo* range of muscle linear and angular displacement.

Muscle	Muscle Linear Displacement						Muscle Angular Displacement					
	Resting Length (mm)	Absolute (mm)		Normalized (L_r)		Coordinate System	Sagittal (deg)		Coronal (deg)		Axial (deg)	
		Precision (± 3 SD)	*In vivo* range (mean)	Precision (± 3 SD)	*In vivo* range (mean)		Precision (± 3 SD)	*In vivo* range (mean)	Precision (± 3 SD)	*In vivo* range (mean)	Precision (± 3 SD)	*In vivo* range (mean)
Ant. Digastric	24.09	0.09	4.59	0.004	0.190	Mandible	0.370	21.308	1.641	60.613	0.400	2.850
Dig. Tendon	18.07	0.12	0.83	0.006	0.046	Cranium	0.412	14.119	0.877	9.691	0.591	5.475
Genioglossus	19.81	0.12	7.72	0.006	0.390	Mandible	0.352	28.168	0.593	11.796	0.757	14.722
Geniohyoid	40.34	0.08	10.14	0.002	0.252	Mandible	0.188	15.401	1.676	140.956	0.178	2.449
Hyoglossus	52.73	0.15	11.46	0.003	0.218	Mandible	0.264	10.281	0.448	12.446	0.380	10.336
Mylohyoid	22.34	0.14	8.75	0.006	0.395	Mandible	0.266	33.999	0.422	20.816	0.298	39.687
Palatoglossus	11.31	0.11	3.22	0.010	0.285	Mandible	0.793	28.542	2.638	153.491	1.054	16.792
Post. Digastric	41.29	0.21	1.92	0.005	0.046	Cranium	0.134	6.867	0.249	5.462	0.280	2.991
Styloglossus	38.22	0.12	7.74	0.003	0.203	Cranium	0.225	15.773	0.814	38.285	0.430	4.715
Stylohyoid	52.61	0.21	3.04	0.004	0.058	Cranium	0.209	10.462	0.197	4.963	0.329	5.425

Reproduced from Orsbon et al. 2018.

For each cycle, the range of each kinematic variable was calculated and the mean range was compared against the precision study results (Tables 3.4 and 3.5).

All *in vivo* kinematic ranges were greater than the precision of the system (± 3 SD), and most (80%) were at least an order of magnitude greater (Tables 4 and 5). The mean precision of absolute linear velocity, normalized linear velocity, and angular velocity among all muscles was 7.58 mm s^{-1}, 0.278 lengths s^{-1}, and 29.8 deg s^{-1}, respectively. Overall, the results indicate that the precision of both displacement and velocity are sufficient for kinematic analysis, but given the variability in precision, measurement- and muscle-specific precision values should be used.

Sensitivity analysis

Posterior mylohyoid was found to exhibit the widest *in vivo* range of all of the measured kinematic variables and was therefore used to investigate the extent to which using inaccurate or imprecise muscle attachment sites affects kinematic measurements. Four false attachment points on the mandible's surface were reconstructed 3.37 to 4.11 mm anterior, inferior, posterior, and superior to the actual attachment point. The range of each variable (*Var*) obtained for each cycle and was then averaged across all cycles for the true and false attachment points. Percent error was calculated as:

$$Error = \frac{Var_{True} - Var_{False}}{Var_{True}} \times 100 \quad \text{(E3.8)}$$

Relatively small inaccuracies in muscle attachment location introduce significant error into most kinematic measurements (Figure 3.7, Table 3.4). Averaging across chewing and swallowing cycles, measurements made from false muscle attachment sites differed from those

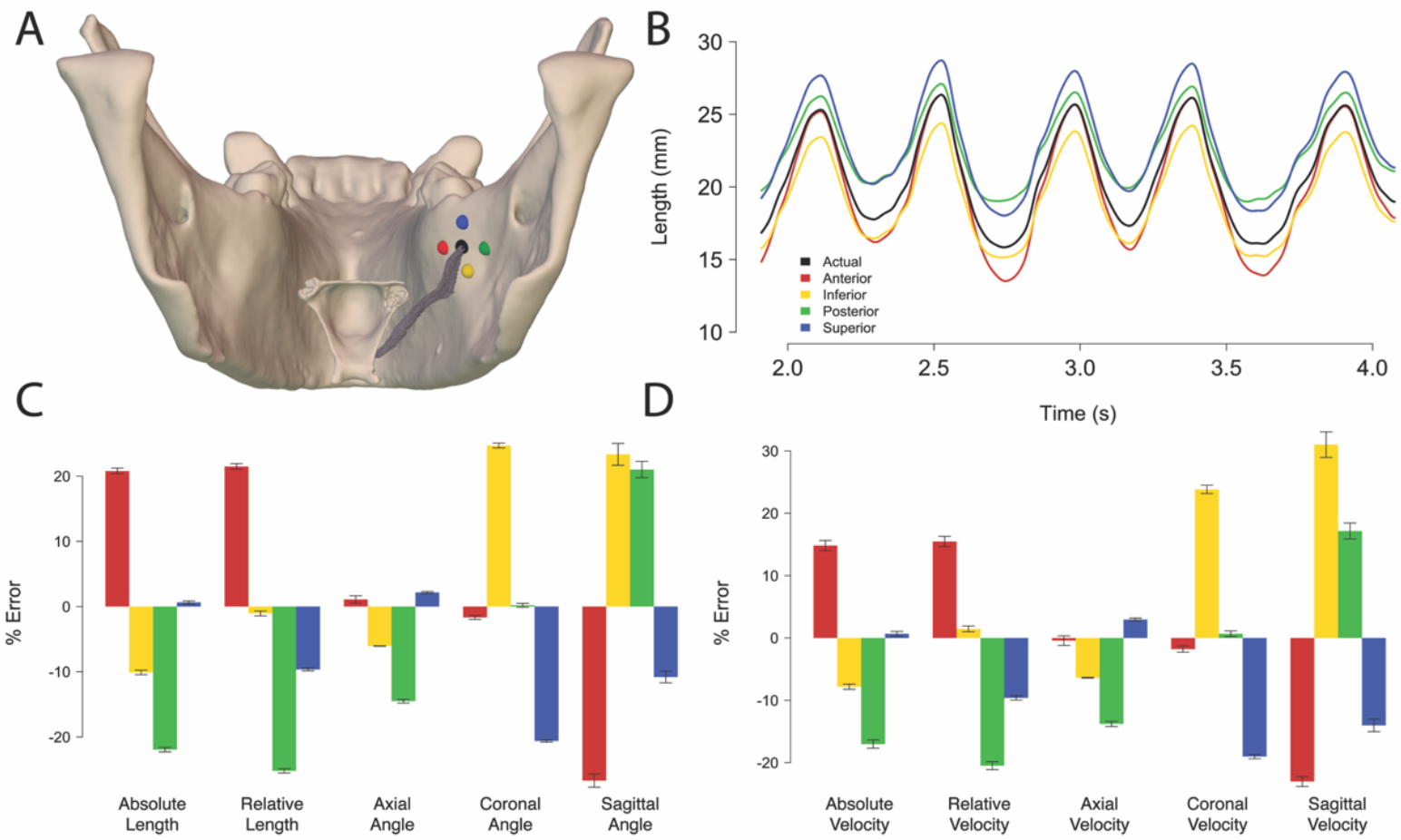

Figure 3.7: Mylohyoid kinematics using actual and estimated mandibular insertion points. (A) Mandible, basihyoid, and mylohyoid fascicle (gray) in posterior view. The locations of the various attachment points are shown as colored spheres. The black sphere is the actual insertion location, while the following colors have been displaced as follows: anteriorly, red; inferiorly, yellow; posteriorly, green; superiorly, blue. (B) Mylohyoid length during a feeding sequence. The colored lines correspond to the same color attachment site in A. Both the absolute value and range of mylohyoid length vary among the different attachment sites. (C) Error in the range of length measurements based on each false attachment location com- pared to the measurements based on the actual attachment location. (D) Error in the range of velocity measurements based on each false attachment location compared to the measurements based on the actual attachment location. Reproduced from Orsbon et al. 2018.

Table 3.4. Mean range of mylohyoid kinematics measured using actual and displaced mandibular insertion points.

Insertion Location	Resting Length (mm)	Mean Range of Mylohyoid Linear Kinematics				Coordinate System	Mean Range of Mylohyoid Rotational Kinematics					
		Absolute (mm s^{-1})		Normalized (L_r s^{-1})			Sagittal (deg s^{-1})		Coronal (deg s^{-1})		Axial (deg s^{-1})	
		Displacement	Linear Velocity	Displacement	Linear Velocity		Angle	Angular Velocity	Angle	Angular Velocity	Angle	Angular Velocity
Actual	22.34	8.75	177.79	0.395	8.017	Mandible	33.999	729.132	20.816	381.114	39.687	783.111
Anterior	22.24	10.58	203.43	0.480	9.225	Mandible	25.284	562.852	20.506	374.187	40.251	778.626
Inferior	20.30	7.86	164.02	0.390	8.140	Mandible	42.665	967.020	25.928	472.027	37.288	732.984
Posterior	23.28	6.83	148.06	0.295	6.397	Mandible	40.632	848.157	20.819	383.693	33.866	674.868
Superior	24.87	8.81	179.04	0.357	7.249	Mandible	29.937	620.890	16.521	308.443	40.507	806.427

Reproduced from Orsbon et al. 2018.

of the actual attachment site by an average of 13.2% (range: 0.1% to 49.8%). Even if the range approximated the actual measurements, the absolute value was nonetheless different, as in the case of the superiorly displaced landmark and absolute length measurements.

Electromyography

Electromyography (EMG) data from all animals were processed using a 30 Hz high-pass Butterworth filter that filtered forward and back to eliminate phase shifts using the *butter* and *filtfilt* functions of the signal R package (Signal 2013). We used different low-pass cutoffs among the different animals because EMG data were collected at different sampling rates (2000-10000 Hz). Low-pass cutoffs ranged from 1000 to 3000 Hz. Filtered data were full-wave rectified and integrated using a root-means squared algorithm integrated over 5 ms intervals, which also functioned to down sample the data to match the cineradiography frame rate of 200 Hz.

Each channel's noise threshold was determined using a method similar to that proposed by Thexton (1996). In brief, Thexton's method uses a runs test to determine the noise threshold, which involves comparing ordered and randomized EMG data. At low thresholds, noise leads to an increased number of threshold crossings (i.e., separate runs) in ordered and randomized data as time progresses. However, at higher thresholds, the number of runs in ordered EMG data will be limited to the sum of the number of separate activity and noise bouts but in randomized EMG data will decrease at a slower rate. The selected threshold optimizes the difference in run number between ordered and randomized EMG data. Our method differed in that we used an average threshold of 30 runs tests for each channel, and a threshold from a temporal subset of each trial in some channels. For each channel, a trial in which the animal exhibited clear periods of activity

and noise was chosen for the runs test. In some channels, the entire trial was used. However, when the total duration of activity exceeded that of noise, the algorithm produced a threshold that cut off salient bursts of activity. In these circumstances, the input data for the runs test was narrowed to a smaller window in which the total duration of activity was roughly equal to that of noise. After determining the channel's threshold in the trial used for the runs test, this threshold was applied to the other trials in the dataset. Every channel was visually inspected for a goodness of fit before applying the threshold to all trials.

ANALYSIS OF TONGUE BASE RETRACTION BIOMECHANICS

Extrinsic muscle orientation was measured using the approach described above. A muscle was defined as having a predominantly posterior orientation when its sagittal angle was greater than 135 degrees and less than 225 degrees.

Intrinsic muscle kinematics were inferred from changes in tongue dimensions measured as the Euclidean distance between lingual markers along a single axis. Posterior tongue height was defined as the Y-axis distance between the posterior surface marker and the dorsum of the hyoid. Posterior tongue width was defined as the Z-axis distance between the two lateral posterior markers. Posterior tongue length was defined as the X-axis distance between the posterior and middle surface markers (Figure 3.8).

Tongue volume

Although increases in all three dimensions of the posterior tongue would necessarily support the conclusion that the tongue regionally changes in volume, it is possible for volume to increase even if one or two dimensions decrease in size. Therefore, tongue volume was also

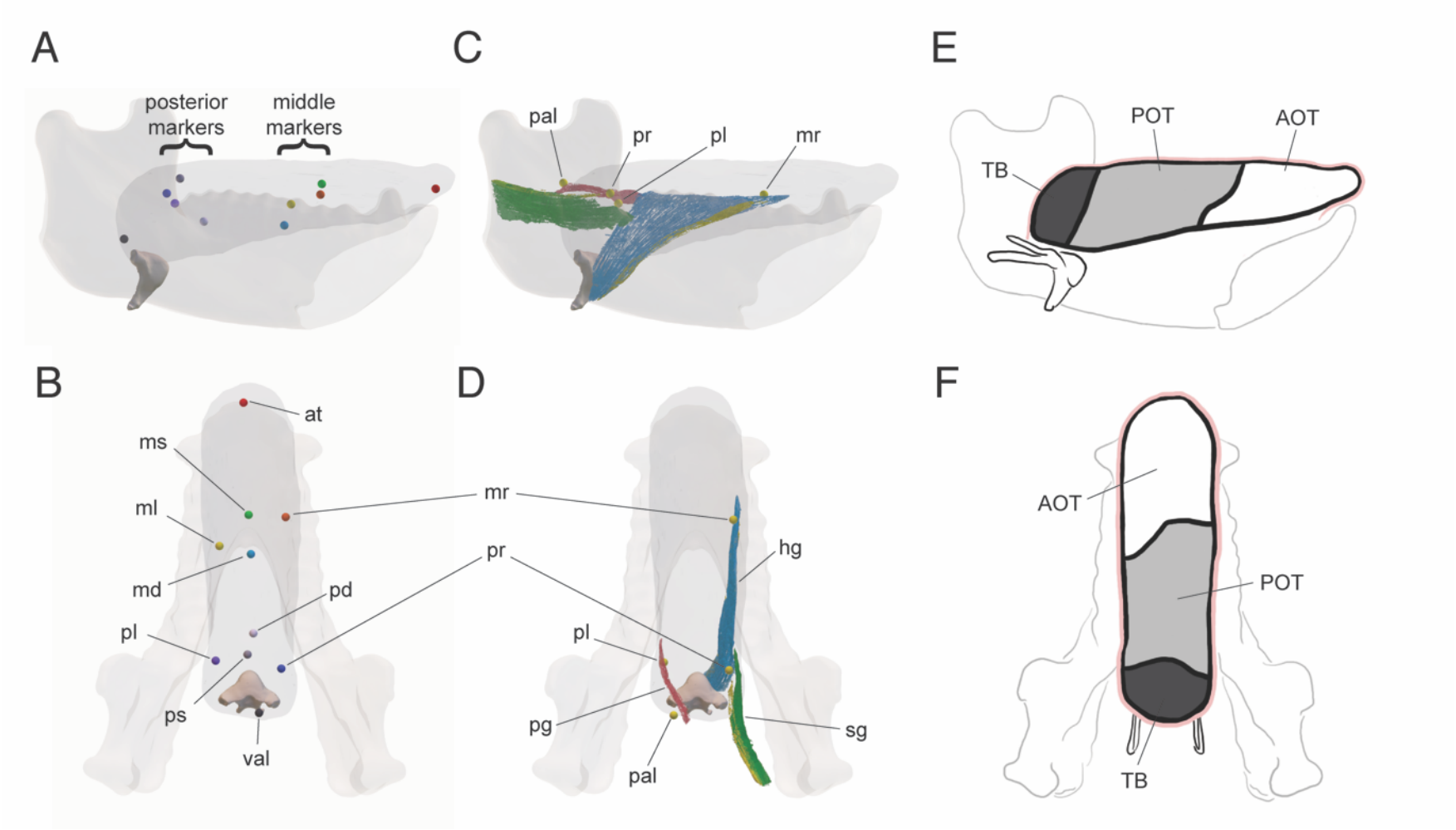

Figure 3.8: Relationships of implanted markers to reconstructed muscles and tongue volumes in Monkey JB. A, C, E) Lateral views. B, D, F) Axial views. A, B) Marker locations. C, D) Markers (gold) relative to hyoglossus (hg, blue), palatoglossus (pg, pink), and styloglossus (sg, green). E, F) Illustration of volume divisions of the tongue: the anterior oral tongue (AOT, white) was bound by the anterior tongue (at) and middle markers; the posterior oral tongue (POT, gray) was bound by the middle markers, posterior markers, and the hyoid; the tongue base (TB, dark gray) was bound by the posterior markers, the hyoid, and the vallecula marker.

modeled. Simple convex models have the advantage of computational simplicity, but the tongue can form distinctly concave shapes (Abd-El-Malek 1955; Stone and Lundberg 1996). For each frame, we generated a 3D volume of the was created by generating a polygonal mesh using the following alpha shape algorithm developed by Dr. Tingran Gao (Department of Statistics, University of Chicago).

The alpha shape algorithm models the tongue as a concave shape consisting of three geometric primitives delimited by two coronal surfaces generated from instantaneous tongue posture (Figure 3.9). The two surfaces were constructed from two closed spline curves each interpolating a set of four implanted markers, respectively: the first, the middle coronal surface, was at the border between the anterior and posterior oral tongue and was defined by the middle superficial, middle right, middle left, middle deep markers, and the second, the posterior coronal area, was at the border between the posterior oral tongue and the tongue base and was defined by the posterior superficial, posterior right, and posterior left markers and a reconstructed on the dorsal surface of the hyoid. The posterior deep marker was not used because of significant disparities in posterior deep marker position among animals compared to the more regularly spaced superficial markers, and because the hyoid delimits the inferior border of the tongue.

Splines were fit using the splinefun function of the R base package with the method set to "natural". For the sake of stability, each coronal surface was determined by initially fitting the corresponding set of four implanted markers using a natural spline that wraps around the ordered set with three full loops of 300 points each, starting and ending at the middle deep or dorsal hyoid marker for the middle and posterior coronal splines, respectively. Then, the segments of the spline outside of the second complete loop were discarded. A minimal surface (Osserman 2002) was then constructed for each coronal surface by solving a minimal surface equation with

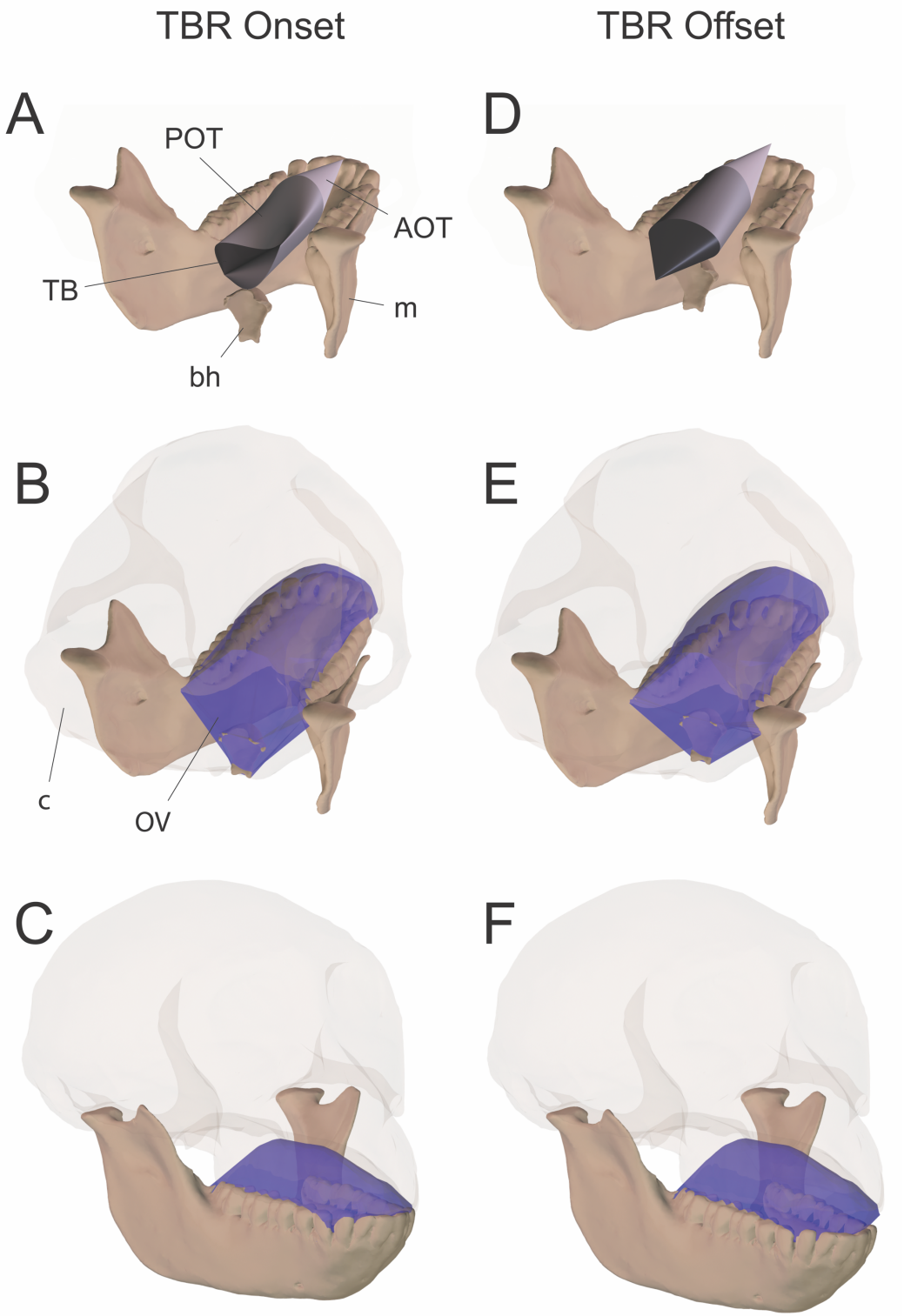

Figure 3.9: Tongue and oral volume at the time of tongue base retraction (TBR) onset and offset in a rhesus macaque (Monkey Ki). Figures show posterolateral (A, B, D, E) and anterolateral (C, F) views of tongue (grayscale) and oral volumes (blue). Abbreviations: AOT, anterior oral tongue volume; bh, basihyoid; c, cranium; OV, oral volume; POT, posterior oral tongue volume; TB, tongue base volume.

the x-, y-, and z- coordinates of the coronals as boundary conditions. For this purpose, first each coronal surface was projected onto a two-dimensional plane spanned by the first two principal directions, then a triangular mesh was constructed for the planar domain enclosed by the projected image, and finally a system of three Poisson equations defined on the planar triangular mesh was solved to obtain the x-, y-, and z-coordinate functions for the minimal surface. This methodology closely follows the surface editing algorithm based on cotangent Laplacians on irregular triangular meshes (Sorkine et al. 2004). The minimal surface of the middle and posterior coronal splines as a boundary will be referred to as the middle and posterior coronal surface in the rest of this section. Note that although each minimal surface was constructed from solving planar Poisson equations, the resulting surface was not flat in general unless the boundary curve actually resides in a plane.

The two coronal surfaces divided the tongue into three adjacent portions. For each, a triangular mesh was constructed with the shape of a geometric primitive and its 3D mesh volume was calculated as the sum of all the signed volumes (e.g., Marschner and Shirley 2015) of the tetrahedrons spanned by the triangular faces with respect to an arbitrarily fixed origin. The total sum of the signed volumes did not affect the final result, but the centroid of the corresponding geometric primitive was picked for definiteness. The three geometric primitives were:

1. *Anterior oral tongue*: A cone with the middle coronal surface as base and the anterior tongue marker as apex;
2. *Posterior oral tongue*: A deformed cylinder with the middle and posterior coronal areas as two bases;
3. *Tongue base*: A cone with the posterior coronal area as base and the vallecula marker as apex.

To construct the posterior tongue volume in a natural way and avoid artificial distortions, the middle and posterior coronal surfaces were resampled evenly with respect to their circumferences. This resampling achieved an equal number of points, starting with the middle deep marker and reconstructed dorsal hyoid marker as the starting points for resampling the middle and posterior coronal areas, respectively. The side surfaces of the posterior oral tongue volume were created by generating line segments that connected pairs of matched samples on the resampled middle and posterior coronal splines. The matchings were defined by first pairing the two anchor points and then progressively propagating the correspondences to the rest of the evenly spaced new samples.

Oral cavity volume was measured using a 3D alpha shape (Figure 3.9). The oral cavity was defined as the space bounded superiorly by the mucosa of the hard palate; anteriorly and laterally by the lingual surfaces of the teeth, mandibular symphysis, and mandibular corpus as far inferiorly as the mandibular attachment for the mylohyoid; inferiorly by a reconstructed mylohyoid raphe running from the inferior pole of the hyoid to the mandibular symphysis immediately inferior to the origin of geniohyoid; and posteroinferiorly by the anterior surface of the hyoid. These boundaries are assumed to be either rigid (hard palate, teeth, mandible, and hyoid) or linear (mylohyoid raphe). Using Autodesk MeshMixer 2018 (Autodesk, San Rafael CA), OBJs of each of these rigid surfaces were created from the hyoid and mandible bone models as well as a model of the segmented cranial teeth and hard palate mucosa. The kinematics of 4684 – 8308 total bony landmarks were then reconstructed and served as the input values for the alpha shape function in the alphashape3D package in R (v1.3, Lafarge and Paterio-Lopz 2017). Volumetric measurements were taken from the resulting alpha shape for each frame.

Temporal Alignment

Changes in extrinsic muscle length, tongue dimensions, and regional tongue volume were measured as the difference in their values between the onset and offset of tongue base retraction. Tongue base retraction onset was set as the time at which the posterior superficial marker was at its most anterior point before beginning to move posteriorly. Tongue base retraction offset was set as the time at which the vallecula marker was at its most posterior point after tongue base retraction offset.

Intercuspal phase was operationally defined as the period of the swallow when mandibular pitch velocity was less than two standard deviations of each animal's precision study velocity from zero.

Statistical Analyses

All statistical comparisons were conducted using either a one-sample t-test or a paired t-test using the t.test function in base R package, which assumes variance heterogeneity by default. A p-value of less than 0.05 was considered statistically significant. Pearson correlation matrices were generated from hyolingual kinematic variables using the cor.table function of the picante package in R (Kembel et al. 2014). Threshold p-values were adjusted in multiple comparisons using a Bonferroni correction.

ANALYSIS OF HYOID EXCURSION BIOMECHANICS

Each swallow cycle was defined from maximum gape to maximum gape. Data were then aligned with the onset of tongue retraction as a proxy for onset of posterior movement of the bolus and for comparison with data from Chapter 4. During swallow cycles, absolute hyoid position was measured as the XYZ coordinates of a marker implanted in the hyoid midline, and absolute muscle length and orientation were measured as described above. To normalize muscle length, *post mortem* lengths, as opposed to *in vivo* rest lengths, were used because variation in craniocervical and craniothoracic posture could not be controlled for among all of the animals. Although all animals were restrained around their necks and two (Monkeys He and Ch) were head restrained, the torso was free to move within the restraining chair. In contrast, after sacrifice all animals were fixed in a neutral posture, in which the neck was slightly flexed, there was minimal deviation of the midline of the face from the midsagittal plane, the mandible was slightly depressed, and the tongue was slightly protruded. Additionally, the connection between the sternohyoid and the sternum was maintained throughout fixation.

To measure the amount of concentric, isometric, and eccentric activity in each cycle and tongue base retraction, the total number of frames in which each muscle was at or above 5% of maximal activity was counted. For each of these frames with supra-suprathreshold muscle activity, muscle velocity was measured—negative velocities indicated concentric activity, while positive velocities indicated eccentric activity. Isometric activity was indicated by velocities that were within two standard deviations of precision study velocity of zero (see above). The number of frames for each type of activity per cycle was then divided by the number of frames in the cycle or the number of frames per tongue base retraction to measure the proportion of cycle time or active time, respectively, that each muscle spent in each type of activity.

Electromyography data were additionally smoothed with a 50 Hz low-pass Butterworth filter for visualizing average muscle activity and velocity during swallowing. For this visualization (See Figure 5.7), activity and velocity values were averaged across all cycles for each 5 ms interval from 200 ms before to 200 ms after the onset of tongue retraction.

The effect of muscle rotation on hyoid kinematics was measured using two methods: first, via ratios of hyoid displacement and velocity to muscle length change and velocity; and second, by analyzing the range of muscle orientation throughout the swallow to determine the plane in which rotation contributed to hyoid kinematics, if at all. Architectural gear ratios are measured as the ratio of whole muscle velocity to fiber velocity (Brainerd and Azizi 2005; Azizi et al. 2008). Gear ratio (GR) was defined slightly differently in this study because hyoid muscle rotation, and therefore gearing, is determined not by muscle bulging but rather how much other hyolingual muscles shorten.

Two types of ratios were measured because most muscles did not show distinct periods of constant velocity. The first considers the average velocity of the hyoid and muscle by measuring the ratio of hyoid displacement to muscle length change from movement onset to offset along a given axis ($GR_{\bar{X}}$ and $GR_{\bar{Y}}$). Because both measurements occur over the same time scale, their ratio compares the average velocity of hyoid movement to the average shortening velocity of the muscle. One exception was hyoglossus—GR was measured during tongue base retraction because the lingual attachment of hyoglossus moved minimally during this timeframe (see Chapter 4), otherwise GR was highly variable due to variation in lingual kinematics during the swallow. The second compares peak hyoid and muscle shortening velocities (GR_{Xp} and GR_{Yp}). Peak hyoid axial velocity did not occur simultaneously with peak muscle shortening velocity in many muscles; therefore, GR_{Xp} and GR_{Yp} were measured at the time of peak muscle shortening

velocity. Gear ratios were measured along the X-axis for geniohyoid, Y-axis for mylohyoid and stylohyoid, and both X- and Y-axes as well as their hypotenuse for hyoglossus. To minimize the effect of minor rotations of the hyoid on hyoid displacement and velocity, hyoid kinematics for calculating GR were measured as the displacement of velocity of the attachment site for each respective muscle.

Muscle fiber rotation produces minimal displacement along the X- and Y-axes at certain orientations. In coronal and sagittal planes, changes along the Y-axis are minimal when rotating through 90° and 270° degrees and maximal when rotating through 0° and 180° degrees (Figure 3.6). In sagittal planes, changes along the X-axis are minimal when rotating through 0° and 180° and maximal when rotating through 90° and 270° degrees. Coronal angles were not reported for geniohyoid because, as a midsagittal muscle, it has a minimal mediolateral component—therefore, small translations of the hyoid attachment site along the mediolateral axis resulted in large changes in coronal orientation that were of little biomechanical consequence because of the small size of the mediolateral component. In contrast, coronal orientations are included for hyoglossus, mylohyoid, and stylohyoid because they all have appreciable mediolateral trajectories.

In addition to measuring muscle orientation within the two-dimensional coronal and sagittal planes, three-dimensional alignment with specific axes was also measured. Three-dimensional alignment measures how a muscle's geometry contributes to axial force-displacement tradeoffs (see below). Perfect alignment with a given axis was defined as 0° relative to the plane created by the orthogonal axes, similar to fiber pennation angle in pennate muscles (Gans and Bock 1965).

Muscle geometry effects how much of a muscle's force is aligned with a given axis of movement and how much a muscle must shorten to generate that movement (Gans and Bock 1965). As a muscle becomes more aligned with a given axis, the magnitude of the force vector aligned with that axis—i.e., axial force—increases. If 0° indicates perfect alignment with a given axis, then the relative magnitude of axial force is proportional to cos Θ. For example, when holding muscle force production constant, a muscle which displaces the hyoid along the Y axis will produce the largest superiorly oriented forces when it is perfectly parallel to the Y axis. On the other hand, as Θ approaches 0°, the amount of Y-axis displacement per degree ($dY/d\Theta$) decreases proportionally to the derivative of the Y axis force component, sin Θ. This *axial force-displacement trade-off* was first noted by Brainerd and Azizi (2005) and describes how muscle orientation affects the ability of a muscle to produce force along a given axis and to produce movement through rotation.

The axial force-displacement trade-off assumes that muscle force is constant at different orientations. However, the axial force-displacement tradeoff is complicated by the force-velocity curve, in which force decays exponentially as velocity increases (Hill 1938). Because the force-velocity curve results from changes along a single dimension—length—it is referred to here as the *metric force-velocity curve*, which is empirically determined. More orthogonal orientations may allow muscles to shorten at lower velocities in order to maintain a given output hyoid velocity because fiber rotation amplifies how much they displace the hyoid. To clarify whether force loses due to rotation were greater than, less than, or equal to force gains due to slower shortening, the relationship between axial force-velocity trade-offs and the metric force-velocity curve were modeled under isovelocity conditions, in which axial velocity remains constant but

fiber velocity is free to vary. This *geometric force-velocity curve*, which is theoretical rather than empirical, also assumes that muscle activity remains constant among different conditions.

A geometric force-velocity model was built to evaluate how axial force production changes as a function of initial fiber length and orientation in a muscle with a fixed width—in other words, a fixed-gear muscle. This model was used for analyzing the geometric force-velocity curve in mylohyoid within the coronal plane because the distance between the attachment points are fixed due to symphyseal fusion. Essentially, the model assesses how mylohyoid force production is affected by having a higher or lower (i.e., descended) hyoid position relative to the mandible when hyoid elevation distance and velocity are held constant. Two models were generated, one which changed hyoid position by changing fiber length while maintaining mandibular width, and another which changed hyoid position by changing mandibular width while maintaining fiber length.

In the first model, model inputs included hyoid axial displacement magnitude (dY) and the mediolateral (i.e., Z-axis) distance between the mylohyoid origin and insertion (Z), from which relative fiber velocity, fiber force, and axial force were calculated. The model assumes that sarcomere length does not change as fiber length or mandibular width changes. The following calculations were used to determine the model's outputs:

$$dY_n = \frac{dY}{dY} \tag{E3.9}$$

$$Z_n = \frac{Z}{dY} \tag{E3.10}$$

$$L_{start} = \frac{Z_n}{\sin\alpha} \tag{E3.11}$$

$$Y_{start} = \frac{Z_n}{\tan\alpha} \tag{E3.12}$$

$$Y_{end} = Y_{start} - dY_n \tag{E3.13}$$

$$\beta = tan^{-1}\left(\frac{Z_n}{Y_{end}}\right) \quad \text{(E3.14)}$$

$$L_{end} = \frac{Z_n}{\sin\beta} \quad \text{(E3.15)}$$

$$dL = L_{start} - L_{end} \quad \text{(E3.16)}$$

$$\tau_c = \frac{dL_{max}}{v_{max}} \quad \text{(E3.17)}$$

$$v = \frac{dL}{\tau_c} \quad \text{(E3.18)}$$

$$F = \frac{F_0 b - av}{v + b} \quad \text{(E3.19)}$$

$$F_R = \frac{F(\sin\beta - \sin\alpha)}{\beta - \alpha} \quad \text{(E3.20)}$$

where α is the initial fiber angle ranging from 0 to $\pi/2$ radians; β is the final fiber angle, L_{start} and L_{end} are fiber length at the beginning and end of shortening; dL_{max} is the maximum shortening generated by the model across values of α; v_{max} is the maximum velocity normalized to 1.0; τ_c is a time-scaling parameter in units of seconds that normalizes the velocity of the model with the largest dL (i.e., dL_{max}) to 1.0 s^{-1}; which effectively scales all relative shortening velocities by the maximum shortening velocity predicted by the model (Zajac 1989); F_0 is force at $v = 0$—i.e., maximum force—and is normalized to 1.0; a and b are empirically determined constants both set at 0.25 (Hill 1938; Zatsiorsky and Prilutsky 2012); and F_R is mean axial force as the fibers rotate (Benninghoff and Rollhaeser 1952; Brainerd and Azizi 2005). Initial fiber angles where L_{start} was greater than three times dY (indicating extreme hyoid descent) and the resulting β was less than zero (indicating inversion of the mylohyoid) were excluded before determining the time constant for normalizing muscle velocity.

A second geometric force-velocity model was built to evaluate how axial force production changes as a function of mandibular width while initial fiber length was held

constant. This was also a fixed-gear muscle, but instead of simulating hyoid descent by increasing or decreasing fiber length, hyoid position was changed by only changing initial fiber angle. In other words, a wider mandible had a higher hyoid with larger fiber angles, while a narrower mandible had a lower hyoid with smaller fiber angles. Model inputs were hyoid axial displacement magnitude (dY) and the weighted average of maximum mylohyoid length (L), from which relative fiber velocity, fiber force, and axial force were calculated. The following calculations were used to determine the model's outputs:

$$L_n = \frac{L}{L} \tag{E3.21}$$

$$dY_n = \frac{dY}{L} \tag{E3.22}$$

$$Z_n = \sin \alpha \tag{E3.23}$$

$$Y_{start} = \cos \alpha \tag{E3.24}$$

Once L_n, dY_n, Z_n, and Y_{start} were determined, equations 4.13-20 were used to solve for force. As with the previous model, initial fiber angles where the resulting β was less than zero (indicating inversion of the mylohyoid) were excluded from the results before determining the time constant for normalizing muscle velocity.

COMPUTATIONAL MODELING AND MORPHOLOGICAL PERTURBATIONS

A computational model of hyoid kinematics was developed using R (R Core Team 2018). This model predicts hyoid range of motion from craniofacial and hyoid anatomy. The model was developed using *in vivo* data as described below.

For each animal, the coordinates of the following muscles' attachment sites were measured post-mortem: anterior digastric, posterior digastric, geniohyoid, mylohyoid, and

stylohyoid. Post-mortem muscle length was defined as the Euclidean distance between these attachment points as described above. All muscle lengths observed during feeding behavior were then normalized by *post mortem* muscle length. As discussed above, *post mortem* lengths were used to normalize *in vivo* muscle length. Ultimately, normalizing by *post mortem* muscle length improved the predictive power of the model as indicated by increased area under the curve (AUC, see below) of specificity versus sensitivity compared to a model based on *in vivo* resting length (0.878 vs 0.785, respectively).

Model constraints

Constraints on muscle shortening and stretch capacity have been used successfully to predict hyoid range of motion in rabbits (Anapol 1988). Anapol (1988) assumed that muscle cannot shorten more than 30% or stretch more than 50% of its length when the jaws were closed. The same limitations were used in this study. The lengthening limit was selected based on observations of force deficits after passively stretching muscle is beyond 50 % of its initial length, although this limit may overestimate range given that force deficits begin at lower levels of stretch when muscle is actively stretched (Brooks et al. 1995). Moreover, passive manipulations of joints—which is functionally similar to determining a range of motion by muscle extension limits alone—can grossly overestimate the range of motion actually used *in vivo* (Kambic et al. 2017). Therefore, limits on muscle shortening were also imposed.

The shortening limit was selected based on the limits imposed on muscle shortening by morphology of a sarcomere. Myosin length was assumed to be conserved across vertebrates at approximately 1.60 μm, as was Z-disc length (0.05 μm) (Walker and Schrodt 1974; Winters et al. 2011). Actin filament lengths vary across species and are 2.36 μm in macaques and 2.59 μm

in humans, assuming a Z-disc length of 0.05 µm (Walker and Schrodt 1974). Based on formulas provided and empiric values in Gordon et al. (1966) and Otten (1987) and the filament lengths above, optimal sarcomere length in macaques and humans is 2.51 µm and 2.74 µm, respectively, and length-tension curves were constructed for each species (Figure 3.10). Force drops off sharply at about 65 % and 60 % of optimal sarcomere length in macaques and humans. Although post-mortem studies of human suprahyoid sarcomere length indicate that these muscles are may be

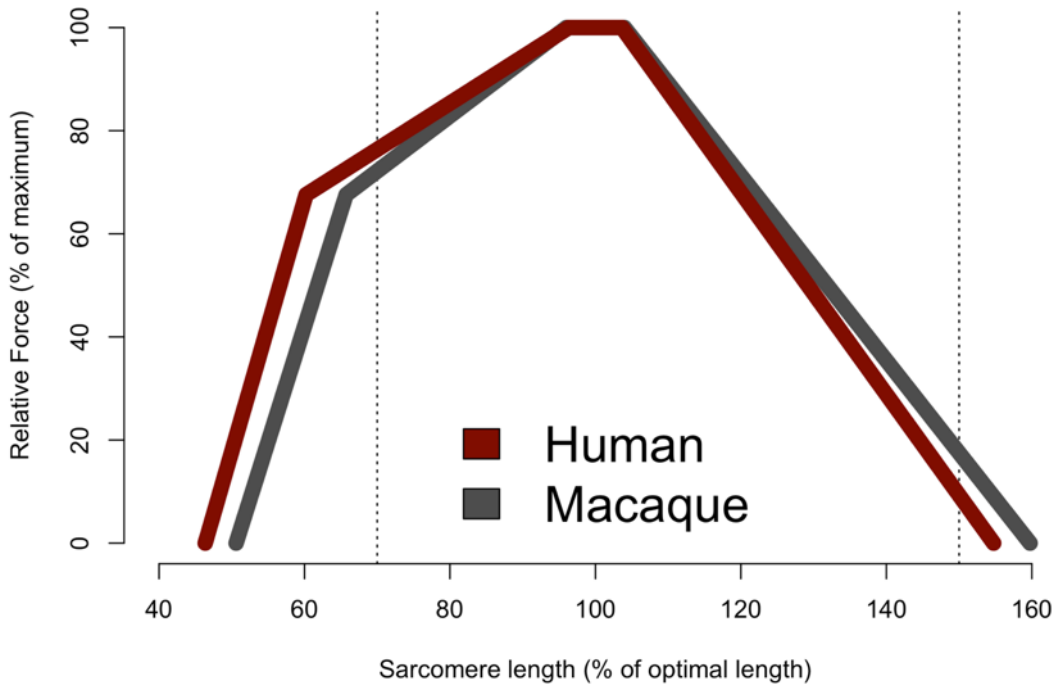

Figure 3.10: Length-tension curve in humans and macaques. Red, human length-tension curve; gray, macaque length-tension curve; vertical dashed lines, 70 % and 150 % of optimal fiber length.

near the plateau (Van Eijden et al. 1997; Pearson et al. 2011), sarcomere lengths may differ *in vivo* because the hyoid is not constrained by joint surfaces, and the posture assumed by the hyoid *post mortem* may not be reflective of its posture or sarcomere lengths *in vivo* (German et al.

2011). A limit of 70 % of initial length represents a conservative approximation—in human-like simulations 60% will overestimate shortening if muscles are on the ascending limb and underestimate shortening if muscles are on the descending limb of the length tension curve. Moreover, 70 % falls within one standard deviation of the mean vertebrate *in vivo* operating range of 81 ± 17% (Burkholder and Lieber 2001).

In addition to using these physiological constraints to estimate maximal range of motion, the model estimated a functional range of motion using maximum and minimum normalized lengths observed *in vivo* during swallowing. These constraints were selected because increasing or decreasing muscle relative length change may affect these muscles' force capacity estimated from the length-tension curve (Gordon et al. 1966). In other words, this study is concerned with predicting functional range of motion in addition to the maximum range of motion. For each swallow, maximum and minimum normalized muscle lengths were measured as described above. Mean muscle maximum and minimum lengths across all animals were then calculated using a weighted average. Each muscle's maximum and minimum length were then increased or decreased, respectively, by the product of the muscle's maximum or minimum length standard deviation and 1.54, as these ranges were found to generate the best fitting model (see "Model validation" below).

Additional limitations were placed on muscle orientation. In models that did not include the digastric, the mylohyoid could not rotate below the average minimum coronal angle (Decreases in mylohyoid coronal angle result in hyoid elevation, see Figure 3.6), and geniohyoid and hyoglossus could not have their insertions on the hyoid more anterior than their origins. Some models included the digastric muscles by simulating an attachment point on the dorsolateral basihyoid at the junction with the greater horn, which is near where the human

digastric connects to the hyoid via a fascial sling (Ozgur et al. 2010; Standring 2015). In these models, the same limitations as above applied with an additional limitation—the digastric insertion could not elevate above a line connecting the origin of the two bellies. This limitation assumes that the digastric can linearize by shortening but not invert after achieving linearization, which would require muscle lengthening as the hyoid elevates. To apply this limitation, an equation predicting the Y-axis values for this line was generated using the lm function in R, and simulated values greater than the predicted Y-axis value were considered inviable.

Model creation

A generalized macaque resting posture was generated by conducting a generalized Procrustes analysis (GPA) using the gpagen function of the geomorph package in R (Adams et al. 2017). The coordinates of the muscle attachment sites, hyoid position, and cranial and mandibular coordinate system origins were used as the GPA landmarks. The data were transformed into a cranial coordinate system using the same custom-written R scripts used for kinematic analysis described above. Because these landmarks were transformed into a cranial coordinate system, aligning the data by principle axes was unnecessary, and this condition was set to FALSE in the gpagen function. The resulting consensus coordinates were used as the resting posture of the model.

Human-macaque hybrid model parameters were adjusted manually to minimize disparities in muscle length with human reference values from the literature. Two studies report total muscle length, one *post mortem* (Pearson et al. 2011) and another *in vivo* (Okada et al. 2013). *Post mortem* muscle lengths were extracted from Figure 3 of Pearson et al. (2011) using DataThief (Tummers 2006). However, the figure is two dimensional and mediolateral

displacement of attachment sites are not reported in the Pearson et al. (2011) study, and two-dimensional measurements necessarily underestimate muscle length. To correct for this underestimation, macaque muscle length was measured both in three dimensions in a sagittal plane, and the Pearson et al. values were then multiplied by the ratio of macaque 3D muscle length to 2D muscle length. *In vivo* muscle lengths measured in three dimensions were also collected from Table 2 of Okada et al. (2013). Although the table contains maximum muscle lengths, the authors state that in most individuals "maximal muscle length corresponded to the length at rest" (Okada et al. 2013). These studies do not report human values that could be used to normalize muscle lengths. Therefore, muscle lengths were normalized using an average human mandible length from the literature (Ross et al. 2009).

The model parameters were then manually adjusted to minimize differences among the relative lengths of model muscles and available *post mortem* and *in vivo* data. The differences in relative muscle length among this and other studies in the literature as well as the parameters selected for this study are found in Tables 3.5 and 3.6 below. Except for hyoid compression and mandible width, input parameters defined how posture was changed as a proportion mandibular length, defined as the sagittal distance from condylion to infradentale (Ross et al. 2009). To generate the human-macaque hybrid model, facial shortening was first simulated by decreasing the sagittal distance between posterior condylion and infradentale by 37.24 %, given that the human mandible is 33.46% shorter than predicted for its body mass, whereas the macaque is 3.78 % longer (Ross et al. 2009). This was achieved by solving for the X-axis coordinate of infradentale that shortened sagittal mandibular length by 37.24 %—this X-axis coordinate was set as the new infradental position. A retraction coefficient was then calculated from the ratio of the difference between the original and new infradental X-axis coordinates to the original X-axis

coordinate and was found to be -0.3879. The X-axis distances from the geniohyoid and hyoglossus origins were then similarly measured, and these coordinates were displaced posteriorly by the product of this distance and the contraction coefficient. Mylohyoid, the posterior suprahyoid muscles, and the hyoid itself were assumed to be unaffected by facial shortening and accommodated by changes in muscle length unless otherwise specified by the model (e.g., the hyoid descends or the styloid process is longer). Figure 3.11 demonstrates how the original macaque model compares with the hybrid model.

All other parameters were then adjusted manually in a step-wise fashion to minimize differences between model relative muscle lengths and literature relative muscle lengths as stated above (Table 3.5). First, to simulate dorsoventral compression of the hyoid, hyoid insertion point Y-axis coordinates were brought closer to the centroid of all hyoid markers. The input parameter for dorsoventral compression determined the percentage by which these markers were brought closer to the centroid Y-axis coordinate. For example, an input parameter of 100 % homogenized all hyoid Y-axis coordinates, while an input parameter of 0 % left all markers in place. The following parameters were then adjusted until muscles were of intermediate length relative to literature values: for mylohyoid, the hyoid was inferiorly displaced; for geniohyoid, the symphysis was anteriorly displaced; for anterior digastric, the origin was displaced to the new geniohyoid and further protracted and depressed; for posterior digastric and stylohyoid, the basicranium was displaced anteriorly and inferiorly; for stylohyoid, the styloid process was retracted and elevated after basicranial flexion. The exact changes made are found in Table 3.6.

Table 3.5: Human-macaque hybrid model raw and relative muscle length vs. literature values

	AD	GH	HG	MH	PD	StyH
Raw Length	0.175	0.131	0.230	0.178	0.345	0.268
Relative Length	0.427	0.321	0.562	0.435	0.843	0.655
% different from Okada et al. 2013	-5.1 %	-2.0 %	—	+2.1 %	-1.7 %	+9.7 %
% different from Pearson et al. 2011	+5.1 %	+1.9 %	—	-2.1 %	+ 1.8 %	-9.7 %

AD, anterior digastric; GH, geniohyoid; HG, hyoglossus; MH, mylohyoid; PD, posterior digastric; StyH, stylohyoid

Table 3.6: Changes in model conditions for the Human-macaque hybrid simulation

Condition	Effect
Shortened Mandible (SM)	Anterior digastric, geniohyoid, and hyoglossus origins posteriorly displaced by 37.2 % of mandibular length (ML)[4]
Physiological Length Limitations (PL)	Minimum and maximum muscle length are 70 % and 150 % of initial length.
Hyoid Descent (HD)	Hyoid marker and muscle insertions displaced inferiorly by 14.1% of ML
Hyoid Compression (HC)	Hyoid locator and muscle insertions brought 90 % closer to the centroid of all hyoid markers
Vertical Symphysis (VS)	Geniohyoid origins anterior displaced by 9.525 % of ML; if digastric is included, anterior digastric is displaced 15 % of ML anteriorly and 4.7625 % of ML inferiorly
Basicranial Flexion (BCF)	Posterior digastric and stylohyoid origins displaced anteriorly and inferiorly by 12.75 % and 19.0 % of ML.
Digastric (Dig)	Digastric bellies insert into hyoid; digastric origin relocated to geniohyoid origin
Mandibular Width (MW)	Included as a parameter in the model, but not needed to make relative muscle length approximate literature values
Styloid Process	Stylohyoid origin displaced posteriorly and superiorly by 2.48 % and 2.49 of ML

[4] Mandibular length defined as mean the sagittal distance between infradentale and the posterior surface of the condyles bilaterally (Ross et al. 2009).

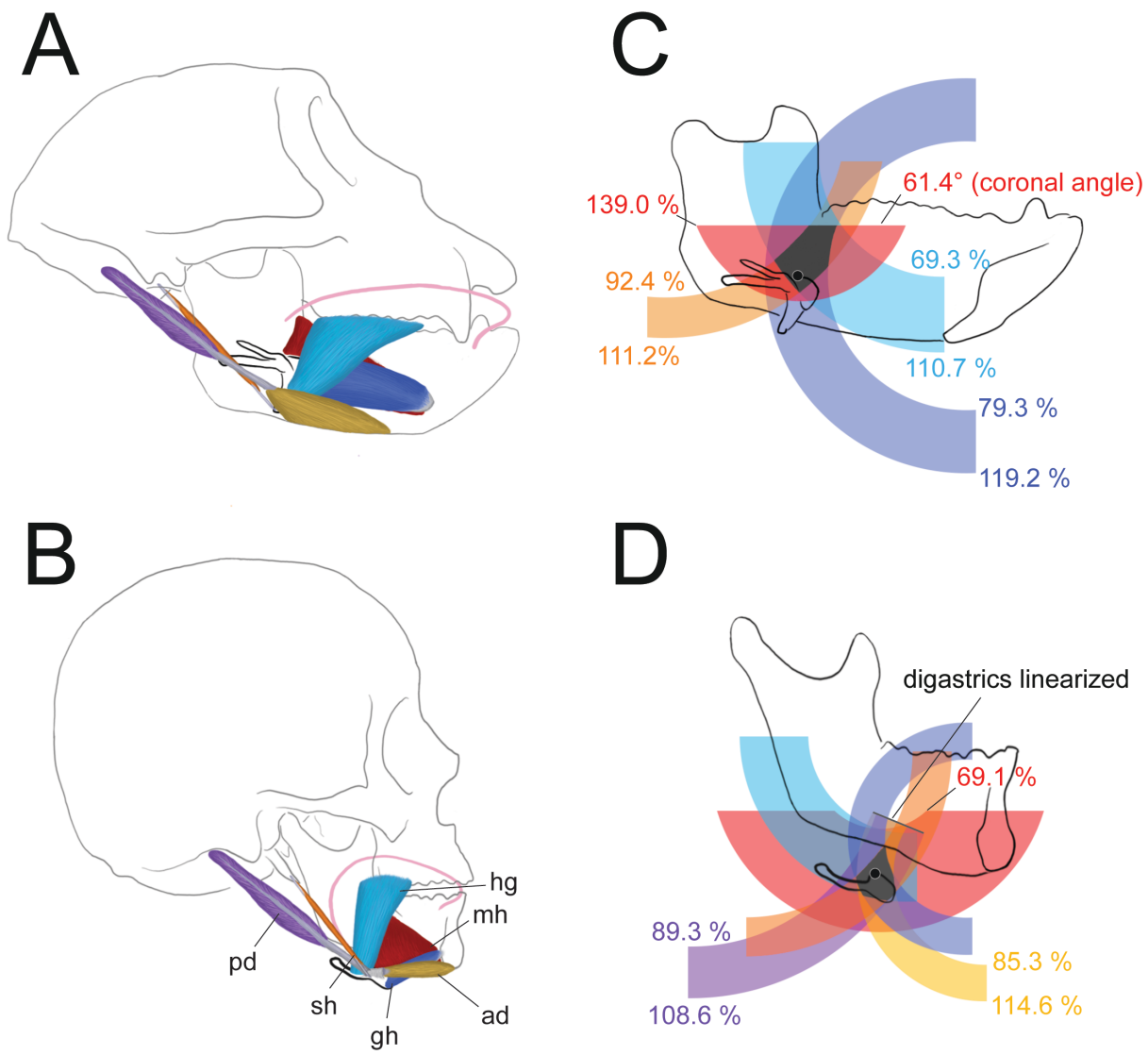

Figure 3.11: Macaque and hybrid models for hyoid range of motion and their constraints. A) Macaque hyolingual anatomy. B) Human hyolingual anatomy. C) The macaque model's range of motion (gray polygon) is determined by the overlap of the range of motion of geniohyoid (dark blue), hyoglossus (light blue), mylohyoid (red), and stylohyoid (orange). Mylohyoid does not reach its shortening limit because it reaches its fiber angle limit in coronal planes (28.6°) beforehand. D) Hybrid model is additionally limited by anterior digastric (yellow) and posterior digastric (purple) range of motion. In C and D, muscle length limits are reported as a percentage of *post mortem* length, and the black dot on the hyoid indicates the point that moves through the range of motion. Digastric bellies' range of motion is further limited by the line at which the digastric as a whole linearizes.

Kinematic simulation

The kinematic simulation compared muscle kinematics against the model's constraints at different hyoid positions using custom-written code in R. Based on the minimal rotational and mediolateral movements observed *in vivo*, the hyoid was assumed to neither rotate nor deviate from the midline. Although simulations varied hyoid position in only two dimensions, muscle length and orientation were measured in three dimensions. For model validations, the simulation evaluated 10,000 points within a square area from (-25, -50) to (25, 0), measured in a cranial coordinate system in millimeters. For model simulations, the simulation increased the sampling density to 40,000 points within a square area from (-0.20, -0.30) to (0.20, 0.10), measured in arbitrary units in a cranial coordinate system. The hyoid marker was translated to each of these cells, and the difference between the hyoid resting position and each cell was used to translate the muscle insertion locations. Muscle length and, if applicable, orientation and position, were then measured and compared against the model limitations. If the model failed any of the conditions, then the cell coordinates were considered inviable and recorded as such. If all conditions were met, the results were considered viable and were included in the range of motion (Figure 3.11).

To evaluate model performance, the minimum distance between all points in the range of motion and an excursion target was measured for each model. An excursion target is here defined as a kinematic endpoint for hyoid translation that is assumed to produce safe swallowing kinematics. If the minimum distance between all of the points and the excursion target is less than the distance between points within the range of motion, then the excursion target fell within the range of motion.

Macaque kinematics, sagittal mandibular length, and body mass were collected using the same animals used in the studies described above. Maximum hyoid protraction and elevation were often not simultaneous. To prevent overestimating hyoid excursion, hyoid protraction and elevation were measured in a cranial coordinate system at the time of maximum excursion from the *post mortem* hyoid position in each macaque. Protraction and elevation from this *post mortem* hyoid position were then averaged for each animal. These averages were then normalized by each individual's mandibular length and body mass.

The following human data were collected from the literature: hyoid kinematics (Perlman 1995; Kim and McCullough 2008), mandibular length (Ross et al. 2009), and body mass (Ross et al. 2009). The Perlman et al. (1995) and Kim and McCullough (2008) studies were chosen in particular because they measured hyoid protraction and elevation simultaneously at the time of maximum excursion. Other studies report maximum protraction and elevation, but as stated above, maximum protraction and elevation were often not simultaneous in this study's macaques. Therefore, using maximum protraction and elevation could overestimate hyoid excursion, and so only the data from Perlman et al. (1995) and Kim and McCullough (2008) were used to ensure that human hyoid excursion was not also overestimated. These protraction and elevation values were then normalized by literature values for mandibular length and body mass (Ross et al. 2009). Results of these normalizations are included in Chapter 6. Because the model is primarily concerned with the effects of geometry on hyoid kinematics, excursion targets were scaled by mandibular length. Models with unmodified mandibular length had kinematic targets derived from macaque data. Models with shortened mandibular length had kinematic targets derived from human data.

Model validation

An ideal model predicts an individual's hyoid range of motion from the individual's anatomy and the model's assumed muscle length limitations without false positives or negatives (Type 1 and Type 2 error, respectively). When average muscle length limitations were used, false positives were low, but the false negative rate was high. As a result, hyoid excursion would be underestimated by the model. Decreasing minimum muscle length and increasing maximum muscle length by a proportion of standard deviations for each muscle could decrease the risk of false negatives but increase the risk of false positives. As such, the best proportion by which to change muscle length limitations was unclear.

A similar error-reduction dilemma is presented when choosing cutoff values for diagnostic tests that are used to determine a patient's disease status or risk of developing disease (Obuchowski 2003). To resolve this dilemma, two ratios—sensitivity and specificity—are often used to quantify a test's predictive power at each cutoff value for a diagnostic test (Obuchowski 2003). In the case of the range of motion model, diagnostic cutoff values are analogous to the proportion of each muscle's standard deviation to be subtracted from or added to minimum or maximum muscle length, respectively. Sensitivity, or the true positive rate, describes the test or model's ability to minimize false negatives and is measured as the ratio of true positive results to total positive results. When false negatives are minimized, the true positive rate, i.e., sensitivity, approaches 1. Specificity, or true negative rate, describes the test or model's ability to minimize false positives and is measured as the ratio of true negative results to total negative results.

The receiver operating characteristic (ROC) curve quantifies how sensitivity and specificity change as a function of the cutoff value. To create an ROC curve, one plots sensitivity versus 1 – specificity (i.e., the false positive rate) (Lusted 1971). The term ROC implies that the

individual receiving the resulting information has some flexibility to operate at any point along the curve depending on how the test will be used (Obuchowski 2003). For example, if minimizing type 2 error is more important, as it is in most screening tests, then one would use a cutoff with a larger sensitivity and smaller specificity. If one wishes to minimize both types of error, then the cutoff value which minimizes the differences of both sensitivity and specificity from 1. This value is quantified as the point with the minimum distance from the upper-left hand corner of the plot, which represents a perfect model with a sensitivity (true positive rate) and specificity (true negative rate) of 1. Such an approach was applied in this study.

A model's predictive power can be described by the area under the curve (AUC) of the ROC curve. A perfect model or test has an area of 1.0 and is represented by a square ROC curve, while a completely random test has an area of 0.5 and is represented by a line from 0, 0 to 1, 1 that is also known as the chance diagonal (Obuchowski 2003). The AUC reflects model accuracy and provides the probability that, given a randomly selected point inside the *in vivo* ROM and a randomly selected point outside of the *in vivo* ROM, the point inside the *in vivo* ROM will fall within the predicted ROM and the point outside of the *in vivo* ROM will fall outside the predicted ROM (Obuchowski 2003). AUC was calculated by summing the area of rectangles with a height of the value of sensitivity and a width of the difference in specificity between each multiple of standard deviation:

$$AUC = \sum_{i=1}^{17} Sensitivity \cdot \Delta Specificity \tag{E3.25}$$

The integrated AUC of a natural spline fitted to the sampled multiples of standard deviations was only 0.1% greater than the AUC calculated directly from the sampled multiples using E3.25, and the latter is reported in the results.

To quantify the *in vivo* and predicted ROM, viable cells identified by the model and *in vivo* coordinates were used to create alpha hulls, which are generalized versions of a convex hull which allow for concavities in the polygon. The tolerance for concavities is determined by the input alpha parameter. Lower alpha values reduce the minimum radius of concavity curvature that can be included in the hull, but values that are too low result in collapsing of the polygon due to oversensitivity. The lowest alpha value tolerated differed at some standard deviation multiples but was 0.05 in most cases. Alpha hulls were created using the ahull function of the alphahull package in R. The model generates many predicted values which are collinear, yet alpha hull algorithms do not tolerate collinear points. To resolve this problem, a small amount of random noise (< 1e-5) was added to each coordinate. The extrema were then extracted and used to construct polygons of the predicted and *in vivo* range of motion. A separate polygon was then constructed from the overlapping area using the joinPolys function of the PSBmapping function in R. The areas of the model ROM (A_{model}), *in vivo* ROM ($A_{in\ vivo}$), and overlapping ROM ($A_{overlap}$) were then calculated from these polygons using the areahull function of the alpha hull package. The area that would be used to define true negatives and false positives could, in theory, be infinite and artificially inflate specificity. To control for this possibility, the total population of cells was limited to the product of the anterior and superior excursion ranges, each of which was multiplied by 1.25. The resulting area (A_{total}) was larger than the predicted area at most multiples of standard deviation. In cases where the predicted area was larger than the total population of cells, specificity was less than zero, and these values were corrected to zero manually. Additionally, minor differences in area values due to alpha value selection could cause the overlapping area to be greater than the *in vivo* area even when the *in vivo* area was completely enclosed within the predicted area. Consequently, all sensitivity values greater than

one were manually corrected to one. The equations used to calculate sensitivity and specificity were as follows:

$$P = A_{model} \tag{E3.26}$$

$$N = A_{total} - A_{model} \tag{E3.27}$$

$$TP = A_{overlap} \tag{E3.28}$$

$$FP = A_{model} - A_{overlap} \tag{E3.29}$$

$$FN = A_{in\ vivo} - A_{overlap} \tag{E3.30}$$

$$TN = A_{total} - (FN + TN + FP) \tag{E3.31}$$

$$Sensitivity = \frac{TP}{P} \tag{E3.32}$$

$$Specificity = \frac{TN}{N} \tag{E3.33}$$

where P was positive area, N was negative area, TP was true positive area, FP was false positive area, FN was false negative area, and TN was true negative area. Sensitivity and specificity were measured for the multiples of standard deviation (hereafter referred to as 'multiples') with values ranging from 0 to 4.0 by increments of 0.25 for a total of 17 multiples.

An ROC curve was generated from the sensitivity and specificity for each multiple. A natural spline function was used to interpolate points along this curve. The point which minimized the distance between the curve and a value of (0, 1.0) on the graph was selected as the multiple for the model (multiple = 1.54, see Chapter 6).

CHAPTER FOUR: THE MECHANISM OF TONGUE BASE RETRACTION: EVIDENCE FOR A HYDRAULIC LINKAGE BETWEEN THE TONGUE AND HYOID

INTRODUCTION

Tongue base[5] retraction (TBR) is an essential component of airway protection during swallowing because it clears the airway before respiration resumes and helps to flip the epiglottis over the laryngeal inlet (McConnel 1988; Dejaeger et al. 1997, Knigge and Thibeault 2016, Pearson et al. 2016). This posterior displacement of the tongue base is hypothesized to be due to a combination of extrinsic (styloglossus, hyoglossus) and intrinsic (transverse lingual) muscle shortening (Napadow et al. 1999; Felton et al. 2007; Gilbert et al. 2007; Gassert and Pearson 2016). Specifically, shortening of the hyoglossus and styloglossus are hypothesized to pull the tongue base posteriorly, while transverse muscles decrease tongue width resulting in hydrostatically driven increases in its length and depth—i.e., the magnitude of the tongue's anteroposterior and superoinferior dimensions, respectively (Hiiemae and Crompton 1985; Napadow et al. 1999; Felton et al. 2007, Gilbert et al. 2007, Gassert and Pearson 2016; Pearson et al. 2016). Studies using midsagittal dynamic MRI observed increases in posterior tongue length and depth to infer that the tongue decreases in width during swallowing (Napadow et al. 1999; Felton et al. 2007; Gilbert et al. 2007). Moreover, studies of muscle activity in many

[5] As discussed in Chapter 1, several terms have been used to describe the different parts of the tongue. The oral tongue is the anterior two-thirds of the tongue anterior to the circumvallate papillae. In this study, markers located halfway between the posterior-most circumvallate papillae and the tongue tip, or apex, separate the oral tongue into an anterior oral tongue (or tongue blade) and posterior oral tongue (or tongue body). The pharyngeal tongue is the posterior one-third of the tongue posterior to the circumvallate papillae (Standring 2016). In this study, the pharyngeal tongue is synonymous with the tongue base or base of tongue referred to in the clinical literature (e.g., Logemann and Bytell 1979; Logemann et al. 1998; Pauloski et al. 2000; Veis et al. 2000; Lazarus et al. 2002). The tongue base is not to be confused with the tongue root, which forms the inferior aspect of the tongue where it is attached to the hyoid and mandible and is spatially related to mylohyoid and geniohyoid (Standring 2016).

mammals, including humans, have demonstrated that styloglossus and hyoglossus are indeed active during swallowing (Doty and Bosma 1956; Thexton et al. 1998; Naganuma et al. 2001; Thexton et al. 2012; Gassert and Pearson 2016). However, this extrinsic/intrinsic muscle shortening hypothesis heavily relies on three untested or recently falsified assumptions: 1) the tongue does not shear—that is, that the lateral tongue retracts the same distance as the tongue midline, 2) the styloglossus and hyoglossus shorten during TBR and 3) tongue volume is regionally conserved during TBR.

In their MRI study of tongue deformation during swallowing, Napadow et al. (1999) assumed that the tongue does not experience intrinsic shear deformation in axial and coronal planes. If true, then one can extrapolate the superoinferior and anteroposterior positions of the tongue midline to the lateral portions of the tongue and vice versa. But, if tongue midline movements do not match those of the lateral tongue, then this non-sagittal shear strain renders previous estimates of tongue mediolateral width inaccurate. A study of swallowing in cats found no qualitative differences in the amount of retraction between the midline and lateral tongue (Thexton and Mcgarrick 1988); however, this hypothesis has not been tested in humans or nonhuman primates.

The assumption that the function of styloglossus and hyoglossus during tongue retraction can be inferred from morphology and muscle activity patterns alone is almost certainly unjustified. Hyolingual muscle function depends not on the muscle's morphology and activity level but also its length and velocity (Thexton 1984; Dickinson et al. 2000; German et al. 2011; Orsbon et al. 2018). Muscles can be active during either shortening (concentric activation), lengthening (eccentric activation), or stasis (isometric activation), with each of these velocities implying different functional roles for the muscle (Dickinson et al. 2000). In order to

demonstrate that styloglossus and/or hyoglossus cause TBR, they must decrease in length as the tongue base retracts. Alternatively, if the tongue shears in coronal and axial planes, then the lingual insertions of the styloglossus and hyoglossus may not retract, and thus stylogossus may be isometric, whereas hyoglossus shortening would be associated with hyoid excursion rather than tongue retraction.

Some studies raise the possibility that mammalian tongues can exhibit regional changes in volume. Potential fluctuations in local tongue volume arise not from violations of the incompressibility of muscle tissue itself, but rather from interactions with other tissue types. In a nectar-feeding glossophagine bat, *Glossophaga soricina*, blood erects lingual papillae to increase the volume of nectar acquired with each lap (Harper et al. 2013). This hydraulic mechanism involves displacement of blood volume from the vessels within the tongue body to sinuses in the papillae, similar to tumescence in mammalian erectile tissue, although the mechanism (and context) differs. Consequently, the volume of the muscular hydrostat portion of the tongue may change if pressure within the tongue body during protrusion exceeds intravascular pressures and causes vessel collapse. Similarly, tongue protrusion in the echidna (*Tachyglossus*) is thought to be facilitated by a "musculohydraulic process" in which cavernous sinuses fill with blood (Doran and Baggett 1970; Doran and Baggett 1971). Regional changes in volume have also been observed in pigs during chewing, ingestion, and drinking (Liu et al. 2008; Liu et al. 2009), but the mechanical basis of these regional volume changes is unclear.

Although vascular sinuses similar to those in glossophagine bats and echidnas have not been reported in pigs or primates, regional tongue volume could change due to passive tongue deformation by active shortening in muscles that do not directly insert into the tongue, namely the suprahyoid muscles. If suprahyoid muscle shortening regionally displaces tongue volume to

produce TBR, then the suprahyoid muscles and tongue would constitute a hydraulic mechanism, "which involves displacement of fluid from one location in order to cause shape change or exert force elsewhere" (Kier 2012). Although hydraulic mechanisms are prevalent throughout invertebrates and vertebrates—including echinoderm tube feet, mammalian penises, and even mammalian tongues as described above (Doran and Baggett 1970; Kier 2012; Harper et al. 2013; Vogel 2013)—no study has probed the possibility that muscular hydrostats could function hydraulically. Because muscle tissue is composed predominantly of water, a relaxed muscular hydrostat could function more like a liquid, passively deforming and regionally changing volume as a result of activity in non-lingual muscles. In the case of the hyolingual apparatus, the oral cavity constitutes a 'lumen' which contains a deformable but incompressible tongue volume, much like conventional biological hydraulic mechanisms involve a lumen filled with an incompressible liquid. Hyoid excursion and mouth floor elevation decrease the volume of this lumen and force the tongue volume to displace posteriorly because the tongue displacement is blocked superiorly by the hard palate, anterolaterally by the tooth row, and inferiorly by the stiffened mouth floor. In such a scenario, the suprahyoid muscles essentially squeeze the tongue backwards, analogous to how the tongue itself squeezes the bolus backwards during swallowing as the posterior sweep of the palate-tongue contact point pushes the bolus posteriorly (Chapter 1; Franks et al. 1984; German et al. 1992; Palmer et al. 1992).

Hypotheses

This study tests three hypotheses regarding the mechanisms of TBR during swallowing. First, the hypothesis that extrinsic muscle shortening causes TBR is tested by measuring how much each of the extrinsic muscles shortens during swallowing. The extrinsic

muscle hypothesis is falsified if the tongue base retracts more than these muscles, in the case of hyoglossus, if its lingual insertion does not retract as the muscle shortens.

Second, the hypothesis that intrinsic muscle shortening causes TBR is tested by measuring dimensional changes in the tongue during swallowing. The intrinsic muscle hypothesis can be falsified by two outcomes: all three dimensions of the tongue base increase, and/or the tongue base increases in volume. (The former necessitates the latter, but not vice versa because volume can still increase even if one or two dimensions decrease.)

Third, the hypothesis that hyoid protraction and mouth floor elevation cause TBR via a hydraulic linkage between the tongue and suprahyoid muscles is tested by comparing the temporal structure of changes in the volumes of the tongue and oral cavity. This hypothesis is falsified if tongue base volume does not increase as the hyoid elevates and protracts, the mouth floor elevates, and oral volume decreases.

RESULTS

Some measurements of muscle length and tongue kinematics were not possible in all animals, although nearly all variables were measured in at least two animals. In Monkey Ch, the palatal palatoglossus marker and lingual hyoglossus markers were not implanted close enough to the muscle to justify using these markers to measure muscle lengths. In Monkey He, palatal palatoglossus markers were not implanted due to concerns that these markers would occlude tongue markers in future neurophysiological experiments. Additionally, Monkey He's vallecular marker extruded during healing. In Monkey Ki, the posterior deep marker was implanted more deeply than the other markers and was adjacent to the hyoid. Consequently, its kinematics were very different from the same marker in other animals (Figures A2-5), but were more similar to

those reported by Nakamura et al. (2017). Accordingly, the posterior tongue markers in Nakamura et al. (2017) were in a similar location to Monkey Ki's posterior deep marker. Lastly, Monkey Ki did not receive digastric markers. For each of these exceptions, the animal was subsequently excluded from analyses that aggregated measurements across animals.

Hyolingual Kinematics During Tongue Base Retraction

Hyolingual kinematics were similar across animals. During tongue base retraction (TBR), the midline posterior markers retracted and elevated significantly more than lateral posterior tongue markers ($p < 0.002$); more anterior markers tended to protract and, because the mandible depressed during TBR, depress slightly (Figures 4.1, A1-5).

Does extrinsic muscle contraction explain TBR?

On average, hyo-, palato-, and styloglossus were predominantly posteriorly oriented during TBR ($135° < \Theta_{sagittal} < 225°$; superior = 90°, posterior = 180°, inferior = 270°). Because all three muscles maintained an orientation between 90 and 270 degrees throughout TBR, each muscle was theoretically capable of producing posteriorly-oriented forces necessary for TBR.

If extrinsic muscles caused TBR, then one would expect that these muscles shorten as much as the tongue base retracts. Tongue base retraction distance significantly exceeded shortening distances of palatoglossus and styloglossus, but not hyoglossus. As shown in Figure 4.2, retraction of the posterior surface (6.85 ± 1.88 mm, mean ± SD), posterior deep (4.32 ± 0.89 mm), and vallecular (3.97 ± 1.57 mm) markers was much greater than shortening of either palatoglossus (-0.06 ± 1.27 mm) or styloglossus (0.43 ± 1.32 mm) ($p < 0.001$). Hyoglossus

shortening (4.74 ± 1.30 mm) most closely approximated TBR magnitude; however, right lateral tongue markers—implanted where the right hyoglossus inserts into the tongue—tended to slightly protract (0.93 ± 1.63 mm) (Figure 4.1, in orange). Moreover, the hyoid elevated (2.05 ± 0.71 mm) and protracted (4.30 ± 1.51 mm) as hyoglossus shortened. All differences among tongue marker retraction and muscle length change were statistically significant after Bonferroni correction except for the differences between posterior deep and vallecular marker retraction and between posterior deep retraction and hyoglossus shortening in both mandibular and cranial coordinate systems.

Does intrinsic muscle contraction cause TBR?

If intrinsic muscles caused TBR, then one would expect that the tongue would decrease in width or height as the tongue base retracts so that tongue volume remains constant. Tongue base (TB) and posterior oral tongue (POT) volume increased (0.72 mL ± 0.22 mL, 417 % ± 217 % and 0.99 mL ± 0.63 mL, 27.9 % ± 16.7 %, respectively) while anterior oral tongue (AOT) volume remained relatively constant during TBR (-0.04 ± 0.12 mL, -1.5 % ± 11.5 %) (Figure 4.3). The width of the TB and posterior POT (i.e., the interface between the two volumes) changed little (-0.10 ± 1.37 mm) while this interface's depth (3.53 ± 2.04 mm), TB length (3.22 mm ± 1.08 mm), and POT length (7.88 ± 1.71 mm) increased. In contrast, AOT dimensions changed little during TBR (width: 0.30 ± 1.02 mm, depth: -0.55 ± 0.95 mm, length: -0.62 ± 1.44 mm).

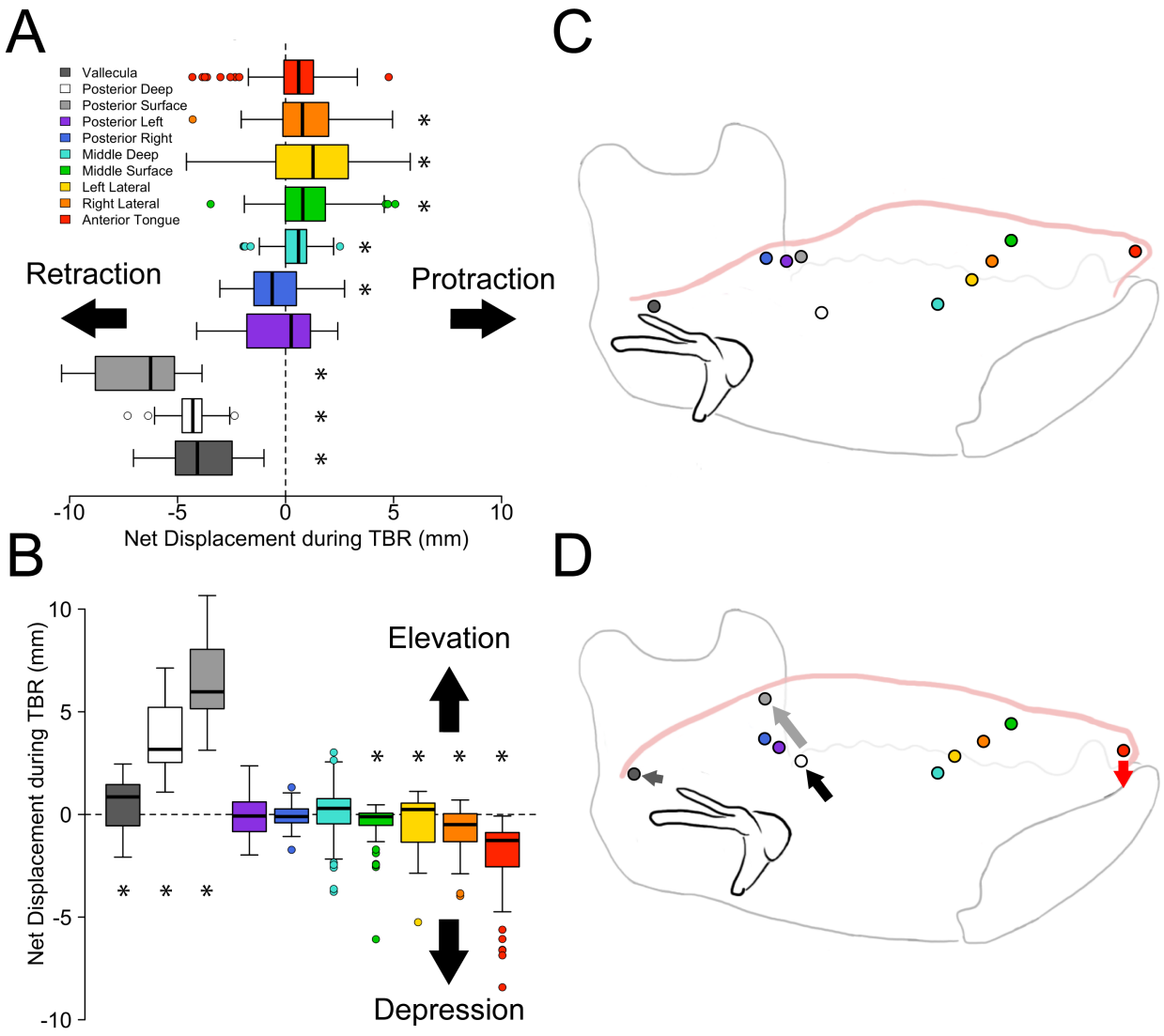

Figure 4.1: Tongue kinematics during tongue retraction in cranial coordinate system. Measurements were taken relative to the marker's position at the start of TBR. Positive values indicate protraction or elevation, negative values indicate retraction or depression. A) Tongue marker anteroposterior displacement. B) Tongue marker superoinferior displacement. C) Illustration representative of observed hyolingual posture and marker position at retraction onset and D) offset. Data are averaged across all monkeys. Boxes indicate the interquartile range, thick bars indicate median, error bars indicate data range, and circles are outliers. Asterisks indicate the mean is significantly different from zero using a one-sample t-test. Arrows indicate marker trajectories. Colors correspond to the following markers: red, anterior; orange, right lateral; yellow, left lateral; green, middle surface; light blue, middle deep; dark blue, posterior right; purple, posterior left; gray, posterior surface; white, posterior deep; dark gray, vallecula. Measurements are in a cranial coordinate system (CCS). The same measurements taken in individual monkeys as well as within a mandibular coordinate system are included in Figures A1-5.

Table 4.1: Muscle orientation ($\Theta_{sagittal}$) during tongue base retraction (cranial coordinate system)

Monkey	Hyoglossus		Palatoglossus		Styloglossus	
	Mean	Range	Mean	Range	Mean	Range
C	—	—	—	—	168.89°	151.02°-178.07°
H	227.60°	203.60°-252.99°	—	—	175.50°	151.20°-183.38°
J	211.90°	186.97°-222.94°	166.97°	131.81°-186.57°	167.73°	153.66°-183.63°
K	227.10°	212.27°-240.02°	137.81°	94.87°-174.57°	185.89°	169.86°-191.80°
Overall	223.17°	186.97°-252.99°	151.14°	94.87°-186.57°	174.42°	151.02°-191.80°

$135° < \Theta_{sagittal} < 225°$; superior = 90°, posterior = 180°, inferior = 270°

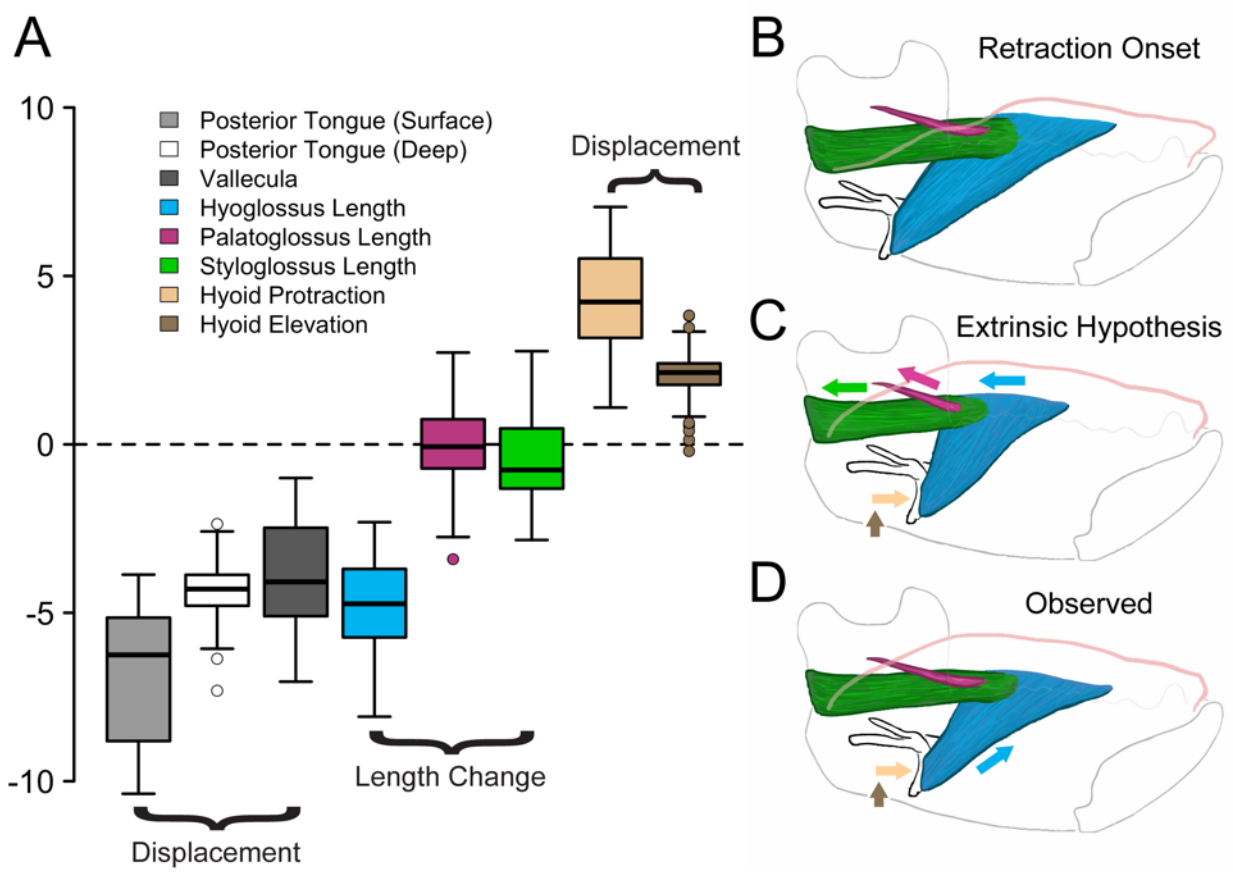

Figure 4.2: Hyolingual and muscle kinematics during TBR in a cranial coordinate system. A) Positive values indicate hyoid protraction, hyoid elevation, or muscle lengthening; negative values indicate TBR or muscle shortening. B) Representative observed extrinsic muscles and hyolingual posture at TBR onset. C) Extrinsic muscle length and hyolingual posture at the end of TBR, as predicted by the extrinsic hypothesis. D) Representative observed extrinsic muscle length and hyolingual posture at the end of tongue retraction. Boxes indicate the interquartile range, thick bars indicate median, error bars indicate data range, circles are outliers. Arrows indicate the trajectory of hyoid movement and muscle shortening.

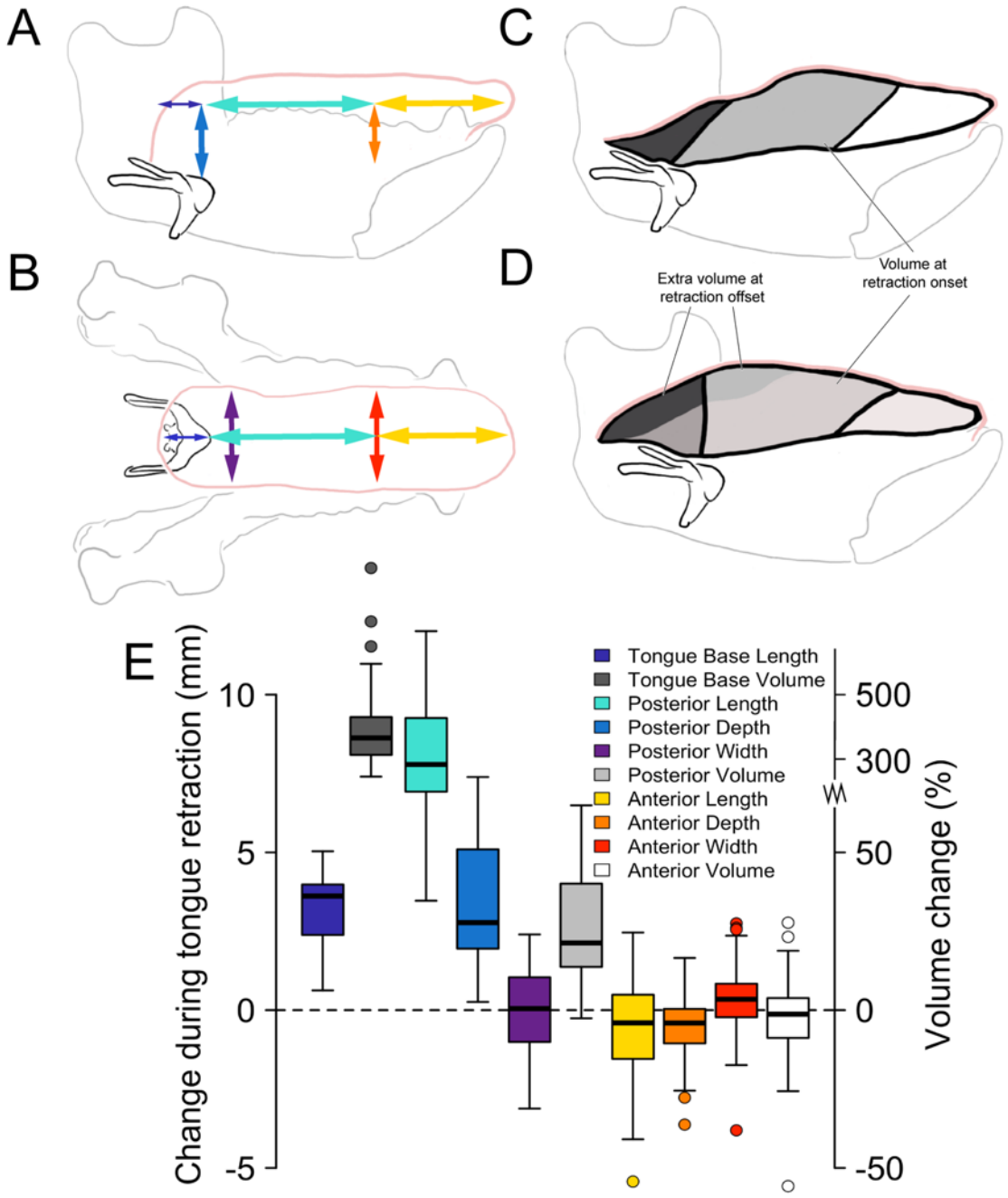

Figure 4.3: Changes in tongue dimensions during TBR in a cranial coordinate system. A, B) Lateral and transverse views of the tongue, with arrows corresponding to colors in legend in E. C, D) Lateral views of the tongue at C) retraction onset and D) retraction offset. The tongue volume is broken into three parts: anterior (white), posterior (light gray), and tongue base (dark gray). E) Box plots of changes in tongue dimensions and volume during retraction. Data were averaged across all monkeys. Boxes indicate the interquartile range, thick bars indicate median, error bars indicate data range; filled circles are outliers. Because the tongue base and posterior oral tongue share a common interface, posterior width and depth are equal to tongue base width and depth.

Does a hydraulic mechanism explain TBR?

After finding that TB and POT volume increased during TBR, tongue volume and dimensions were compared with oral volume over time (Figure 4.4). If regional changes in tongue volume—i.e., a hydraulic mechanism between the tongue and hyoid apparatus—caused TBR, then one would expect that tongue base volume would increase as oral volume decreases due to hyoid excursion. Oral volume decreased rapidly during the intercuspal phase before TBR and during early TBR, albeit with low levels of jaw depression (Figure 4.5); however, oral volume began to increase before the end of TBR in all animals as the mandible continued to depress. This increase in oral volume suggests that during the later stages of TBR, the oral cavity did not function as a closed container for the tongue volume. The POT initially increased in volume rapidly, reached its maximum volume during the middle of TBR, and then declined slightly as oral volume began to increase. As POT volume became relatively static or declined slightly, TB volume nonetheless continued to increase until shortly after TBR offset despite slightly decreased TB width and, to a lesser extent, depth during late TBR (Figure 4.6). The results suggest that retraction of the interface between the TB and POT is driven by decreased oral volume as the hyoid protracts and elevates, whereas retraction of the vallecular marker (i.e., the posterior TB) is driven by a combination hyoid excursion and hydrostatic deformation once the dorsal tongue has been anchored against the hard palate.

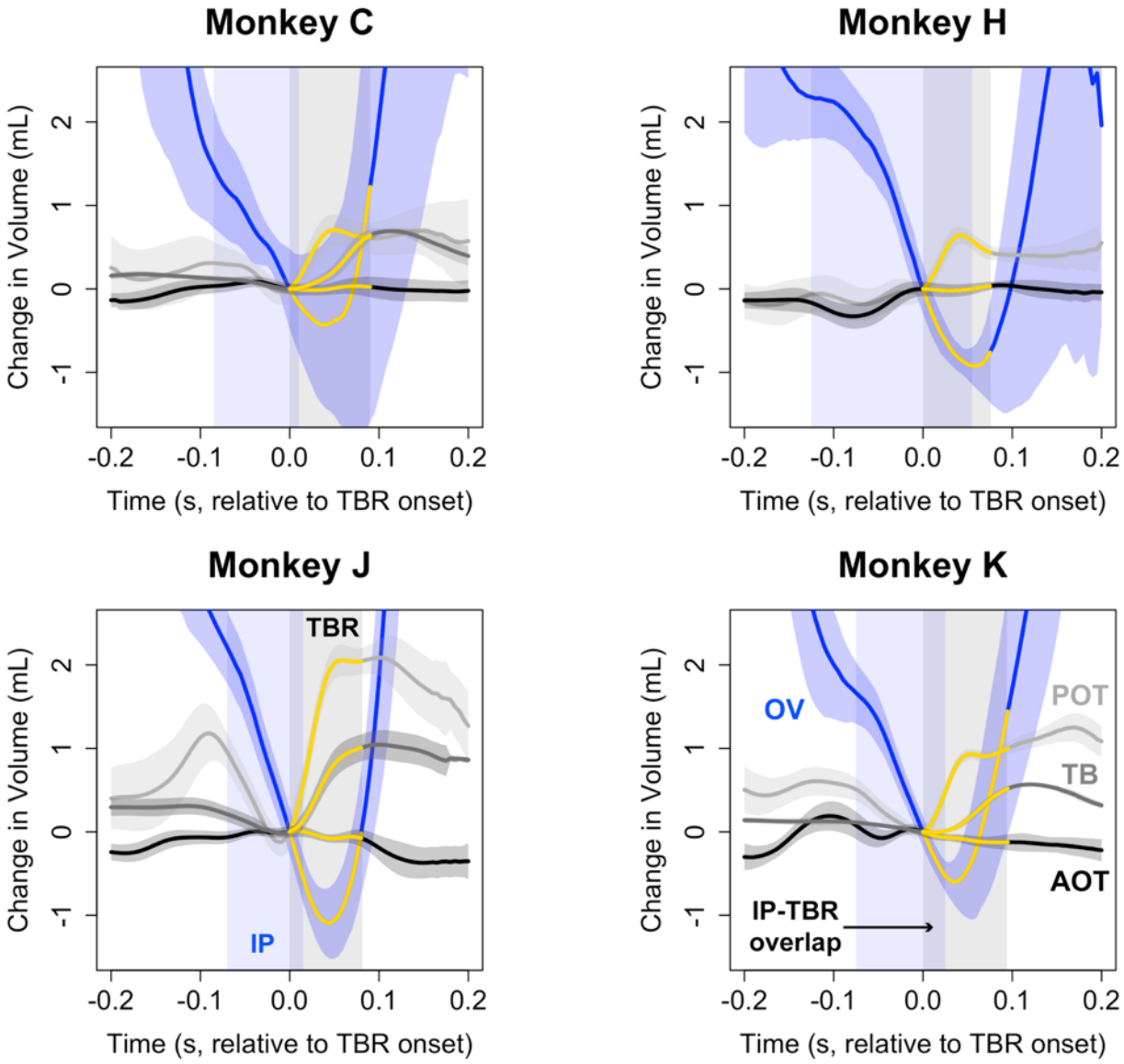

Figure 4.4: Oral and tongue volume change during intercuspal phase and TBR. Volumes were measured relative to TBR onset. Oral volume modeled using an alpha hull with alpha = 6. Tongue volume modeled using concave meshes. Volumes are measured relative to the volume at the time of tongue retraction onset. Dark traces indicate the mean value at each time stamp; lighter shades are standard deviations. Monkey He did not have a vallecular marker and tongue base volume was not measured in this animal. Color code for rectangles and lines: blue rectangle, intercuspal phase (IP); gray rectangle, tongue base retraction (TBR); blue line, oral volume (OV); black line, anterior oral tongue (AOT); light gray line, posterior oral tongue (POT); dark gray line, tongue base (TB); yellow lines, volume during TBR. Data aligned to TBR onset (Time = 0.0).

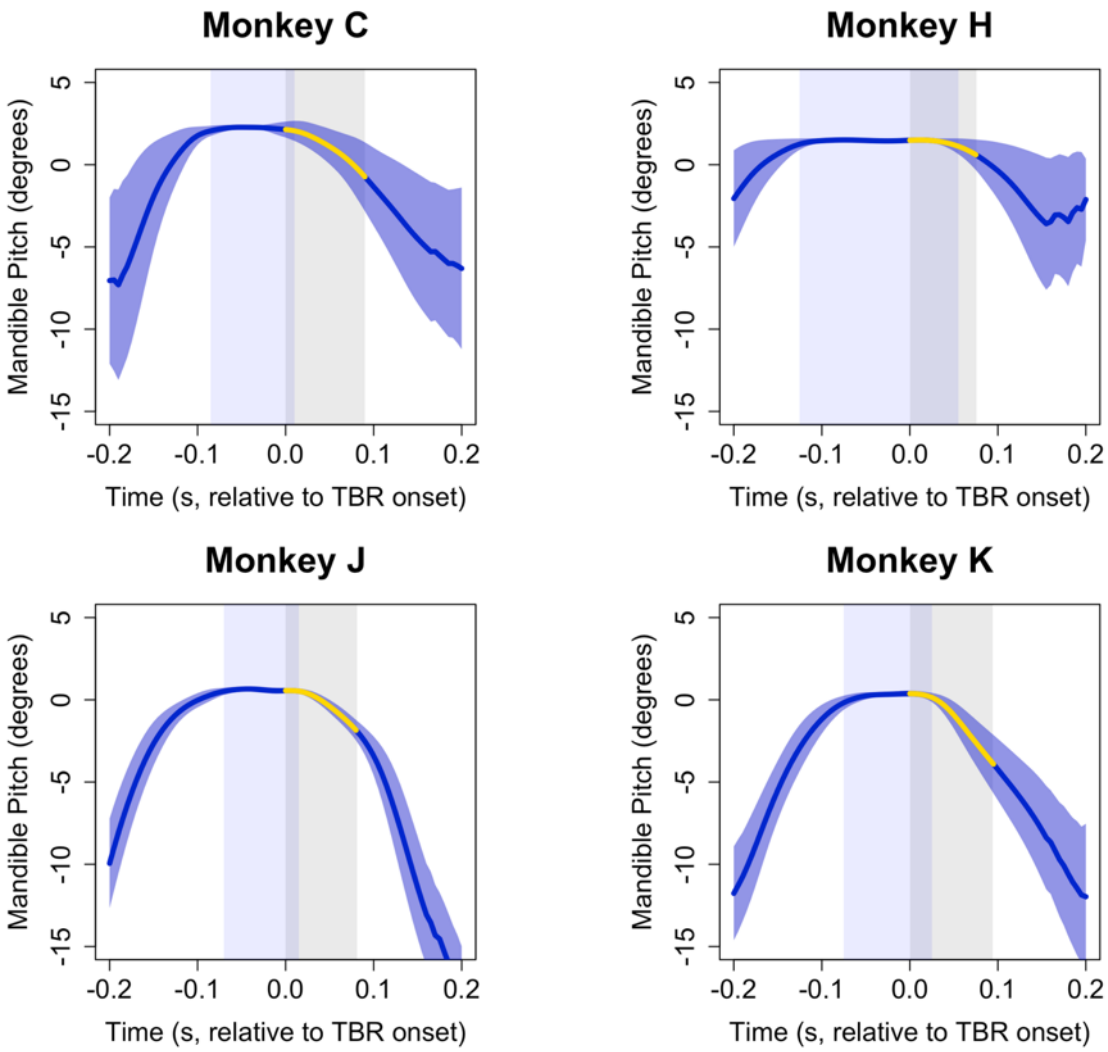

Figure 4.5: Mandibular pitch during tongue base retraction. A pitch angle of 0° or less indicates that the mandibular cusps are superior to the cranial cusps, i.e., intercuspation. Because the animals had different levels of cusp height due to variable wear patterns, intercuspal phase was operationally defined as when pitch velocity was less than 2 SD of pitch velocity measured during the precision study (see Chapter 3). Dark trace indicates the mean value at each time stamp; lighter shades are standard deviations. Color code for lines and rectangles: blue rectangle, intercuspal phase (IP); gray rectangle, tongue base retraction (TBR); blue line, mandibular pitch; yellow line, pitch during TBR. Data aligned to TBR onset (Time = 0.0).

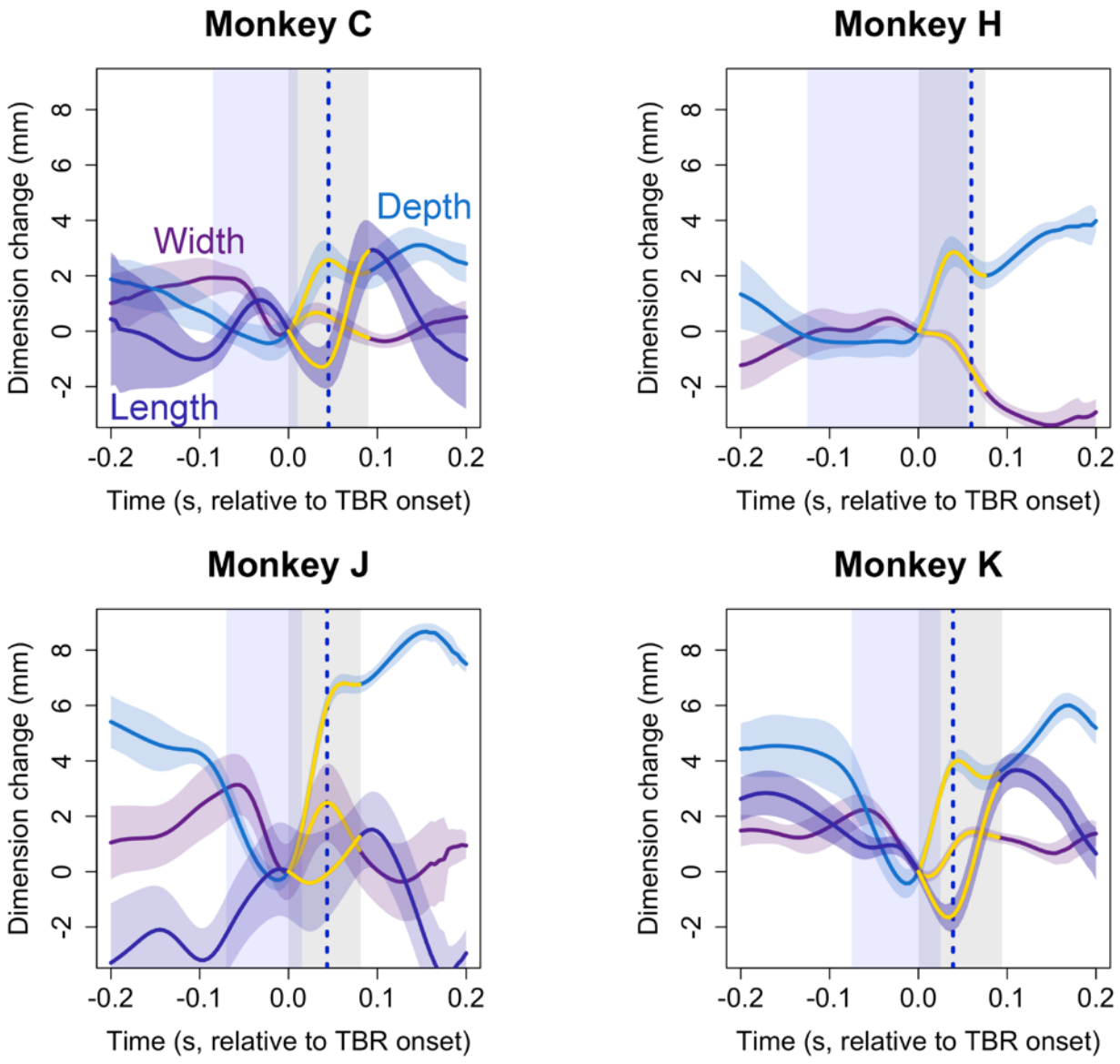

Figure 4.6: Tongue base dimensions during tongue base retraction. Dark trace indicates the mean value at each time stamp; lighter shades are standard deviations. Color code for lines and rectangles: blue rectangle, intercuspal phase (IP); gray rectangle, tongue base retraction (TBR); dashed blue line, time of minimum oral volume; dark blue line, tongue base length; light blue line, tongue base depth; purple line, tongue base width; yellow lines, dimensions during TBR. Dimension changes are measured relative to values at TBR onset. Data aligned to TBR onset (Time = 0.0).

Hyoid movement had a dynamic relationship with tongue expansion and retraction. In both mandibular and cranial coordinate systems, the hyoid elevated and protracted throughout and usually prior to TBR. Hyoid elevation began before TBR and was most rapid as oral volume declined during early intercuspal phase and before TBR onset (Figures 4.7 and 4.8). During TBR, hyoid elevation reached a period of relatively constant velocity until maximum POT volume, after which hyoid elevation resumed decelerating. In contrast, hyoid protraction began at variable times before the onset of TBR, reached peak velocity during TBR, and continued after TBR offset.

Several aspects of hyoid kinematics were significantly correlated with tongue base kinematics. Within a cranial coordinate system, greater hyoid protraction and excursion between TBR onset and the time of minimum oral volume was associated with greater retraction in all tongue base markers and greater overall excursion in the posterior surface marker (Table 4.4); no other correlations between hyoid and tongue base kinematics in a cranial coordinate system were significant. Within a mandibular coordinate system, greater hyoid elevation was associated with greater elevation and total excursion of all tongue base markers (Table 4.2). At the time of maximum TBR, greater hyoid protraction was associated with greater vallecula marker protraction, and greater hyoid elevation was associated with greater elevation of all tongue base markers (Table 4.3). For displacement prior to minimum oral volume, greater hyoid protraction was associated with greater retraction in all tongue base markers, and greater hyoid excursion was associated with greater overall displacement of the posterior surface marker and greater retraction of the posterior surface and deep markers (Table 4.4). At the time of minimum oral volume, the vallecula marker was more elevated when the hyoid was more elevated (Table 4.5). No other correlations between hyoid and tongue base displacement or velocity were significant

among all animals. Additionally, there were several significant positive correlations within the tongue base, particularly at the time of maximum TBR (Table 4.3), from TBR onset until minimum oral volume (Table 4.4), and at minimum oral volume (Table 4.5).

There were no significant correlations between peak velocities of the hyoid and tongue base, and their peak velocities were significantly different. Compared to maximum absolute hyoid velocity, maximum absolute velocities for the posterior surface, posterior deep, and vallecula markers were, on average, 144 %, 79 %, and 23% greater than in a mandibular coordinate system and 198 %, 110 %, and 68 % greater in a cranial coordinate system, respectively, and these differences were statistically significant ($p < 0.001$).

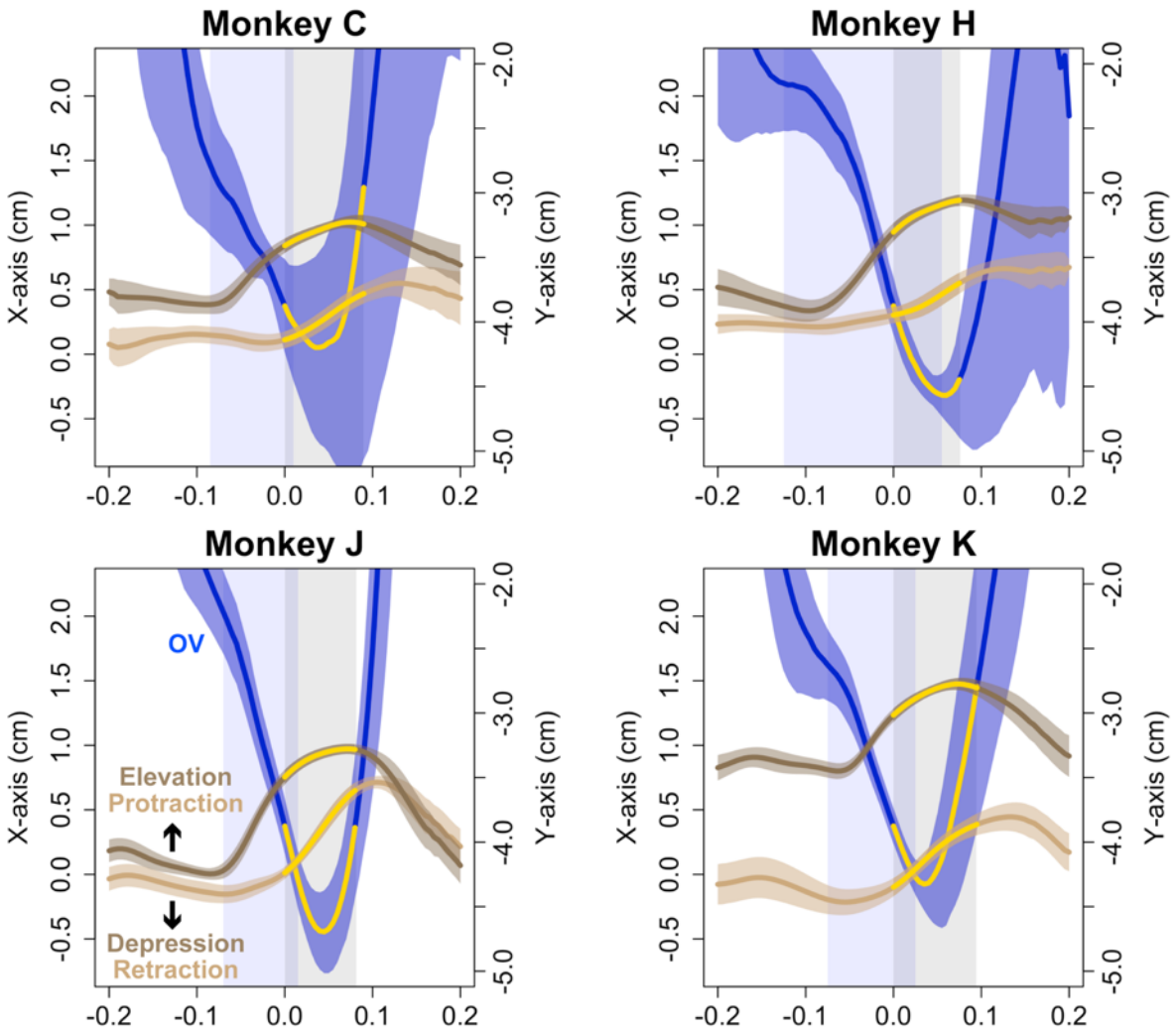

Figure 4.7: Oral volume change and hyoid displacement. Oral volume traces are identical to those in Figure 4.4. Dark traces indicate the mean value at each time stamp; lighter shades are standard deviations. Color code for lines and rectangles: blue line, mandibular pitch; blue rectangle, intercuspal phase (IP); light brown line, hyoid protraction; dark brown line, hyoid elevation; light gray line, posterior oral tongue (POT); dark gray line, tongue base (TB); gray rectangle, tongue base retraction (TBR); yellow lines, volume and position during TBR. Data aligned to TBR onset (Time = 0.0).

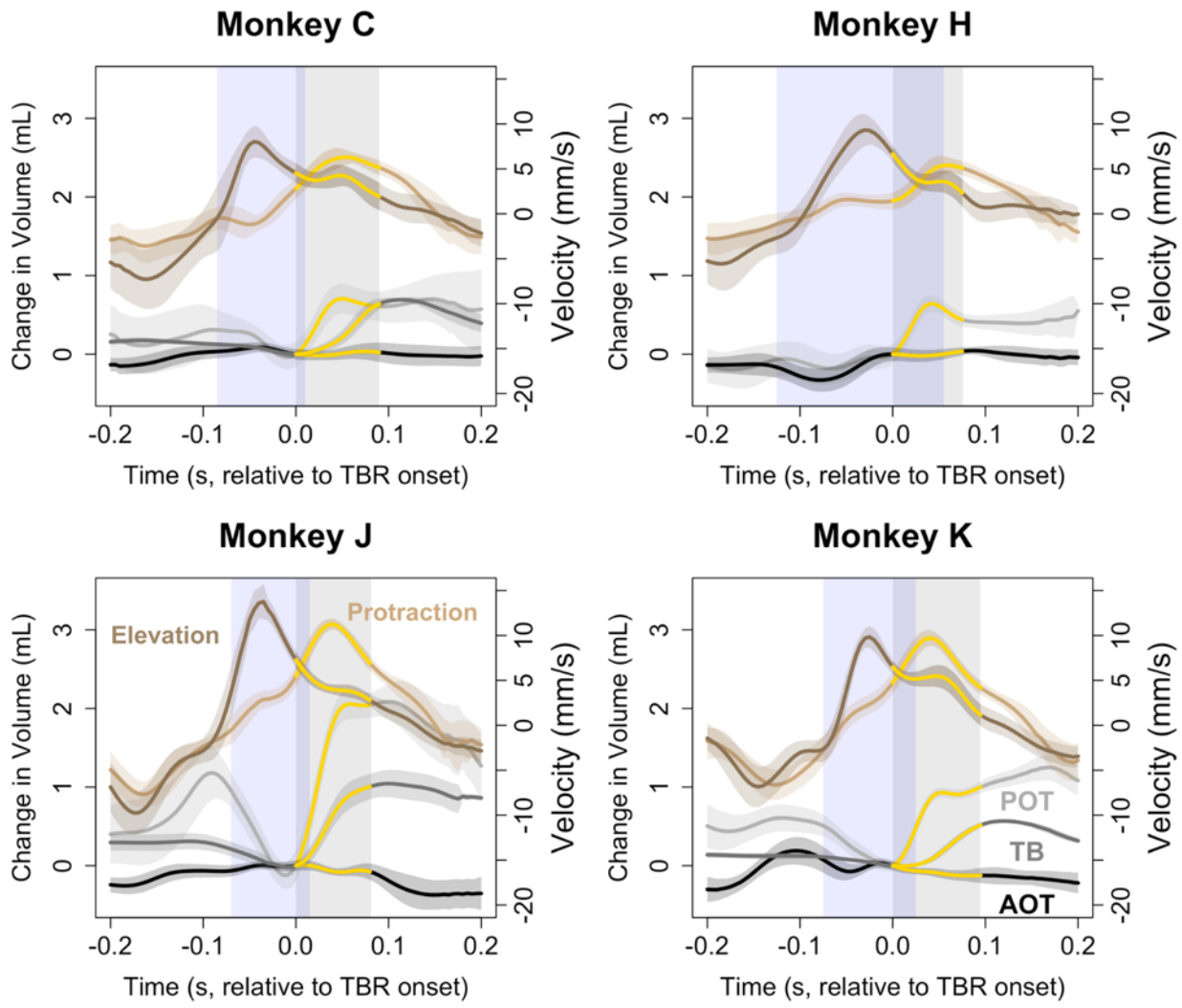

Figure 4.8: Tongue volume change and hyoid elevation and protraction velocity. Volumes are measured relative to the volume at the time of tongue retraction onset. Positive velocity indicates elevation and protraction, negative velocity indicates depression and retraction. Dark traces indicate the mean value at each time stamp; lighter shades are standard deviations. Color code for lines and rectangles: blue line, mandibular pitch; blue rectangle, intercuspal phase (IP); light brown line, hyoid protraction; dark brown line, hyoid elevation; light gray line, posterior oral tongue (POT); dark gray line, tongue base (TB); gray rectangle, tongue base retraction (TBR); yellow lines, volume and velocity during TBR. Data aligned to TBR onset (Time = 0.0).

Table 4.2: Correlation matrix for hyoid and tongue base displacement during tongue base retraction

	HX	HY	HT	PSX	PSY	PST	VX	VY	VT	PDX	PDY	PDT
HX			0.90/0.84									
HY			0.84		0.81			0.90			0.82	
HT	< 0.001	< 0.001			0.78			0.72			0.74	
PSX										0.84		
PSY		< 0.001	< 0.001					0.77			0.78/0.91	
PST												0.84/0.81
VX									-0.92	0.77		
VY		< 0.001	< 0.001		< 0.001					0.65		
VT							< 0.001					
PDX				< 0.001			< 0.001	< 0.001				
PDY		< 0.001	< 0.001		< 0.001			< 0.001				
PDT						< 0.001						

Values above the diagonal are average Pearson correlation coefficients across all animals. Values below the diagonal are average p-values. Blue values are in a cranial coordinate system. Red values are in a mandibular coordinate system. Purple indicates the p-value for both coordinate systems. X, X-axis; Y, Y-axis; T, total excursion; H, hyoid; PS, posterior surface; V, vallecular; PD, posterior deep. N = 99 swallows.

Table 4.3: Correlation matrix for hyoid and tongue base displacement at maximum tongue base retraction

	HX	HY	PSX	PSY	PDX	PDY	VX	VY
HX							0.79	
HY				0.86		0.84		0.85
PSX					0.93/0.87			
PSY		p < 0.001				0.96		0.78/0.89
PDX			< 0.001				0.68/0.74	0.64
PDY		< 0.001		< 0.001			0.71	0.73
VX					< 0.001	< 0.001		
VY		< 0.001		< 0.001	< 0.001	< 0.001		

Values above the diagonal are average Pearson correlation coefficients across all animals. Values below the diagonal are average p-values. Blue values are in a cranial coordinate system. Red values are in a mandibular coordinate system. Purple indicates the p-value for both coordinate systems. X, X-axis; Y, Y-axis; H, hyoid; PS, posterior surface; V, vallecular; PD, posterior deep. N = 99 swallows.

Table 4.4: Correlation matrix for hyoid and tongue base displacement prior to minimum oral volume

	HX	HY	HT	PSX	PSY	PST	VX	VY	VT	PDX	PDY	PDT
HX			0.95/0.96	-0.84/-0.87		0.84/0.88	-0.74/-0.67			-0.84/-0.84		
HY			0.83									
HT	< 0.001	< 0.001		-0.83/-0.85		0.87/0.90	-0.72			-0.83/-0.81		
PSX	< 0.001		< 0.001			-0.95/-0.94				0.90/0.91		
PSY											0.83/0.86	0.89/0.91
PST	< 0.001		< 0.001	< 0.001						-0.93/-0.92		0.86/0.86
VX	< 0.001		< 0.001					0.73		0.73/0.73		
VY							<0.001					
VT												
PDX	< 0.001		< 0.001	< 0.001		< 0.001	< 0.001					-0.82/-0.78
PDY					< 0.001							0.81/0.84
PDT					< 0.001	< 0.001				< 0.001	< 0.001	

Values above the diagonal are average Pearson correlation coefficients across all animals. Values below the diagonal are average p-values. Blue values are in a cranial coordinate system. Red values are in a mandibular coordinate system. Purple indicates the p-value for both coordinate systems. X, X-axis; Y, Y-axis; T, total excursion; H, hyoid; PS, posterior surface; V, vallecular; PD, posterior deep. N = 99 swallows.

Table 4.5: Correlation matrix for hyoid and tongue base displacement at minimum oral volume

	HX	HY	PSX	PSY	PDX	PDY	VX	VY
HX								
HY								0.72
PSX					0.93		0.91	
PSY							-0.18	0.78/0.86
PDX			< 0.001				0.68/0.70	
PDY								
VX			< 0.001	< 0.001	< 0.001			-0.190
VY		< 0.001		< 0.001			0.002	

Values above the diagonal are average Pearson correlation coefficients across all animals. Values below the diagonal are average p-values. Blue values are in a cranial coordinate system. Red values are in a mandibular coordinate system. Purple indicates the p-value for both coordinate systems. X, X-axis; Y, Y-axis; H, hyoid; PS, posterior surface; V, vallecular; PD, posterior deep. N = 99 swallows.

DISCUSSION

Limitations

This study is subject to several limitations. Due to the time-intensive nature of data processing, data were collected from only four animals (two males, two females) and for one food type (red grapes). Grapes were selected because macaques are generally motivated to eat them while seated in a primate chair, regardless of satiety. Future work needs to quantify whether this phenomenon is generalizable to foods and liquids of various material properties.

The correlative findings supporting the third (hydraulic) hypothesis cannot discriminate among alternative causes of TBR: hyoid protraction and TBR could be hydraulically linked, or TBR could occur through an undiscovered mechanism that is independent of hyoid kinematics. In the latter case, hyoid excursion and TBR could simply occur simultaneously without a common mechanical driver due to motoneuron synchronization of hyoid excursion and TBR within the brainstem or by corticobulbar neurons. However, this scenario would require the tongue to retract through an undiscovered mechanism that uses neither a hydraulic linkage nor extrinsic muscle shortening, nor intrinsic muscle shortening. More experimental work involving mechanical and lesion-based *in vivo* models is required to further test the hydraulic linkage hypothesis. Lesion studies in which the geniohyoid is paralyzed or otherwise perturbed could discriminate among these hypotheses. Ideally, several conditions would be tested to rule out compensatory mechanisms through extrinsic or intrinsic muscle activity.

Volume measurements should be weighed as overall trends rather than accurate measurements until the tongue volume measurement method can be validated against a gold standard. For example, TB volume increases may be overestimated, considering that the dorsal hyoid was used as a landmark to define the boundary between the TB and POT (see Chapter 4).

Therefore, parts of this volume are a product of not only TBR but also hyoid protraction. However, TB length increases from mid-TBR until shortly after TBR offset and was measured as the anteroposterior distance between the posterolateral and vallecula markers. Therefore, any artifacts introduced by using the hyoid as a boundary between the TB and POT likely only exaggerate trends rather than reverse them.

Lastly, these results may not be generalizable to humans, given that the macaque basihyoid has relatively more surface area than the human hyoid due to the former's more shield-like shape (Howell and Straus 1933; Nishimura 2003). Aspects of this study could be replicated in humans using lateral view videofluoroscopy by placing radiopaque markers on the tongue surface (Matsuo and Palmer 2010) not only in the midline but also on the tongue's lateral edges to assess whether the human midline retracts more than the lateral edges, as it does in macaques.

Summary of Results and Hypotheses

As was reported by Franks et al. (1984), the more posterior parts of the tongue began to retract as the hyoid began to protract. These findings are in contrast to Nakamura et al. (2017), in which the posterior tongue marker moved anteriorly as the hyoid protracted. These differences can be attributed to differences in marker location within the tongue—markers in this study and the study by Franks et al. were more superficial than those in Nakamura et al. Simultaneous retraction and elevation are also contrary to the findings of Kahrilas et al. (1993), who claimed that the "illusion of rolling tongue motion was created by the tongue surface motions occurring out of phase in the distal relative to the proximal tongue. This is analogous to a wave in the ocean which gives the illusion of moving forward, even though each particle is actually only moving up and down." The results presented here demonstrate that the macaque tongue indeed

retracts and indicate that tongue profile kinematics may not be a reliable indicator of internal tongue kinematics; therefore, markers should be placed on the tongue in humans to ensure that homologous points are tracked when digitizing data.

Does extrinsic muscle contraction explain TBR?

These data refute the hypothesis that posterior extrinsic tongue muscles—hyoglossus, palatoglossus, and/or styloglossus—produce TBR. Although hyoglossus shortens sufficiently to account for TBR, its lateral insertion into the tongue does not move posteriorly during shortening. These kinematic findings demonstrate that, assuming hyoglossus is active during shortening, hyoglossus functions to elevate and protract the hyoid. Thus, although hyoglossus does not produce TBR directly, it may contribute to TBR through a hydraulic linkage with the tongue (see below). Although styloglossus is active during swallowing in macaques (Doty and Bosma 1956; Chapter 5), its length change cannot account for the observed amount of TBR; styloglossus may function isometrically to produce higher pressures at the tail of the bolus (McConnel 1988).

Does intrinsic muscle contraction cause TBR?

The macaque tongue does not function according to the classic theory of muscular hydrostats, in which regional volume is constant because increases in one tongue dimension are accompanied by decreases in others (Kier and Smith 1985; Smith and Kier 1989). Previous research in humans demonstrating similar increases in tongue base depth and length assumed that tongue width decreases (Napadow et al. 1999). However, although the POT shows small decreases late in TBR, the POT and TB volume increase as AOT volume remains relatively

constant. These data do not necessarily refute the biomechanical applicability of muscular hydrostat theory to the macaque tongue in all behaviors, but rather demonstrate that the tongue can at times function hydraulically—moving and generating force by regionally displacing volume (see below; Kier 2012; Vogel 2013).

Does a hydraulic mechanism explain TBR?

This study suggests a novel mechanism of tongue base movement that involves regional changes in tongue volume caused by suprahyoid muscle shortening. TB and POT share a common interface—markers defining posterior border of the POT are the same as those defining the anterior border of the TB. Therefore, posterior expansion of the POT by definition contributes to TBR. During the early stages of TBR, POT and TB volume increase as oral volume decreases, which is consistent with the hydraulic linkage hypothesis. However, oral volume increases during the latter half of TBR, and therefore minimal oral volume is not necessary for the tongue base to continue retracting after the POT stops expanding. Although the magnitude of hyoid excursion at the end of TBR did not predict the amount of TBR, the magnitude of hyoid excursion and TBR were tightly correlated until minimum oral volume was reached. After minimum volume, hyoid protraction and elevation continue, and the tongue base increases in volume as it slightly decreases in depth and width. Therefore, the later stages of TBR may involve a combination of hydraulic displacement of tongue volume by the hyoid and classic hydrostatic deformation. Low magnitude changes in gape may be tolerated during swallows as long as the tongue can contact the hard palate and maxillary teeth to prevent superoanterior displacement of tongue volume as the hyoid elevates and protracts. However, as

the reader may easily appreciate, if the tongue cannot contact the hard palate and teeth, as when the jaws are wide open, swallowing is indeed very difficult and somewhat uncomfortable.

THE BIOMECHANICS OF TONGUE BASE RETRACTION

The novel mechanism of TBR proposed here raises several questions: How is tongue volume displaced? How does this displacement cause retraction? How do these observations reconcile with previous work? What are the functional and clinical implications of these findings? What is the function of styloglossus during swallowing? How does a hydraulic mechanism reconcile with other previous work? Is TBR possible if the hyoid has been removed? What are the implications of a hydraulic linkage for swallowing motor control? Although many of these questions will require further experimentation to firmly resolve, the following discussion uses the data at hand to present new hypotheses about the biomechanics of TBR.

How is tongue volume displaced?

During early TBR, POT volume increases as oral volume—the volume bounded by the teeth, hard palate, mandibular corpus, mylohyoid, and anterior surface of the hyoid—decreases due to hyoid excursion and mouth floor elevation. Posterior oral tongue volume increased more than the oral volume decreased, suggesting that our methodology may overestimate posterior oral tongue volume changes and/or underestimate oral volume changes. It is clear, however, that oral volume compression is a result of hyoid protraction and mouth floor elevation because oral volume decreases even as the mandible depresses slightly during TBR. These patterns of volume change meet the definition of a hydraulic linkage, "which involves the displacement of fluid from one location in order to cause shape change or exert force elsewhere" (Kier 2012). Given

that POT volume increases as oral volume decreases, the hyoid and the POT are arguably hydraulically linked. In such a linkage, the hyoid superoanterior excursion and mouth floor elevation cause TBR by squeezing the tongue out of the space bounded by the hard palate, tooth row, and mouth floor, forcing the tongue posteriorly. Essentially, the hyoid functions as a piston for the POT, which itself functions as a piston for the bolus (McConnel 1988).

Muscular hydrostats are assumed to "optimize speed and flexibility during deformation…while sacrificing force production" because they lack levers (Gilbert et al. 2007). However, biological hydraulic systems can indeed amplify force and displacement by varying the surface area of input and output forces, as is commonly done with automobile hydraulic brakes (Vogel 2013). Nonetheless, given that the POT moves further, and up to 198 % faster than, the hyoid, a hyolingual hydraulic linkage arguably amplifies tongue displacement and velocity. Such patterns of velocity amplification are not surprising given that the area of interface between the root of the tongue and the hyoid plus the mouth floor is larger than the cross-sectional area of the tongue base.

While POT expansion in early TBR could be due to a hydraulic linkage, most of TB expansion occurs as oral volume increases during late TBR. Therefore, an alternative mechanism to reciprocal changes in oral and regional tongue volume must drive the later stages of TBR. Early TBR involves both retraction and elevation, and this elevation brings the POT into contact with the hard palate. This contact with the hard palate is an essential component of the squeeze-back mechanism of swallowing, in which this point of contact forces the bolus posteriorly as the contact point itself moves posteriorly (Franks et al. 1984). During late TBR, the hyoid continues to protract and, to a lesser degree, elevate as the TB decreases in depth and width, although the magnitude of each is variable among animals. Decreased tongue depth and slight decreases in

POT volume suggest that the hyoid compresses the POT against the hard palate during late TBR. Because AOT volume changes are minimal and anterior and anterolateral markers are relatively stationary, POT compression by the hyoid and mouth floor virtually requires that POT volume be displaced posteriorly. Alternatively, because TB width decreases slightly during late TBR, classic hydrostatic deformation may yet contribute to tongue base retraction. However, because TB volume increases during late TBR, hydrostatic deformation cannot be the only mechanism of TBR at that time.

Additional experiments increasing the marker density in the TB and POT are necessary to resolve these uncertainties and address the exact nature of tongue base deformation. Nonetheless, two hypotheses about volume displacement can be ruled out: first, given that the anterior tongue does not change volume, posterior oral tongue expansion is not due to internal shearing resulting in extrusion of the more central portions of the anterior tongue posteriorly; and second, that the later portions of TBR do not require reciprocal changes in tongue and oral volume.

How does tongue volume displacement cause tongue retraction?

The exact nature of tongue internal deformation during TBR will require further investigation, but some hypotheses can be generated from the data at hand and previous studies of primate tongue morphology. The correlational analyses presented here demonstrate that superficial and deep tongue base movements are coordinated, presumably through mechanical coupling. Although deep posterior and vallecular marker displacements were less than that of the superficial tongue marker, retraction and elevation of the former markers increased as the latter retracted and elevated more. Therefore, the tongue base midline seems to function as a single

unit that translates posteriorly and superiorly relative to the lateral edges of the tongue—in other words, the TB shears in coronal and axial planes during TBR.

The design of the primate tongue may facilitate such internal shearing. Anisotropic materials with load-bearing elements oriented at 0° and 90° to the plane of shearing will tend to exhibit high shear strain (Gordon 1981). To draw everyday analogies, building scaffolding has diagonal struts or braces at 45° to the horizontal to prevent collapse of the scaffolding due to shear stress, and tall bookshelves tend to exhibit high shear strains when pushed horizontally. The intrinsic lingual muscles are oriented orthogonal and parallel to the long axis of the tongue, and transverse fibers insert into a midline tendon rather than span the width of the tongue (Takemoto 2001; Takemoto 2008). When considering a coronal cross-section of the tongue (Figure 4.9), inferiorly or superiorly directed forces at the tongue midline would cause midline depression or elevation, respectively, via shear strain.

Midline tongue depression occurs during swallowing and speech and is thought to be due to genioglossus shortening (Abd-El-Malek 1955; Stone and Lundberg 1996). This hypothesis is further supported by electromyographic and kinematic data presented in Chapter 5. However, genioglossus shortening alone is not sufficient to produce midline depression via shear because the lateral edges of the tongue must be stabilized against inferior translation by either isometric palatoglossus or styloglossus activity or wet adhesion forces between the palate and tongue. Coactivation with hyoglossus is an unlikely mechanism because of its posteroinferior orientation, would also depress the lateral edges.

Tongue elevation might occur via shearing in the opposite direction to depression by genioglossus. Regional volume displacement by the hyoid as discussed above may apply mucosally-oriented forces deep to the intrinsic muscles that would cause them to shear in the

opposite direction (Figure 4.9). Such shearing could explain not only midline elevation but also retraction because the orientation of the intrinsic muscles changes from anterior to posterior near the POT/TB boundary, such that vertical intrinsic fibers are oriented more anteroposteriorly in the TB (Takemoto 2001; Takemoto 2008) (Figure 4.10).

The tongue's stiffness in response to shear stress can be quantified as its shear modulus, which is measured in units of pressure, i.e., pascals (Vogel 2013). To give an intuitive sense of the kind of stiffness described by the shear modulus, solids such as bone (5000 MPa) resist shear displacement whereas low-viscosity liquids such as water (0 MPa) do not (Vogel 2013). The tongue at rest similarly has a liquid-like, low shear modulus (0.002-0.003 MPa) (Cheng et al. 2011; Y. Wang et al. 2011). Active whole tongue and regional tongue stiffness are unknown, but at maximum voluntary contraction, limb muscle is more akin to a cartilage-like solid at 0.200 MPa (Bensamoun et al. 2006; Nordez and Hug 2010; Bouillard et al. 2011; Ateş et al. 2015). Therefore, tongue stiffness probably depends on intrinsic muscle activity level. Importantly, the more posterior regions of the tongue, including the tongue base, probably have less variable stiffness than other areas of the tongue because they have relatively less muscle and more connective and glandular tissue in both humans (Sanders and Mu 2013) and macaques (Figure B1). Whether the tongue's low shear modulus is a function of the tongue's fiber architecture (see above), muscle and connective tissue material properties, or a combination of both will require further investigation.

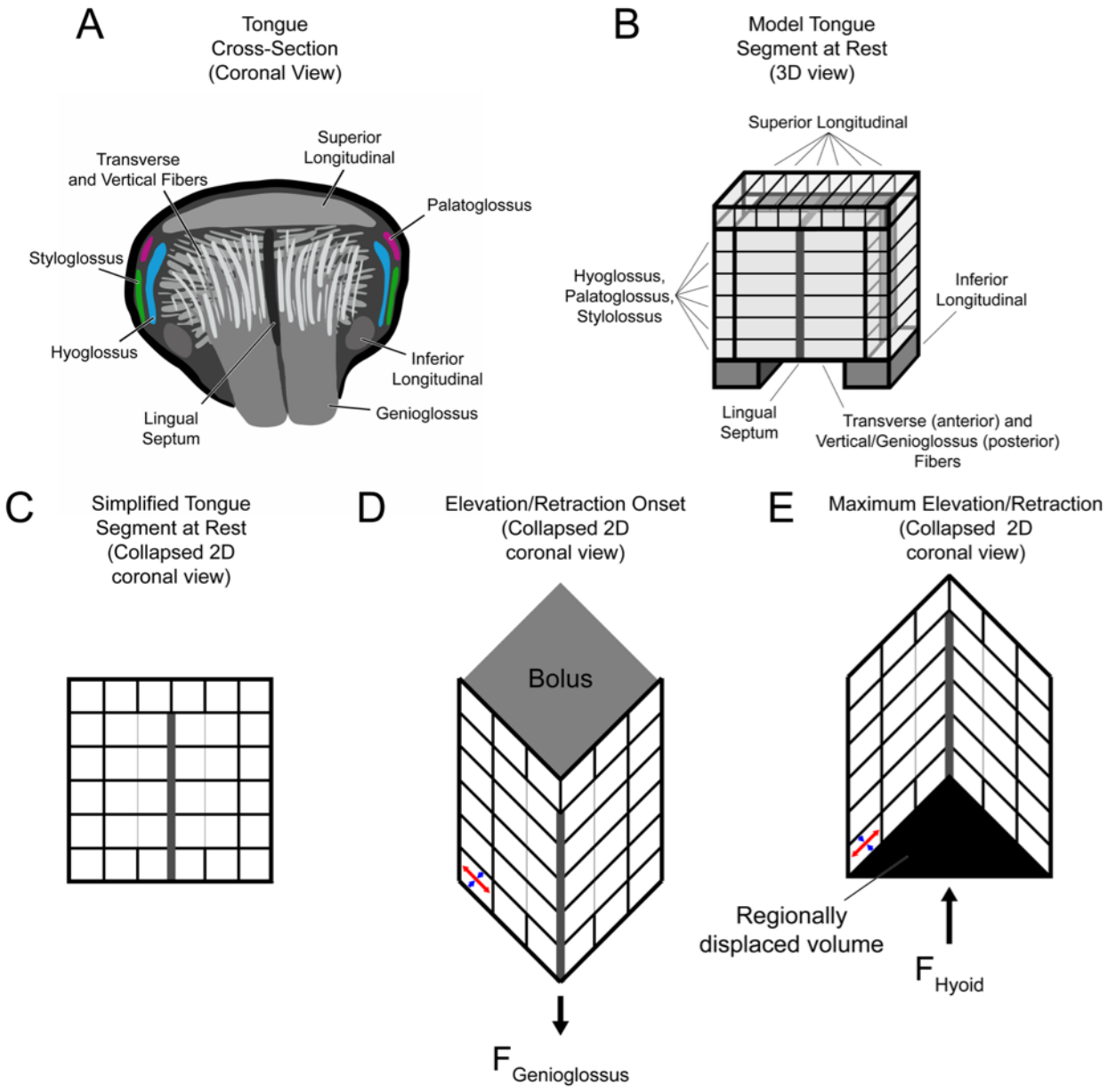

Figure 4.9: Primate tongue morphology and patterns of shear deformation in coronal planes. A) Illustration of a macaque tongue coronal cross-section based on diceCT. Vertical, transverse, and genioglossus fibers are oriented orthogonal to the long axis of the tongue, while superior and inferior longitudinal, palatoglossus, and styloglossus fibers are oriented parallel to the long axis. Hyoglossus fibers are oblique to the long axis in a parasagittal plane but simplified to being parallel in the coronal plane. B) Simplified 3D model of A. C) Simplified 2D model of B. D) Shearing stress produced by genioglossus shortening causing tongue midline depression. E) Shearing stress produced by hyoid excursion causing tongue midline elevation.

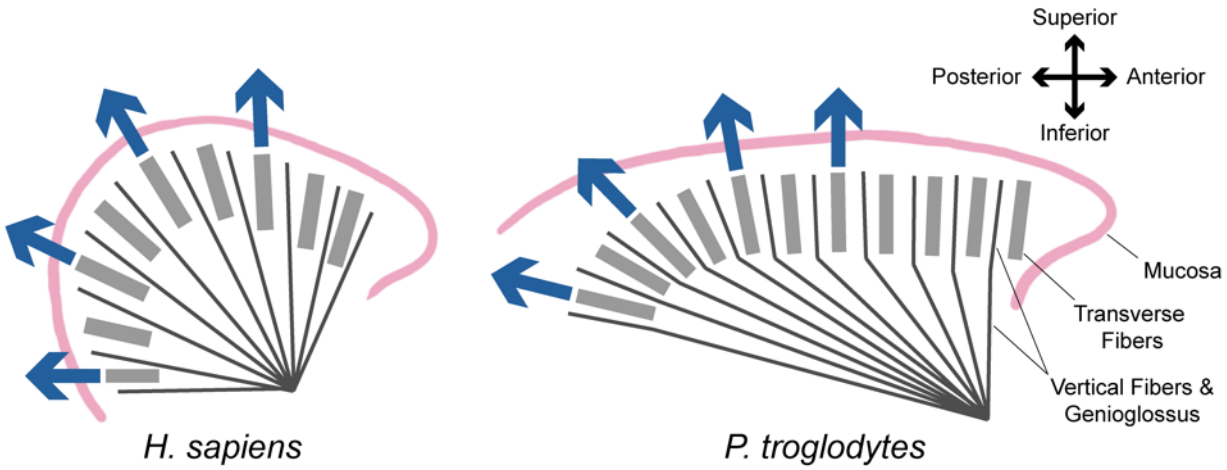

Figure 4.10: Changes in the orientation of primate intrinsic tongue muscles and genioglossus from anterior to posterior in both humans (*Homo sapiens*) and chimpanzees (*Pan troglodytes*). Intrinsic tongue muscles and genioglossus (gray bars and lines, respectively) change orientation from being more superoinferiorly oriented in the anterior tongue to being more anteroposteriorly oriented in the tongue base. Blue arrows indicate direction of movement produced by intrinsic shearing. Intrinsic shearing results in elevation more anteriorly and retraction more posteriorly. Modified from Takemoto 2008.

What are the functional and clinical implications of shearing?

Although the tongue is typically thought of as a deformable solid, the tongue's low shear modulus and the observed shearing behavior within the tongue suggest that the tongue may have facultative liquid-like properties during swallowing, depending on the level of intrinsic muscle activation. Importantly, a fundamental feature of liquids is that increased applied forces result in increased rates of deformation, i.e., velocity (Denny 2016), so that suprahyoid muscle weakness may manifest as slow posterior oral tongue and tongue base retraction if the tongue behaves like a liquid during TBR. If TBR velocity depends on suprahyoid muscle force, then suprahyoid muscle strengthening or maneuvers like the effortful swallow would be expected to increase the velocity of TBR. Many studies of the effortful swallow have reported increased suprahyoid EMG activity and tongue base pressures (Lazarus et al. 2002; Huckabee et al. 2005; Huckabee and

Steele 2006; Witte et al. 2008; Takasaki et al. 2011; Doeltgen et al. 2017), while more recent studies make conflicting reports on the effect of the effortful swallow on hyoid and bolus velocity (Jang et al. 2015; Molfenter et al. 2017). Future work could compare TBR velocity in effortful versus regular swallows and assess whether palatal pressure recordings—which are a product of lingual and suprahyoid force production—are correlated with TBR velocity.

In addition to the intralingual shearing described above, these data indicate that shearing in sagittal planes—specifically, between the geniohyoid and genioglossus—is necessary for the hyoid to protract as tongue volume is displaced posteriorly. In other words, this plane allows geniohyoid and genioglossus to slide past each other as they move in opposite directions during swallowing. The connective tissue between genioglossus and geniohyoid may be filled with compliant connective tissue with a high elastin content and low shear modulus, as there is between skin and underlying tissues (Kawamata et al. 2003), which provides minimal resistance to shear but returns the tissues to their resting position once shearing forces are removed.

An increase in this plane's shear modulus would require the geniohyoid to produce more force during shortening to achieve normal hyoid protraction. The stiffness of the connective tissue between geniohyoid and genioglossus could be increased by either decreased tissue compliance as a result of decreased elastin and increased collagen (i.e., the spring between the muscles is stiffer) or increased overall amount of connective tissue as a result of fibrosis (i.e., there are more springs between the muscles). Consequently, both hyoid protraction and TBR could be hindered, a potentially devastating combination for swallowing safety. Indeed, radiation-induced fibrosis is thought to be one of the main causes of dysphagia in head and neck cancer patients, among whom poor tongue base retraction is the most common finding (Logemann et al. 2006; Logemann et al. 2008; King et al. 2016). Whether surgical, therapeutic,

or pathological processes affect midline shearing or the stiffness of geniohyoid-genioglossus plane in particular warrants further investigation.

However, there appears to be a limit to how much the hyoid can move relative to the tongue, and excessive hyoid protraction may be detrimental to TBR. In a mandibular coordinate system—which negates the effect of mandibular depression on hyoid and tongue kinematics—the vallecular marker is less retracted when the hyoid is more protracted at the end of TBR, perhaps because the extreme protraction drags the tongue base with it (Table 4.3). Poor hyoid protraction is frequently seen in dysphagic patients (Steele et al. 2011; Hoffman et al. 2013), but it is possible that maximal tongue base pressures could be reduced if extreme hyoid protraction results in slight tongue base protraction, i.e., less retraction. Alternatively, TBR may be reduced if tissue stiffness increases, thus limiting movement of the TB relative to the hyoid.

What is the function of styloglossus during swallowing?

Previous studies have demonstrated that the macaque and human styloglossus are active during swallowing (Doty and Bosma 1956; Gassert and Pearson 2016), and this study demonstrates that such activity is likely isometric. Limited styloglossus shortening would theoretically provide two benefits to pressure production at the tail of the bolus after TBR is complete. First, less length change could keep styloglossus in a more favorable region of its length-tension curve, whereas shortening may involve force losses as the sarcomeres enter the ascending limb of the length-tension curve (Ramsey and Street 1941; Gordon et al. 1966). Alternatively, if styloglossus is on the descending part of its length-tension curve before TBR, then shortening may improve its force production during its isometric phases. However, this possibility is countered by the second benefit of not shortening, which is that muscles that

passively shorten to a given length produce more isometric force than those which actively shorten to the same length (Abbott and Aubert 1952; Edman et al. 1993; Herzog and Leonard 1997). In other words, shortening results in residual force depression during isometry. While the hypothetical benefit deriving from the length-tension curve will require further work involving sarcomere length measurement and length-tension curve modeling, the residual force depression would apply regardless of sarcomere length.

How does a hydraulic mechanism reconcile with previous work?

As mentioned previously, several studies have argued that the mechanism of TBR involves a combination of styloglossus, hyoglossus, and transverse lingual muscle shortening (Napadow et al. 1999; Felton et al. 2007; Gilbert et al. 2007; Gassert and Pearson 2016). The evidence, assumptions, and limitations of these claims will now be reviewed in the context of this study's results.

Using 2D midsagittal tagged MRI in humans, Napadow et al. (1999) found, similarly to this study, that the tongue base greatly increased in depth and length of the tongue during TBR. Because their study was limited to two dimensions, increased depth and length were used to *infer* that the decreased width and that styloglossus shortened, based on two assumptions: "the out-of-plane axial strain was calculated by knowing the 2D strain condition, assuming that tongue muscle is incompressible (hence isochoric) and that out-of-plane shear strains are negligible" (Napadow et al. 1999). However, the results of this study suggest that (in macaques) TB and POT volumes increase (417 % and 27.9 %, respectively) during retraction, and that these tongue regions shear in coronal and axial planes as the midline elevates and retracts while the lateral tongue remains relatively stationary. Some shearing in the coronal and transverse planes is to be

expected if the midline of the tongue is capable of forming a depression between its lateral edges, as has been observed previously (Abd-El-Malek 1955; Stone and Lundberg 1996). In contrast, the expansion of the POT and TB was unexpected and suggests that the assumption of regional volume conservation is not universally valid in the tongue. Therefore, our results invalidate both Napadow et al.'s assumptions and so also the conclusion that TBR necessarily involves styloglossus, hyoglossus, and transverse muscle shortening.

Follow-up work by Felder et al. (2007) used a slightly different technique that allowed measurement of 3D strain from 2D images in axial and sagittal views. This MRI study examined tongue strain in the coronal plane and found evidence of mediolateral compression of the tongue, but the results here demonstrate that tongue base volume can increase despite decreased tongue width. However, Felder et al. only measured the oral stages of the swallow—when the oral tongue elevates to contact the hard palate—but not to the later pharyngeal phases when the tongue base retracts. The study interval spanned the time of palatal pressure onset until 400 ms after onset for coronal slices and 600 ms after onset for sagittal slices, yet vallecular pressure onset—which corresponds with retraction of the region (McConnel 1988)—is approximately 650 ms *after* palatal pressure onset (Steele and Huckabee 2007), and bolus transit through the oropharynx alone lasts about 570 ms (McConnel 1988). Application of similar methods during timeframes which include the pharyngeal stages of the swallow—and therefore TBR—would provide the critical strain data necessary to test the hydraulic linkage hypothesis in humans.

Other studies of hyolingual biomechanics have used muscle functional MRI, which uses increased T2 signals to infer whether a muscle was active during activity conducted immediately prior to the scan (Meyer and Prior 2000). Using this method, Gassert and Pearson (2016) argued that hyoglossus and styloglossus are active during swallowing in humans. While these muscles

can be accessed surgically in animal models, it is difficult to obtain muscle activity recordings from these muscles in humans. However, as noted previously, evidence of muscle activity is necessary but insufficient to draw conclusions about hyolingual muscle function (Thexton 1984; German et al. 2011). Gassert and Pearson's study also assessed whether activity increased after performing the Mendelsohn maneuver, which maintains the hyolaryngeal apparatus in an elevated position and the tongue base retracted against the posterior pharyngeal wall after the swallow. Interestingly, although tongue base contact with the posterior pharyngeal wall is maintained throughout the Mendelsohn maneuver (Lazarus et al. 2002), metabolic by-product accumulation in the hyoglossus and styloglossus is actually lower after the Mendelsohn maneuver than after regular swallows (Gassert and Pearson 2016). These findings suggest that these muscles are either less active, active for less time, or a combination of both during the Mendelsohn maneuver. If styloglossus and hyoglossus activity is less in either or both magnitude or duration, how then does the tongue remain retracted during the Mendelsohn maneuver? One answer may be a hydraulic mechanism—the hyoid's semi-protracted and more elevated position during the maneuver may displace sufficient tongue bulk to keep the tongue retracted without additional activity from styloglossus. Furthermore, hyoid elevation musculature is redundant (Pearson et al. 2011), and an elevated position could be maintained in the absence of increased hyoglossus activity by the anterior digastric, mylohyoid, posterior digastric, and stylohyoid. Moreover, given that the hyoid also elevates and protracts during TBR in humans (McConnel 1988), it is unlikely that hyoglossus shortening simultaneously retracts the tongue in humans.

Pearson et al. (2016) compared the trajectory of hyolingual kinematics in dysphagic patients with and without epiglottal inversion. They found that reduced TBR was associated with poor epiglottal inversion, whereas differences in hyoid kinematics were not significant between

the two groups. While these findings would seem to suggest that TBR is independent of hyoid kinematics, the limitations of this study must be considered. The subjects included in this study were all dysphagic—therefore, their hyoid kinematics cannot be assumed to be normal. All of these patients may have already had impaired hyoid excursion, and variable amounts of TBR in these patients may have been due to variability in compensation by extrinsic or intrinsic muscle shortening. Additionally, differences in mandibular kinematics between groups were as large as those observed in TBR, yet measurements were not taken in a mandibular coordinate system. Therefore, differences in hyoid kinematics may have been masked by mandibular kinematics. Moreover, this study conflicts with others demonstrating a link between hyoid excursion and epiglottal flipping (Logemann et al. 1992; Van Daele et al. 1995; Paik et al. 2008; Seo et al. 2014). The link between hyoid excursion, TBR, and epiglottal flipping needs be investigated more thoroughly to resolve these conflicting interpretations of swallowing biomechanics.

Lingual strengthening exercises specifically target intrinsic and extrinsic tongue muscles, which theoretically should improve TBR. However, lingual exercises have been unsuccessful in resolving dysphagia in head and neck cancer patients, in which poor TBR and hyolaryngeal excursion are common (Logemann et al. 2006; Logemann et al. 2008; O'Connell et al. 2008; Lazarus et al. 2014). Among a patient population with poor TBR, which included a near majority of head and neck cancer patients, Veis et al. (2000) found that most of these individuals could move the tongue further posteriorly via voluntary maneuvers than during swallowing. The authors suggested that these voluntary maneuvers may be able to strengthen weak tongue retractors without requiring the patients to engage in swallowing and risk aspirating. Although it is possible that these patients' TBR strength was so weak that they could not overcome intrabolus pressures to fully retract, these results alternatively suggest that either separate motor

pathways or separate muscles are responsible for voluntary and deglutitive TBR. In the latter case, styloglossus and/or hyoglossus shortening may yet generate tongue base kinematics for these voluntary maneuvers. The fact that yawning in particular could generate large TBR in these patients is particularly interesting—yawning is a wide-gaped behavior, yet swallowing with a wide gape is difficult to initiate and uncomfortable to execute, even if a bolus is transported into the valleculae beforehand. If styloglossus and/or hyoglossus are under such voluntary control, then exercises that specifically target these muscles' strength and coordination with other muscle groups may allow the tongue's redundant musculature to compensate for a failed hydraulic mechanism (Huckabee and Macrae 2014; Slovarp et al. 2016).

If suprahyoid muscles produce TBR through a hydraulic mechanism, then these muscles should be active during TBR. Several studies have demonstrated that palatal tongue pressure, suprahyoid muscle activity, and hyoid kinematics are temporally coordinated, with suprahyoid activity preceding tongue pressure and hyoid movement (Palmer et al. 2008; Taniguchi et al. 2008; Ono et al. 2009; Hori et al. 2013). Park et al. (2017) demonstrated that suprahyoid muscle activity precedes tongue base pressure and hyoid movement onset; although tongue base pressure onset was approximately 70 ms before hyoid movement onset, their confidence intervals were overlapping. This limited evidence from the human literature supports the hypothesis that suprahyoid muscle activity and tongue kinematics and kinetics are temporally coordinated.

Is tongue base retraction possible when if the hyoid has been removed?

Swallowing performance in patients following laryngectomy—surgical removal of part or all of the hyolaryngeal apparatus with the aim of curing locally invasive laryngeal cancer (Genden et al. 2007)—could be leveraged as a pseudo-experiment to attempt to falsify the

hydraulic linkage hypothesis by examining whether removal of the hyoid is associated with impaired TBR and swallowing performance in general. There are different degrees of laryngectomy—supraglottic laryngectomy larynx superior to the vocal folds, supracricoid laryngectomy removes the larynx superior to the cricoid cartilage, and total laryngectomy removes the entire hyolaryngeal apparatus (Genden et al. 2007). Depending on the extent of tumor growth, the entire hyoid and/or parts of the tongue base may also be removed in supraglottic or supracricoid laryngectomy (Ogura et al. 1961; Ogura 1979; Sobol and May 1990). Because patients vary in the extent of structures resected, some have correlated the preservation of specific structures with post-operative swallowing performance. Hyoid preservation does not correlate with a shorter time to oral feeding after supraglottic laryngectomy, and contact between the tongue base and posterior pharyngeal wall and normal tongue base pressures are nonetheless commonly observed despite hyoid resection (Flores et al. 1982; Hirano et al. 1987; McConnel et al. 1986; McConnel et al. 1987; Hamlet et al. 1990; Sulikowski 1991; Beckhardt et al. 1994). However, only one of these studies (Sulikowski 1991) analyzed swallowing kinematics, and none measured differences in tongue base retraction magnitude in these patients. Moreover, reduced hyolaryngeal excursion, TBR duration, and TBR magnitude are common in partial laryngectomy patients (Logemann et al. 1994; Lewin et al. 2008).

Although the observation that some patients still have normal tongue base pressures and contact between the tongue base and posterior pharyngeal wall after hyoid removal challenges the hydraulic linkage hypothesis proposed here, reconstruction technique may affect post-surgical outcomes. After removing the hyoid and part of the thyroid cartilage during a supraglottic laryngectomy, the defect is closed by suturing the remaining thyroid cartilage to the

base of the tongue and remaining hyoid periosteum onto which the suprahyoid muscles attach (Hirano et al. 1987; Sobol and May 1990). Therefore, the thyroid cartilage may serve as a neohyoid and replace the hydraulic functions of the hyoid in these patients. Additionally, there is variation in hyoid-sparing approaches to supraglottic laryngectomy—either the infrahyoid muscles (Sobol and May 1990) or the suprahyoid muscles (Ogura 1979) can be incised to gain access to the larynx for surgical removal. To date, no study has compared the functional outcomes of these techniques or whether incising hyoid musculature alone leads to functional defects.

Post-operative changes in motor control may also underlie the relative preservation of swallowing performance after removal of the hyoid. Contact between the TB and posterior pharyngeal wall may be preserved due to compensatory superior constrictor shortening in response to altered sensory feedback (Pauloski and Logemann 1995; Fujiu et al. 1995; Humbert et al. 2012). Moreover, the other extrinsic and intrinsic lingual muscles may alter their behavior to produce the work of TBR when the hydraulic linkage between is impaired. Tongue base retraction duration after partial laryngectomy—with hyoid removal but sparing of the tongue base—trends toward but does not reach normal over a course of three months following surgery (Logemann et al. 1994), which suggests that the surgery impairs TBR even though the tongue base is left intact and supports the hypothesis that new TBR motor patterns are being learned over the course of recovery.

Ultimately, falsification of the hydraulic linkage hypothesis requires more scientific rigor than retrospective analyses of laryngectomy patients can provide. These conflicts between clinical practice and biomechanical theory highlight the primary limitation of using patients in pseudo-experiments comparing control or pre-operative function with post-operative function:

hyoid removal is not studied in isolation but rather occurs in a variable patient population with variable tumor sizes and locations and variable comorbidities (Sobol and May 1990). Therefore, there are many potential confounding variables that could underlie the apparent lack association between hyoid preservation status and post-operative swallowing function, and tightly controlled animal experiments that control for not only operative technique but also changes in motor control over recovery are necessary to falsify the hydraulic linkage hypothesis.

What are the implications of a hydraulic linkage for swallowing motor control?

Mechanical linkages reduce the degrees of freedom necessary to control the movement of an apparatus, which in turn may simplify its motor control (Zatsiorsky and Prilutsky 2012). A hydraulic linkage would passively coordinate the movements of not only the hyoid and the tongue but also the tongue with the larynx and upper esophageal sphincter opening, thus ensuring that high pressures at the tail of the bolus are generated simultaneously with low pressures at the head of the bolus to grant the bolus safe and swift passage past the larynx. Simplification of motor control may be particularly important in infant mammals, which must suddenly transition from intermittent swallowing *in utero* (Bowie and Clair 1982), where aspiration of sterile amniotic fluid is of little consequence, to juggling swallowing with sucking and breathing during feeding sessions (German et al. 1998; Crompton et al. 1997). Conversely, loss of this hydraulic linkage may make TBR more complex for the central nervous system to control, in which case dysphagia may result from poor coordination rather than poor strength. Tongue base retraction rehabilitation may therefore require more training in swallowing skill and coordination among the remaining functional muscles than the strength of individual muscles (Huckabee and Macrae 2014).

CONCLUSIONS

The data refute the hypothesis that tongue base retraction is due to shortening of hyoglossus, palatoglossus, or styloglossus. Although hydrostatic deformation may facilitate the final stages of tongue base retraction, the tongue base and posterior oral tongue volume increase the oral volume accommodating the tongue decreases due to hyoid protraction and elevation. These reciprocal changes in volume support the hypothesis that tongue retraction is driven by a hydraulic linkage between the hyoid and the tongue.

CHAPTER FIVE: FUNCTIONAL MORPHOLOGY OF THE HYOLINGUAL MUSCLES OF *MACACA MULATTA*: *IN VIVO* MEASUREMENTS AND GEOMETRIC DETERMINANTS

INTRODUCTION

The suprahyoid muscles have several functions during feeding in humans and non-human primates. Chapter 4 discussed the role of hyoid elevation and protraction in tongue base retraction during swallowing. Because the larynx is suspended from the hyoid by the thyrohyoid membrane and thyrohyoid muscle (Standring 2015; Nishimura 2003), this hyoid excursion aids in airway protection by elevating and protracting the larynx. Laryngeal elevation facilitates contact between the arytenoids of the larynx and the laryngeal surface of the epiglottis, preventing entry of the bolus into the airway (Logemann et al. 1992; Inamoto et al. 2011). Because the upper esophageal sphincter (UES) is attached to the larynx—specifically to the cricoid cartilage—hyolaryngeal protraction opens the UES after it relaxes during the pharyngeal stages of the swallow (Cook et al. 1989; Jacob et al. 1989; Kahrilas et al. 1991). Hyoid protraction may also flip the epiglottis over the airway, providing an additional physical barrier against penetration (Logemann et al. 1992; Seo et al. 2014; Pearson et al. 2016a).

Given the important role of suprahyoid muscles in airway protection, it is not surprising that reductions in hyoid displacement and velocity are commonly found in patients with dysphagia (Hamlet et al. 1991; Wang et al. 2010; Hoffman et al. 2013; Steele and Cichero 2014; Seo et al. 2016), and increased hyoid displacement and velocity after rehabilitation therapy are associated with improved swallowing performance (Sia et al. 2015). Pearson and colleagues have related specific hyolaryngeal and pharyngeal kinematics to the underlying morphology to infer

which muscles should be targeted in therapy (Pearson et al. 2011; Pearson et al. 2012; Pearson et al. 2013; Gassert and Pearson 2016; Pearson et al. 2016). This approach is analogous to gait analysis which associates changes in gait to pathological function of individual muscles (e.g., the Trendelenburg gait and medial gluteal weakness), and rehabilitation targets these muscles using muscle-specific exercises and biofeedback (Petrofsky 2001; Tate and Milner 2010). However, the basic mechanisms of hyoid excursion remain unclear because it is difficult to access individual suprahyoid muscles for EMG recordings. Moreover, muscle length cannot be accurately measured from 2D videofluoroscopy, the most common method for measuring hyoid kinematics *in vivo*. Without a basic understanding of mechanisms of hyoid excursion, it is difficult to design, implement and evaluate rehabilitation therapies.

Currently, suprahyoid muscles are assumed to produce hyoid elevation and protraction through active shortening. Although these muscles are hypothesized to also behave isometrically and eccentrically (Thexton 1984), the potential functions of such activity are unknown. Knowing whether and when muscles are concentrically, isometrically, or eccentrically active would help determine the kinds of exercises used during swallowing rehabilitation. Because different types of exercise produce different neuroplastic and myoplastic responses, exercises which match the type of activity observed *in vivo* produce superior functional outcomes to those which do not match or only partially match (Thorstensson et al. 1976; Coyle et al. 1981; Gür et al. 2002). This principle of rehabilitation is known as task-specificity and is thought to facilitate transfer of improvements in exercises to improvement in the targeted function (Stathopoulos and Ducchan 2006; Hubbard et al. 2009).

Moreover, the geometric arrangement of hyolingual muscles allows hyoid movement to occur not only as a result of muscle shortening, but also of fiber rotation. Recent research on the

biomechanics of other pennate muscles emphasizes the fact that, while rotation of hyolingual muscles may enhance hyoid translational velocity, this comes at the expense of muscle force production (Brainerd and Azizi 2005; Azizi et al. 2008; Randhawa et al. 2013; Azizi and Roberts 2014; Holt et al. 2016). As argued in Chapter 2, the geometric arrangement of hyolingual muscles is analogous to a complexly pennate muscle. Because these trade-offs are analogous to the gearing of skeletal muscles via morphological variation in muscle attachment site or physiological variation in body posture and joint kinematics (Biewener 1989; Carrier et al.1994; Carrier et al. 1998; Biewener et al. 2004; Iriarte-Diaz et al. 2017), such trade-offs are quantified with an architectural gear ratio (AGR) of whole muscle to fiber velocity. However, much of the dynamic nature of a pennate muscle's AGRs is due to how these muscles bulge during shortening, which is probably a function of both force production and connective tissue properties (Azizi et al. 2008; Holt et al. 2016). In comparison, most individual primate hyolingual muscles have simple architecture (Howell and Straus 1933; Pearson et al. 2011) and are free to bulge in any direction relative to its line of action. Because the amount of rotation each muscle experiences is instead determined by how much other hyolingual muscles shorten, a gear ratio is generated for each muscle separately and termed as such below.

If suprahyoid muscles lose force as a result of rotation, then eccentric activity prior to shortening (i.e., stretch-shortening cycles, Chapter 2) may preserve or even enhance force production. Thus, evidence of non-concentric activity and fiber rotation has important implications for understanding how force-velocity tradeoffs affect suprahyoid muscle performance during swallowing as well as determining what rehabilitation strategies are optimal for treating dysphagia. Moreover, relating gear ratios to hyolingual geometry will lay a foundation for future work evaluating the morphological basis of swallowing performance.

Aims and Hypotheses

This chapter has two aims: to relate the observations about tongue base retraction and hyoid kinematics made in Chapter 4 to observations about muscle behavior presented here; and to test two hypotheses about suprahyoid muscle function. The first hypothesis, that hyolingual muscles only function concentrically, is tested by comparing EMG recordings to muscle velocity measurements. This concentric-only hypothesis is falsified if hyolingual muscles reach peak activity during shortening but exhibit additional periods of isometric and/or eccentric activity, or if hyolingual muscles reach peak activity during isometric and/or eccentric activity. The second hypothesis, that muscle shortening is the sole cause of hyoid protraction and elevation, is tested by measuring the ratio of hyoid excursion velocity to muscle velocity, a ratio analogous to the architectural gear ratio in pennate muscles (Azizi et al. 2008). This hypothesis is falsified if the hyoid moves faster than the suprahyoid muscles shorten. The biomechanical basis and consequences of hyoid velocity amplification is further examined using mathematical models.

RESULTS

After inspecting the location of electrodes on diceCT scans, electrodes were confirmed to be in the anterior digastric, genioglossus, geniohyoid, and mylohyoid muscles in all four animals. One animal had one channel for styloglossus (Monkey Ch), while another had one channel for posterior digastric (Monkey JB). Because Monkey Ki did not have markers implanted in the digastric tendon, anterior digastric velocity data were not available for this animal.

How is muscle behavior related to tongue base retraction?

Data on behavior—activity, length, orientation—of genioglossus, geniohyoid, mylohyoid, digastric, hyoglossus and stylohyoid during swallowing are summarized in Figures 5.1-5.6.

Geniogossus exhibits low-level activity during TBR in all animals, and a distinct burst of activity in two animals (Figure 5.1). In three animals, maximum activity in genioglossus is observed before TBR as the genioglossus fibers shorten. These fibers subsequently lengthen and exhibit either low-level activity or a small burst of activity during TBR.

Geniohyoid passively lengthens before TBR in three out of four animals. Geniohyoid actively shortens during TBR (Figure 5.2) and in three out of four animals TBR corresponds with peak geniohyoid activation. Geniohyoid fascicles rotate superiorly during TBR as the hyoid continues elevating.

Posterior mylohyoid reaches peak activity and actively shortens and rotates in coronal planes before TBR (Figure 5.3). During TBR, it begins to rotate in sagittal planes and continues to shorten with less activity. Onset of sagittal rotation near the beginning of TBR is consistent with the beginning of hyoid protraction at that time (Chapter 4).

The anterior and posterior digastric muscles show opposite patterns of length change—the anterior digastric lengthens before and shortens during TBR, while the posterior digastric shortens before and lengthens during TBR (Figure 5.4). In Monkeys Ch and He, the anterior digastric is active during lengthening before TBR onset. As with mylohyoid, peak anterior digastric activity precedes TBR onset in three out of four animals. The anterior digastric rotates superiorly throughout retraction, indicating continued elevation of the mouth floor. However, anterior and posterior digastric activity during TBR is minimal in one animal (Monkey JB).

Muscle activity data were not available for hyoglossus or stylohyoid because electrode pairs were not confirmed to be within their muscle fascicles *post mortem*. As expected from hyoid kinematics and muscle length change reported in Chapter 4, hyoglossus shortens before and during TBR and rotates minimally to become slightly more superiorly oriented as the hyoid protracts (Figure 5.5). In contrast, stylohyoid shortens during hyoid elevation before TBR and lengthens slightly as the hyoid protracts during TBR (Figure 5.6). Throughout stylohyoid shortening and TBR, stylohyoid rotates in sagittal planes to become more posteriorly oriented.

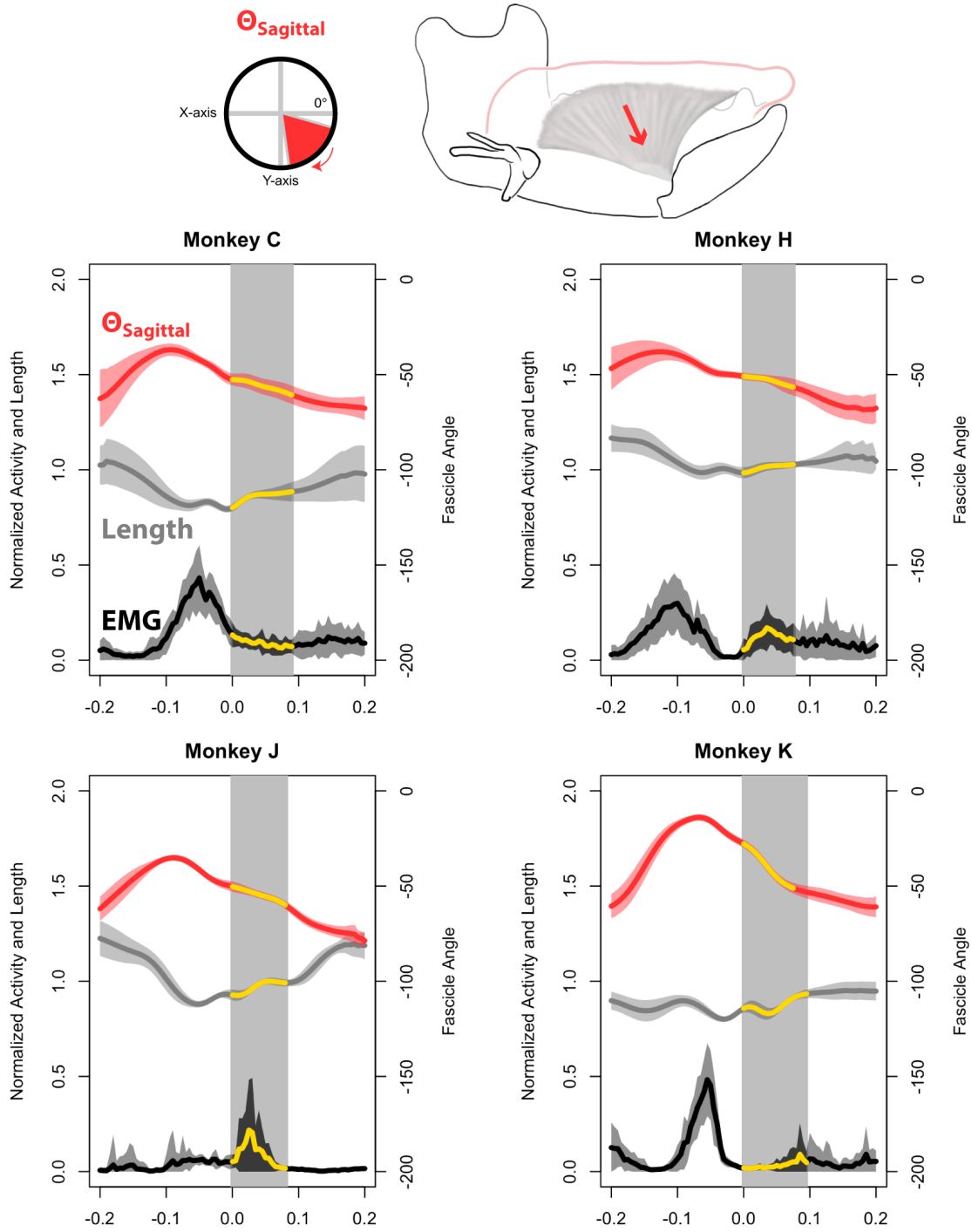

Figure 5.1: Genioglossus normalized activity, normalized length, and orientation during swallowing. Normalized EMG traces are shown in black. Genioglossus normalized length is shown in gray. Genioglossus sagittal orientation is shown in red—more negative values indicate a more superoinferior orientation. Dark traces indicate mean values; lighter shades are standard deviations. Vertical gray bars indicate the mean duration of tongue retraction and coincide with the yellow portions on the muscle length and EMG traces. Data are aligned to the onset of tongue base retraction (Time = 0.0). The origin of the compass is aligned with the marker in the tongue.

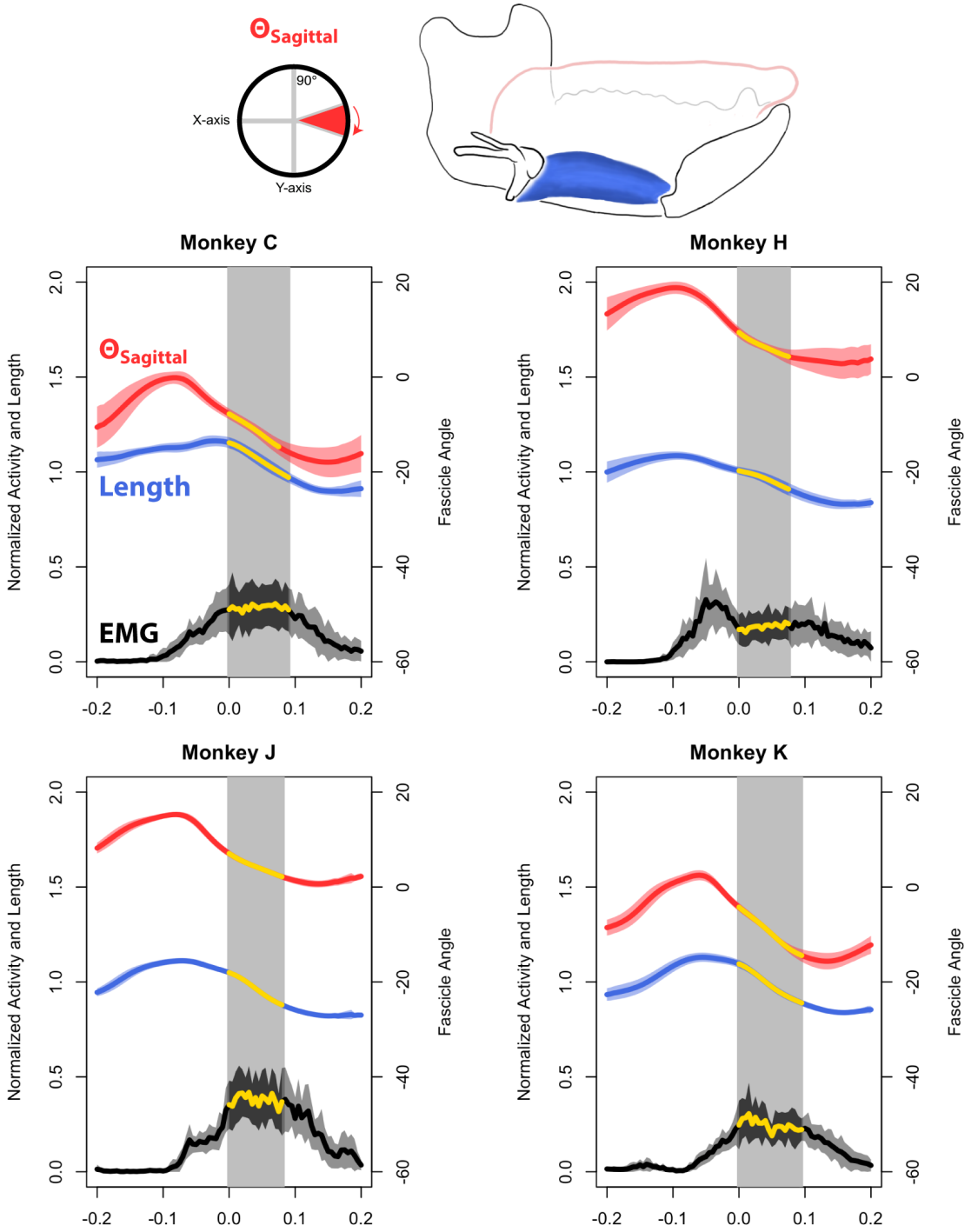

Figure 5.2: Geniohyoid normalized activity, normalized length, and orientation during swallowing. EMG traces are shown in black. Geniohyoid normalized length is shown in blue. Dark traces indicate mean values; lighter shades are standard deviations. Vertical gray bars indicate the mean duration of tongue retraction and coincide with the yellow portions on the muscle length and EMG traces. Data are aligned to the onset of tongue base retraction (Time = 0.0). The origin of the compass is aligned with the attachment on the hyoid.

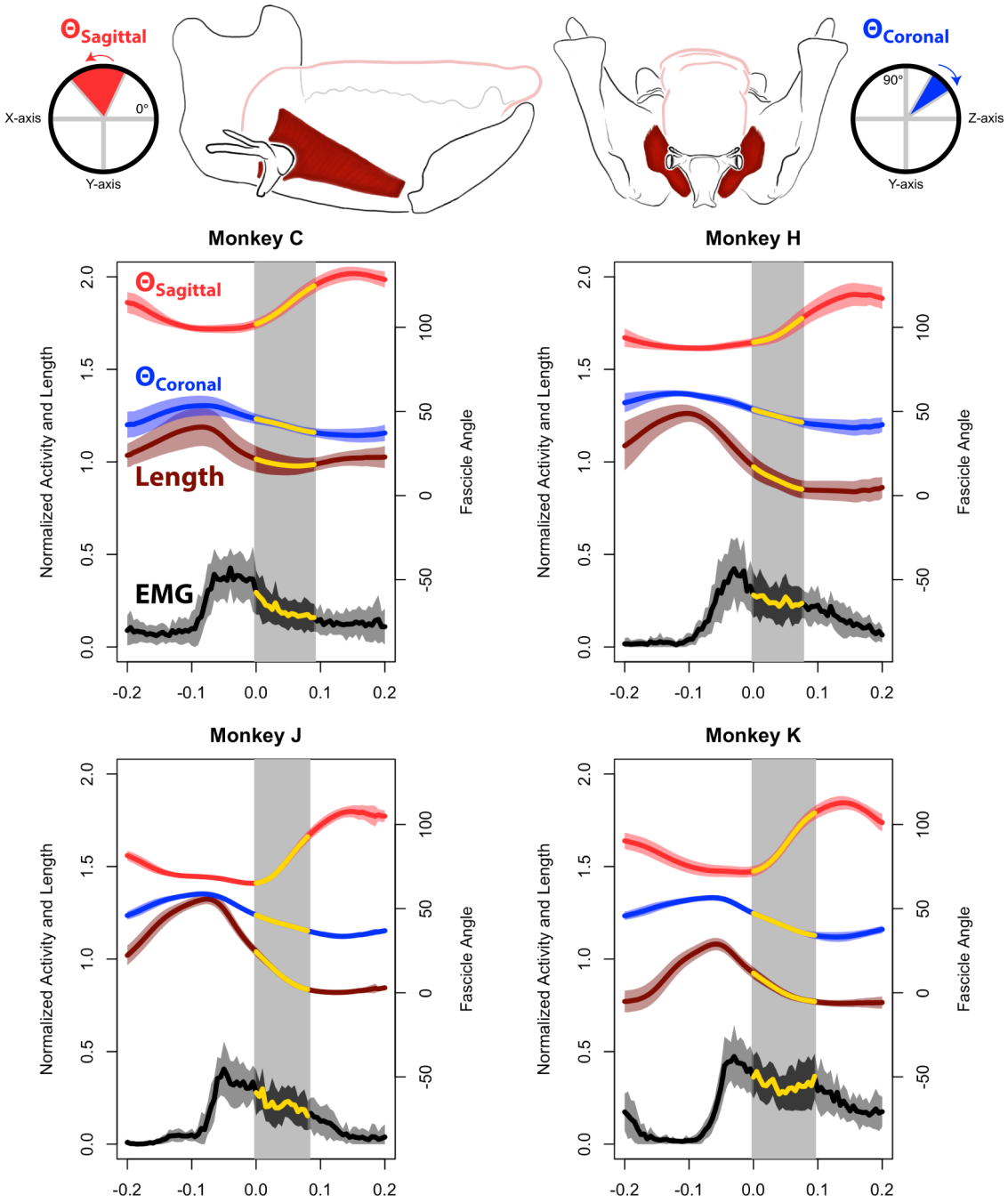

Figure 5.3: Mylohyoid normalized activity, normalized length, and orientation during swallowing. EMG traces are shown in black. Mylohyoid normalized length is shown in dark red. Mylohyoid sagittal angles are shown in red. Mylohyoid coronal angles are shown in blue. Dark traces indicate the mean values; lighter shades are standard deviations. Vertical gray bars indicate the mean duration of tongue retraction and coincide with the yellow portions on the muscle length and EMG traces. Data are aligned to the onset of tongue base retraction (Time = 0.0). The origin of the compass is aligned with the attachment on the hyoid.

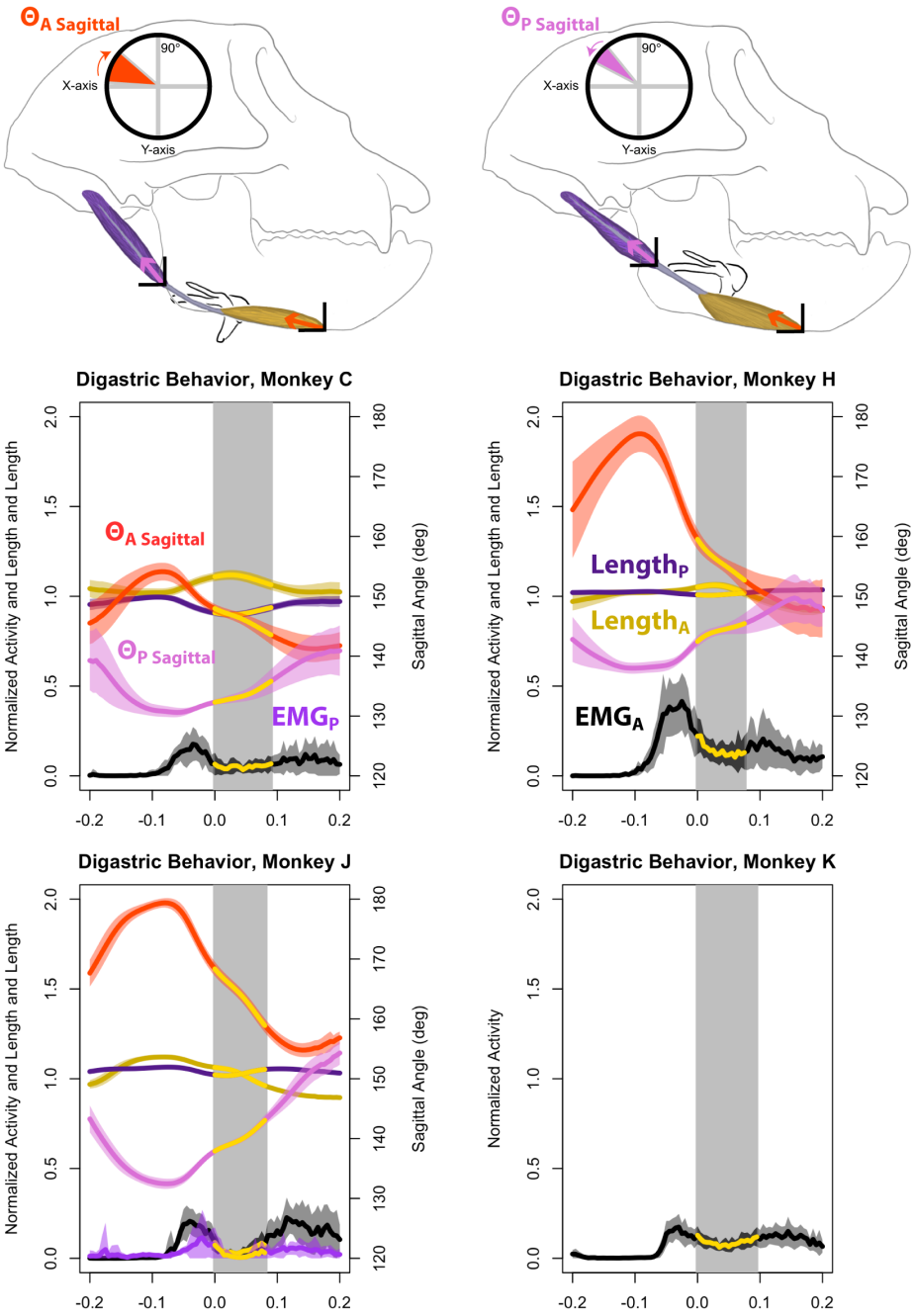

Figure 5.4: Digastric activity, normalized length, and orientation during swallowing. Anterior digastric EMG traces are shown in black, posterior digastric shown in purple. Anterior digastric normalized length is shown in gold. Posterior digastric normalized length is shown in dark purple. Orientation of the anterior and posterior digastrics in the sagittal planes are shown in orange and pink, respectively—180 degrees indicates a purely posterior orientation, while lower values indicate progressively more superior orientations. Dark traces indicate the mean values; lighter shades are standard deviations. Vertical gray bars indicate the mean duration of tongue retraction and coincide with the yellow portions on the muscle length, orientation, and EMG traces. Data are not available for Monkey Ki because it did not have markers implanted in the anterior digastric. Data are aligned to the onset of tongue base retraction (Time = 0.0). The origin of the anterior digastric compass is aligned with the attachment on the mandible. The origin of the posterior digastric compass is aligned with the attachment into the digastric tendon.

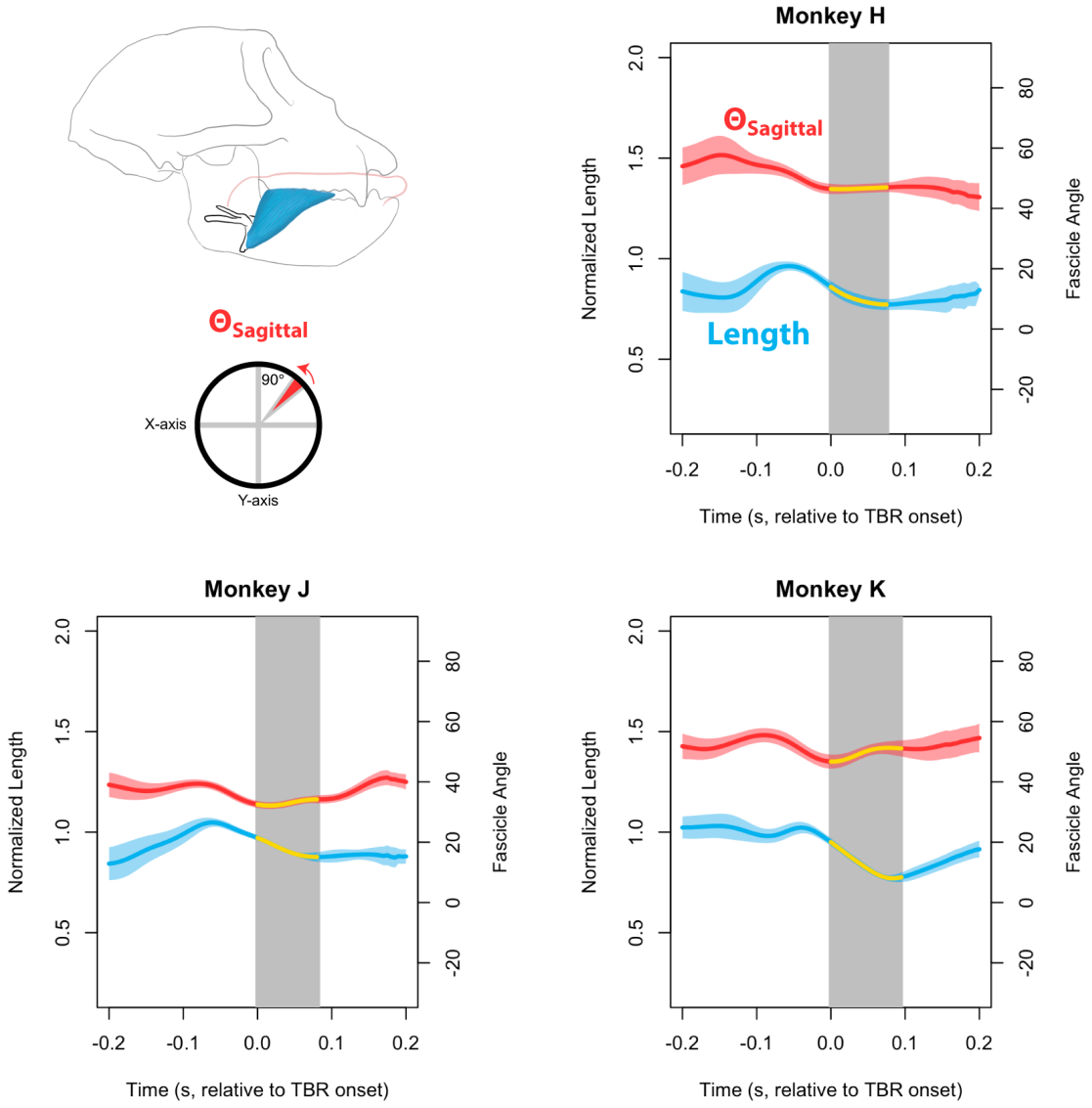

Figure 5.5: Hyoglossus normalized length during swallowing. Hyoglossus normalized length is shown in light blue. Orientation of the hyoglossus in the midsagittal plane is shown in red—90° indicates a purely superior orientation, 0° indicates a purely anterior orientation. Dark traces indicate the mean values; lighter shades are standard deviations. Vertical gray bars indicate the mean duration of tongue retraction and coincide with the yellow portions on the muscle length and orientation traces. Data are not available for Monkey Ch because the marker was implanted too far medially. Data are aligned to the onset of tongue base retraction (Time = 0.0). The origin of the compass is aligned with the attachment on the hyoid.

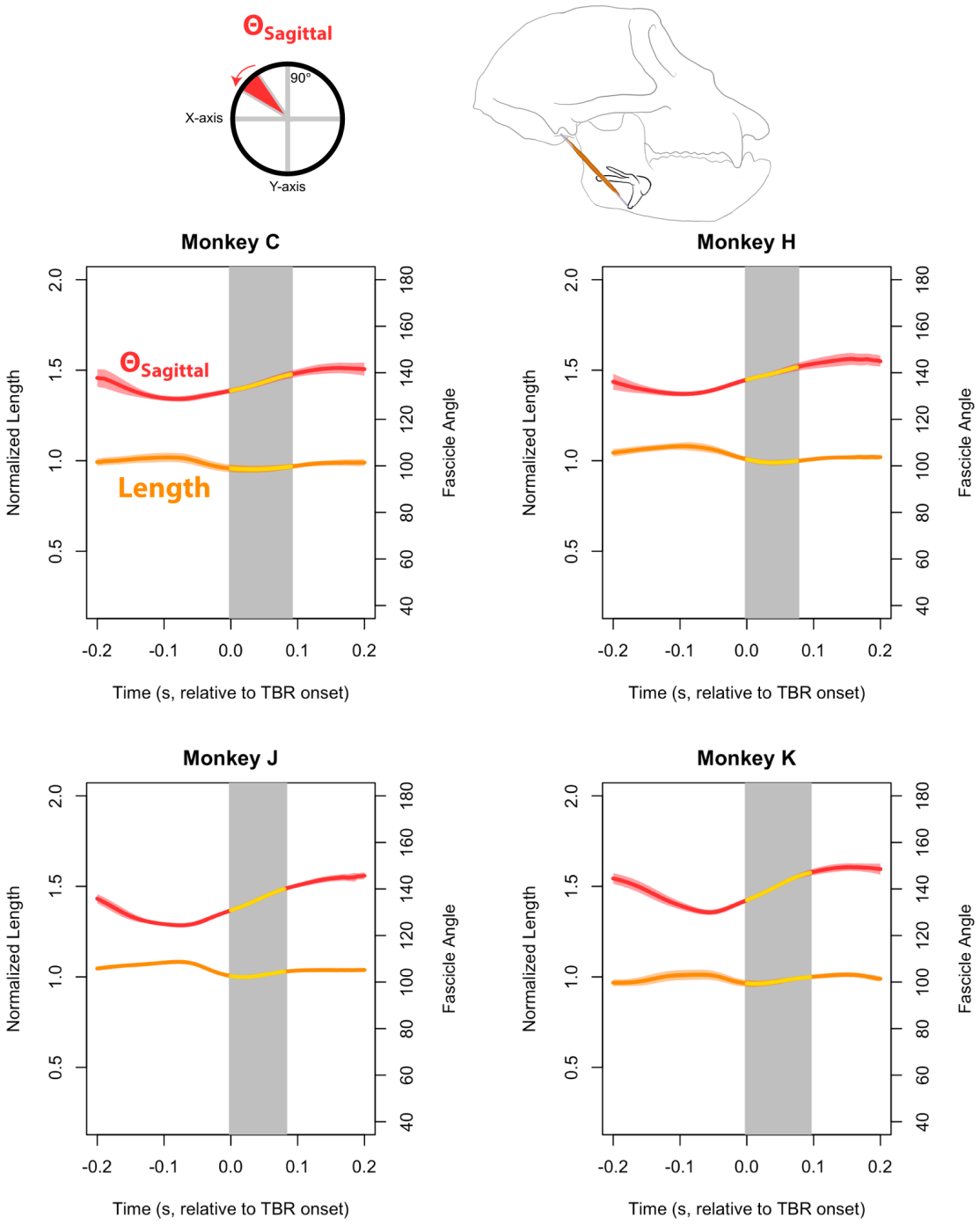

Figure 5.6: Stylohyoid normalized length during swallowing. Stylohyoid normalized length is shown in orange. Orientation of the stylohyoid in sagittal planes is shown in red—90° indicates a purely superior orientation, 0° indicates a purely anterior orientation. Dark traces indicate the mean values; lighter shades are standard deviations. Vertical gray bars indicate the mean duration of tongue retraction and coincide with the yellow portions on the muscle length and orientation traces. Data are aligned to the onset of tongue base retraction (Time = 0.0). The origin of the compass is aligned with the attachment on the hyoid.

Are hyolingual muscles concentrically, isometrically, or eccentrically active during swallowing?

The patterns of length change described above were analyzed by directly comparing muscle velocity to activity levels. Muscles showed variable patterns of concentric (active shortening), eccentric (active lengthening), and isometric activity (active without changing length) among muscles and among animals during swallowing (Figure 5.7).

Genioglossus activity and velocity were particularly variable among animals. Three animals showed concentric activity before tongue base retraction (Monkeys Ch, He, and Ki), and three showed either a burst or sustained low-level isometric or eccentric activity during tongue base retraction (Monkeys Ch, He, and JB). The earlier onset of the pre-retraction genioglossus burst corresponds with the observation that this animal formed a trough in the midline tongue earlier in the swallow than the other animals.

Geniohyoid was concentrically active throughout tongue base retraction in all four animals and exhibited variable activity before the onset of tongue base retraction: Monkeys Ch and Ki had submaximal isometric activity, Monkey He had maximal concentric activity, and Monkey JB had submaximal concentric activity.

Mylohyoid was concentrically active before tongue base retraction in all animals. This main burst of mylohyoid concentric activity was preceded by variable amounts of active stretch at low velocities and low activity levels. The main mylohyoid burst was followed by variable types of activity—Monkey Ch had isometric and eccentric activity, Monkeys He and Ki had relatively sustained isometric activity before activity declined, and Monkey JB had declining isometric activity. Among animals with digastric markers, eccentric activity is observed in Monkeys Ch and He before TBR, while concentric activity is uniformly observed during late TBR.

Given that styloglossus and posterior digastric electrodes were only viable for one animal each and the amount of inter-individual variability observed among the animals, these muscles activity patterns may not be generalizable but are nonetheless reported here. Styloglossus shifted from being concentrically active early in the swallow to being primarily eccentrically active during TBR. Posterior digastric was concentrically active immediately before TBR, as during hyoid elevation, and showed a second period of lower-level activity that was isometric and then concentric late in the swallow.

The proportion of the swallow and TBR that each muscle spent in each type of activity was measured to quantify these activity patterns. With the exception of geniohyoid, activity type distributions were variable across the swallow as a whole (Figure 5.8). However, patterns among animals and within muscle groups were more consistent among animals during TBR, with suprahyoid muscles being predominantly concentrically active and lingual muscles being predominantly eccentrically active (Figure 5.9).

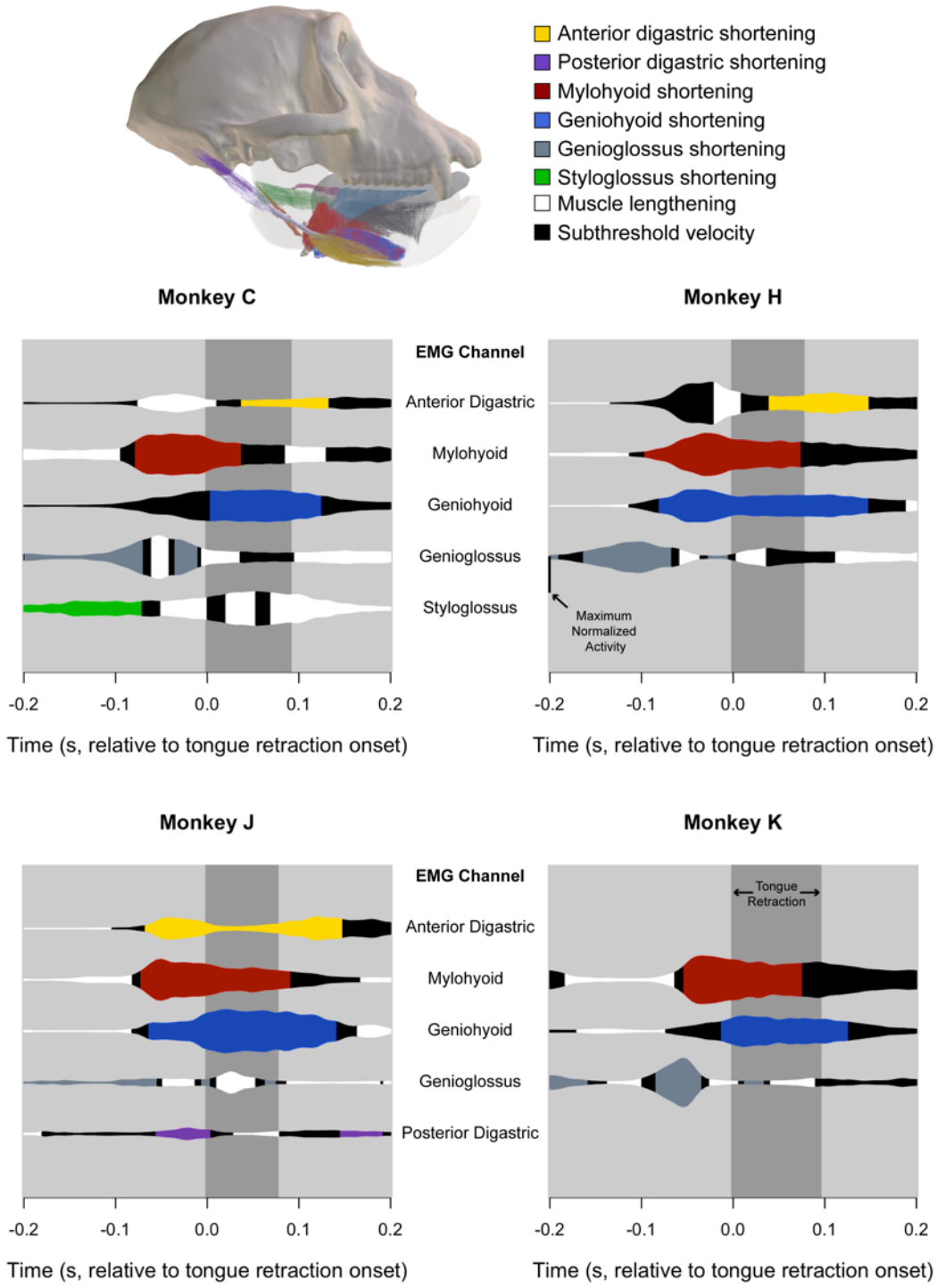

Figure 5.7: Hyolingual muscle activity and velocity. Data are not available for some animals because they either lacked markers (Monkey Ki digastrics) or EMG electrodes were confirmed implanted in the anterior digastric in only one animal (Monkey Ch styloglossus, Monkey JB posterior digastric). Vertical dark gray bar indicates the duration of tongue base retraction. Data are aligned to the onset of tongue base retraction (Time = 0.0).

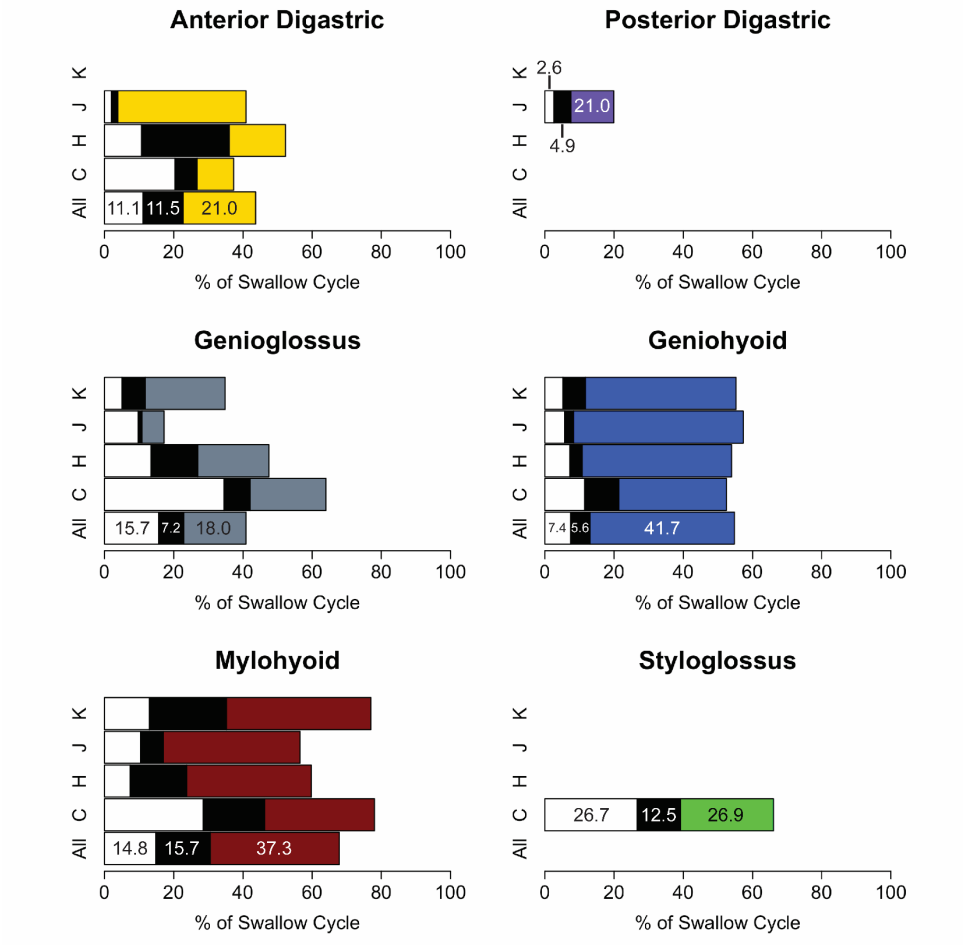

Figure 5.8: Proportion of muscle activity types during swallow cycles. Bar plots illustrate for each animal (C, H, J, K) the mean proportion of the swallow cycle in which a muscle exhibits a given activity type. Color code: white, eccentric activity; black, isometric activity; respective color, concentric activity. Numbers in the lowest bars indicate percentage of the swallow cycle spent in each activity type.

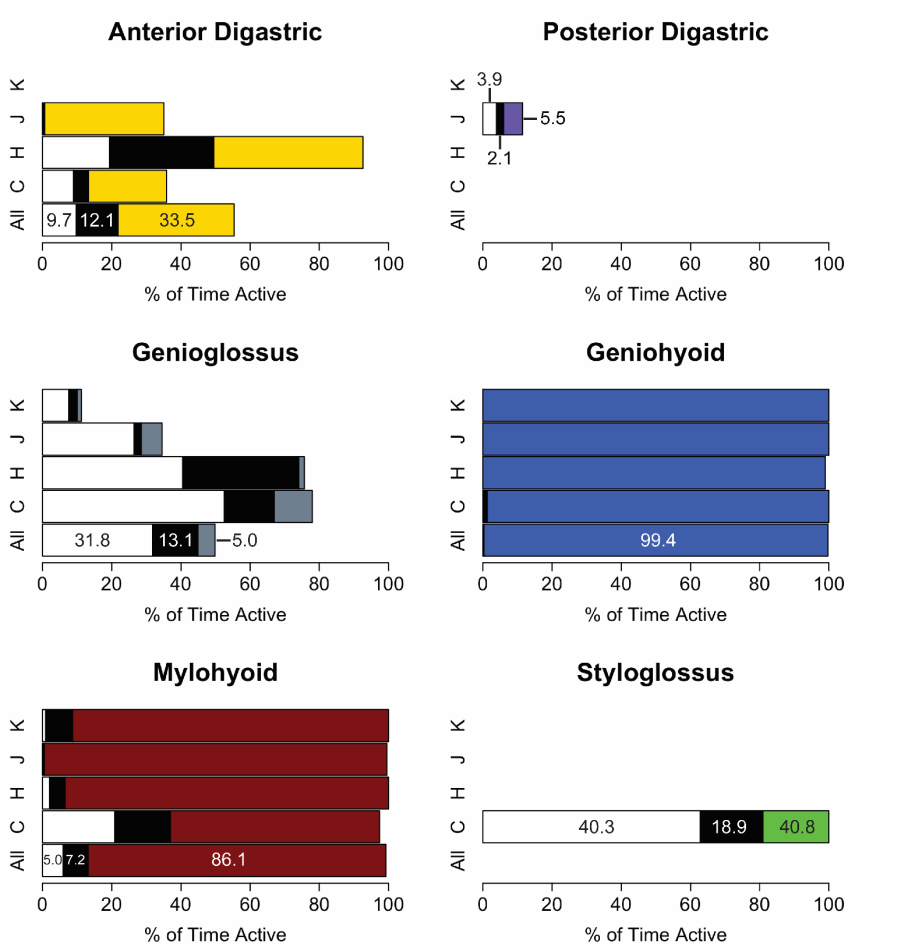

Figure 5.9: Proportion of muscle activity types during tongue base retraction. Bar plots illustrate for each animal (C, H, J, K) the mean proportion of tongue base retraction in which a muscle exhibits a given activity type. Color code: white, eccentric activity; black, isometric activity; respective color, concentric activity. Numbers in the lowest bars indicate percentage of the swallow cycle spent in each activity type.

Is hyoid velocity amplified by suprahyoid muscle rotation?

Gear ratios (GR, the ratio of hyoid velocity to muscle velocity) quantify how much hyoid velocity is amplified by rotation of each muscle; $GR_{\bar{X}}$ and $GR_{\bar{Y}}$ compare average velocity along the X- and Y-axes, respectively, while GR_{Xp} and GR_{Yp} compare velocity at the time of peak muscle velocity. Values greater than 1.00 indicate that the hyoid moves faster than the muscle

shortens. In these results, positive GR values indicate net muscle shortening, while negative GR values indicate net muscle lengthening.

All measured suprahyoid muscles rotated during swallowing, yet there was no clear relationship between the amount of rotation and the amount of hyoid velocity amplification (Table 5.1). Geniohyoid and stylohyoid rotated by similar amounts in sagittal planes, yet stylohyoid GR values were much larger in geniohyoid. Similarly, mylohyoid rotated more than twice as much as stylohyoid, yet stylohyoid velocities were amplified more than mylohyoid velocities. Hyoglossus rotated the least, and GRs depending on whether they were measured based on X-axis, Y-axis, or total displacement. Stylohyoid $GR_{\bar{Y}}$ was particularly high and variable (7.31 ± 42.13). High variation was due to some cycles in Monkey Ch and Monkey Ki where the stylohyoid lengthened during hyoid elevation, reducing the amount of net muscle shortening and inflating $GR_{\bar{Y}}$. In contrast to $GR_{\bar{Y}}$, stylohyoid GR_{Yp} values were fairly consistent across animals (1.61 ± 0.30).

Gear ratio variation correlated with muscle geometry and the direction of rotation. As a muscle becomes more aligned with a given axis, more of its force is oriented along that axis. However, as a muscle becomes more perpendicular to a given axis, rotation produces greater displacement along that axis. This rotational phenomenon is here termed *rotational efficiency* (RE) and is defined as $dY/d\Theta$ (see Chapter 3). This axial force-displacement trade-off is illustrated in Figure 5.10. Geniohyoid was oriented primarily anteroposteriorly, so any fiber rotation contributes minimally to hyoid protraction. Indeed, two animals (Monkeys He and JB) had geniohyoid insertion sites that were more inferior than their mandibular origin, and these animals had $GR_{\bar{X}}$ values of 0.79 ± 0.03 and 0.94 ± 0.01, indicating that fiber rotation reduced hyoid protraction. This reduction occurred the direction of rotation toward 90° was antagonistic

to protraction until the geniohyoid insertion was superior to its origin on the mandible. A simulation of human-like hyoid descent, where the geniohyoid rotated from 120° to 90°, demonstrated that further descent worsened protraction depression due to rotation. In contrast, hyoglossus, mylohyoid, and styloglossus are all oriented at approximately 45° to either direction of hyoid movement, and the direction of rotation was synergistic with their axes of movement (i.e., toward 0°). Consequently, these muscles all exhibited higher GR's, except for hyoglossus $GR_{\overline{Y}}$ and GR_{Yp}. Indeed, although rotation direction was agonistic to hyoglossus' ability to protract, it was antagonistic to its ability to elevate the hyoid—consequently, its $GR_{\overline{Y}}$ was less than 1.00 (0.85 ± 0.20). In general, larger fiber angles increase the magnitude of effects of rotation on hyoid kinematics, and the direction of rotation determined whether rotation amplified or reduced hyoid kinematics.

Table 5.1: Suprahyoid muscle average and peak gear ratios and muscle rotations during swallows.

Muscle	Direction	Gear Ratio		Sagittal Plane			Coronal Plane		
		Average	Peak	Θ_{start}	Θ_{end}	$\Delta\Theta$	Θ_{start}	Θ_{end}	$\Delta\Theta$
GH	X	0.99 (0.14)	1.04 (0.07)	7.49 (9.92)	-7.88 (9.48)	15.37	—	—	—
HG	X	1.13 (0.33)	0.61 (0.4)	50.08 (6.97)	40.3 (6.49)	9.78	77.2 (2.51)	68.88 (3.83)	8.32
HG	Y	0.85 (0.20)	0.65 (0.1)	50.08 (6.97)	40.3 (6.49)	9.78	77.2 (2.51)	68.88 (3.83)	8.32
HG	Total	1.43 (0.29)	0.95 (0.24)	50.08 (6.97)	40.3 (6.49)	9.78	77.2 (2.51)	68.88 (3.83)	8.32
MH	Y	1.68 (0.92)	1.21 (0.16)	80.48 (13.29)	117.64 (11.02)	37.16	57.3 (3.99)	35.13 (4.22)	22.17
StyH	Y	7.31 (42.13)	1.61 (0.30)	128.34 (2.68)	145.26 (3.52)	16.92	68.67 (4.18)	59.31 (5.09)	9.36

GH, geniohyoid; HG, hyoglossus; MH, mylohyoid; StyH, stylohyoid

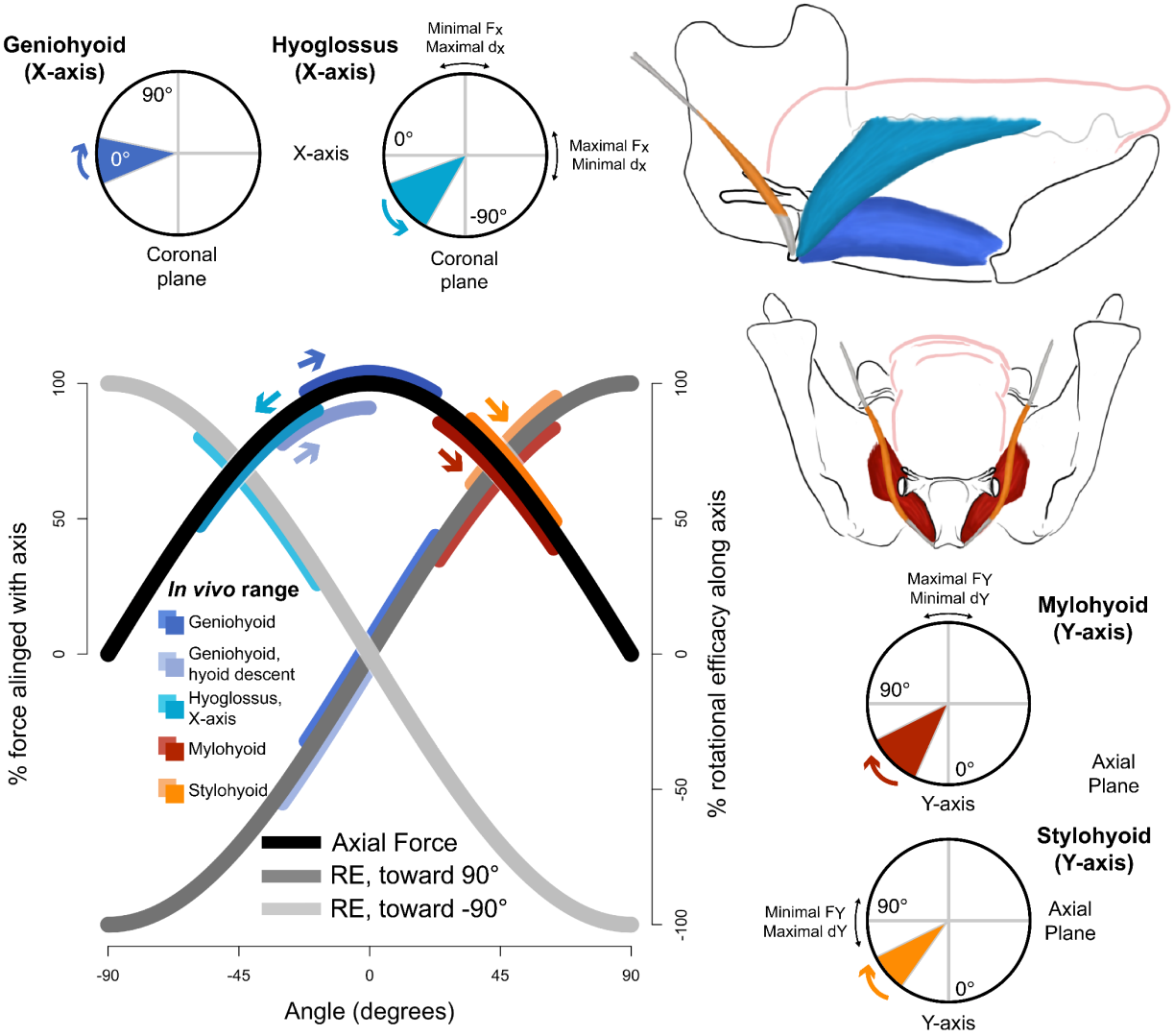

Figure 5.10: Axial force-displacement trade-off in hyolingual muscles. Whether rotational efficiency (RE) increases or decreases depends on whether rotation is toward 90° (light gray) or -90° (dark gray). Colored slices in compasses and colored lines on the graph indicate the range of muscle orientations observed *in vivo*. The origin of each compass is the muscle origin on the hyoid or in the tongue. Color code: black line, axial force; light gray line, RE when rotating toward zero; dark gray line, RE when rotating away from zero; dark blue, geniohyoid; light blue, hyoglossus; red, mylohyoid; orange, stylohyoid.

Although alignment maximizes the relative amount of force produced along that axis (Brainerd and Azizi 2005; Azizi et al. 2008), an aligned muscle can only generate axial movement through fiber shortening. Consequently, force-velocity tradeoffs could decrease the amount of force produced by longer fibers that rotate less compared to shorter fibers that rotate more and shorten less despite their not being aligned with the axis. To test this hypothesis, force production was modeled in a fixed-gear muscle—a muscle with a fixed width, specifically mylohyoid—using a Hill-type model (see Chapter 3). One model changed initial fiber angle by changing muscle length while keeping mandibular width constant, while a second model changed initial fiber angle by changing mandibular width while keeping muscle length constant. The models simulated mylohyoid shortening and consequent hyoid elevation and assumes that the hyoid does not move mediolaterally and always elevates the same amount that was observed *in vivo* (10.1 mm). This displacement (*dY*) was normalized to dY_n by dividing *dY* by itself in the variable fiber length model and by fiber length in the constant fiber length model.

In the variable fiber length model, the *in vivo* range of initial fiber angles (32.7° ± 4.0°) approached the largest normalized fiber velocities and lowest predicted total and axial forces (Figure 5.11). Longer, more axially-oriented fibers found in models with lower hyoids produced the greatest total and axial forces, while the shortest, most orthogonally-oriented fibers in models with higher hyoids generated less force than more axially-oriented fibers but more than those in the *in vivo* initial fiber angle range.

In the fixed fiber length model, the *in vivo* range of initial fiber angles produced intermediate total and axial forces (Figure 5.12). As the mandible widened and initial fiber angle increased, total force increased as fiber velocity decreased, and axial force increased until an

initial fiber angle of 60°. Hyoid elevation by mylohyoid shortening beyond 64.5° was impossible because it required fiber inversion to achieve dY_n.

DISCUSSION

This study sought to determine the muscular mechanisms of hyolingual movement during swallowing by analyzing both linear and angular hyolingual muscle kinematics. Combining linear kinematics with muscle activity determines the prevalence of concentric, isometric, and eccentric activity in hyolingual muscles during swallowing, and this information can be used to determine which rehabilitation exercises will best restore normal function (Burkhead et al. 2007).

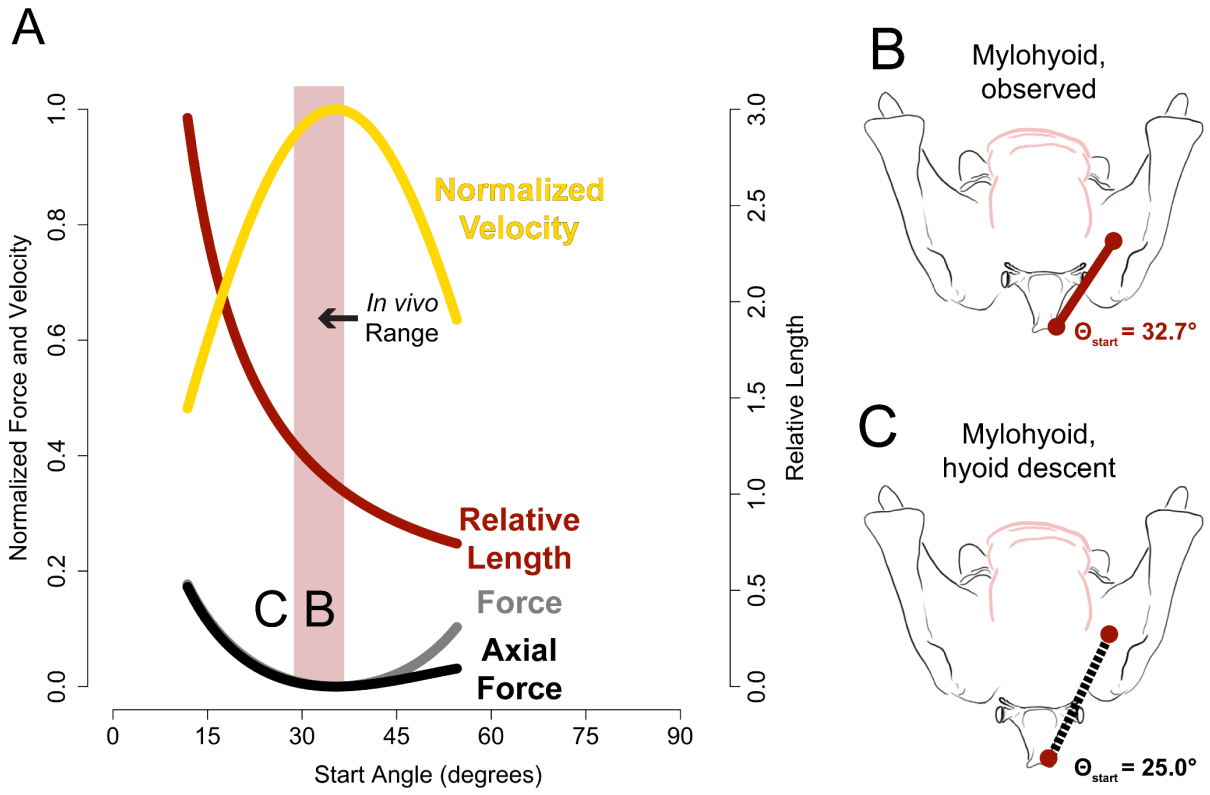

Figure 5.11: Geometric force-velocity curve in mylohyoid as hyoid posture is changed. A) Normalized force (gray), axial force (black), fiber velocity (gold), and starting fiber length (red) at different starting orientations. Lengths less than 69.6 % of *in vivo* length could not generate enough elevation without achieving final angles greater than 90°. Lengths greater than 300% of hyoid Y-axis displacement are not shown. B) Diagram of observed average mylohyoid starting orientation. C) Diagram of mylohyoid with a smaller initial starting angle. A similar orientation could be achieved by displacing the mylohyoid mandibular attachment superiorly relative to the hyoid.

For example, muscles which function primarily isometrically may benefit the most from isometric exercises and force-based biofeedback, while those which function primarily concentrically may benefit most from exercises which are concentric and use velocity- or power-based biofeedback (force x velocity) (Duchateau and Hainaut 1984).

Angular kinematics are important because fiber rotational components of hyolingual kinematics and kinetics are central to links between hyolingual morphology and swallowing performance. Although inquiries into the functional consequences of static and dynamic muscle geometry have long advanced the field of muscle functional morphology (Gans and Bock 1965; Azizi et al. 2008), this is the first time these principles are applied to the hyolingual apparatus.

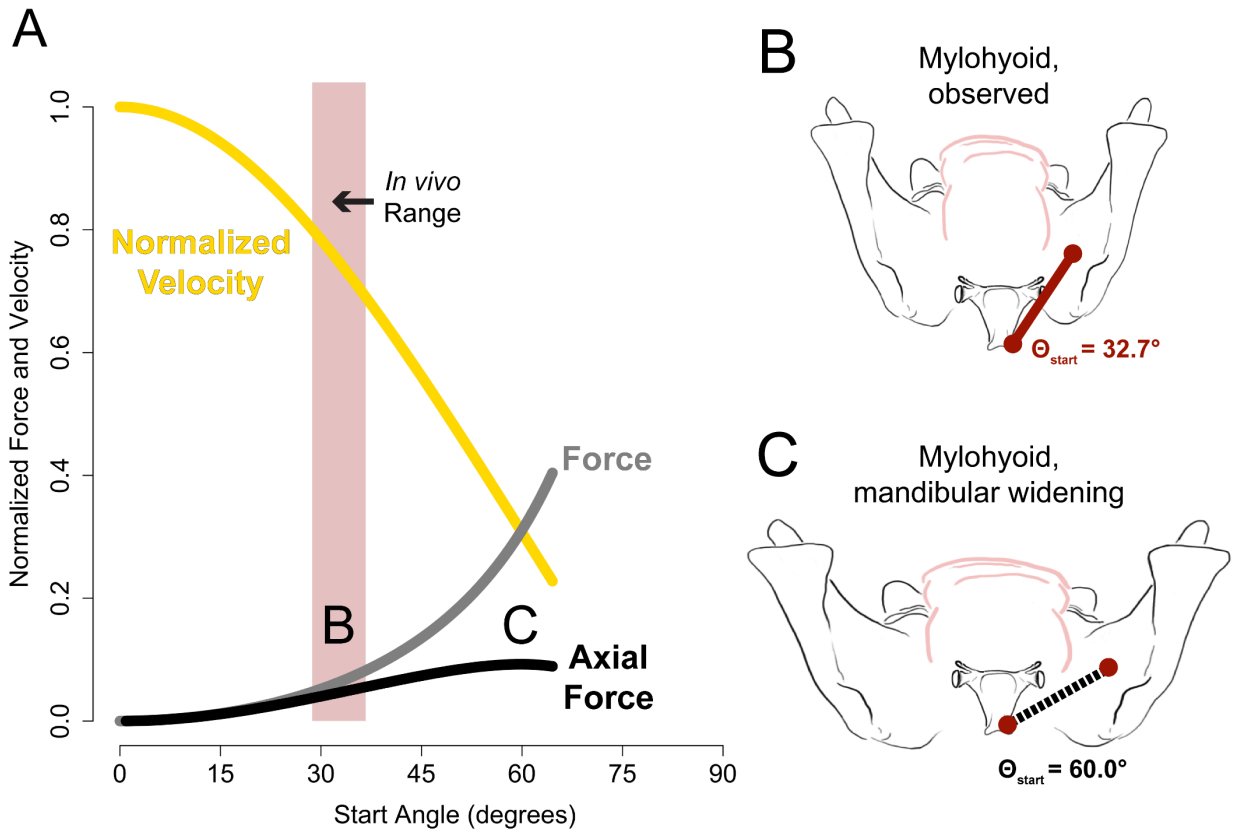

Figure 5.12: Geometric force-velocity curve in mylohyoid as mandibular width is increased. A) Normalized force (gray), axial force (black), fiber velocity (gold), and starting fiber length (red) at different initial fiber angles. Initial fiber angles greater than 64.5° could not generate enough elevation without achieving final fiber angles greater than 90°. B) Diagram of observed average mylohyoid initial fiber angle (32.7°). C) Diagram of optimal initial fiber angle (60°).

Limitations

This study has several limitations. As discussed in Chapter 4, the time it takes to process bi-planar videoradiographic data limited data analysis to four animals and one food type (red grapes). This study also does not evaluate infrahyoid muscle function, yet infrahyoid muscles are complex and are likely to be an important determinant of hyoid excursion (Konow et al. 2010; Wentzel et al. 2011; Yamazaki et al. 2017). Because the animals were restrained by their necks, the manubrium sternum—where sternohyoid and sternothyroid insert—often was not included in the field of view or was not clearly visible. Additionally, markers sutured onto the thyroid cartilage in some animals displayed large variation in inter-marker distance, indicating that they were not rigidly fixed to the cartilage and therefore were unreliable for rigid body kinematics and reconstructing thyrohyoid muscle length. Revision of the primate chair design and surgical implantation of thyroid cartilage markers will allow the functional morphology of these important muscles to be examined in future work.

This study also does not evaluate the effects of electromechanical delay (EMD), in which force onset and offset lag behind muscle activity onset and offset by 7.5-100 ms (Cavanagh and Komi 1979; Norman and Komi 1979; Hylander and Johnson 1989; Hylander and Johnson 1993; Ross et al. 2005; Grosset et al. 2009; Roberts and Gabaldón 2008; Zatsiorsky and Prilutsky 2012). Electromechanical delay also depends on whether the muscle is eccentrically, isometrically, or concentrically active (Cavanagh and Komi 1979, Norman and Komi 1979, citation map). For example, many hyolingual muscles show low levels of active stretch immediately before shortening, and eccentric activity, particularly at higher lengthening velocities, have shorter EMDs (Cavanagh and Komi 1979; Norman and Komi 1979). Moreover, because EMD is thought to be due to sarcomere's shortening to take up slack in the series elastic

element before force can be developed at attachment sites (Cavanagh and Komi 1979; Roberts and Gabaldón 2008; Grosset et al. 2009; Nordez et al. 2009; Zatsiorsky and Prilutsky 2012), passive stretch before shortening could also decrease EMD. Additionally, delays between muscle force and EMD may be dynamic as muscles shift from one type of activity to another, e.g., from fast concentric to slower concentric or relatively isometric activity, as in the muscles of mastication as they transition from jaw closing to the power stroke (Hylander et al. 1987; Hylander and Johnson 1989). However, it is uncertain whether the shorter EMDs would persist as the muscle begins to actively shorten. Because of these uncertainties, only raw EMG timing was used when quantifying the amount of each type of activity observed in each muscle.

Lastly, the tight spatial packing of the hyolingual muscles could introduce cross-talk artifacts in the EMG recordings. For example, these bursts during TBR could also be cross-talk from either the neighboring geniohyoid or intrinsic lingual muscles. If the latter, then the macaque tongue may be more stiff during swallowing than at rest, which argues against the hypothesis that the tongue has more liquid-like than solid-like properties during swallowing, as was proposed in Chapter 4. Similarly, styloglossus activity could be due to crosstalk from the neighboring medial pterygoid.

Do suprahyoid muscles produce tongue base retraction?

The data presented in this chapter are consistent with the hypothesis that hydraulic coupling between the hyoid and tongue drives tongue base retraction (TBR) because the hyoid protractors and elevators are active during TBR and so could produce the forces necessary not only to displace the hyoid but also to displace tongue volume via the hyoid (Chapter 4). However, as discussed in Chapter 4, such correlations could also be due to neurological

synchronization of suprahyoid muscles and muscles generating TBR through an undiscovered alternative mechanism.

The data suggest that, despite their lack of a direct connection with the hyoid, the digastrics also function to elevate the floor of the mouth. Similar to mylohyoid, digastric bellies showed a burst of activity before TBR but decreased activity during TBR. During TBR, both bellies rotated and the digastric muscle as a whole became more linear (Figure 5.4). This linearization involved shortening of posterior digastric and variable patterns of length change in the anterior digastric during early TBR but consistent posterior digastric lengthening and anterior digastric shortening during late TBR. In this way, straightening out of the digastrics may facilitate a hydraulic mechanism of TBR by elevating the floor of the mouth if linearization converts the tensile forces generated by the two bellies of the digastric into a net compressive force acting on the root of the tongue, equal in magnitude and orientation to the vector sum of forces generated by the two digastric bellies.

Although EMG data for hyoglossus and stylohyoid were not successfully obtained, hyoglossus shortened during TBR, whereas stylohyoid lengthened or maintained length as it became more horizontal during hyoid elevation and protraction. Stylohyoid may facilitate mouth floor elevation before TBR, but it does not shorten during TBR and therefore does not directly contribute to the hypothesized hydraulic function of the hyoid as the tongue base retracts.

In summary, these data support the hypothesis that TBR results from the hyoid's displacing tongue volume posteriorly as it elevates and protracts into the tongue (i.e., a hydraulic linkage) because geniohyoid and mylohyoid—and potentially hyoglossus—actively shorten throughout TBR, the digastrics linearize throughout TBR, and TBR coincides with peak geniohyoid activity.

What is the functional significance of concentric activity in suprahyoid muscles and eccentric activity in lingual muscles?

The data presented here demonstrate that the mylohyoid and geniohyoid are primarily concentrically active during swallowing, particularly during TBR. Additionally, mylohyoid has periods of low level eccentric activity before shortening and higher level isometric activity after shortening in most animals, while anterior digastric activity was highly variable during early TBR and consistently concentric in late TBR. The current hypothesis, that suprahyoid muscles are predominantly concentrically active, is supported for geniohyoid but not for mylohyoid or anterior digastric.

Because swallowing is a dynamic activity, some have doubted whether the isometric exercises which dominate swallowing rehabilitation are the most effective treatments (Stathopoulos and Ducchan 2006; Burkhead et al. 2007; Rogus-Pulia and Connor 2016). Given that peak geniohyoid and mylohyoid activity is observed during shortening, these findings suggest that either velocity or power (the product of force and velocity) is more important for suprahyoid muscle swallowing performance than force alone. Exercises that are best at improving muscle shortening velocity and power are different from those which primarily improve muscle strength (Duchateau and Hainaut 1984). Moreover, matching exercises to the specific task being rehabilitated improves functional outcomes better than those which are not task-specific (Thorstensson et al. 1976; Coyle et al. 1981; Gür et al. 2002). These greater improvements related to task-specific exercises are probably due to a combination of neuroplastic and myoplastic responses that improve motoneuron recruitment, coordination, and overall motor control, in addition to remodeling of muscle and connective tissue (Duchateau and Hainaut 1984; McDonagh and Davies 1984; Burkhead et al. 2007; Malas et al. 2013). This

research suggests that dysphagia rehabilitation exercises that incorporate concentric exercises aimed at improving muscle shortening velocity and/or power through concentric activity—such as the Shaker Head Life exercise protocol (Shaker et al. 1997; Shaker et al. 2002) or fast jaw opening exercises which require high shortening velocities in suprahyoid muscles (Matsubara et al. 2018)—may be superior to isometric training aimed at improving suprahyoid muscle strength. Nevertheless, isometric exercises may be beneficial for rehabilitating mylohyoid, which often has a period of isometry at the end of TBR that may function to hold the larynx in an elevated position as the bolus passes the airway and enters the esophagus.

Although suprahyoid muscles are predominantly concentrically active during swallowing and especially TBR, lingual muscles have more balanced eccentric and concentric activity and are predominantly eccentrically active during TBR. Because the markers used to measure genioglossus length (the middle deep marker, see Chapter 3) were essentially stationary relative to the cranium during TBR, active lengthening is probably due to mandibular depression during TBR, which displaces the genioglossus origin away from the tongue. If these results are reflective of true styloglossus activity and are assumed to be generalizable to all macaques, then eccentric and isometric activity by styloglossus may function to stabilize the tongue as the hyoid protracts into the tongue midline. Otherwise, hyoid protraction as the mandible begins to depress may result in protrusion of the entire tongue out of the oral cavity rather than retraction of only the posterior and tongue base midline. Such a function may be particularly important in edentulous populations, where the tooth row is not available to prevent such protrusion, or in patients with xerostomia (poor saliva production) if there is less wet adhesion between the tongue and hard palate. Contrary to the suprahyoid muscles, these findings support the use of isometric exercises to improve styloglossus function.

Does fiber rotation amplify either hyoid velocity or suprahyoid muscle force?

All suprahyoid muscles rotate, but hyolingual muscle geometry and the direction of rotation combine to determine whether rotation amplifies or depresses movement. Other studies have demonstrated architectural gear ratios greater than or equal to 1.00 (Brainerd and Azizi 2005; Azizi and Brainerd 2007; Azizi et al. 2008; Azizi and Roberts 2014; Holt et al. 2016), but this is the first study to demonstrate that a muscle's gear ratio can be less than 1.00 and that fiber rotation can impair movement along a given axis. The results reveal that rotation amplifies muscle velocity in the muscles that rotate away from the axis of movement—mylohyoid and stylohyoid rotate away from the Y-axis, and hyoglossus rotates toward the X-axis. These muscles had larger fiber angles relative to their respective axes of movement, and their higher gear ratios are consistent with a similar study by Brainderd and Azizi (2005) which modeled the effects of initial angle on architectural gear ratios. Therefore, there may be a general principle of the functional morphology of rotating muscle fibers: a larger initial angle predicts a larger gear ratio.

In contrast, rotation reduced protraction velocity in geniohyoid and elevation velocity in hyoglossus, each of which rotated toward their respective axes of movement. This variation in the effects of rotation occurs because rotational efficiency—defined as the proportion of movement along a given axis to total excursion caused by rotation—increases as fibers become more orthogonal to that axis, but decreases as fibers become more parallel. In Monkeys He and JB, in which the geniohyoid insertion was nearly always inferior to geniohyoid's mandibular insertion, geniohyoid shortened more than the hyoid protracted because elevation rotated geniohyoid toward the X-axis. On the other hand, the geniohyoid insertion was higher in Monkeys Ch and Ki, and these animals had more hyoid protraction than geniohyoid shortening

because elevation rotated geniohyoid away from the X-axis. Further hyoid descent predicted more severe reductions in hyoid protraction. Additionally, just as rotation in one direction can amplify movement, rotation in the opposite direction depresses movement. Rotation did not amplify hyoglossus peak velocity, particularly along the Y-axis where GR_{Yp} was not within one standard deviation of 1.00. This lack of amplification was due to the minimal amount of hyoglossus rotation in sagittal planes during TBR which, because of its orientation and direction of rotation, depressed elevation.

Increased rotational efficiency necessarily decreases the alignment of the fiber with the axis of movement and therefore the amount of force produced along that axis, or axial force. Indeed, mathematical and experimental studies of hypaxial and pennate muscles, which also exhibit fiber rotation, have shown that more fiber rotation leads to faster shortening velocities at the expense of muscle force (Brainerd and Azizi 2005; Azizi et al. 2008). However, fiber rotation could also, theoretically, amplify force if morphological changes decrease relative fiber velocity such that fiber force increases more than axial force declines due to non-alignment with the line of action. Previous mathematical models of dynamically geared muscles found that more orthogonal starting angles produce higher AGRs and less force (Brainerd and Azizi 2005), but these models assume a constant fiber shortening velocity rather than a constant whole muscle velocity, as was simulated here. In the fixed-gear mathematical models of mylohyoid presented here, more obliquely oriented fibers generate more force than fibers in the *in vivo* range, but this increased fiber force only translates into larger forces along the Y-axis if fiber length is held constant, i.e., if increased initial angle is due to mandibular widening rather than fiber shortening. Indeed, simulations of hyoid descent via fiber lengthening predict greater force production by more aligned fibers that rotate less, consistent with the findings of Azizi et al.

(2008) but for an additional reason—namely, these fibers are also longer and so experience lower relative velocities, consistent with expectations from muscle architectural theory (Gans and Bock 1965, Chapter 2).

How does hyolingual geometry affect swallowing performance?

The data presented here suggest a possible functional conflict between geniohyoid and mylohyoid performance created by hyoid descent during human ontogeny and evolution (Negus 1949; Lieberman and Crelin 1971; Lieberman et al. 1972; Crelin 1973; Falk 1973; Lieberman et al. 2001; Lieberman 2011). As suggested in the Chapter 1, hyoid elevation and protraction are important for swallowing performance because of their functions in laryngeal closure (Logemann et al. 1992; Inamoto et al. 2011; Seo et al. 2014), upper esophageal sphincter opening (Cook et al. 1989; Jacob et al. 1989; Kahrilas et al. 1991), and, as argued in Chapter 4, tongue base retraction. When caused by fiber lengthening as opposed to decreased mandibular width, hyoid descent improves mylohyoid's capacity to generate superiorly oriented forces but decreases geniohyoid's capacity to displace the hyoid anteriorly. Because of these geometric changes, geniohyoid may need to shorten relatively faster and/or further when the hyoid is low in order to achieve adequate hyoid protraction. This in turn could impair force production due to force-velocity and force-length trade-offs. Alternatively, if hyoid descent is accompanied by increases in geniohyoid muscle length through addition of sarcomeres in series, the longer geniohyoid would be able to shorten absolutely more at a given sarcomere strain, enabling it to function at a narrower, and potentially better, part of its length tension curve (Gans and de Vree 1987; Gans and Gaunt 1991). Thus, through adaptive plasticity, the hyoid can plausibly descend during ontogeny and evolution without detrimental effects on protractile force and displacement.

Indeed, hyoid descent could even improve performance if it is also accompanied by increases in hyoglossus muscle length without significantly reducing its anteroposterior alignment. However, hyoid descent must be balanced against other changes in hyolingual anatomy that have emerged over human evolution, namely shortening of the face and mandible (Bilsborough and Wood 1988; Ross et al. 2009)—which decreases geniohyoid and hyoglossus length due to posterior displacement of the geniohyoid origin—and a vertically oriented mandibular symphysis (Aiello and Dean 2002; W. Liu et al. 2010), which increases geniohyoid length due to anterior displacement of the geniohyoid origin. To discriminate among these hypotheses and to detect any potential functional (or dysfunctions) interactions arising from different combinations of morphological features, Chapter 6 uses a computational model to simulate the consequences of hyoid descent on hyoid range of motion.

CONCLUSION

The data on hyolingual muscle behavior presented here are consistent with the hypothesis that TBR is the result of a hydraulic linkage with the hyoid driven by concentric activity in suprahyoid muscles, especially geniohyoid. The suprahyoid muscles are predominantly concentrically active during swallowing, especially during TBR, while lingual muscles demonstrate more eccentric activity. The data further reveal that hyoid movement is not a product of suprahyoid muscle shortening alone: not only can hyoid displacement and velocity be amplified by fiber rotation, but they can also be depressed, depending on the direction of rotation. Changes in rotational efficiency and fiber length caused by hyoid descent, which is observed in humans, may impair the ability of the geniohyoid muscle to protract the hyoid.

Computational modeling promises to further elucidate the effects of changing morphology on swallowing function in humans and non-human primates.

CHAPTER SIX: DID SWALLOWING SHAPE THE HUMAN MANDIBLE AND HYOLINGUAL APPARATUS?

INTRODUCTION

Among the many features accumulated in the human skull over the course of evolutionary history, facial shortening and the descent of the hyoid and larynx are thought to be pivotal for the origin of speech (Lieberman et al. 1969; Laitman et al. 1997; Lieberman et al. 1992; Lieberman 2012). As infants, non-human primates are relatively orthognathic, or flat faced, and they become more prognathic with age; archaic and modern humans, in contrast, remain orthognathic throughout life (Aiello and Dean 2002; Lieberman et al. 2002). Facial shortening can be achieved by retracting the entire face relative to the cranial base, and this facial retraction continued until relatively recently in human evolution (< 500 kyr) and is one the distinguishing features of *Homo sapiens* from other species of *Homo* (Lieberman et al. 2002). The tongue, hyoid, and larynx rest near the base of the mandible in extant non-human primates and infant humans, but they descend relative to the mandible and palate during human ontogeny (Negus 1949; Falk 1973; Crelin 1973; Laitman, Crelin, and Conlogue 1977). This facial shortening and hyolingual and laryngeal descent yield equally proportioned superior and horizontal elements of the supralaryngeal vocal tract (SVT), which is argued to be necessary for producing unambiguous vowels and therefore 'clear' speech (Peterson and Barney 1952; Lieberman et al. 1969; Stevens 1989; Lieberman et al. 1992; Lieberman 2012). Hyolingual descent has also been hypothesized to produce a vocal tract that is "maladapted to swallowing and respiration compared to the non-human [vocal tract]", based on the assumption that

separation of the soft palate and epiglottis by the tongue base increases the risk of choking (Lieberman et al. 1992). This *maladaptive vocal tract hypothesis* (MVT) posits that the descent of the larynx and hyoid—which also causes descent of the tongue base—expands the size of the oropharynx, creating a larger space in which the bolus can mix with air and increasing the risk of penetration of food into the airway and consequent choking (Figure 1.1) (Negus 1949).

Recent findings on the potential vocal capabilities of nonhuman primates cast doubt on the hypothesis that hyolingual and laryngeal descent are necessary adaptations for clear speech. Fitch and coworkers show that macaques could produce unambiguous vowels if they phonated at the same time that they held postures within the animal's normal range of orofacial behavior (Fitch et al. 2016). Similarly, Boë et al. (2017) demonstrated that baboons produce a range of vowel sounds much the same as human children. Moreover, comparative evidence suggests that a descended hyoid and/or larynx is also present in greater and lesser apes (Wall et al. 1994; Nishimura 2003; Nishimura et al. 2006), red deer (Fitch and Reby 2001), Mongolian gazelles (Frey et al. 2008), koalas (Charlton et al. 2011; Charlton et al. 2013), many felids (Weissengruber et al. 2002), and anteaters (Perez et al. 2010; Borges et al. 2017), none of which are known to exhibit high rates of choking. A lower hyoid and larynx create a longer airway, which lowers the pitch of vocalization and may confer fitness benefits via sexual selection (Fitch and Reby 2001; Charlton et al. 2011, Charlton et al. 2013). However, alternative hypotheses regarding the role of functional constraint or the potential adaptive value of tongue, hyoid, and laryngeal descent also need to be falsified in order to conclude that the human vocal tract is the result of natural selection for speech performance.

Re-consideration of the hypothesized links between human oropharyngeal morphology and choking also raises questions about the MVT hypothesis. In non-human mammals, including

non-human primates, swallowing is preceded by accumulation of a food bolus in the valleculae at the base of the tongue, and the bolus is separated from the airway by the overlapping epiglottis and soft palate (Hiiemae et al. 1981; Franks et al. 1984). In humans, the valleculae are exposed to air from the nasopharynx due to descent of the tongue base, hyoid, and larynx into the neck. Hence, the MVT hypothesis posits that bolus accumulation there would pose a threat to the airway, requiring that humans maintain a seal between the soft palate and the posterior tongue to keep food from collecting in the valleculae (Dantas et al. 1990). However, it is now clear that humans, like other mammals, do in fact accumulate some food in the valleculae prior to the swallow (Palmer et al. 1992; Hiiemae and Palmer 1999). Moreover, stage II transport of food into the valleculae prior to the swallow is not due to poor bolus control occasioned by hyoid descent, but rather is intentional, active transport independent of gravity (Palmer et al. 1992b; Palmer 1998; Hiiemae and Palmer 1999; Matsuo and Palmer 2015). One would also expect that if a bolus in the valleculae posed a danger to the airway, then respiration would be inhibited when the bolus is present. Although bolus transport to the valleculae is coordinated with expiration, humans do not inhibit respiration after this active transport (Matsuo et al. 2008; Matsuo and Palmer 2015). The fact that humans actively, and regularly, store food in the valleculae prior to swallowing and continue to breathe after having done so effectively falsifies a critical assumption underlying the MVT: that food in the expanded oropharynx is difficult to control and thus constitutes a danger to the airway.

Review of the clinical literature also suggests that selective pressure against the human airway configuration may not be as great as proponents of the MVT suggest when they cite that choking—or asphyxiation due airway obstruction by either a foreign body or laryngospasm caused by the presence of a foreign body in the airway—is a common cause of accidental death

(Lieberman 2012; Lieberman 2017; National Safety Council 2017). Foreign body airway obstruction (FBAO) has an incidence of only ca. 10 in 100,000 (0.01%) in the general population and, in the decade prior to the introduction of the Heimlich maneuver, caused death in only 0.66 adults per 100,000 (0.00066%) (Heimlich 1974; Heimlich 1975; Mittleman and Wetli 1982; Sakai et al. 2014). Even if every individual with FBAO died, the infrequency of choking raises serious doubts about the notion that an adaptive behavior, such as speech, is necessary to drive selection for a modern human airway. In short, if natural selection had to overcome an increased risk of FBAO in order to select for clear speech in adults, the fitness costs are arguably minimal. In fact, the risk of FBAO is actually higher among infants, when the larynx is high in the neck, than among older children and non-elderly adults when it is lower: 55% of FBAO in children under the age of five occur in infants under the age of one (Vilke et al. 2004; Sakai et al. 2014).

Although FBAO is rare in humans, entry of the bolus into the airway is strikingly common. Penetration—entry of the bolus into the larynx superior to the vocal folds—occurs in 11 % to 83 % of healthy individuals, with more older individuals exhibiting penetration (Robbins et al. 1992; Daggett et al. 2006; Butler et al. 2009; Allen et al. 2010; Butler et al. 2010; Todd et al. 2013). Some of these studies also suggest that aspiration—entry of the bolus into the airway below the vocal folds—occurs in up to 30 % of older adults (Butler et al. 2009; Butler et al. 2010; Todd et al. 2013), although others suggest that aspiration is not regularly observed in healthy individuals (Robbins et al. 1992; Daggett et al. 2006; Allen et al. 2010). However, humans are not alone in having a high prevalence of penetration—healthy piglets also commonly penetrate and, less frequently, aspirate, despite their intranarial larynges (Holman et al. 2013; Holman et al. 2014; Gould et al. 2015; Gould et al. 2016).

A new hypothesis for the functional significance of a low tongue and hyoid in humans.

Given the weak evidence that the human hyolingual apparatus is maladapted for swallowing because it increases the risk of choking, and recent evidence suggesting that its configuration is not necessary for speech, what, if any, fitness advantage does a low hyolingual apparatus and larynx actually confer? Rather than being a cause of poor swallowing performance, I hypothesize that the low position of the hyolingual apparatus, in addition to changes in mandibular morphology, may in fact be necessary to maintain swallowing performance in the evolutionary context of facial shortening. Shortening of the face through evolution, unless accompanied by decreases in tongue anteroposterior dimensions, would move the hyoid and tongue base too far posteriorly, decreasing the cross-sectional area of the airway, the back of which lies against the vertical and anteriorly curving cervical spine associated with erect bipedalism (Lieberman et al. 2001, Lieberman 2011). However, if facial shortening were accommodated by a reduction in tongue volume, then tongue base retraction may be impaired (Chapter 4).

Additionally, physiological limits on muscles effecting swallowing performance put serious constraints on decreases in hyolingual length. Specifically, decreases in the length of the geniohyoid would limit both the range of motion and the velocity of the hyoid, interfering with its role in bolus transport, epiglottal flip, upper esophageal sphincter opening, and tongue base retraction during swallowing (Steele et al. 2011, Pearson et al. 2015, Seo et al. 2016; Chapter 4). The average strain of the human geniohyoid during swallowing is about 30% (Okada et al. 2013), approximating the maximum whole muscle shortening strain observed for most muscles, including those of the hyoid (Anapol 1988, Gans and Bock 1965). For a given average geniohyoid fiber length of 35 mm (Pearson et al. 2011), 30 % shortening strain yields 10.5 mm

of absolute shortening. If the geniohyoid decreased its resting length from 35 to 25 mm, accommodating a 10 mm increase in airway diameter to maintain patency after 10 mm of facial shortening, this would translate into 7.5 mm of shortening strain, a decrease of shortening strain of roughly one-third. In humans, similar reductions in anterior hyoid excursion increase the risk of penetration or aspiration of the bolus into the airway by more than 50 % (Steele et al. 2011). Shortening of the geniohyoid would also impact shortening velocity because longer muscles shorten absolutely faster than shorter muscles (Gans and Bock 1965).

Thus, because anterior hyoid displacement and velocity are primarily attributable to geniohyoid activity (Pearson et al. 2011, Palmer et al. 1992, Chapter 5), I hypothesize that moving the hyolingual apparatus and larynx down into the neck may be necessary to maintain geniohyoid length, and hence shortening distance and velocity, in the face of profound facial shortening. This hypothesis would also explain why humans have a vertically oriented mandibular symphysis, as opposed to a more obliquely inclined simian shelf (Aiello and Dean 2002). A vertical symphysis displaces the attachments of the geniohyoid, anterior belly of the digastric and genioglossus muscles anteriorly, as another mechanism for maintaining geniohyoid length (Coquerelle et al. 2010, Coquerelle et al. 2013). Notably, the mandibular symphysis has become vertical very recently in human evolution, as late as the Early Upper Paleolithic (50 kyr), and greater verticality is associated with a more protuberant chin that may compensate for losses in strength associated with this change in symphyseal orientation (Dobson and Trinkaus 2002; Liu et al. 2010), although the adaptive value of the chin is still debated (Daegling 2012; Pampush and Daegling 2016). To paraphrase Lauder in the current context **[additional text in bold]**:

> In a highly constrained system in which the structural elements are tightly coupled by both functional and morphogenetic interactions **[the dependence of hyolingual biomechanics on**

> **craniofacial morphology]**, certain types of structural modification **[hyoid descent, a vertical symphysis, and chin projection]** might be predicted to occur given a certain initial morphology **[a shorter face]**, regardless of the nature of the extrinsic factors **[the advantages of speech]**. These patterns of change do not require deterministic explanations and are largely due to the network of constraints within the initial system. (Lauder 1981, 434)

Thus, if a minimum geniohyoid length is necessary to swallow safely, then explanations of hyolingual morphology could rest on intrinsic functional constraints alone rather than relying on the tenuously adaptive value of equivalent SVT proportions for clear speech (i.e., an "extrinsic factor"). In this case, even if an equally proportioned SVT *is* necessary for clear speech, such morphology may well be an exaptation for clear speech if it was initially generated by functional constraints. Ordinarily in functional morphology research, such hypotheses about adaptation or maladaptation would be tested in a comparative framework (Lauder 1981; Ross 1999; Ross et al. 2002). However, no other extant species have converged on *Homo sapiens*' cumulative suite of a descended hyolingual apparatus and larynx, an orthognathic face, and a vertical spine with anterior curvature, or lordosis, of the cervical vertebrae. Therefore, validated computational approaches are necessary to better understand whether and how functional constraints on feeding performance have driven morphological change in the course of human evolution and continue to affect humans during ontogeny. Modeling hyolingual function will give invaluable insight into how morphology affects biomechanics and performance in not only extant and extinct taxa, but also in organisms that have never existed because of possible functional or developmental constraints.

Aims and Hypotheses

Constraints on muscle shortening and stretch capacity have been used successfully to predict hyoid range of motion in rabbits (Anapol 1988)—similar constraints on muscle

lengthening and shortening were employed in this study, as described in detail in Chapter 3. Building on methods first described by Anapol (1988), this chapter uses a combination of *in vivo* measurement and mathematical modeling to explore relationships between craniofacial and hyolingual morphology, biomechanics, and performance, addressing two specific aims.

The first aim is to develop a biomechanical model of hyolingual range of motion based on *in vivo* data used in Chapters 3-5. The input variables of the model were the coordinates of the muscle attachment sites (i.e., muscle length and orientation) and hyoid starting posture (i.e., position relative to the mandible). Physiological parameters are average hyolingual muscle length and rotation ranges determined using XROMM. Model output is the overall size and shape of the volume enclosing the hyolingual range of motion (see Chapter 3). The output of the model is compared against *in vivo* macaque data to determine its goodness of fit.

The second aim is to use this model to estimate how changes in craniofacial and hyolingual morphology over human evolution affect hyolingual range of motion as a proxy for swallowing performance. Model morphological inputs are varied to mimic changes observed over human evolution and ontogeny. Facial shortening shortens the geniohyoid and hyoglossus by moving their origins posteriorly, while a vertical mandibular symphysis lengthens the geniohyoid by moving its origin anteriorly. Hyoid descent lengthens the suprahyoid musculature and reorients these muscles more superoinferiorly. Dorsoventral compression of the hyoid brings suprahyoid insertion points closer together along the Y-axis. Basicranial flexion shortens the posterior digastric and stylohyoid. These changes are modeled individually as well as in combination to determine how each one affects hyoid range of motion and whether certain combinations produce synergistic effects. Rather than applying these models to specific fossils, the aim is to determine how general trends observed—or not observed—in the evolution of

hominin craniofacial and vertebral morphology may have affected hyolingual biomechanics and performance.

RESULTS

Model development and validation

As stated in Chapter 3, the model was developed by measuring muscle length and orientation at each point within an area of interest and evaluating whether these values fell within the limits defined by the model. When average maximum and minimum muscle length or fiber angle were used as the limits for each muscle, false positives were very low, but the false negative rate was high. To balance the risk of under- or over-estimating hyoid range of motion, minimum muscle length and maximum muscle length were decreased and increased, respectively, by a multiple of standard deviations for each muscle. To select the multiple that best captured range of motion while minimizing false negatives and false positives, a receiver operator characteristic (ROC) curve was generated by comparing the true positive (sensitivity) and true negative (specificity) rates for each multiple (Chapter 3). Based on this ROC curve for different standard deviation multiples, a multiple of 1.54 standard deviations was used to expand the range of the muscle length limit parameter for all models using macaque muscle physiology (Figure 6.1). The model's area under the curve (AUC) essentially quantifies how accurately the model segregates the results into two categories. More formally, it is the probability that, given one randomly selected point within the *in vivo* ROM and another randomly selected point outside of the *in vivo* ROM, the point inside the *in vivo* ROM will fall within the predicted ROM and the point outside of the *in vivo* ROM will fall outside the predicted ROM (Obuchowski 2003). A perfect model has an AUC of 1.00, while a random model has an AUC of 0.50. The model

presented here had an AUC of 0.88. At a standard deviation of 1.54, sensitivity was 0.80 and specificity was 0.82 (Figure 6.2).

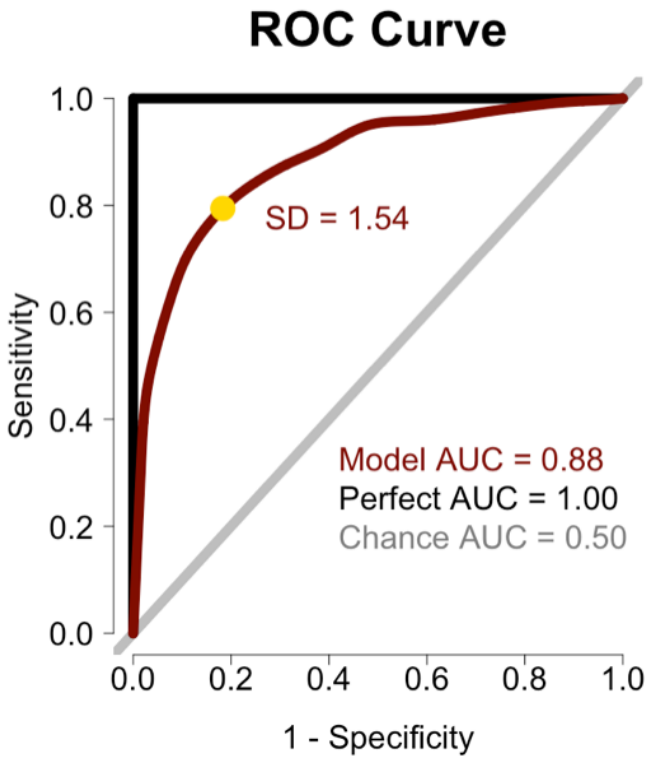

Figure 6.1: Receiver operator characteristic (ROC) curve for different standard deviation multiples of mean minimum and maximum length. Black, perfect model ROC curve; gray, chance diagonal ROC curve; red, model ROC curve; gold, best-fit standard deviation multiple.

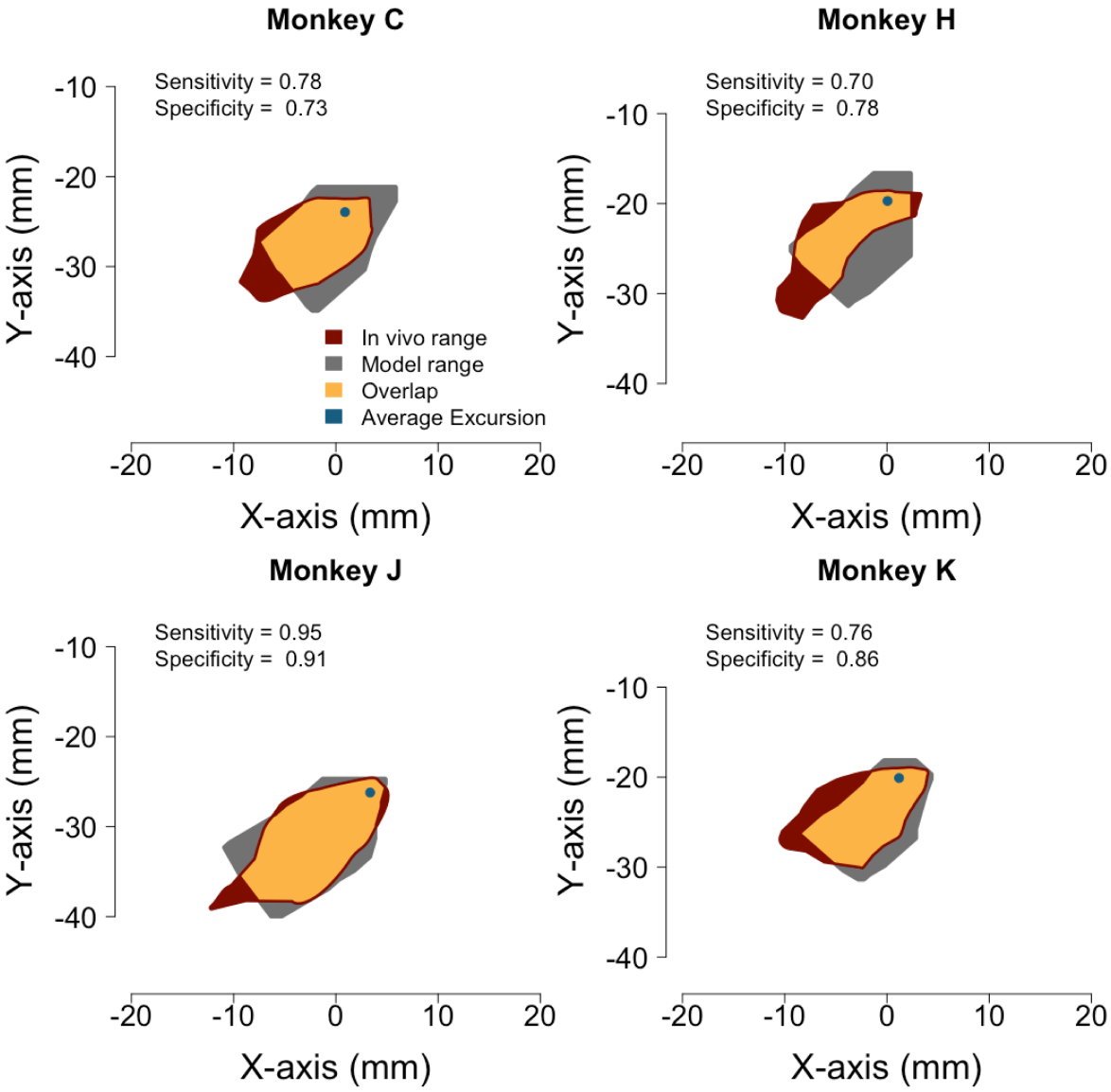

Figure 6.2: Sensitivity and specificity of model ROM and in vivo ROM for each macaque. Sensitivity is equal to the true positive rate, specificity is equal to the true negative rate. Red, *in vivo* range; gray, false positives of model range; gold, true positives of model range; white background, true negatives; blue dot, point of average maximum excursion across all swallows for each animal.

Given that the digastric "tendon is attached to the inferior border of the hyoid bone by a thick non-elastic membrane" (Hilloowala 1975), it was uncertain whether the digastrics needed to be included in the model. To resolve this uncertainty, kinematics of the marker implanted in

the insertion of the anterior digastric into the digastric tendon were compared to hyoid kinematics. Although hyoid and digastric tendon kinematics were significantly correlated with each other ($r^2 > 0.75$, $p < 0.001$), the mean slope of the regression lines for anterior digastric tendon and hyoid X- and Y-axis displacements were 1.788 and 1.603 and the range of motion of the hyoid was larger than that of the digastric tendon (Figure 6.3; data not available for Monkey Ki because it did not have digastric markers). These findings indicated that anterior digastric kinematics did not constrain the hyoid; therefore, the digastric was not included in the original model.

Differences in hyoid excursion between humans and macaques

Relative to mandibular length, the human hyoid protracts 38.5 % more, elevates 38.0 % more, and translates 36.1 % more overall than macaques (Table 6.1). However, relative to body mass, the human hyoid protracts 18.6 % less, elevates 17.9 %, and translates 19.4 % less overall than macaques. Elevation was significantly greater than protraction in macaques ($p = 0.036$), and the ratio of protraction to elevation at the time of maximum hyoid excursion was similar between humans (0.933) and macaques (0.948).

Table 6.1: Absolute and normalized hyoid excursion in macaques and humans

Animal	Mandible Length (mm)	Body Mass (kg)	Units	Protraction (X-axis)	Elevation (Y-axis)	Total
Macaque	89.2	8.05	mm	5.20	5.51	7.69
			lengths	0.060	0.065	0.090
			$mm \cdot kg^{-1/3}$	2.59	2.757	3.84
Human	99.3	60.2	mm	8.28	8.87	12.1
			lengths	0.083	0.089	0.122
			$mm \cdot kg^{-1/3}$	2.11	2.26	3.10

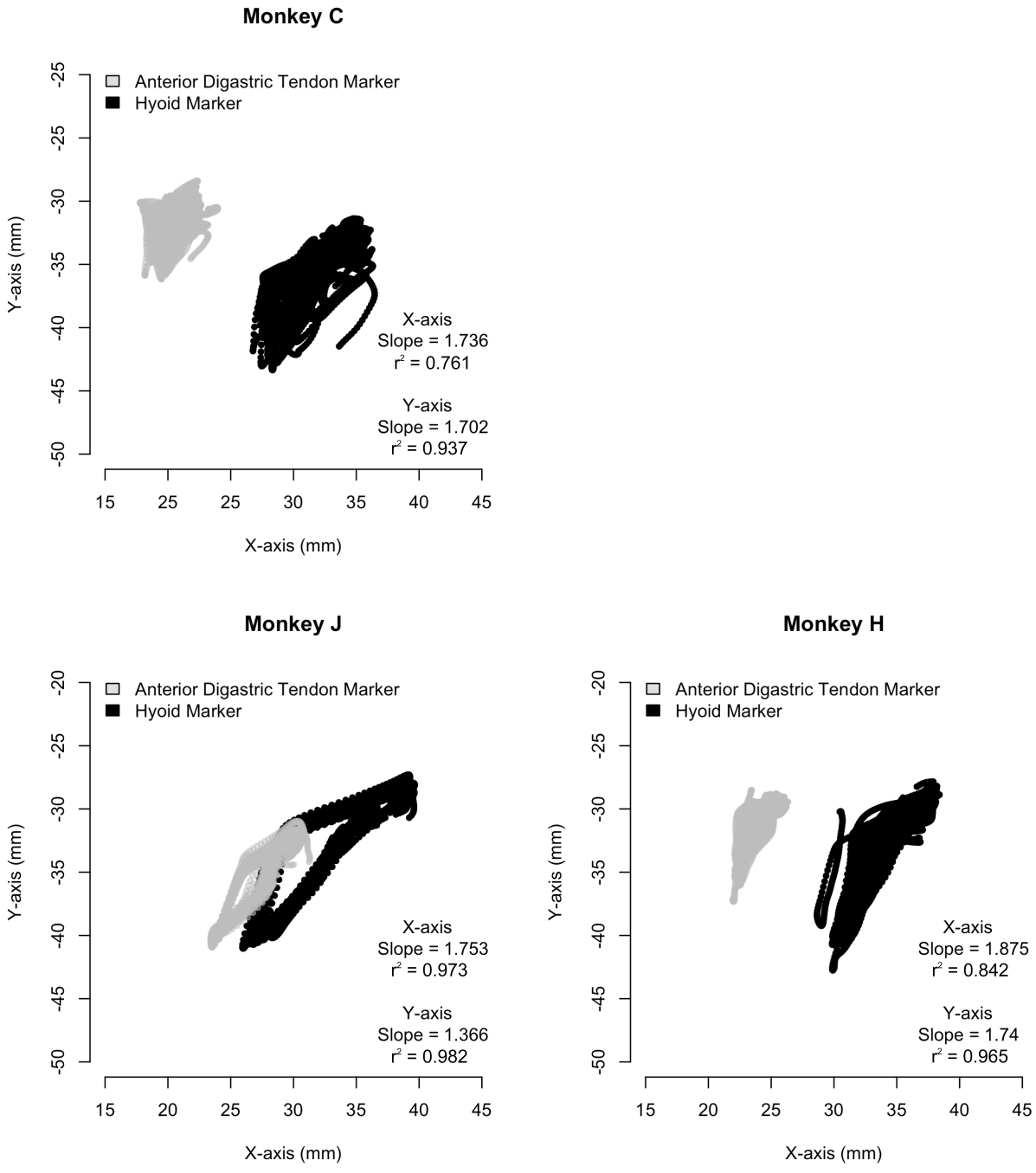

Figure 6.3: Anterior digastric tendon and hyoid range of motion. Hyoid kinematics range of motion is larger than that of the anterior digastric tendon. Slopes and coefficients of determination (r^2) are reported for each axis separately. Color code: black, hyoid sagittal range of motion; gray, anterior digastric tendon marker range of motion.

Because this study lacks a sufficient taxonomic sample to infer the effects of body mass on swallowing kinematics, this study focuses on how geometry influences movement. The kinematic targets were determined by multiplying the magnitude of excursion measured in mandibular lengths by the model's mandibular length. Macaque relative excursion was used for models with unchanged mandibular length (length = 0.653 units), and human relative excursion was used for models with sagittal length shortened by 37.2 % (length = 0.410 units, see Chapter 3). Unchanged models had a target of 0.039 units of protraction and 0.042 units of elevation, while shortened models had a target of 0.034 units of protraction and 0.037 units of elevation. The ratio of the maximum distance between neighboring simulation points to the predicted total excursion distance gave a measure of model uncertainty in case the simulation did not sample densely enough. As a percentage, model uncertainty was 4.9 % for unchanged models and 5.7 % for shortened models. Therefore, unchanged models that came within 95.1 % of the predicted excursion distance were judged to have sufficient excursion, while this percentage was 94.3 % for shortened models.

Five sets of simulations were run to evaluate how craniofacial and hyolingual morphology as well as assumptions about muscle physiology affect swallowing performance. Tables 6.2-3 report absolute and relative muscle length for each model. Overall, hyoid descent (HD) increases all suprahyoid muscle lengths, while a vertical symphysis (VS) increases geniohyoid and anterior digastric lengths. Together, HD and VS increased geniohyoid length more than either did separately but decreased anterior digastric length compared to VS alone. Mandibular shortening decreases geniohyoid and hyoglossus length by 77 % and 35 %, respectively. For the reasons stated above, the digastrics were only included in human-macaque hybrid models. Relative geniohyoid length was increased to 90 % of its original length relative to

mandibular length when both HD and VS were present in SM models, although absolute length was 44 % of its original length. Hyoid descent brought hyoglossus back to 95 % of its original absolute length and increased its relative length by 51 % in SM models.

Gear ratios describe the relative amount of hyoid movement for a given amount of muscle shortening over the same amount of time, i.e., velocity—because this model does not measure instantaneous muscle velocity, only average gear ratio is considered here (Tables 6.4-5). Hyoid descent reduced both mylohyoid and geniohyoid gear ratios. The geniohyoid gear ratio declined to less than 1.00 while the mylohyoid gear ratio remained above 1.00. Similar trends were observed in the human-macaque hybrid models, although the absolute values differed slightly due to the effect of hyoid compression on hyoid muscle insertion location. In posterior digastric, the gear ratio was negative in hybrid models with more protraction because the muscle lengthened over the course of excursion, which was observed *in vivo* in macaques (Chapter 5). Gear ratios are not reported for models in which no movement was possible because the hyoid's initial position was superior to the line connecting the origins of the digastric.

Table 6.2: Simulated conditions, swallowing performance, and muscle length

Simulation	Swallowing Performance (% of Target Excursion, no PL | PL)	Absolute Muscle Length (arbitrary units)					
		Anterior Digastric	Geniohyoid	Hyoglossus	Mylohyoid	Posterior Digastric	Stylohyoid
Original	98.2	—	0.254	0.294	0.144	—	0.356
HD	100.2	—	0.265	0.356	0.223	—	0.427
VS	98.2	—	0.316	0.294	0.144	—	0.356
HD+VS	100.2	—	0.325	0.356	0.223	—	0.427
SM	101.8 | 101.8	—	0.058	0.192	0.144	—	0.356
SM+HD	41.7 | 58.5	—	0.097	0.278	0.223	—	0.427
SM+VS	101.8 | 101.8	—	0.12	0.192	0.144	—	0.356
SM+HD+VS	61.5 | 90.2	—	0.143	0.278	0.223	—	0.427
Hybrid	0.0 | 0.0	0.089	0.068	0.148	0.11	0.307	0.215
Hybrid +HD	46.3 | 47.1	0.089	0.08	0.23	0.178	0.345	0.268
Hybrid +VS	0.0 | 0.0	0.191	0.125	0.148	0.11	0.307	0.215
Hybrid +HD+VS	81.1 | 93.4	0.175	0.131	0.230	0.178	0.345	0.268

Table 6.3: Simulated conditions, swallowing performance, and muscle length normalized by mandibular length

Simulation	Swallowing Performance (% of Target Excursion)	Muscle length, normalized by mandibular length					
		Anterior Digastric	Geniohyoid	Hyoglossus	Mylohyoid	Posterior Digastric	Stylohyoid
Original	98.2	—	0.389	0.45	0.221	—	0.545
HD	100.2	—	0.406	0.546	0.342	—	0.654
VS	98.2	—	0.484	0.45	0.221	—	0.545
HD+VS	100.2	—	0.498	0.546	0.342	—	0.654
SM	101.8 | 101.8	—	0.143	0.468	0.352	—	0.868
SM+HD	41.7 | 58.5	—	0.237	0.679	0.544	—	1.042
SM+VS	101.8 | 101.8	—	0.292	0.468	0.352	—	0.868
SM+HD+VS	61.5 | 90.2	—	0.349	0.679	0.544	—	1.042
Hybrid	0.0 | 0.0	0.218	0.165	0.36	0.269	0.75	0.525
Hybrid +HD	46.3 | 47.1	0.216	0.194	0.562	0.435	0.843	0.655
Hybrid +VS	0.0 | 0.0	0.466	0.304	0.36	0.269	0.75	0.525
Hybrid +HD+VS	81.1 | 93.4	0.427	0.321	0.562	0.435	0.843	0.655

HD, hyoid descent; PL, physiological limits of muscle length; SM, short mandible; VS, vertical symphysis

Table 6.4: Simulated conditions, swallowing performance, and muscle gear ratios with macaque muscle physiology

Simulation	Swallowing Performance (% of Target Excursion)	Gear Ratios for Average Velocity							
		DigA, X	DigA, Y	GH, X	HG, X	HG, Y	MH, Y	DigP, Y	StyH, Y
Original	98.2	—	—	1.21	0.71	0.77	1.68	—	32.92
HD	100.2	—	—	0.81	0.68	0.76	1.21	—	3.82
VS	98.2	—	—	1.15	0.71	0.77	1.68	—	32.92
HD+VS	100.2	—	—	0.84	0.68	0.76	1.21	—	3.82
SM	101.8	—	—	12.21	0.85	0.93	1.61	—	21.35
SM+HD	41.7	—	—	0.82	1.09	0.87	1.12	—	8.51
SM+VS	101.8	—	—	1.63	0.85	0.93	1.61	—	21.35
SM+HD+VS	61.5	—	—	0.69	0.81	0.92	1.13	—	3.23
Hybrid	0.0	—	—	—	—	—	—	—	—
Hybrid +HD	46.3	0.19	2.03	0.14	0.10	1.05	1.19	2.35	1.64
Hybrid +VS	0.0	—	—	—	—	—	—	—	—
Hybrid +HD+VS	81.1	1.07	2.45	0.60	0.43	0.98	1.22	7.45	2.87

Table 6.5: Simulated conditions, swallowing performance, and muscle gear ratios with muscle physiology limits

Simulation	Swallowing Performance (% of Target Excursion)	Gear Ratios for Average Velocity							
		DigAX	DigAY	GHX	HGX	HGY	MHY	DigPY	StyHY
SM	101.8	—	—	12.21	0.85	0.93	1.61	—	21.35
SM+HD	58.5	—	—	0.7	0.87	0.91	1.13	—	3.78
SM+VS	101.8	—	—	1.63	0.85	0.93	1.61	—	21.35
SM+HD+VS	90.2	—	—	0.67	0.76	0.94	1.16	—	3.04
Hybrid	0.0	—	—	—	—	—	—	—	—
Hybrid +HD	47.1	0.74	0.78	0.69	0.85	0.90	1.20	-4.30	24.08
Hybrid +VS	0.0	—	—	—	—	—	—	—	—
Hybrid +HD+VS	93.4	1.05	1.38	0.73	0.72	0.94	1.28	-7.73	8.98

HD, hyoid descent; PL, physiological limits of muscle length; SM, short mandible; VS, vertical symphysis; X, X-axis gear ratio; Y, Y-axis gear ratio; DigA, anterior digastric; GH, geniohyoid; HG, hyoglossus; MH, mylohyoid; DigP, posterior digastric; StyH, stylohyoid

The first set of simulations tested whether the models could meet the excursion target if the hyoid was descended (HD), if the symphysis was vertical (VS), or both (HD & VS). The target of 0.039 units of protraction and 0.042 units of elevation was met in all conditions (Figure 6.4). Hyoid descent displaced the entire ROM inferiorly, increased anterior ROM, and decreased superoanterior ROM. A vertical symphysis slightly increased anterior and superoanterior ROM. Although the maximum point of superoanterior excursion was slightly reduced in models with HD alone, including VS restored some of this region of the ROM.

The second set of simulations tested the same conditions as the first while simulating a shortened mandible (SM) (Figure 6.5). In the following simulations with short mandibles, the target was reduced to 0.034 units of protraction and 0.037 units of elevation as described above. In addition to geniohyoid and hyoglossus shortening presented above, mandibular shortening changed hyoglossus orientation from 39° to 78° relative to the X-axis—that is, the hyoglossus became more superoinferiorly oriented. The target was met in the SM and SM+VS conditions, albeit through extreme geniohyoid rotation in the SM model (GR = 12.21). The target was not met in the SM+HD (41.7 %) or SM+HD+VS (61.5 %) conditions.

The third set of simulations tested the same conditions as the second while using the physiological limits (PL) of muscle length change (70-150% of initial length) for the simulations (Figure 6.6). The target was met in models with a high hyoid, but using PL increased but did not fully restore excursion in SM+HD (58.5 %) or SM+HD+VS (90.2 %).

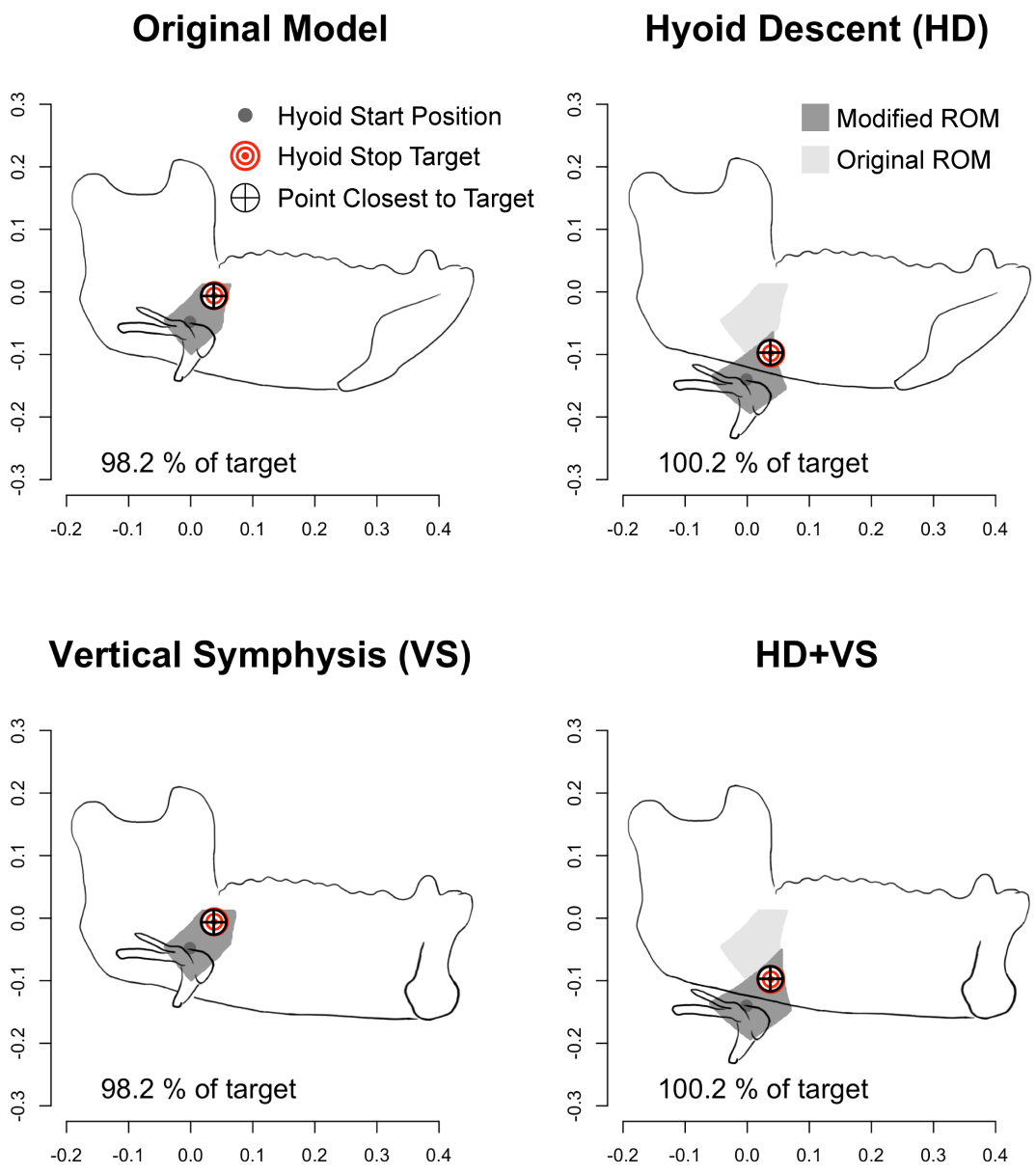

Figure 6.4: Effect of hyoid descent and a vertical symphysis on range of motion (ROM) in the original macaque model. X-axis is anteroposterior, Y-axis is superoinferior. Mandible and hyoid silhouettes demonstrate how model anatomy has been modified. Values reported in bottom left report predicted excursion as a percentage of target excursion. Color code: dark gray circle, hyoid starting position; red and white concentric circles, hyoid excursion target; black crosshairs, point in the ROM closest to the excursion target; gray polygon, model ROM; light gray polygon, ROM of the original, unmodified model.

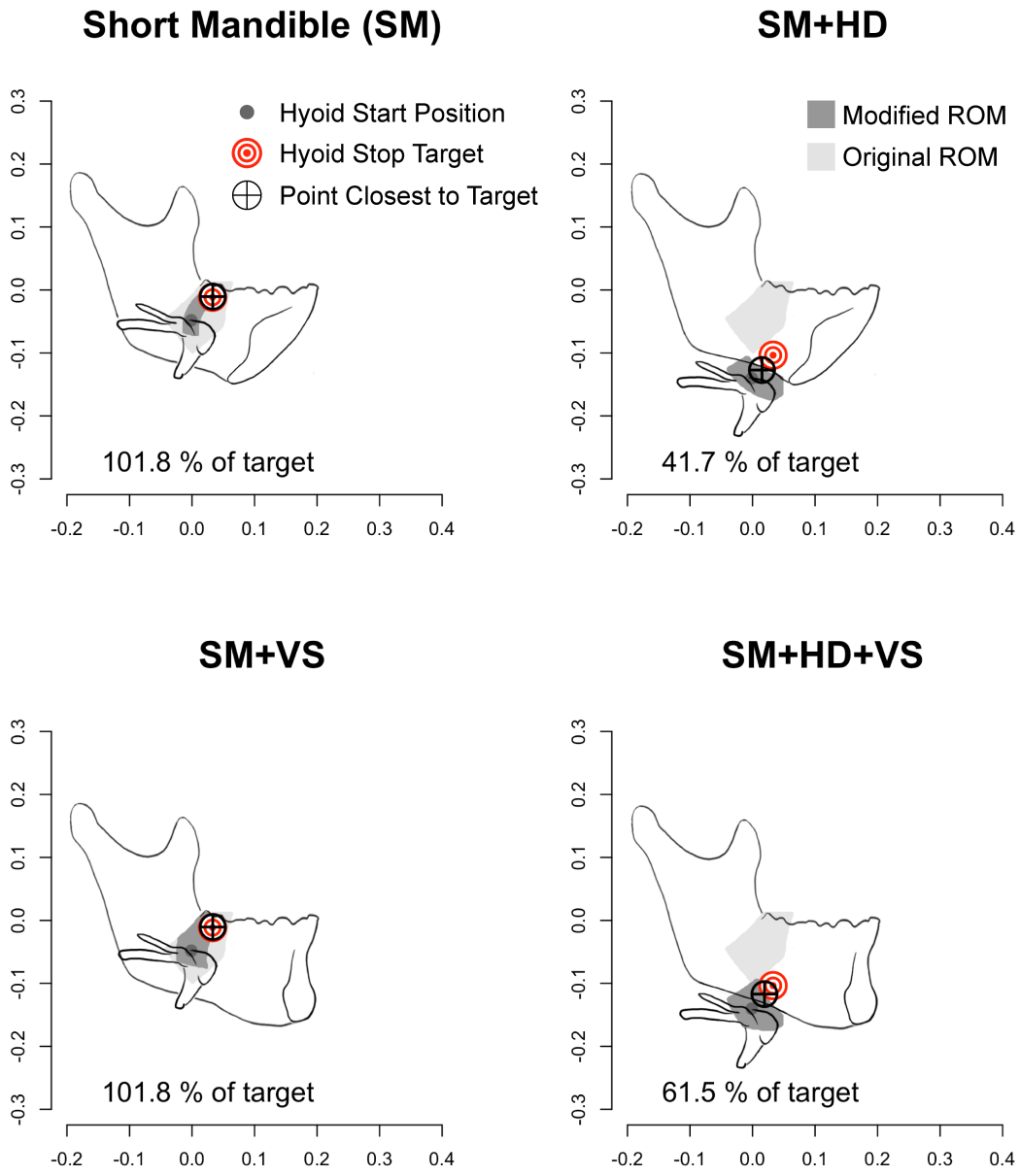

Figure 6.5: Effect of hyoid descent and a vertical symphysis on range of motion (ROM) in models with a short mandible (SM). X-axis is anteroposterior, Y-axis is superoinferior. Mandible and hyoid silhouettes demonstrate how model anatomy has been modified. Values reported in bottom left report predicted excursion as a percentage of target excursion. Color code: dark gray circle, hyoid starting position; red and white concentric circles, hyoid excursion target; black crosshairs, point in the ROM closest to the excursion target; gray polygon, model ROM; light gray polygon, ROM of the original, unmodified model.

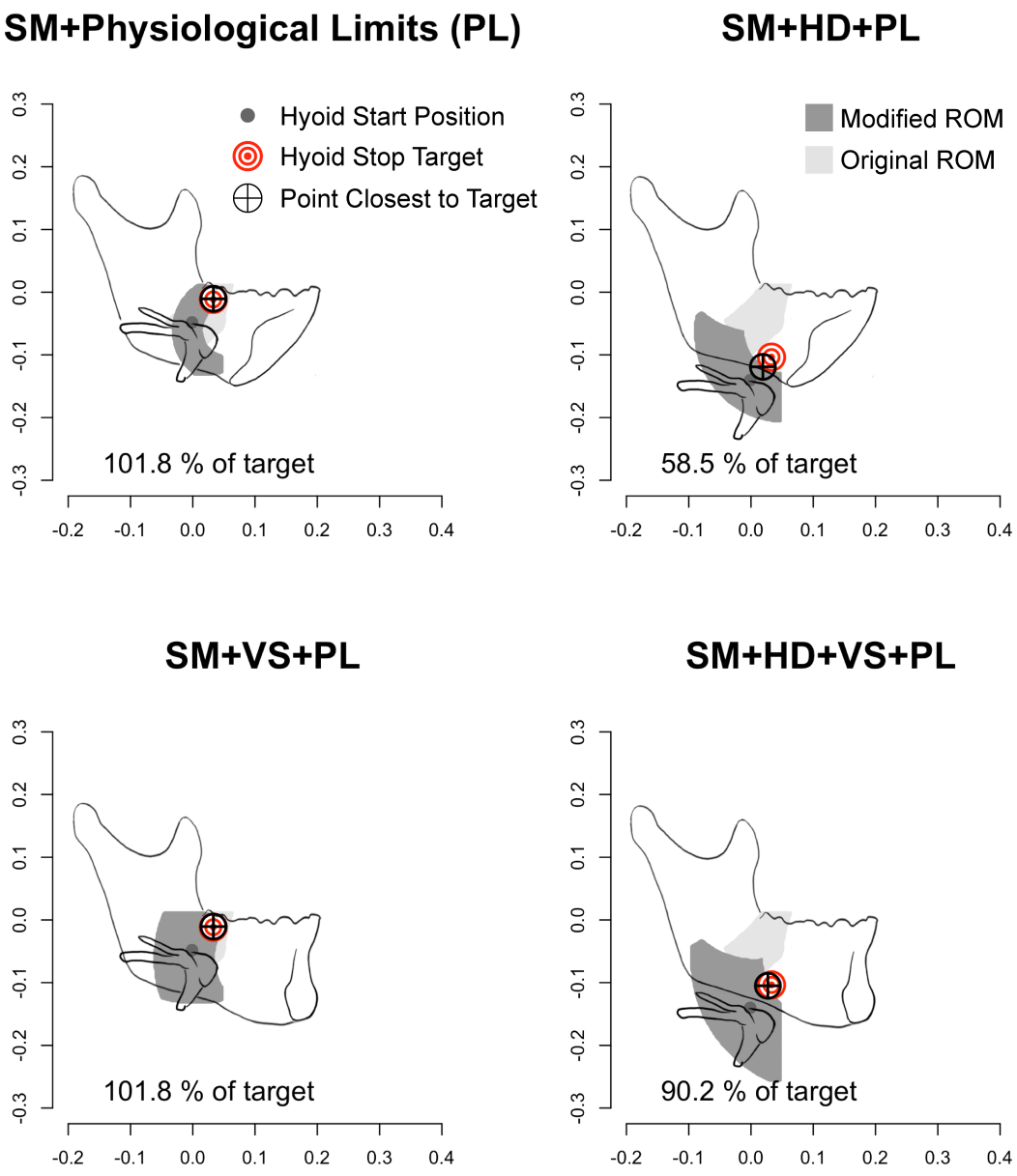

Figure 6.6: Effect of hyoid descent and a vertical symphysis on range of motion (ROM) in models with a short mandible (SM) using physiological length limits (PL). X-axis is anteroposterior, Y-axis is superoinferior. Mandible and hyoid silhouettes demonstrate how model anatomy has been modified. Values reported in bottom left report predicted excursion as a percentage of target excursion. Color code: dark gray circle, hyoid starting position; red and white concentric circles, hyoid excursion target; black crosshairs, point in the ROM closest to the excursion target; gray polygon, model ROM; light gray polygon, ROM of the original, unmodified model.

The fourth set of simulations used the hybrid model while changing whether HD, VS, or both were present or absent (Figure 6.7). In these hybrid models, the mandible was shortened, hyoid shape was vertically compressed, the digastrics inserted onto the dorsolateral basihyoid, the posterior digastric and stylohyoid origins were displaced anteriorly and inferior, the anterior digastric originated at the mandibular symphysis anterior and inferior to the geniohyoid origin, and the styloid process was slightly shortened (see Chapter 3). Macaque muscle length limits were used in these simulations. No models could reach their targets, although the hybrid+HD+VS had more excursion (81.1 %) than hybrid+HD (46.3 %) and the SM+HD+VS condition (61.5 %). Excursion was not possible without hyoid descent for two reasons. First, compression of the hyoid elevated the mylohyoid attachment site and consequently shortened mylohyoid and decreased its coronal angle closer to the limit observed in macaques. Second, the digastrics were already nearly linearized when the hyoid was in a high position, and the model assumed that the hyoid could not elevate any more once the digastrics were linearlized.

The fifth set of simulations tested the same conditions as the fourth set while using PL, akin to the third set (Figure 6.8). As with the fourth set, no models met their targets, although hybrid+HD+VS again had the greatest excursion (93.4 %) and was greater than the SM+HD+VS+PL simulation (90.2 %), although the difference between them (3.2 %) was less than the uncertainty of the model due to sampling density (5.7 %). As with the previous simulations, hyoid excursion was not possible without HD.

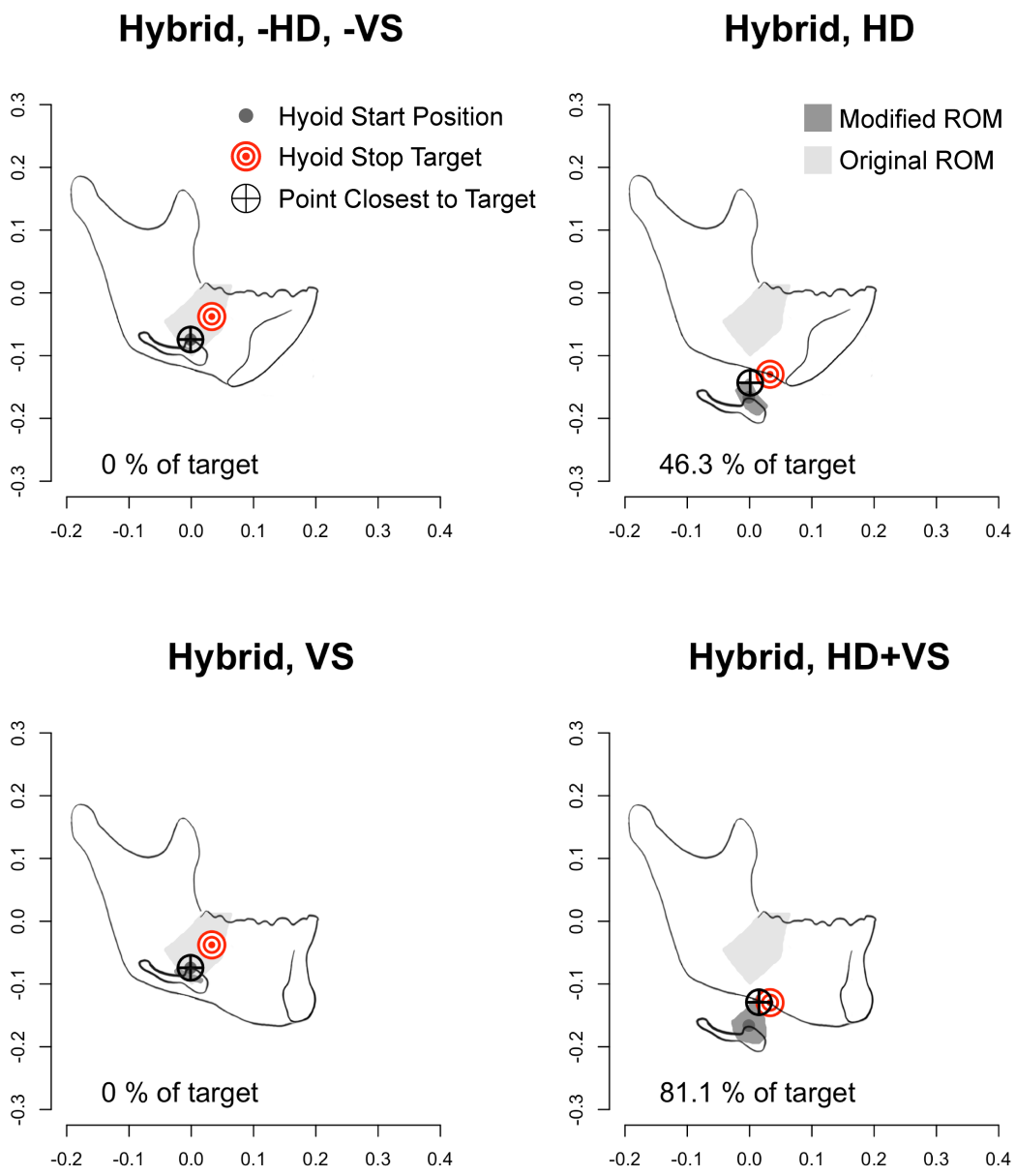

Figure 6.7: Effect of hyoid descent and a vertical symphysis on range of motion (ROM) in hybrid models. X-axis is anteroposterior, Y-axis is superoinferior. Mandible and hyoid silhouettes demonstrate how model anatomy has been modified. Values reported in bottom left report predicted excursion as a percentage of target excursion. Color code: dark gray circle, hyoid starting position; red and white concentric circles, hyoid excursion target; black crosshairs, point in the ROM closest to the excursion target; gray polygon, model ROM; light gray polygon, ROM of the original, unmodified model.

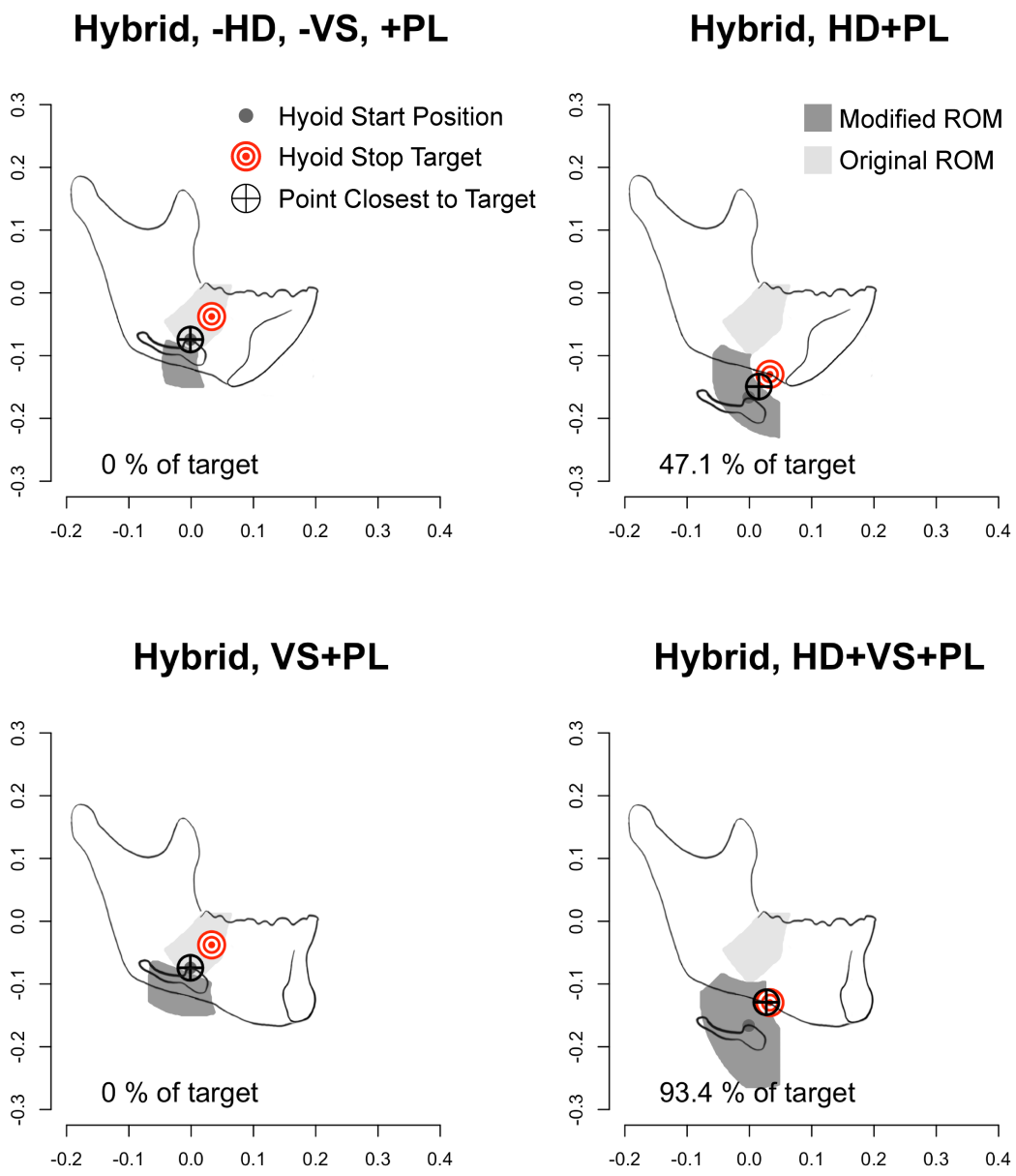

Figure 6.8: Effect of hyoid descent and a vertical symphysis on range of motion (ROM) in hybrid models using physiological length limits (PL). X-axis is anteroposterior, Y-axis is superoinferior. Mandible and hyoid silhouettes demonstrate how model anatomy has been modified. Values reported in bottom left report predicted excursion as a percentage of target excursion. Color code: dark gray circle, hyoid starting position; red and white concentric circles, hyoid excursion target; black crosshairs, point in the ROM closest to the excursion target; gray polygon, model ROM; light gray polygon, ROM of the original, unmodified model.

The sixth set of simulations were generated *post hoc* and examined the effects of including the digastric attachment to the hyoid and mylohyoid rotation limitations on non-descended hominoid models (Figure 6.9). Removing the digastric slightly improved anterior excursion, while removing the mylohyoid rotation did not affect superoanterior excursion because the hyoid's initial position was already above the line connecting the digastric origins. Only removal of both constraints produced sufficient hyoid excursion, and in this model the mylohyoid had an initial coronal angle of 56° and a final angle of 78°, compared to the original limit of 61°. The mylohyoid and geniohyoid gear ratios in this less constrained model were 3.27 and 2.85 compared to the Hybrid +HD+PL model's 0.69 and 1.20. When the VS was then removed from this less constrained hybrid model (ROM not shown), the target could again be reached with the same amount of mylohyoid rotation and gearing, but geniohyoid stretched and the geniohyoid gear ratio was consequently -3.04. Additionally, among all models with both the mylohyoid and digastric constraints removed, the target could be reached using macaque muscle physiology.

Additional figures demonstrating the effects of changing single parameters in the original macaque model and the hybrid model are included in Appendix C.

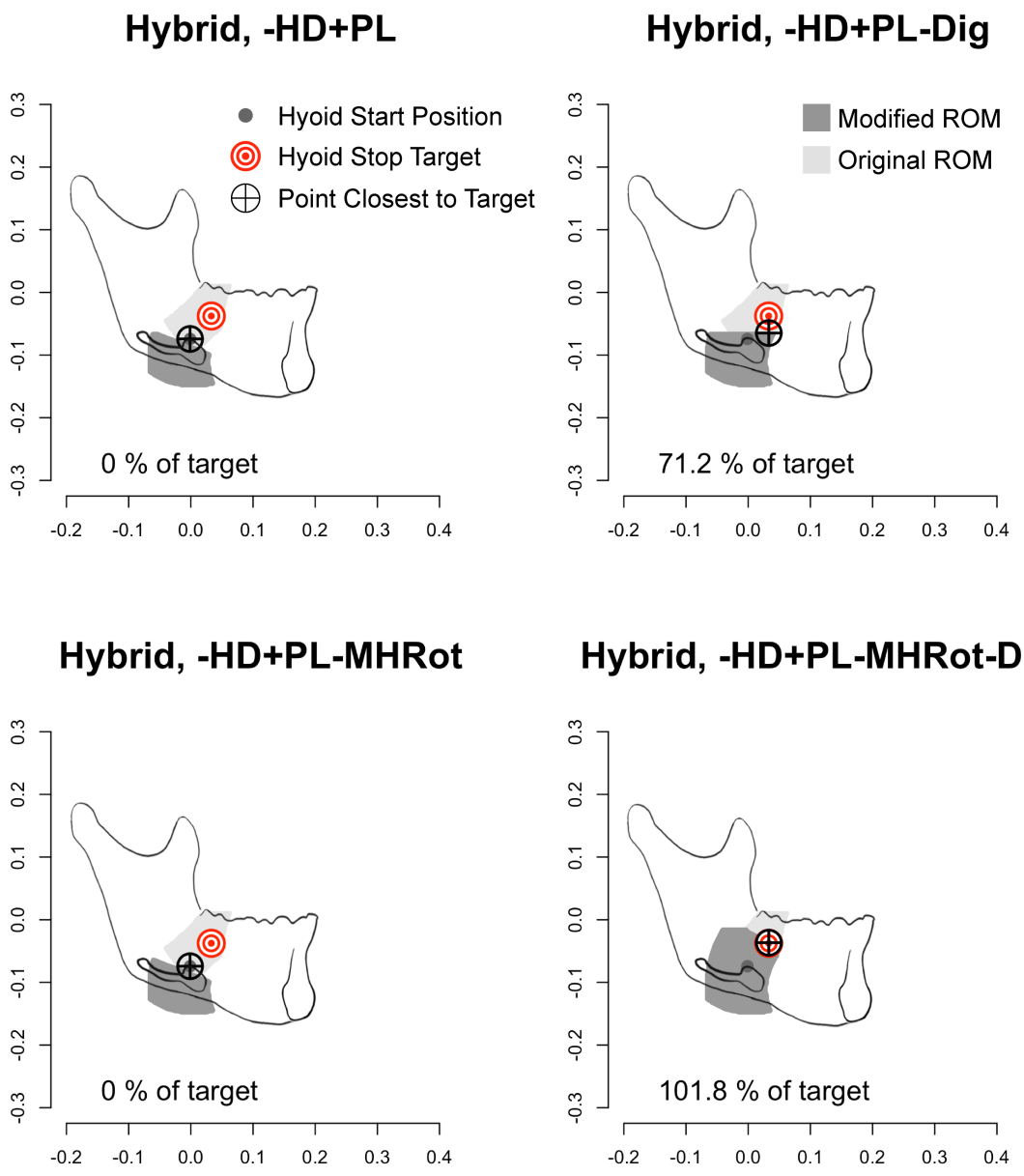

Figure 6.9: Effect of including the digastrics and mylohyoid rotation limits on range of motion (ROM) in a hybrid model using physiological length limits (PL). X-axis is anteroposterior, Y-axis is superoinferior. Mandible and hyoid silhouettes demonstrate how model anatomy has been modified. Values reported in bottom left report predicted excursion as a percentage of target excursion. Color code: dark gray circle, hyoid starting position; red and white concentric circles, hyoid excursion target; black crosshairs, point in the ROM closest to the excursion target; gray polygon, model ROM; light gray polygon, ROM of the original, unmodified model.

DISCUSSION

This study was performed to determine how changes in hyolingual and craniofacial morphology affect swallowing performance. Previous studies have evaluated the suitability of the airway for producing vowels (Peterson and Barney 1952; Lieberman et al. 1969; Stevens 1989; Lieberman et al. 1992; Lieberman 2012) and potential adaptations—or lack thereof—of the mandible for speech (DuBrul and Sicher 1954; Daegling 2012). Although hyoid descent has been hypothesized to be detrimental to swallowing performance because it increases the volume in which air and food can mix in the oropharynx (Negus 1949; Lieberman et al. 1992), more recent studies of feeding physiology cast doubt on this claim. Humans, like other mammals, regularly store food in the oropharynx prior to swallowing (Hiiemae et al. 1981; Franks et al. 1984; Palmer et al. 1992; Hiiemae and Palmer 1999; Matsuo and Palmer 2015) and do so independent of gravitational effects (Palmer 1998). Therefore, it seems unlikely that the central nervous system would regularly transport food into the oropharynx if such presents a choking hazard to the airway. However, it is possible that swallowing performance may nonetheless be either positively or negatively affected by craniofacial changes observed over human evolution and development. For example, based on the findings in Chapter 4, impaired hyoid excursion may also impair tongue base retraction and, therefore, clearing of the oropharynx before respiration resumes. If hyoid descent or craniofacial changes negatively affect hyoid excursion or suprahyoid muscle force production, then human swallowing performance may be less than optimal not because of an inherent design flaw in airway anatomy—as is commonly postulated—but rather because of fundamental constraints on underlying musculoskeletal biomechanics.

Chapter 5 argues that hyoid excursion is a result of not only muscle shortening but also rotation. Hyoid descent would theoretically improve mylohyoid's ability to generate superiorly oriented forces and displacement because such descent increases mylohyoid length and aligns mylohyoid with the superoinferior axis. However, descent could have one of two consequences on hyoid protraction. Descent places geniohyoid on an unfavorable part of the axial force-displacement curve, and consequently its gear ratio would be less than 1.00. In other words, as the hyoid descends, the geniohyoid would shorten more than the hyoid protracts. However, hyoid descent would also increase geniohyoid length, which could offset losses in protraction due to gearing deficits by increasing the absolute distance that the geniohyoid can shorten. Moreover, there may be synergistic effects between hyoid descent and having a more vertically oriented mandibular symphysis as opposed to an obliquely inclined simian shelf, given that the former increases geniohyoid length.

To address these uncertainties, a computational model was developed and trained on *in vivo* data to simulate the hyoid's range of motion (ROM) as morphology changes. Although Falk (1975) and Arensburg et al. (1990) have argued that a high hyoid would be detrimental to hominid swallowing performance, this is the first study to quantitatively test the hypothesis that changes in craniofacial and hyolingual shape affect swallowing performance.

Limitations

This study faces several limitations, and the models discussed here present new hypotheses that can be further tested through experimental and comparative approaches.

This model only examines the effect of shape change and assumes that hyoid performance scales with mandibular length. However, body mass may affect the actual excursion target

location. For example, if swallowed bolus size scales negatively with body mass, as bite size volume does in anthropoid primates (Perry et al. 2015), then the magnitude of hyoid excursion required for a safe swallow may decrease because hyoid excursion directly relates to bolus size (Molfenter and Steele 2011). This hypothesis is weakly supported by the observation here that human hyoids move approximately 20 % less than macaques when scaled by body mass. More hyolingual kinematic data from within and outside of primates are necessary to further evaluate whether the differences observed in this two-species comparison carry any functional significance (Garland and Adolph 1994).

As stated in Chapters 4 and 5, these data are limited to four individuals feeding on grapes. Bolus volume was not controlled in this study, and hyoid excursion is known to increase with bolus size (Molfenter and Steele 2011). If mean macaque excursion was underestimated, macaques may not significantly differ from humans in hyoid excursion relative to body mass. However, if such data were available for model development, then the length limits derived from *in vivo* data would respond accordingly.

The human-macaque hybrid model was created by manually adjusting input parameters until relative muscle lengths matched literature values. While this produced a realistic morphology, potential errors arising from this approach could be resolved by obtaining attachment coordinates from CT scans (e.g., Okada et al. 2013) of living humans or digitizing attachment sites on cadaveric specimens (e.g., Pearson et al. 2011, 2012).

Except for mylohyoid, hyoid gear ratios reported from the model differ from those reported in Chapter 5. For example, geniohyoid gear ratio here was 1.21, whereas *in vivo* it was 0.99. The anteroposterior axis hyoglossus gear ratio was 0.71, whereas *in vivo* it was 1.13. Stylohyoid superoinferior gear ratio was 32.92, whereas in *in vivo* it was 7.31. These values are likely

different because the starting position of the hyoid is based on a *post mortem* posture, which was more superior and anterior than the position of the hyoid before the onset of elevation and protraction during swallowing.

Lastly, adequate hyoid excursion is necessary but not sufficient for adequate swallowing performance. For example, it is unclear whether hyoid descent affects the central nervous systems' use of sensory feedback to coordinate suprahyoid and infrahyoid muscle activity with the muscles of the soft palate, pharynx, and larynx. Additionally, given that the larynx is suspended from the hyoid and shows variable degrees of mechanical linkage with the hyoid across primates (Nishimura 2003), the biomechanical consequences of laryngeal descent relative to the hyoid warrants further study.

What are the effects of mandibular shortening, hyoid descent, and symphyseal shape on static and dynamic morphology?

Hyoid descent increased all suprahyoid muscle lengths except anterior digastric, while a vertical symphysis increased and mandibular shortening decreased, respectively, geniohyoid and anterior digastric lengths. These findings are to be expected given that the methodology involved in simulating each of these changes involves inferior and anterior displacement of muscle attachment sites, respectively.

Mandibular shortening without a vertical symphysis profoundly decreases geniohyoid length—geniohyoid decreases by 77 % absolutely and 63 % relative to mandibular length for a 37 % decrease in mandibular length. This drastic reduction occurs because the model assumes that the hyoid is not posteriorly displaced when the mandible shortens because posterior displacement of the hyoid would be limited by the cervical spine and its associated prevertebral

musculature. Although mandibular shortening may be accommodated by posterior displacement of the hyoid in quadrupedal animals, a vertical spine may have been present as early as about 7 myr in *Sahelanthropus tchadensis*, an early hominid, and was well established in *Australopithecus sp* and *Homo sp*, (Zollikofer et al. 2005; Lieberman 2011). A vertical symphysis and hyoid descent together lengthened geniohyoid more than either did separately, and a vertical symphysis alone increased geniohyoid length more than hyoid descent alone. Notably, having a vertical symphysis and hyoid descent brought geniohyoid length back to 90 % of its length relative to the mandible but only 44 % of its original absolute length. The persistent deficiencies in absolute and relative geniohyoid length even after hyoid descent and symphyseal reorientation partially underlie the finding that increased muscle shortening is required in human-macaque hybrid models.

Increased muscle shortening was also required because of the effects of hyoid descent on geniohyoid gearing. As expected from the predictions made in Chapter 5, hyoid descent decreased the gear ratios of both mylohyoid and geniohyoid. Based on observations of greater force produced by lower gear pennate muscles (Azizi et al. 2008) and modeling results in Chapter 5, less rotation in mylohyoid may increase superiorly oriented force production. The mylohyoid gear ratio remained above 1.00 in all conditions, but the geniohyoid gear ratio was less than 1.00 in all HD models, indicating that the hyoid always moved less than geniohyoid shortened when the hyoid was descended. In the short mandible model with a high hyoid, the geniohyoid gear ratio was extremely high at 12.21, meaning that hyoid protraction was achieved almost entirely through rotation. However, the kinetic consequences of gear ratios of less than 1.00 is less clear because reported architectural gear ratios are greater than 1.00 (Brainerd and Azizi 2005; Azizi et al. 2008; Randhawa et al. 2013; Azizi and Roberts 2014; Holt et al. 2016);

presumably, this type of rotation would result in increased force and decreased velocity compared to fibers that do not rotate. However, as stated above, hyoid descent and a vertical symphysis both increased geniohyoid length, and the following simulation sets were run to determine whether these increases in length could overcome potential deficits imposed by hyoid descent.

Are a vertical symphysis and hyoid descent alone compatible with swallowing?

The first set of simulations demonstrated that models with HD, VS, and their combination all can reach the excursion target. However, there were subtle differences in the overall ROM. Superoanterior excursion was increased in VS and decreased in HD, whereas directly anterior excursion was increased in both. In combination, VS mitigated some of the losses in superoanterior excursion caused by HD but did so by increasing elevation more than protraction. Assuming that hyoid excursion is a reliable predictor of swallowing performance, these findings demonstrate that VS or HD could be well-tolerated by primates with mandibles that scale with their body size, especially if a more vertical symphysis is present.

Are a vertical symphysis and hyoid descent necessary to maintain swallowing performance when the mandible is shortened?

The second set of experiments simulated mandibular shortening by posteriorly displacing the geniohyoid and hyoglossus origins. The target could be reached after mandibular shortening when the hyoid was in a high position through a combination of mylohyoid shortening and geniohyoid rotation (Chapter 5). However, the geniohyoid has a high gear ratio, and consequently the hyoid protracts more than 12 times more than geniohyoid shortens. This ROM

seems biologically implausible because anteriorly directed forces would be miniscule if this fiber rotation decreases axial force, as it does in muscles with a high architectural gear ratio (Azizi et al. 2008). Therefore, geniohyoid may not generate enough force to overcome the inertia of its surrounding structures or the passive stiffness of antagonistic muscles such as sternohyoid, stylohyoid, or even the middle pharyngeal constrictors. Additionally, whereas low forces in a high gear stylohyoid can be compensated for by its synergists, mylohyoid and hyoglossus, especially as the hyoglossus becomes more vertically oriented with facial shortening, hyoglossus' more vertical orientation also means that geniohyoid loses its synergist and so a mechanism for compensating for force losses incurred by a large gear ratio. In contrast to the model with the simian shelf, the geniohyoid gear ratio when the symphysis was vertical was 1.63, which is more realistic and similar to the mean *in vivo* mylohyoid gear ratio (1.68, Chapter 5). Overall, the data support the hypothesis that healthy swallowing requires a minimum distance between the hyoid and the mandibular symphysis so that geniohyoid can actually shorten rather than rotate to produce sufficient protraction. As the mandible decreases in length beyond this minimum distance, the symphysis must become vertical to maintain swallowing performance.

If the hyoid is low, superoanterior excursion is limited, and predicted swallowing performance is reduced. Unlike in the first experiment where the target could be reached with a descended hyoid, excursion losses when the mandible was shortened were profound (41.7 % of target excursion). Although these losses were mitigated by a vertical symphysis and its attendant increases in geniohyoid length (61.5 %), these findings nonetheless demonstrate that mandibular shortening and hyoid descent together present a significant challenge to maintaining swallowing performance with macaque muscle physiology. Therefore, the same simulations were run utilizing the physiological limits of muscle shortening and lengthening (70-150 % of initial

length). Models with hyoid descent using the physiological limits were still deficient in excursion toward the swallowing target but less so than with macaque physiology (without VS: 41.7 % vs 58.5 %; with VS: 90.2 % vs 61.5 %). Moreover, in the hybrid models with hyoid descent, the geniohyoid gear ratio increased closer to 1.00 when physiological limits were used, indicating that deficits in protraction caused by hyoid descent were somewhat mitigated by greater muscle shortening. Nonetheless, these HD models could not reach the target, and strictly speaking the data do not support the hypothesis that, in absence of any other morphological changes, HD and VS can preserve swallowing function when the mandible is shortened. On the other hand, the data support the hypothesis that VS improves swallowing performance irrespective of hyoid posture when the mandible is shortened.

Are a vertical symphysis and hyoid descent necessary to maintain swallowing performance when simulating more human conditions?

Hyoid descent, a short mandible, and a vertical symphysis are not the only differences between humans and other primates. In addition to these traits, the fourth and fifth set of simulations use models with three other conditions that made the relative muscle lengths relative to mandibular length more human-like: basihyoid dorsoventral compression, and basicranial modifications, digastric origin at the mandibular symphysis, and digastric insertion on the dorsolateral hyoid. While humans share a dorsoventrally compressed basihyoid with other hominoids (i.e., greater and lesser apes) (Nishimura 2003), the highest levels of basicranial flexion in primates are found only among hominids (e.g., *Australopithecus* and *Homo sp.*) (Ross and Ravosa 1993; Ross and Henneberg 1995). Although the macaque digastric "tendon is attached to the inferior border of the hyoid bone by a thick non-elastic membrane" (Hilloowala

1975), the hyoid had a larger range of motion than the tendon marker in the anterior digastric, indicating that this membrane did not restrict hyoid range of motion, at least in protraction and elevation. In contrast, the human digastric essentially inserts into the hyoid via a fascial sling (Ozgur et al. 2010; Standring 2015), and so this muscle was included in the hybrid models.

The fourth set of simulations used the hybrid conditions with macaque physiology, whereas the fifth used physiological limits. In the hybrid models with high hyoids, superoanterior ROM was extremely limited without both hyoid descent and a vertical symphysis, primarily due to two limitations on hyoid elevation. First, hyoid compression elevated the insertion of the mylohyoid, which both shortened the muscle and increased its fiber angle relative to the Y-axis. Second, the digastric insertion on the hyoid was above the digastric linearization limit when in a high position. The model with both hyoid descent and a vertical symphysis produced the most superoanterior excursion with macaque physiology (76.4 %) and approached sufficient excursion with physiological limits (92.0 %). These results demonstrate that, in the context of additional human-like morphological features of the cranium and hyolingual apparatus, the entire biomechanical suite of hyoid descent, a vertical symphysis, and increased muscle excursion would be required to maintain swallowing performance. However strict application of the 94.3 % of the target displacement requires rejection of hypothesis that sufficient performance is maintained.

Given that the macaque hyoid is not rigidly coupled to the digastrics and that it is theoretically possible for the mylohyoid to reach fiber angles as high as 90° relative to the Y-axis, it is possible that the hybrid model with a high hyoid was overly constrained. To test this hypothesis, these constraints were removed in *post hoc* simulations using hybrid models with a vertical symphysis and without hyoid descent. Sufficient excursion was only reached when both

the mylohyoid rotation limits were relaxed and the digastrics were excluded from the model. In this model, the target was reached when mylohyoid rotated from 52° to 72° in a coronal plane. Based on modeling in Chapter 5, such rotation is not only theoretically possible but also may generate larger superiorly oriented forces because the increased rotation reduces fiber shortening velocity and increases fiber force production despite being less aligned with the superoinferior axis. However, when this same model had a simian shelf, geniohyoid actually had to stretch in order for the model to reach the target. Again, these results demonstrate that a high hyoid with a short mandible is theoretically possible, but such a configuration is only biologically realistic if accompanied by a vertical symphysis.

A deglutitive origin for the modern symphysis? Hyoid descent with modification.

Three important traits distinguish the faces of *Homo sapiens* from more archaic species of *Homo*: a more retracted (i.e., shorter) face (Lieberman et al. 2002), a more vertical symphysis (Liu et al. 2010), and a more protuberant chin (Elder 1855; Wallis 1917; Dobson and Trinkaus 2002). In fact, a chin is so unique to humans that it is considered by some to be "a hallmark of modern humanity" (Dobson and Trinkaus 2002). Importantly, these three traits covary: the chin protrudes more as the symphysis becomes more vertical, and the symphysis becomes more vertical as the mandible shortens (Figure 6.10) (Dobson and Trinkaus 2002).

A more vertical inclination reduces the symphysis' ability to resist stresses that tend to pull the two halves of the mandible laterally—i.e., wishboning stress, or lateral transverse bending (Hylander 1984; Dobson and Trinkaus 2002; Groening et al. 2011). Although a protuberant chin increases symphyseal strength somewhat, a vertical symphysis with a chin is still weaker under wishboning stress than an obliquely oriented symphysis (Dobson and Trinkaus

2002; Groening et al. 2011). This weakness suggests that wishboning stresses became less important in the mandible's loading regime over human evolution, probably because a shorter mandible—a result of facial retraction—decreases the moment arm of muscles producing wishboning itself (Daegling 1993).

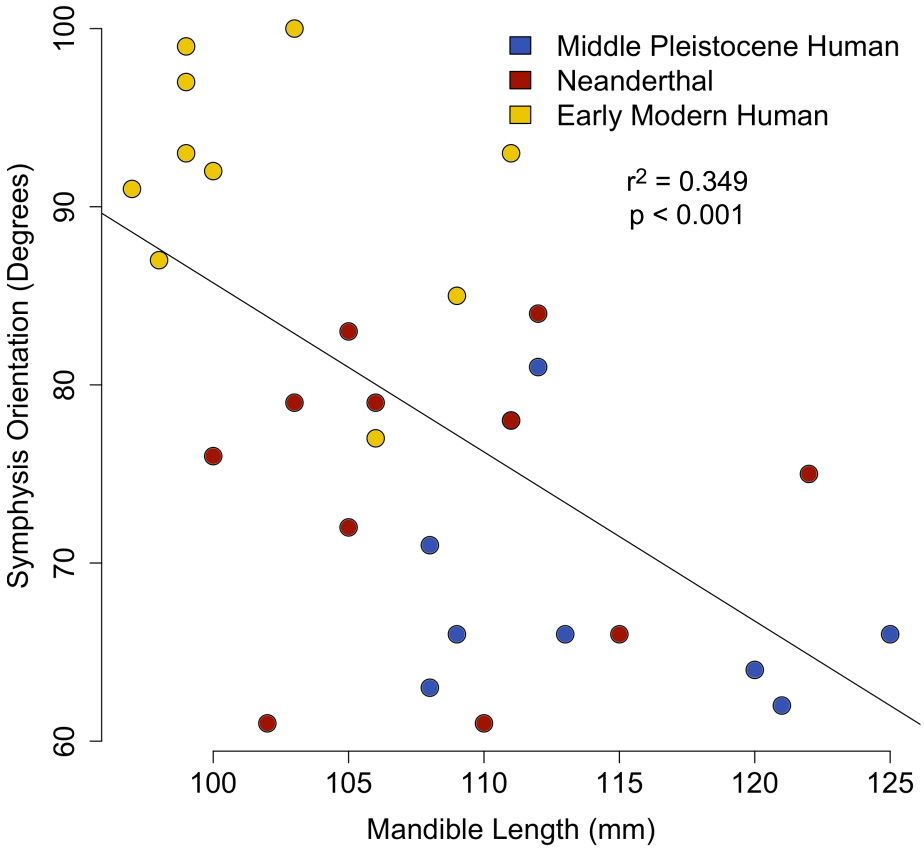

Figure 6.10: Mandibular length versus symphysis orientation in Pleistocene humans. Data from Dobson and Trinkaus 2002.

However, a new question arises from the finding that inclined symphyses without chins and vertically oriented symphyses with chins are equally strong in other kinds of loading (Dobson and Trinkaus 2002; Groening et al. 2011): if a simian shelf and a vertical symphysis

have equivalent strength under non-wishboning stresses, then why did recent and modern humans shift to a vertical symphysis (Daegling 1993)? DuBrul and Sicher (1954) proposed a spatial packing hypothesis, wherein the vertical symphysis resulted from bipedalism because continued retraction of the face—and shortening of the mandible—would have compressed the oropharyngeal structures against the vertical cervical spine. This hypothesis has been described as "frustratingly difficult to evaluate" (Daegling 1993) and does not resolve the question of why the oropharyngeal structures—including geniohyoid and the tongue itself—could not instead reduce their anteroposterior length to avoid such problems.

This research provides a plausible answer to the question of why the symphysis became vertical by falsifying the hypothesis that swallowing performance would be unaffected by reductions in mandibular length. When the mandible is shortened and a simian shelf is maintained, the geniohyoid cannot protract the hyoid sufficiently by shortening—it can only reach target hyoid displacements by primarily rotating and, in some cases, stretching. Given that force production likely drops as a result of this rotation (Azizi et al. 2008), it is unlikely that the geniohyoid in such a fictional morphology would be able to produce enough force to facilitate laryngeal closure, open the upper esophageal sphincter, or displace tongue volume. Simulating a vertical symphysis, however, results in more plausible muscle kinematics when the hyoid is high. A vertical symphysis also nearly meets the swallowing performance target when the hyoid is descended, although greater muscle shortening is required. In conclusion, the human mandible is probably shaped by trade-offs in swallowing and masticatory performance—the simulations presented here support the hypothesis that swallowing performance drove the evolution of the human vertical symphysis, while the comparative biomechanics of symphyseal strength supports the hypothesis that masticatory performance drove the evolution of the human chin as the

symphysis became more vertical (Dobson and Trinkaus 2002; Groening et al. 2011, but see Daegling 2012 and Pampush and Daegling 2016).

Is the human hyoid apparatus maladapted to swallowing?

The simulations offer several insights into how swallowing performance may be affected by changes in craniofacial shape and hyoid posture that have occurred over the course of human evolution. Hyoid descent was of little consequence by itself, and only when combined with mandibular shortening were the models unable to reach their targets. These findings suggest that the primary obstacle to human swallowing performance is not the size of the oropharynx, as is posited by the maladaptive vocal tract (MVT) hypothesis, but rather suprahyoid muscle length. This length deficiency hypothesis (LD) hypothesis is supported by a limited number of studies of muscle length change in humans demonstrating that the geniohyoid and mylohyoid shorten by up to 30-40 % of their maximum lengths during swallowing (Okada et al. 2013; Feng et al. 2015). The LD hypothesis is also supported by the clinical literature, in which 86 % of dysphagic pediatric patients with facial malformations had abnormally short mandibles, i.e., micrognathia (Baudon et al. 2009; van de Lande et al. 2017). The treatment for micrognathia is mandibular distraction, i.e., mandibular lengthening, which restores feeding function in most patients (Breik et al. 2016). Interestingly, micrognathia-related dysphagia appears to be worse in infants (van de Lande et al. 2017)—given that the hyoid descends during the first year of life (Lieberman et al. 2001), hyoid descent and its consequent increases in suprahyoid muscle length may sufficiently compensate for deficiencies imposed by a pathologically short mandible.

Because hybrid simulations with hyoid descent and vertical symphyses could only approach the excursion target through increased muscle shortening, adult humans may routinely

function near the extremes of suprahyoid muscle function, which has two implications. First, human suprahyoid muscles may also need to shorten relatively faster to maintain coordination with palatal, pharyngeal, and laryngeal muscles. If so, then relative muscle force and power during shortening would be reduced compared to macaques. Second, suprahyoid muscles may have little tolerance for decreased functionality. Tolerance for functional deficits is sometimes called physiological reserve in the clinical literature and provides an indication of how well an organ system can handle physiological insults or increased demand (Burkhead et al. 2007). This concept is similar to how the safety factor of bone describes the difference between typical bone loads and those loads which cause the bone to fail (Currey 2013). In the case of swallowing, this reserve could be quantified as difference between the minimum muscle force or velocity necessary for safe swallowing and the maximum force and velocity of that muscle. Physiological reserve is essential for feeding, lest one grow too tired from breakfast to continue eating and drinking throughout the day (Humbert and Vose 2018). Once physiological reserve is depleted, patients tend to decompensate and perform worse—in the case of the muscular system, this manifests as fatigue and increased perceived effort (Burkhead et al. 2007). In the case of swallowing musculature, the high functional demands placed on suprahyoid muscles could make them prone to decompensation or failure with only slight decreases in maximum displacement or velocity output.

The suprahyoid muscles may, however, compensate for deficiencies in length through physiological adaptations which increase their serial sarcomere number. Having more sarcomeres in series decreases the amount of strain each sarcomere experiences for a given amount of whole fiber strain, which would also decrease fiber velocity and increase fiber force (Winters et al. 2011). In this case, the infrahyoid muscles may have a critical function in

providing low amounts of active stretch to the suprahyoid muscles during feeding or tonic stretch during rest, both of which would stimulate increased serial sarcomere number (Williams and Goldspink 1973; Butterfield et al. 2005). As demonstrated in Chapter 5, the macaque mylohyoid routinely shows low levels of active stretch before shortening, which implies that infrahyoid muscles are active at that time. Because hyoid descent makes the geniohyoid slightly more superoinferiorly oriented, sternohyoid would also be an antagonist for geniohyoid in humans and so could lead to increased serial sarcomere number in both elevators and protractors of the hyoid.

Although physiological adaptation may allow organisms to bridge some gaps in performance imposed by morphological changes, maintaining a connection between the digastric and a high hyoid could nonetheless be detrimental swallowing performance. Given that mylohyoid and anterior digastric coactivate during non-human primate swallowing (Vitti and Basmajian 1977; Wall et al. 1994; Chapter 5), it is unlikely that such an attachment would be beneficial in a high hyoid without fundamentally changing swallowing motor patterns (Falk 1975). If the digastrics were attached, then the digastrics would have to either invert—in this case, the anterior digastric would then function as an antagonist to mylohyoid—or, because tendons and ligaments offer no resistance to compression, the hyoid may have been able to elevate a short distance independent of the digastric before inverting the fascial sling and pulling the sling back into tension. The ROM constraints imposed by attachment of the digastrics to the hyoid raise an important question: why do humans maintain this connection and descend the hyoid rather than retain a high hyoid and no connection between the digastrics and the hyoid, similar to orangutans (Chapman 1880; Sonntag 1924; Winkler 1991; Wall et al. 1994; Diogo et al. 2013b)?

Mandibular shortening may have created the conditions in which maintaining a connection between the digastric and the hyoid as well as hyoid descent were advantageous. The hyoglossus loses much of its synergistic protraction capabilities because of mandibular (and tongue) shortening. Because geniohyoid alone would then have to produce most of the protraction power, such a redundant-less configuration may be particularly prone to failure and have a low physiological reserve. Additionally, increased geniohyoid rotation away from the anteroposterior axis in a high hyoid would likely decrease anteriorly-directed forces (Azizi et al. 2008; Chapter 5). This is not to say that such an arrangement would be impossible. Rather, a short mandible creates a scenario in which hyoid descent might be favorable because, despite its accompanying requirement for increased fiber excursion, rotation brings geniohyoid fibers into better alignment with the anteroposterior axis and allows for the anterior digastric to facilitate hyoid protraction. Given that the human anterior digastric's physiological cross-sectional area—which correlates with muscle force—is 20 % greater than the geniohyoid's (Pearson et al. 2011) and anterior digastric strain is 39 % less than geniohyoid (Chapter 3), such gains in anteriorly directed power would likely exceed losses incurred by increased geniohyoid excursion.

Therefore, hyoid descent allows the anterior digastric to facilitate hyoid protraction if the hyoid maintains an attachment to the digastric tendon, as it is in most hominoids except orangutans (Chapman 1880; Sonntag 1924; Winkler 1991; Wall et al. 1994; Ozgur et al. 2010; Diogo et al. 2011; Diogo et al. 2012; Diogo et al. 2013a; Diogo et al. 2013b; Standring 2015). The loss of anteriorly-directed force from hyoglossus associated with mandibular shortening may have created the conditions in which connection between a descended hyoid and the digastric tendon via a fascial sling may have provided a selective advantage, potentially through either the ability to swallow larger boluses and so consume more food quickly or increased physiological

reserve. Indeed, the human anterior digastric frequently has additional bellies, some of which are oriented anteroposteriorly and directly connect the mandible and hyoid (e.g., Sargon 1994; Guelfguat et al. 2001; Ozgur et al. 2010), which supports the hypothesis that the human anterior digastric facilitates hyoid protraction.

Although sufficient hyoid excursion is possible with a high hyoid if constraints related to digastric and mylohyoid rotations are removed, tongue length and volume—like geniohyoid—would have to decrease (Lieberman 2011), unless compensated by increased width or height. Unlike geniohyoid, however, whole tongue volume would not substantially increase with a vertical symphysis; only genioglossus length would increase. Conservation of tongue volume may be a particularly strong selective pressure if a hydraulic mechanism of tongue base retraction—in which tongue volume is displaced by hyoid excursion and mouth floor elevation (Chapter 4)—was prevalent among human ancestors. Given that increases in tongue width and height are limited by the width of the tooth row and height of the palate, the only way to maintain tongue volume in the presence of mandibular shortening is through hyoid descent (Lieberman 2011). Future work will need to expand this model to tongue base range of motion to evaluate the consequences of volume reduction on tongue base retraction.

Regardless of the exact chronology of how the human hyolingual apparatus emerged, the arguments above detail how hyoid descent may actually be advantageous to swallowing performance rather than outright maladaptive as some profess. Despite the potential benefits of hyoid descent, many of these muscles, especially geniohyoid, nonetheless must shorten near their maxima to generate sufficient hyoid excursion for safe swallowing (Okada et al. 2013). Such high functional requirements may explain why the choking epidemiology curve is bimodal, with higher incidences among those younger than two and older than sixty (Sakai et al. 2014)—motor

control may be underdeveloped in the young (especially if many choking events are due to oral exploratory behaviors rather than feeding) and declining in the elderly. Moreover, age-related sarcopenia and increased connective tissue stiffness may further contribute to age-related declines in swallowing performance if they impact the ability of hyolingual muscles to rotate, as they do in pennate muscles (Randhawa and Wakeling 2013; Holt et al. 2016). Ultimately, the data suggest that mandibular shortening has altered the human suprahyoid muscles and tongue to become a high functioning, but somewhat fragile, apparatus. Infants may be buffered from this fragility despite poor motor control by having a high larynx which better physically separates milk and air than the adult configuration (Negus 1949). In older adults, suprahyoid muscles may begin to lose their physiological reserve after reproduction, in which case there may be little selective pressure for the suprahyoid muscles to have more physiological reserve.

Can hyoid posture be predicted from craniofacial morphology?

This question cannot be definitively answered with the data at hand. As discussed above, it is unclear whether a high hyoid and smaller tongue volumes could be tolerated as the face shortens (Lieberman 2011). If not, then it may be possible to predict hyoid position from mandibular length. Studies of the scaling tongue dimensions, mandibular length, and hyoid posture with body mass may be particularly useful in resolving these uncertainties. Primates (Ross et al. 2009), felids (Weissengruber et al. 2002), canids (Schmitt and Wallace 2014), and xenarthrians (Casali and Perini 2017) all exhibit a wide range of mandibular lengths and/or hyoid positions and may provide a fruitful comparative dataset for these questions.

CONCLUSIONS

The data support the hypothesis that, when the mandible is shortened, a vertical symphysis is necessary to maintain swallowing performance. The data weakly support the hypothesis that hyoid descent is necessary to maintain swallowing performance. Sufficient hyoid displacement is possible if a high hyoid and a vertical symphysis are present, but anteriorly-directed force production would likely be reduced. Moreover, a high hyoid would require reductions in tongue volume that may not be tolerated if a hydraulic linkage between the hyoid and the tongue base requires a minimum tongue volume to successfully execute tongue base retraction. Additionally, descent may benefit swallowing performance by allowing the digastric maintain its insertion onto the hyoid, which would allow the anterior digastric to facilitate hyoid protraction. Future work should further validate this model and its assumptions in humans, other species of primates, and mammals in general.

CHAPTER SEVEN: CONCLUDING THOUGHTS ON THE PRIMATE HYOID APPARATUS AND ITS HYDROSTAT

This dissertation aimed to establish the biomechanical basis of the primate squeeze-back mechanism of swallowing—specifically, the relationship between tongue base retraction and hyoid excursion. In doing so, I have proposed a novel mechanism of tongue base retraction, demonstrated why suprahyoid muscle rehabilitation should target velocity and power rather than mere strength, and argued that swallowing performance has shaped not only the hyolingual apparatus but also the mandibular symphysis over the course of recent human evolution. In this conclusion, I summarize my findings, discuss the implications of my work, propose future directions, and offer parting thoughts about the inner workings of the hyoid and its hydrostat.

SUMMARY

In Chapter 1, I discussed the basics of swallowing and why studying hyolingual biomechanics and the squeeze-back mechanism can be fruitful not only for clinical practice but also evolutionary biology and anthropology. I argued that a better understanding of the biomechanics of swallowing can improve rehabilitation techniques and thereby expedite recovery from dysphagia. More broadly, such knowledge can be used to determine how hyolingual design affects swallowing performance, which is an essential behavior for survival and may exert selective pressures not only on the hyolingual apparatus but on the vertebrate skull as a whole. However, determining the biomechanics of the squeeze-back mechanism requires knowledge of the *in vivo* behavior of the individual hyolingual muscles, and obtaining such information from humans is methodologically challenging. Therefore, because macaques (genus

Macaca) share similar swallowing anatomy and physiology with humans, a macaque model system was employed in testing these functional hypotheses. Specifically, I examined the biomechanics of tongue base retraction, hyoid excursion, and hyolingual descent.

In Chapter 2, I reviewed the muscle functional morphology literature and discussed why morphological and physiological lines of evidence must be integrated to determine muscle function. Muscle is a morphologically and physiologically dynamic tissue, and its capacity to generate force and movement depends not only on muscle mass and fiber velocity but also dynamic muscle geometry. Therefore, study of hyolingual functional morphology requires measuring both muscle length, orientation, and activity over time.

In Chapter 3, I presented a methodology which meets these demands by simultaneously acquiring electromyography and three-dimensional muscle, hyolingual, and craniomandibular kinematics. Integrating diceCT into the XROMM workflow improves on previous approaches by allowing not only three-dimensional data acquisition but also permits the accurate study of the many hyolingual muscles that are surgically remote. These data are then used to develop the computational model used in Chapter 6 to examine how morphology affects swallowing performance.

In Chapter 4, I proposed that the suprahyoid muscles drive tongue base retraction via a novel mechanism of muscular hydrostat movement. Extrinsic and intrinsic tongue muscles do not shorten enough to account for the amount of tongue base retraction observed *in vivo*. Rather, I argue that suprahyoid muscles generate tongue base retraction by regionally displacing tongue volume via hyoid excursion. Although later stages of tongue base retraction may involve some classic hydrostatic deformation, the observed regional increases in volume are consistent with a

hydraulic linkage, in which volume is regionally displaced in one region—the root of the tongue—to exert force or displacement elsewhere—the tongue base.

In Chapter 5, I built on these findings by examining *in vivo* muscle activity and velocity and comparing these against hyoid kinematics. In general, suprahyoid muscles were primarily concentrically active, especially during tongue base retraction. Suprahyoid muscles also rotated during swallowing and tongue base retraction, either amplifying or reducing hyoid displacement depending on the direction of rotation. Active shortening and fiber rotation suggest that the hyolingual apparatus is not prioritizing force production but, rather, either velocity or power. Moreover, mathematical modeling demonstrated that trade-offs in suprahyoid muscle force and velocity can be strongly affected by changes in hyolingual geometry.

In Chapter 6, I further probed this geometric dependence by modeling how changes in craniofacial and hyoid morphology over the course of human evolution affect swallowing. Using hyoid kinematics as a proxy for swallowing performance, the models demonstrate that mandibular shortening would impair swallowing function if not accompanied by other morphological changes, especially a vertical mandibular symphysis. Models with high hyoids could theoretically maintain hyoid excursion; however, they do so through increased fiber rotation, and anteriorly directed forces may be greatly diminished as a result. Moreover, mandibular shortening without hyoid descent would require the tongue to decrease in volume substantially, which may impair the hydraulic linkage between the tongue and the suprahyoid muscles which causes tongue base retraction. Therefore, contrary to previous claims that the human vocal tract is maladapted to swallowing because of hyolingual descent, such descent arguably functions to preserve swallowing function as the face shortens.

IMPLICATIONS

Biomechanical implications

The tongue differs from other muscular hydrostats because of its connectivity with neighboring structures which can affect its movement, including the hyoid and suprahyoid muscles. Indeed, the hyoid itself—the nexus of the neck—connects several essential structures in swallowing into a kinetic chain (Hiiemae and Palmer 2003). Muscular hydrostats were previously assumed to deform through alternating active muscle shortening of antagonistic fibers within the hydrostat. This dissertation broadens the scope of muscular hydrostat biomechanics and suggests that the tongue's morphological connectivity allows it to function passively in a more hydraulic manner, regionally displacing volume due to deformation caused by shortening suprahyoid muscles.

Studies of non-primate mammals—including the hyrax, opossum, and cat—suggest that a hydraulic linkage between the tongue base and hyoid may not be limited to primates. In the hyrax,

> At the start of the swallow, the leading edge of the food held in the oropharynx began to move around the epiglottis at the same time as the soft palate began to elevate. It is probable that posterior movement of the back of the tongue (between the posterior marker and the hyoid) created pressure on the bolus stored in the valleculae pushing the food in a posterior direction. As the leading edge of the stored bolus moved further down and back, the tongue markers and hyoid remained stationary though the region between the hyoid and posterior tongue marker changed in shape. The concavity, in which the food was held, smoothed out so that the bolus moved posteriorly. At the beginning of the tongue/hyoid protraction phase of the swallow cycle, the middle tongue marker and the hyoid moved up and forward as they did in chew cycles with stage II transport but the posterior tongue marker moved up without moving forward. The reduction of anterior movement at this time in a swallow cycle reflects continued posterior movement of the tongue dorsum in the region behind the posterior tongue marker. The changed shape of the bolus showed that the tongue, in conjunction with activity of the pharyngeal constrictors, was continuing to force the bolus towards the oesophagus. As the bolus continued to move down and back into the oesophagus, the tongue markers remained almost stationary…As the entire bolus moved into the oesophagus, the hyoid moved posteriorly. The hyoid movement reflected activity in the region of the tongue that is directly attached to the hyoid which assisted in pushing food into the oesophagus. (Franks et al. 1985, 542-543)

Although the earlier stages involve no hyoid sagittal movement and later stages involves both hyoid and tongue base retraction, the middle stages involve tongue base retraction during hyoid elevation and protraction. Similarly, Thexton (1984) notes a similar phenomenon in cats:

> The importance of the shape of the hyoid orbits in feeding relates to the movement transmitted directly to the tongue. Whereas this transmitted movement particularly affects the movement of the posterior/pharyngeal surface (Hiiemae *et al.* 1981, Thexton 1981), the movements of the anterior parts of the tongue are less influenced and may differ significantly from the movement of the hyoid. During swallowing there are, however, differences even between the movement of the posterior tongue and the hyoid…(1013)

which were described by Thexton and McGarrick (1988):

> In those cycles in which swallowing occurred, the tongue and the hyoid markers moved backwards during jaw closure with the same pattern of movement as in the pure lapping cycles…In early jaw opening, the markers also started to move forwards as in simple lapping cycles…However, during a short interruption in the jaw-opening movement, the posterior and/or middle tongue markers moved upwards towards the soft palate. The posterior part of the tongue, in contact with the soft palate, then moved backwards as the hyoid continued to move firstly forwards and then upwards…At the same time, the tongue became convex dorsally in the transverse axis…During this time, the bolus passed into the pharynx. Two factors produced the upward-backward sweep of the posterior tongue: movement of the tongue base, i.e., hyoid…and change of shape and dimensions within the tongue…The overall movement of the tongue in the swallow period was therefore not just a movement of the tongue base[6] but also a movement within the tongue itself, possibly reflecting styloglossus muscle activity. (336, 338)

However, there are conflicting reports of hyoid kinematic patterns in suckling pigs. Thexton et al. (1998) report hyoid elevation and subsequent *retraction* during tongue base retraction, whereas Gross et al. (2018) report hyoid elevation and subsequent protraction. This difference could arise from surgical technique: Thexton et al. (1998) report implanting a marker "into the tissues adjacent to the hyoid" whereas Gross et al. "sewed markers into the thyroid cartilage and hyoid bone". Interestingly, in this latter study, Gross et al. also report that both hyoid excursion and tongue base retraction were delayed in unsafe swallows. Overall, the comparative literature suggests that simultaneous hyoid superoanterior excursion and tongue base retraction are not unique to primates, and a hydraulic linkage between the tongue base and hyoid may extend to

[6] Thexton and McGarrick (1988) used the term "tongue base" synonymously "hyoid"; they did not use it to mean the posterior 1/3 of the tongue.

non-primate mammals as well. Moreover, such a mechanism may be essential in mammals which lack a styloglossus, including monotremes and many myrmecophagous[7] mammals, the latter of which are lingual feeders (Smith 1992; Reiss 1997).

Hydraulic displacement may also facilitate protrusion in these myrmecophagous mammals. Many of these ant- and termite-eating mammals are described as having long, narrow 'Type II' tongues by Doran and Bagget (1971), some of which have lost their attachment to an extremely descended hyoid due to fusion of the hyoglossus with the sternohyoid into a single muscle, sternoglossus (Chan 1995; Reiss 1997; Naples 1999; Reiss 2000). Although this narrow shape alone is mechanically advantageous for tongue protrusion because small changes in width can cause large changes in length (Kier and Smith 1985), the suprahyoid musculature of the echidna, pangolin, and the giant anteater suggest a hydraulic mechanism may facilitate protrusion in these animals. Their mylohyoids form a muscular tube around the tongue, nearly completely encircling the tongue and oropharynx posteriorly in pangolins and anteaters (Reiss, 1997; Reiss, 2000). In the pangolin, fibers innervated by the facial nerve, possibly homologous with the posterior digastric, continue this tube caudal to the mylohyoid, whereas in the anteater the mylohyoid itself extends caudally in to the neck (Chan 1995, Reiss 1997). As suggested by Reiss (2000), shortening of the muscles forming this tube would decrease the cross-sectional area of the 'lumen' deep to the muscle, resulting in tongue protraction as the tongue volume is displaced anteriorly. This muscular arrangement may facilitate tongue protrusion by protracting the tongue at its base, thus adding to the protraction due to hydrostatic deformation by intralingual fibers shortening alone. Such protraction is functionally analogous to tongue protraction by the genioglossus or geniohyoid, and future work could test the hypothesis that

[7] Ancient Greek: μύρμηξ, múrmēx, 'ant'

hydraulic protraction by mylohyoid is mechanically advantageous because it produces more displacement for a given change in mylohyoid length than either shortening in genioglossus or geniohyoid would. Changing the firing patterns of mylohyoid motoneurons could similarly produce tongue base retraction during swallowing in these animals.

Myrmecophagous mammals are not the only mammals with hyolingual specializations. Hyoid descent is also seen in koalas (*Phascolarctos cinereus*, Charlton et al. 2011, Charlton et al. 2013), some bats (*Epomops sp.*, *Epomophorus sp.*, and *Hypsignathus sp.,* Sprague 1943), and some felids (*Panthera sp.*, Weissengruber et al. 2002). Increased hyoid size is seen in howler monkeys (*Alouatta sp.* Hilloowala 1975), which probably results in a relatively short geniohyoid because the hyoid grows anteriorly toward the symphysis (e.g., Figure 15 of Hilloowala 1975). Moreover, the howler monkey anterior digastric inserts far posteriorly on the mandible and does not connect with the hyoid (Hilloowala 1975). The orangutan (*Pongo sp.*) similarly lacks connection between the digastric and the hyoid, and indeed lacks an anterior belly entirely (Chapman 1880; Sonntag 1924; Winkler 1991). Markedly, the gibbon *(Hylobates sp.*) not only has a more vertically oriented symphysis compared to other Great Apes (Daegling 2001), but its hyoid also sits below the lower mandibular border level with the C3/C4 vertebrae, as it is in humans, and is suspended below the digastric, suspended by a fascial sling (Figure 7.1) (Wall et al. 1994). Given that studying many of these animals in the laboratory is impractical, the modeling approaches presented here create new opportunities to examine hyoid posture, hyolingual shape, and swallowing performance within the broader context of craniofacial design and organismal fitness.

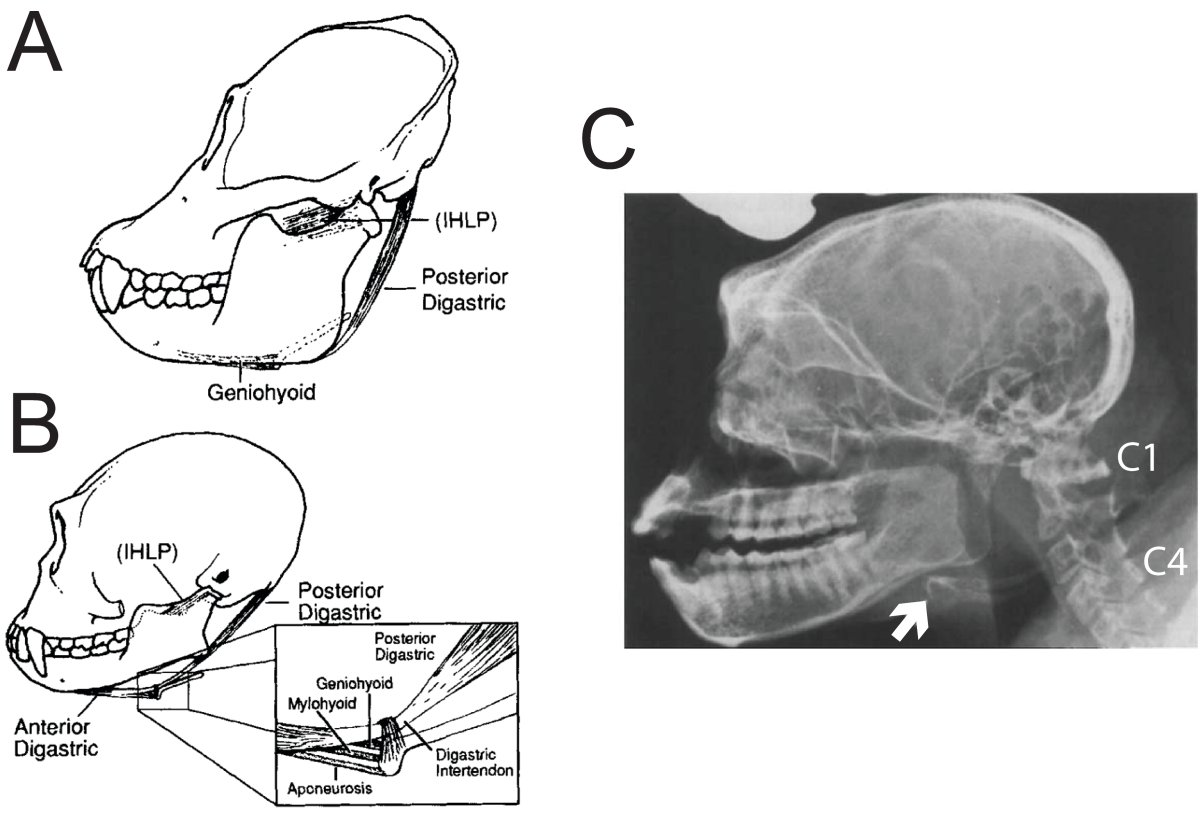

Figure 7.1: Suprahyoid muscle anatomy in the orangutan and gibbon. A) Orangutan skull and hyoid apparatus, lateral view. B) Gibbon skull and hyoid apparatus, lateral view. C) X-ray image of gibbon skull and hyoid apparatus, with cervical vertebrae labeled at C1 and C4 and hyoid position indicated by a white arrow. Modified from Wall et al. 1994.

Clinical implications

Because macaque and human hyolingual kinematics and kinetics are fundamentally similar (Franks et al. 1984; Palmer et al. 1992; Hiiemae et al. 1995; Matsuo and Palmer 2010; Nakamura et al. 2017), this dissertation's findings have translational potential for improving dysphagia treatment and prevention. If the human tongue exhibits similarly high levels of internal shear strain during tongue base retraction, prostheses made of materials with similarly low resistance to shear—perhaps even as simple as liquids—could be developed to enhance swallowing performance in patients with low tongue volume, such as glossectomy patients.

Moreover, patients with poor tongue base retraction may benefit more from rehabilitation exercises that target the suprahyoid muscles that those that do not.

The question then arises of what kind of exercises should be used to rehabilitate dysfunctional suprahyoid muscles. I argue that these exercises should be concentric and aim to improve muscle velocity and power (force x velocity) rather than isometric and solely aim to increase muscle force. Macaques, which have similar anatomy and physiology to humans, exhibit predominantly concentric activity in suprahyoid muscles during swallowing. Computational modeling presented here demonstrates that humans need to shorten geniohyoid relatively more to swallow safely because of facial shortening. Human *in vivo* data corroborate the computational modeling predictions of increased suprahyoid muscle excursion (Okada et al. 2013), and poor hyoid excursion is a known risk factor for dysphagia (Steele et al. 2011; Hoffman et al. 2013; but see Kraaijenga et al. 2016), Given that exercises which match *in vivo* function produce better functional outcomes than those that do not (Thorstensson et al. 1976; Coyle et al. 1981; McDonagh and Davies 1984; Gür et al. 2002; Stathopoulos and Ducchan 2006), these findings suggest that dysphagia rehabilitation should emphasize muscle velocity and/or power rather than strength alone. Indeed, increased hyoid displacement and velocity after rehabilitation therapy are associated with improved swallowing performance (Sia et al. 2015).

Evolutionary and anthropological implications

Computational modeling, combined with the novel mechanism of tongue base retraction proposed here, supports the hypothesis that selection to maintain swallowing performance underlies the emergence of three hallmarks of modern human anatomy: the vertical symphysis, the chin (provided that the chin functions as a mechanical buttress), and the descended hyoid.

Although a high hyoid could be tolerated with a shortened mandible if the digastric was not attached to the hyoid, the large decrease in tongue volume necessary to maintain such a high hyoid (Lieberman 2011) casts doubt on whether such an organism would be able to achieve sufficient tongue base retraction to swallow safely. The proposed length deficiency hypothesis predicts that, because of geometric constraints imposed by facial shortening and hyoid descent, human suprahyoid muscles have to shorten relatively more than other primates to reach the same amount of hyoid excursion for their body size. This deficiency may be tolerated in part because muscle is plastic, and increased serial sarcomere numbers may add to these muscles' physiological reserve. If this length deficiency hypothesis further supported, then humans may currently be under selection to maintain a minimum distance between the mandibular symphysis and the hyoid, particularly in human infants when the hyolaryngeal apparatus is still high (Breik et al. 2016; Lande, Caron, and Pluijmers 2017). This consideration raises the question of what, then, drove—and perhaps, is still driving—human mandibles to shorten?

A major review of the theories driving facial and mandibular shortening in recent humans is beyond the scope of this dissertation, but several theories have been put forth. Facial shortening increases bite force mechanical advantage because it decreases the out-lever length, in which case selection for increased masticatory efficiency or higher relative bite forces could drive facial shortening (Wroe et al. 2010). However, the human face is less able to resist these forces than closely related *Homo* species that are more prognathic and robust (Godinho et al. 2018), and recruiting all jaw adductor muscles bilaterally will tend to put the human temporomandibular joint into tension, which could risk its dislocation (Ledogar et al. 2016). Moreover, bite forces are poorly predicted by mechanical advantage but are well predicted by jaw muscle PCSA, i.e., force (Eng et al. 2013), suggesting that muscular rather than skeletal

morphology is a larger determinant of bite force production in anthropoids. All of these findings suggest that increased bite force is not driving facial shortening. Instead, smaller teeth, which are associated with smaller bite forces and may have been acquired following dietary shifts or pre-oral processing (e.g., cooking) (Robinson 1954; Demes and Creel 1988; Lieberman 2011), may cause the mandible to be shorter because decreased tooth root size allows for a smaller alveolar process in the mandible, particularly if the incisors teeth are upright as in humans (Lieberman 2011). Alternatively, Lieberman (1998) suggests that facial shortening may have facilitated speech by making the horizontal and vertical proportions of the vocal tract more equal to each other. Although recent studies argue against the increased mechanical efficiency hypothesis, smaller tooth size associated with decreased masticatory performance requirements and facial shortening due to selection for more clear speech are not mutually exclusive.

Although the research presented here cannot resolve why the human face became shorter in recent evolutionary history, this dissertation brings new ideas to bear on long-standing unresolved questions about hyolingual and mandibular design—form:function relationships—in primates. For example, although humans have presumably retained a connection between the hyoid and the digastric as a primitive trait (Sonntag 1923; Hilloowala 1975; Wall 1994), howler monkeys and orangutans have no connection between the digastrics and the hyoid as a result of either migration of the anterior belly posteriorly or because the anterior belly was lost, respectively (Chapman 1880; Sonntag 1924; Hilloowala 1975; Winkler 1991). The computational model suggests that such a loss may function to increase hyoid range of motion. For the howler monkey, such a loss may have protected swallowing performance in males as the basihyoid expanded anteriorly under sexual selection for increased lower roaring pitch (Dunn et al. 2015), which functionally resembles mandibular shortening by shortening the geniohyoid. On

the other hand, the hyoid in these monkeys may be massive enough to displace sufficient tongue volume to compensate for decreased geniohyoid shortening during tongue base retraction. In orangutans, the reasons for the loss of the anterior digastric are less clear. The posterior digastric is monofunctional in the orangutan, only activating during jaw opening, whereas in the gibbon it is also active during jaw opening but has a small amount of activity during swallowing (Wall et al. 1994). The data presented here from the one macaque with a verified posterior digastric electrode pair supports a bifunctional role in the macaque as well, although activity was greater during the swallow than jaw opening. Orangutans are unlikely to have deficient geniohyoid length because they do not have particularly posteriorly projecting mandibular symphyses or short mandibles for their body size (Daegling 2001; Ross et al. 2009). Although the reasons for the loss of the anterior digastric may remain obscure until a hyoid range of motion model can be generated for an orangutan, one observation may find an explanation in this dissertation—*in vivo*, the orangutan hyoid is higher relative to the mandible than in gibbons, chimpanzees, or humans (Falk 1973; Wall et al. 1994; Lieberman et al. 2001). Assuming that this higher position is because the orangutan mylohyoid has a larger fiber angle (and not because the inferior border of the mandible is more inferiorly displaced relative to the palate), such a high position may increase mylohyoid's superiorly oriented forces in the absence of synergistic elevation by digastric linearization (Chapter 5, Figure 5.11). Given the broad diversity of craniofacial and hyolingual morphology among not only primates but mammals in general, it is unlikely that humans are alone in facing biomechanical challenges in the face of selection for traits that may interfere with swallowing, and insights from the biomechanics of other organisms may lead to discoveries that inform dysphagia treatment.

FUTURE DIRECTIONS

Materials & methods

One of the primary limitations of the XROMM and diceCT workflows is the amount of time involved in processing data for a single animal. For XROMM, the most time intensive step is digitizing the marker positions. The semi-automatic features of XMALab (Knörlein et al. 2016) expedite the process, but application of computer vision and machine learning to this digitizing program would make hundreds—if not thousands—more cycles available for analysis, akin to feeding studies using infrared light motion capture, e.g., Vicon (Reed and Ross, 2010; Ross et al., 2012; Ross and Iriarte-Diaz, 2014; Takahashi et al., 2017; Iriarte-Diaz et al., 2017). Increased data processing speed would make sampling more individuals feasible, which would be particularly promising for comparisons of phenotypes in transgenic mice or marmosets, lesion studies, or ontogenetic studies. Given that XROMM is currently the only technology that can capture both hyolingual and mandibular kinematics in three dimensions with sufficient temporal resolution for the small mammals frequently used in the laboratory—especially transgenic strains—time invested to improve data processing speed with open-source software would be a valuable endeavor that would ultimately save time and increase the utility of XROMM.

Tongue base retraction via a hydraulic linkage

The data supporting the hydraulic linkage hypothesis are largely correlational, and this hypothesis could be further tested through targeted experiments.

First, these experiments could be replicated in additional rhesus macaque subjects where marker density in the tongue base is increased to improve spatial resolution. Following completion of feeding experiments, the animal could be used in a terminal stimulation procedure

while filmed in the XROMM facility in which muscles are systematically stimulated to determine whether activity in either single muscles or combinations of muscles are sufficient to produce tongue base retraction. I hypothesize that, when the jaws are closed, anterior digastric, geniohyoid, and mylohyoid stimulation are sufficient to produce tongue base retraction.

Second, in the absence of additional living subject availability, fresh tissue could also be manipulated *post mortem* using a linear actuator, currently under development by Kelsey Stilson in the Ross Lab. Because the tissues would have no active tone, these experiments could be used to determine whether hyoid displacement, without suprahyoid muscle shortening and stiffening, is sufficient to cause tongue base retraction. This actuator has variable velocity and power settings, which could be used to test the dependence of tongue deformation on hyoid velocity and suprahyoid muscle force transmitted to the tongue via the hyoid. These experiments could also be used to assess how differences in hyoid shape affect this hydraulic mechanism by using scaled 3D printed hyoids from across primates—for example, the compressed U-shaped hyoids of hominoids versus the cavernous hyoids of howler monkeys.

Lastly, the material properties of the tongue are largely unknown. *In vivo* nerve stimulation experiments could evaluate how tongue material properties change as a function of lingual muscle activity as well as how they vary across different regions of the tongue. The MyotonPRO is a handheld device designed to measure muscle stiffness noninvasively in humans and could be used to measure tongue stiffness (Mooney et al. 2013; Van Deun et al. 2016). However, the size of the device, though handheld, may prohibit its use on the more posterior parts of the tongue unless the temporomandibular joint is dislocated or the hyolingual apparatus is removed from the oral cavity via a submandibular incision, both of which would require converting the experiment to a terminal procedure.

Hyolingual functional morphology

Knowing the sarcomere lengths of the suprahyoid muscles of these animals would allow muscle force to be estimated from *in vivo* velocity and activity. However, as discussed in Chapter 2, current models of *in silico* force struggle under dynamic, submaximal conditions. (Perreault et al., 2003; Wakeling et al., 2012; Lee et al., 2013; Millard et al., 2013; Dick et al., 2017). Nonetheless, relating hyoid posture to each muscle's length-tension curve would yield valuable, albeit crude, insights into the postures at which muscle force production might be greatest, whether muscles are active when they are at that length, and whether muscles pass through their optimum length as they shorten.

One challenge to overcome before obtaining these sarcomere length measurements is the effect of iodine staining on sarcomere length measurements. Iodine staining, even at the low concentrations used in this study, causes skeletal muscle shrinkage in excess of 20 % of its original volume (Vickerton et al. 2013). To measure sarcomere length, fascicles are chemically digested using 30 % nitric acid, an aqueous solution (Loeb and Gans 1986). Because this solution is hypotonic compared to stained muscle, it is uncertain whether formalin fixation is sufficient to resist a tendency for fibers to elongate due to rehydration. With the aid of Prof. Andrea Taylor, experiments to test this hypothesis are currently under development.

Computational model of hyoid range of motion

Before the computational model is applied to non-human or non-macaque species, potential effects of scaling should be accounted for. Specifically, do the spatiotemporal elements of swallowing scale with body mass and mandibular length—that is, do hyoid excursion magnitude, duration, swallowing frequency depend on body size or mandibular length? The

answer to this question is important for establishing the prediction for how far the hyoid needs to move for an animal of a given body size and/or mandibular length. Addressing these uncertainties with experimental or observational data will be challenging—unlike chewing (Ross et al. 2009), hyolingual swallowing kinematics cannot be reliably estimated without videoradiographic equipment. However, common laboratory animals and ontogenetic studies would provide a useful starting point.

The computational model suggests that a vertical symphysis is necessary to maintain swallowing performance. If true, the human mandible and hyolingual apparatus may be the result of trade-offs in masticatory and swallowing performance. Groening at el. (2011) examined the effect symphyseal of cross-sectional shape on their ability to withstand different loads. They found that, under wishboning and dorso-ventral shear, the symphysis with a vertical symphysis and a chin was weaker than a more inclined symphysis shaped like that of a Neanderthal. However, this study did not vary mandibular length, and a vertical symphysis at longer lengths is probably relatively weaker than one at shorter lengths due to a larger moment arm for wishboning torques (Daegling 1993). Additional finite element modeling that includes variable mandibular length could determine a broader spectrum of performance among models to determine whether the current human configuration represents optimal masticatory and swallowing performance.

Lastly, the model could be expanded to include tongue kinematics after the hydraulic linkage hypothesis has been further tested and the relationship between hyoid kinematics, suprahyoid muscle shortening, and tongue base retraction are better understood. Including the tongue in the model would permit testing of the hypothesis that a short mandible and a high hyoid are incompatible because of the necessary decreases in tongue volume (Lieberman 2011).

CONCLUSION

I hope that the ideas presented in this concluding chapter have impressed upon the reader that the time is ripe for more in-depth study of swallowing biomechanics and functional morphology. Many untested hypotheses can now be approached with novel imaging techniques and the budding biomechanical framework presented in this dissertation. New imaging methods like diceCT will bring unprecedented spatial resolution and accuracy to hyolingual morphology without disturbing the posture of the apparatus through dissection—as has been argued previously (German et al. 2011) and as this dissertation has shown, hyoid posture is essential to understanding the function of hyolingual muscles. Mammals have diverse hyolingual apparatuses with variable degrees of connectivity among the cranium, hyoid, mandible, and tongue, yet the relationships within this kinetic chain are only understood for a handful of species. While the models used in this dissertation may be satisfactory for primates, these models probably have little bearing on mammals that lack connectivity between the hyoid and the tongue, such as some myrmecophagous mammals: this highlights the need to study swallowing in organisms that may swallow in extreme ways. Studying these organisms may also have tangential benefits for clinical research if new mechanisms of safe swallowing are discovered. High spatiotemporal resolution methods like XROMM will be essential in clarifying the relationship between swallowing morphology and function and for validating approaches that can evaluate how hyolingual performance may be affected by craniofacial or post-cranial modifications or posture. Given that muscles from the cranium, mandible, pharynx, soft palate, larynx, sternum, and scapula all converge on this nexus of the neck, the hyolingual apparatus may have an underappreciated role in shaping the very structures that have eclipsed it for so long

APPENDICES

APPENDIX A: MEAN TONGUE KINEMATICS IN MANDIBULAR AND CRANIAL COORDINATE SYSTEMS COMBINED AMONG ANIMALS AND WITHIN ANIMALS

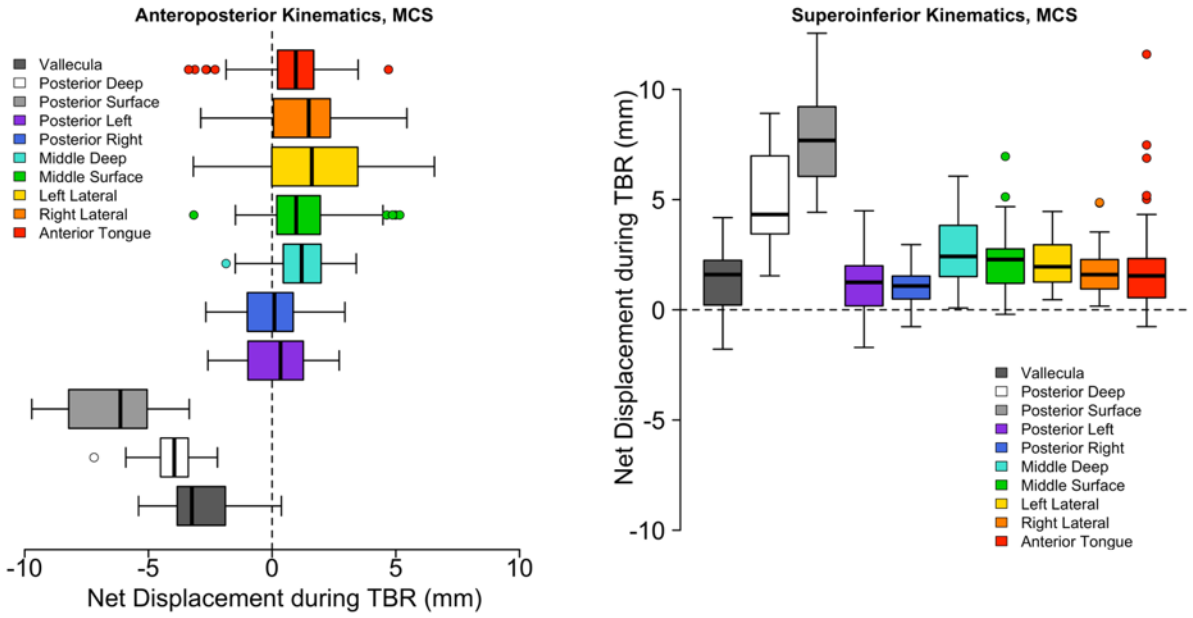

Figure A1: Tongue anteroposterior and superoinferior movement during tongue base retraction in mandibular coordinate system (MCS). Positive values indicate protraction or elevation, negative values indicate retraction or depression. A) Tongue marker anteroposterior movement during tongue base retraction. B) Tongue marker superoinferior movement during tongue base retraction. Posterolateral and more anterior markers appear to show more elevation than in a cranial coordinate system (c.f. Figure 4.1) because the markers remain elevated against the hard palate as the mandible depresses. Data are averaged across all monkeys. Boxes indicate the interquartile range, thick bars indicate median, error bars indicate data range, and circles are outliers. Colors correspond to the following markers: red, anterior; orange, right lateral; yellow, left lateral; green, middle surface; light blue, middle deep; dark blue, posterior right; purple, posterior left; gray, posterior surface; white, posterior deep; dark gray, vallecula.

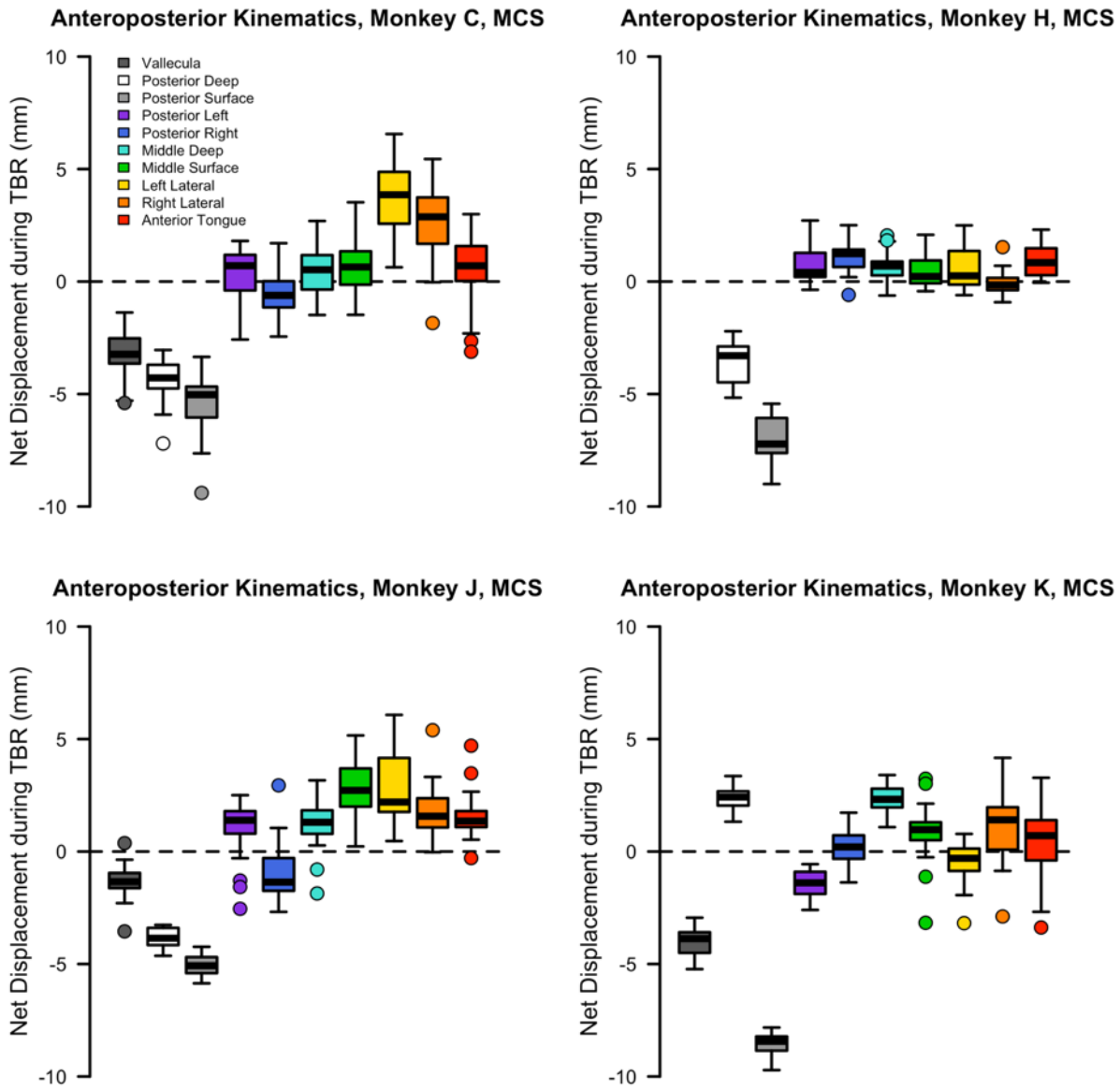

Figure A2: Tongue marker anteroposterior displacement during tongue retraction in individual monkeys in a mandibular coordinate system (MCS). Trends in individuals reflect the overall trends of the aggregated data. There is interindividual variation in the amount of posterior surface marker retraction relative to the posterior deep marker. The relative amount of protraction (and in some cases, slight retraction) of the other markers also varies among individuals. However, the posterior midline markers consistently retract more than the posterior lateral or more anterior markers in every animal. Positive values indicate protraction, negative values indicate retraction. The posterior deep marker of Monkey K protracts because it is more closely related to the hyoid than in other animals.

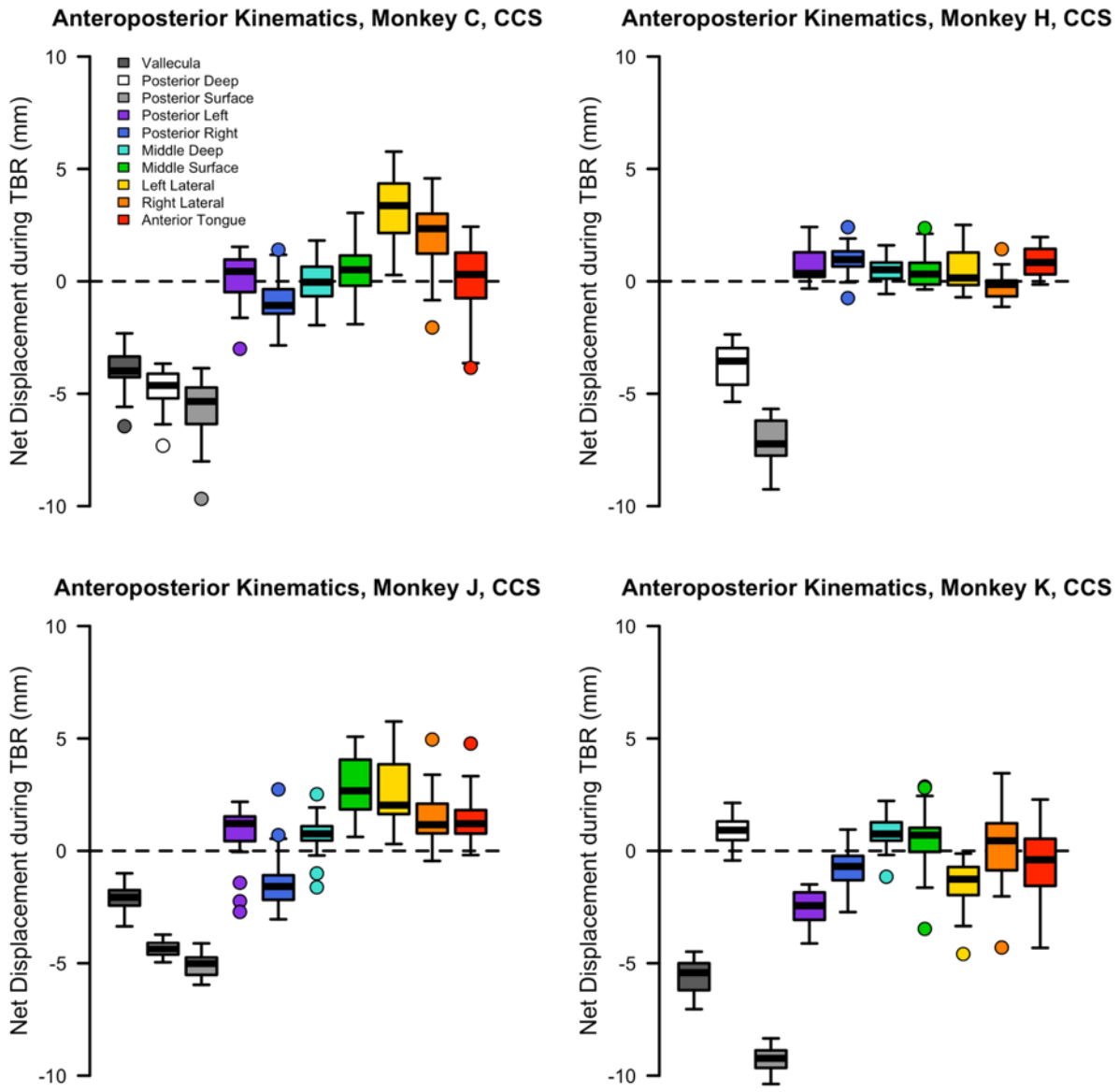

Figure A3: Tongue marker anteroposterior displacement during tongue retraction in individual monkeys in a cranial coordinate system (CCS). Trends in individuals are similar to those observed in a mandibular coordinate system. Positive values indicate protraction, negative values indicate retraction. The posterior deep marker of Monkey K slightly protracts because it is more closely related to the hyoid than in other animals.

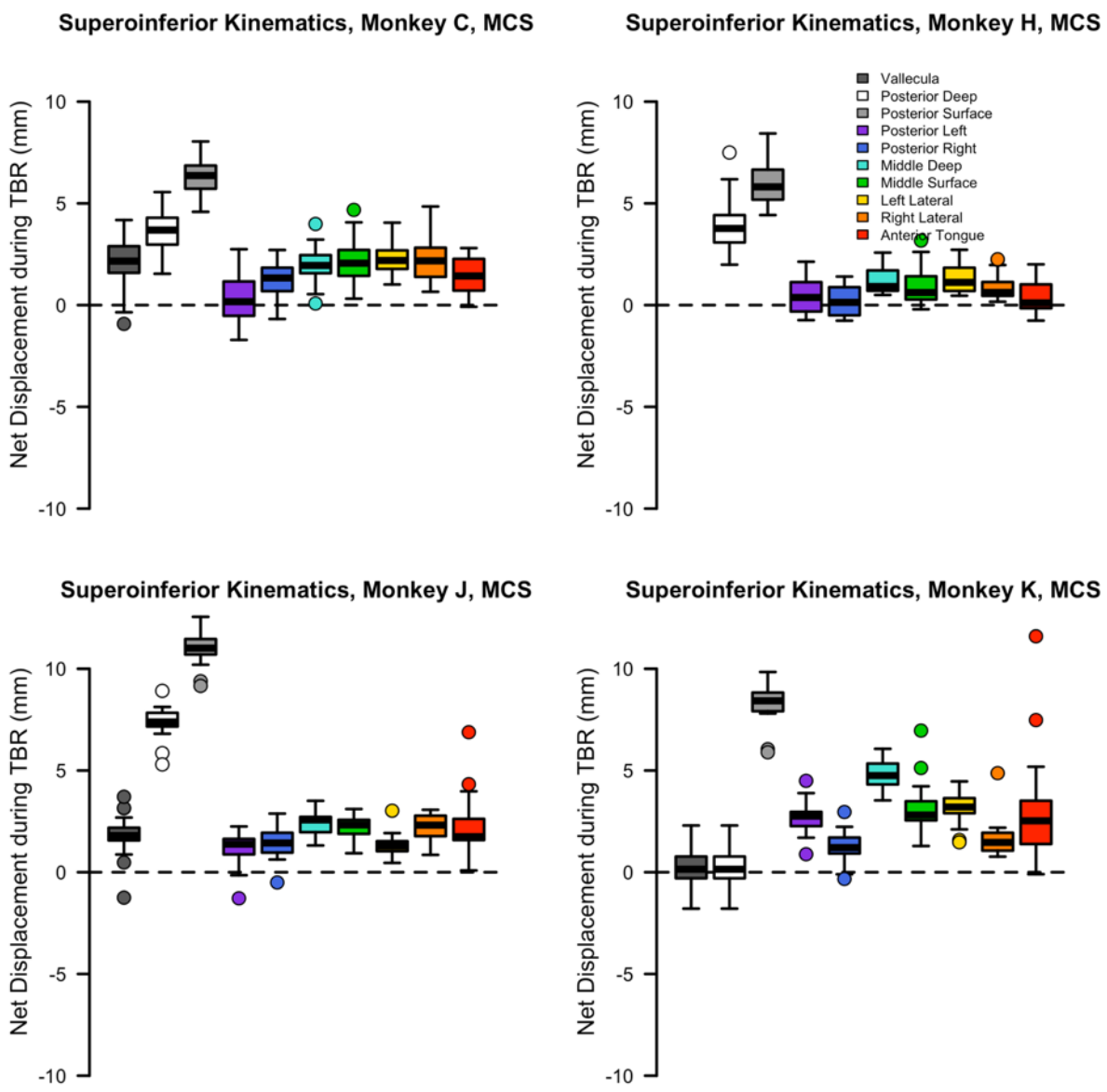

Figure A4: Tongue marker superoinferior displacement during tongue retraction in individual monkeys in a mandibular coordinate system (MCS). Tongue markers elevate relative to the mandible because the mandible depresses slightly at the end of tongue retraction while the tongue remains elevated against the hard palate. Positive values indicate elevation, negative values indicate depression.

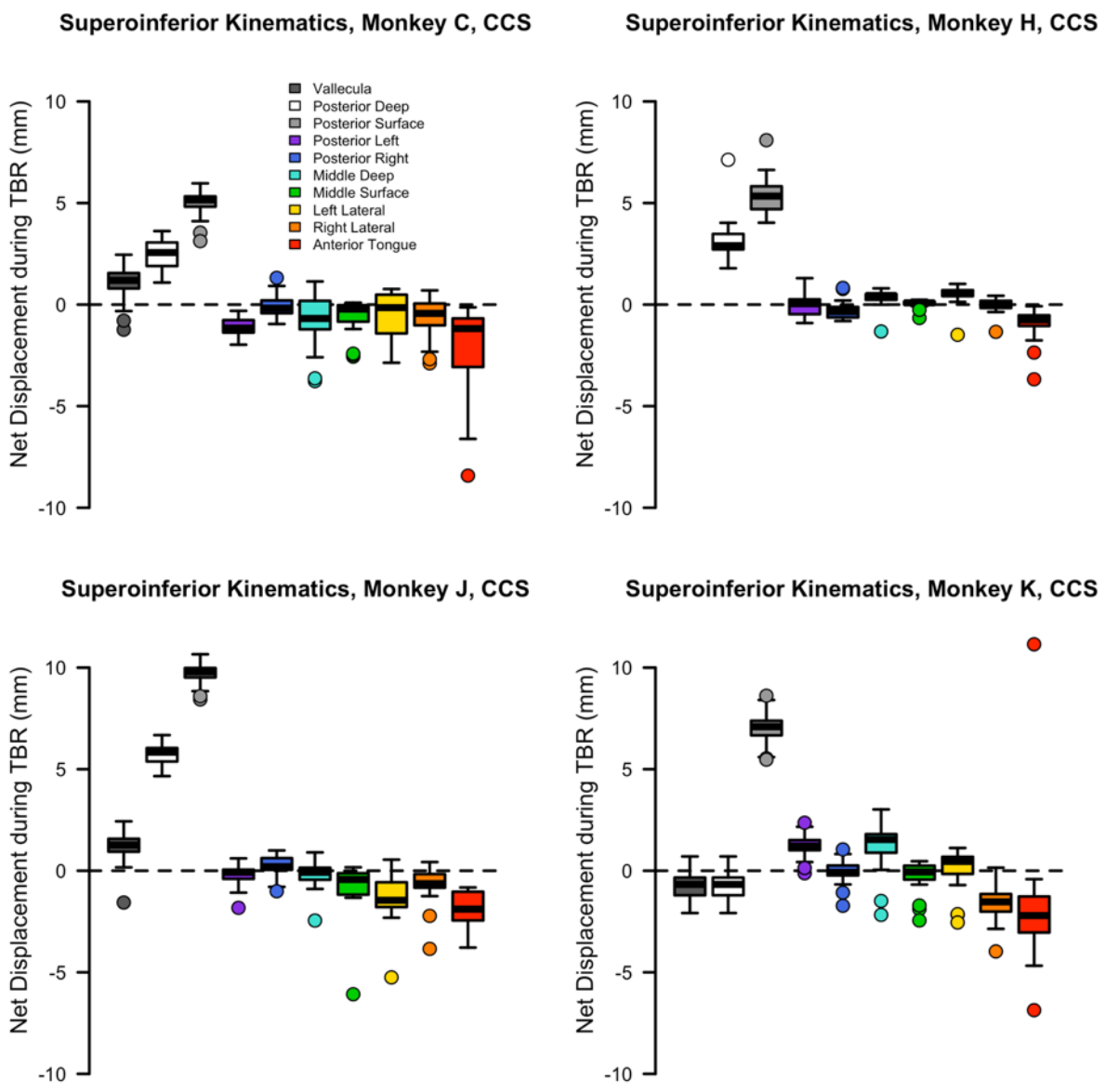

Figure A5: Tongue marker superoinferior displacement during tongue retraction in individual monkeys in a cranial coordinate system (CCS). Except for the posterior deep marker in Monkey Ki, posterior midline markers elevate during tongue retraction, whereas other tongue markers tend to remain stationary or depress relative to the cranium due to slight depression of the mandible later in the swallow. Positive values indicate elevation, negative values indicate depression.

APPENDIX B: DICECT OF A FEMALE RHESUS MACAQUE HYOLINGUAL APPARATUS DEMONSTRATING A LACK OF MUSCLE TISSUE IN THE POSTERIOR ORAL TONGUE AND TONGUE BASE.

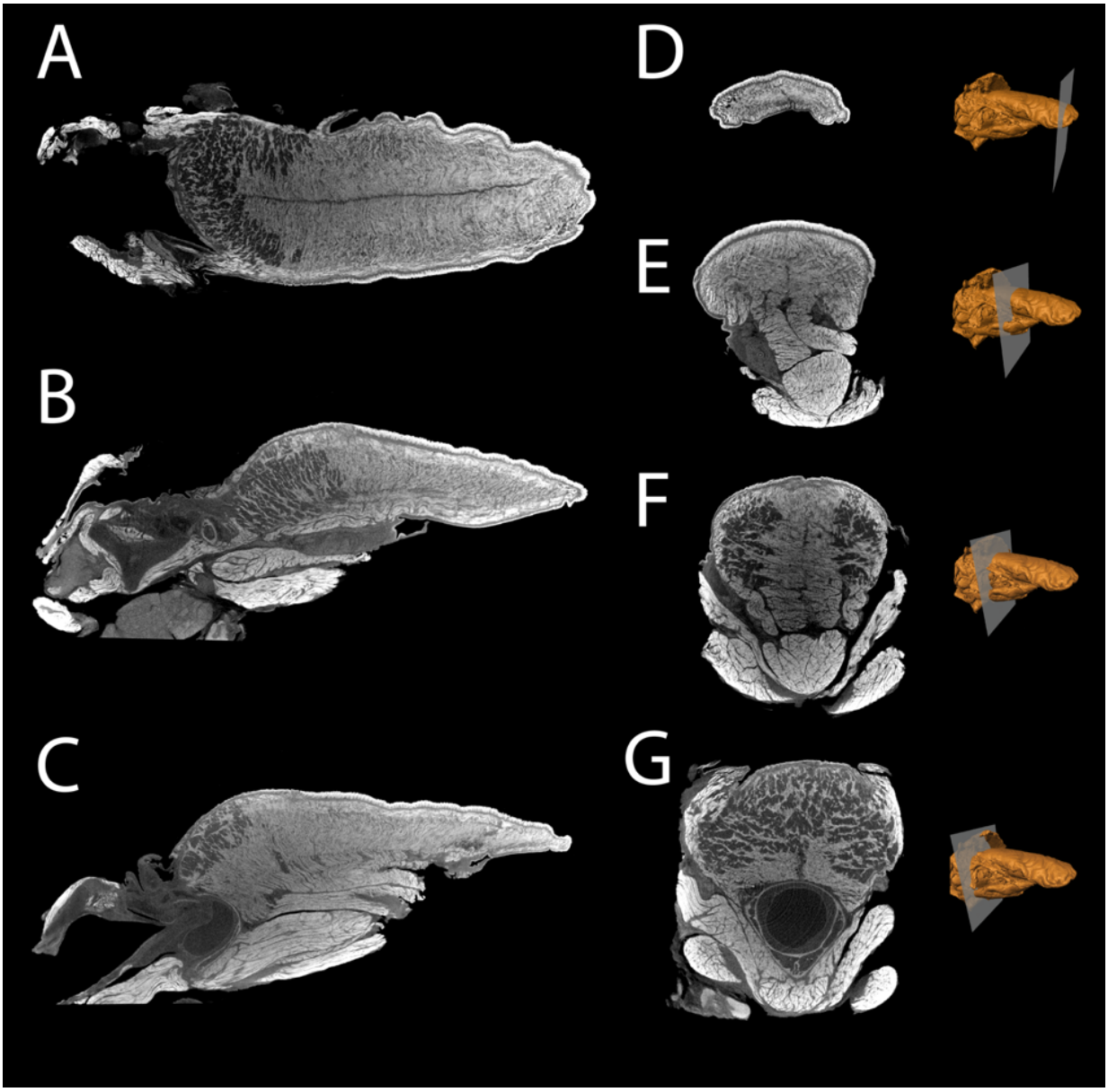

Figure B1: DiceCT of female rhesus macaque not used in XROMM experiments demonstrating a lack of muscle tissue in the posterior oral tongue and tongue base. Brightness indicates tissue density; iodine binds to glycogen in muscle and makes it as dense or denser than bone. The posterior oral tongue and tongue base are hypodense compared to the anterior oral tongue. A) Axial slice at the level of the palatoglossal arch lingual insertion. Up is left. Right is anterior. B) Parasagittal slice. Up is dorsal. Right is anterior. C) Midsagittal slice. Same orientation as B. D-F) Coronal slices. Up is dorsal. Right is right. 3D reconstructions to the right of each slice demonstrate the location of the slices. D) Tongue tip. E) Posterior to anterior oral tongue-posterior oral tongue border. F) Posterior oral tongue. G) Posterior oral tongue-tongue base border. The hyoid and part of the laryngeal air sac (round hypodense structure) are visible ventral to the tongue.

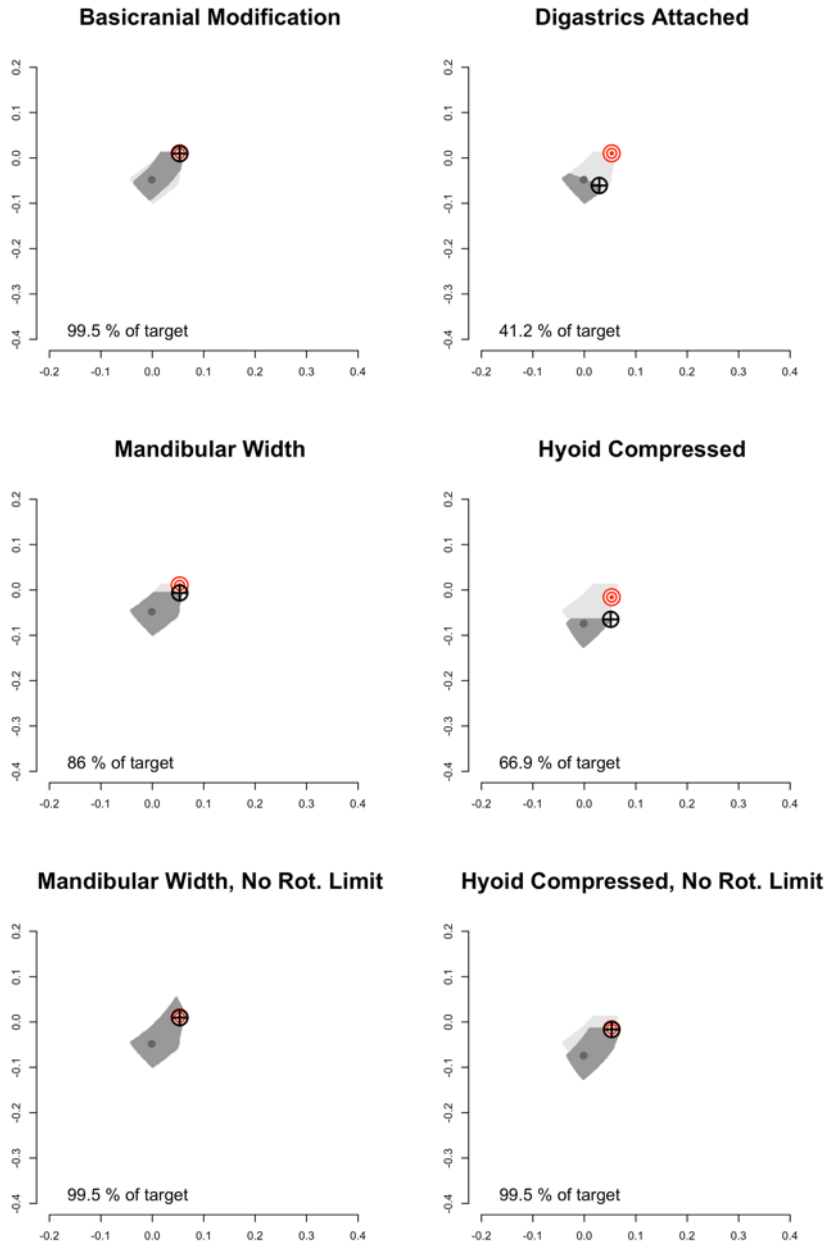

Figure C1: Effect of changing single parameters on the original macaque model. X-axis is anteroposterior, Y-axis is superoinferior. "No Rot. Limit" indicates that the mylohyoid could rotate freely, as long as the insertion on the hyoid was inferior to its origin. Values reported in bottom left report predicted excursion as a percentage of target excursion. Color code: dark gray circle, hyoid starting position; red and white concentric circles, hyoid excursion target; black crosshairs, point in the ROM closest to the excursion target; gray polygon, model ROM; light gray polygon, ROM of the original, unmodified model.

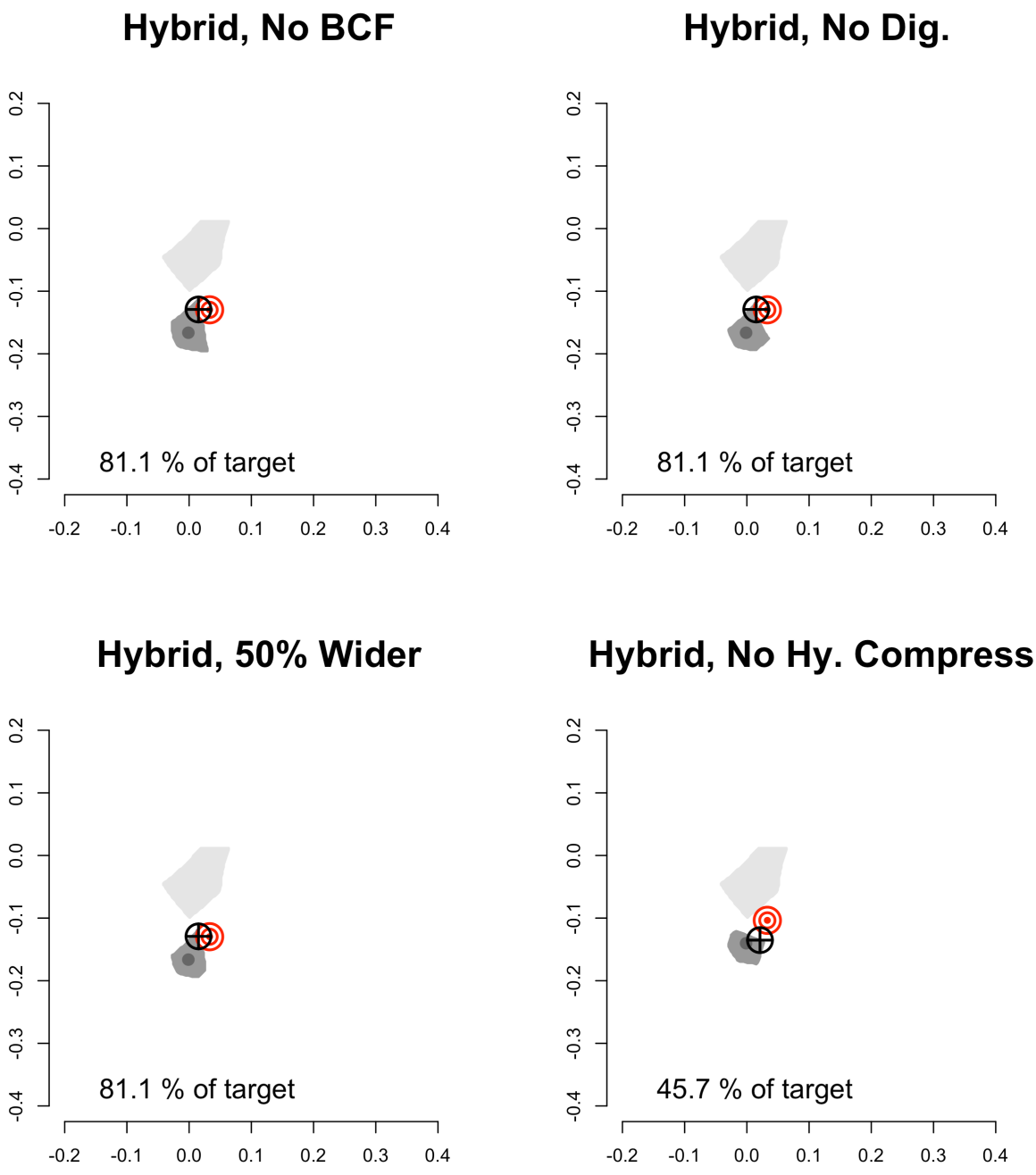

Figure C2: Effect of changing single parameters on the hybrid model. X-axis is anteroposterior, Y-axis is superoinferior. "No BCF" indicates that there was no basicranial flexion simulated, and so the posterior digastric and stylohyoid origins were unmodified. "No Dig." indicates that the digastrics were excluded from the model. "50 % Wider" indicates that the Z-axis distance between the mylohyoid origins was 50 % further apart. "No Hy. Compress" indicates that there was no vertical compression of the insertions on the hyoid. Values reported in bottom left report predicted excursion as a percentage of target excursion. Color code: dark gray circle, hyoid starting position; red and white concentric circles, hyoid excursion target; black crosshairs, point in the ROM closest to the excursion target; gray polygon, model ROM; light gray polygon, ROM of the original, unmodified model.

BIBLIOGRAPHY

Abbott, B. C., and X. M. Aubert. 1952. "The Force Exerted by Active Striated Muscle during and after Change of Length." *The Journal of Physiology* 117 (1): 77–86.

Abd-El-Malek, S. 1955. "The Part Played by the Tongue in Mastication and Deglutition." *Journal of Anatomy* 89 (2): 250–54.

Aerts, P. 1998. "Vertical Jumping in Galago Senegalensis: The Quest for an Obligate Mechanical Power Amplifier." *Philosophical Transactions of the Royal Society B: Biological Sciences* 353 (1375): 1607–20.

Ahn, A. N., R. J. Monti, and A. A. Biewener. 2003. "In Vivo and in Vitro Heterogeneity of Segment Length Changes in the Semimembranosus Muscle of the Toad." *The Journal of Physiology* 549 (3): 877–88.

Aiello, B. R., H. M. King, and M. E. Hale. 2014. "Functional Subdivision of Fin Protractor and Retractor Muscles Underlies Pelvic Fin Walking in the African Lungfish (*Protopterus Annectens*)." *Journal of Experimental Biology* 217 (19): 3474–82.

Aiello, B. R., R. W. Blob, and M. T. Butcher. 2013. "Correlation of Muscle Function and Bone Strain in the Hindlimb of the River Cooter Turtle (*Pseudemys Concinna*)." *Journal of Morphology* 274 (9): 1060–69.

Aiello, B. R., M. W. Westneat, and M. E. Hale. 2017. "Mechanosensation Is Evolutionarily Tuned to Locomotor Mechanics." *Proceedings of the National Academy of Sciences* 114 (17): 4459–64.

Aiello, L., and C. Dean. 2002. *An Introduction to Human Evolutionary Anatomy*. London, UK: Elsevier Academic Press.

Alemseged, Z., F. Spoor, W. H. Kimbel, R. Bobe, D. Geraads, D. Reed, and J. G. Wynn. 2006. "A Juvenile Early Hominin Skeleton from Dikika, Ethiopia." *Nature* 443 (7109): 296–301.

Allen, J. E., C. J. White, R. J. Leonard, P. C. Belafsky. 2010. "Prevalence of Penetration and Aspiration on Videofluoroscopy in Normal Individuals without Dysphagia." *Otolaryngology—Head and Neck Surgery* 142: 208–13.

Altringham, J. D., and D. J. Ellerby. 1999. "Fish Swimming: Patterns in Muscle Function." *The Journal of Experimental Biology* 202 (23): 3397–3403.

Anapol, F., and K. Barry. 1996a. "Fiber Architecture of the Extensors of the Hindlimb in Semiterrestrial and Arboreal Guenons." *American Journal of Physical Anthropology* 99 (3): 429–47.

Anapol, F., and J. P. Gray. 2003. “Fiber Architecture of the Intrinsic Muscles of the Shoulder and Arm in Semiterrestrial and Arboreal Guenons.” *American Journal of Physical Anthropology* 122 (1): 51–65.

Anderson, C. V. 2016. “Off like a Shot: Scaling of Ballistic Tongue Projection Reveals Extremely High Performance in Small Chameleons.” *Scientific Reports* 6: 18625.

Anderson, C. V, and S. M Deban. 2010. “Ballistic Tongue Projection in Chameleons Maintains High Performance at Low Temperature.” *Proceedings of the National Academy of Sciences* 107 (12): 5495–99.

Arce-McShane, F. I., C. F. Ross, K. Takahashi, B. J. Sessle, and N. G. Hatsopoulos. 2016. “Primary Motor and Sensory Cortical Areas Communicate via Spatiotemporally Coordinated Networks at Multiple Frequencies.” *Proceedings of the National Academy of Sciences* 113 (18): 5083–88.

Arce-McShane, F. I., N. G. Hatsopoulos, J. C. Lee, C. F. Ross, and B. J. Sessle. 2014. “Modulation Dynamics in the Orofacial Sensorimotor Cortex during Motor Skill Acquisition.” *The Journal of Neuroscience* 34 (17): 5985–97.

Arensburg, B., L. A. Schepartz, A. M. Tillier, B. Vander-Meersch, and Y. Rak. 1990. “A Reappraisal of the Anatomical Basis for Speech in Middle Palaeolithic Hominids.” *American Journal of Physical Anthropology* 83: 137–46.

Arensburg, B., A. M. Tillier, B. Vasndermeersch, H. Duday, L. A. Schepartz, and Y. Rak. 1989. “A Middle Palaeolithic Human Hyoid Bone.” *Nature* 338: 758–60.

Arnold, E. M., S. R. Hamner, A. Seth, M. Millard, and S. L. Delp. 2013. “How Muscle Fiber Lengths and Velocities Affect Muscle Force Generation as Humans Walk and Run at Different Speeds.” *Journal of Experimental Biology* 216 (11): 2150–60.

Astley, H. C., and T. J. Roberts. 2014. “The Mechanics of Elastic Loading and Recoil in Anuran Jumping.” *Journal of Experimental Biology* 217 (24): 4372–78.

Astley, H. C, and T. J.Roberts. 2012. “Evidence for a Vertebrate Catapult: Elastic Energy Storage in the Plantaris Tendon during Frog Jumping.” *Biology Letters* 8 (3): 386–89.

Ateş, F., F. Hug, K. Bouillard, M. Jubeau, T. Frappart, M. Couade, J. Bercoff, and A. Nordez. 2015. “Muscle Shear Elastic Modulus Is Linearly Related to Muscle Torque over the Entire Range of Isometric Contraction Intensity.” *Journal of Electromyography and Kinesiology* 25 (4): 703–8.

Azizi, E., and E. L. Brainerd. 2007. “Architectural Gear Ratio and Muscle Fiber Strain Homogeneity in Segmented Musculature.” *Journal of Experimental Zoology Part A:*

Ecological and Integrative Physiology 307A: 145–55.

Azizi, E., E. L. Brainerd, and T. J. Roberts. 2008. "Variable Gearing in Pennate Muscles." *Proceedings of the National Academy of Sciences* 105 (5): 1745–50.

Azizi, E., and T. J. Roberts. 2014. "Geared up to Stretch: Pennate Muscle Behavior during Active Lengthening." *The Journal of Experimental Biology* 217 (3): 376–81.

Ballester, A., F. Gould, L. Bond, B. Stricklen, J. Ohlemacher, A. Gross, K. DeLozier, R. Buddington, K. Buddington, N. Danos, and R. Z. German. 2018. "Maturation of the Coordination Between Respiration and Deglutition with and Without Recurrent Laryngeal Nerve Lesion in an Animal Model." *Dysphagia* In press.

Barnes, G. R. G., and D. N. Pinder. 1974. "In Vivo Tendon Tension and Bone Strain Measurement and Correlation." *Journal of Biomechanics* 7 (1): 35–42.

Baudon, J. J., F. Renault, J. M. Goutet, V. Biran-Mucignat, G. Morgant, E. N. Garabedian, and M. P. Vazquez. 2009. "Assessment of Dysphagia in Infants with Facial Malformations." *European Journal of Pediatrics* 168 (2): 187–93.

Beckhardt, R. N., J. G. Murray, C. N. Ford, J. E. Grossman, and J. H. Brandenburg. 1994. "Factors Influencing Functional Outcome in Supraglottic Laryngectomy." *Head & Neck* 16 (3): 232–39.

Benninghoff, A, and H. Rollhaeser. 1952. "Zur Inneren Mechanik Des Gefiederten Muskels" *Pflüger's Archiv für die gesamte Physiologie des Menschen und der Tiere* 254 (6): 527–48.

Bensamoun, S. F., S. I. Ringleb, L. Littrell, Q. Chen, M. Brennan, R. L. Ehman, and K. Nan An. 2006. "Determination of Thigh Muscle Stiffness Using Magnetic Resonance Elastography." *Journal of Magnetic Resonance Imaging* 23 (2): 242–47.

Bernstein, N. 1967. *The Co-Ordination and Regulation of Movements*. Oxford, NY: Pergamon Press.

Biewener, A. A. 1990. "Biomechanics of Mammalian Terrestrial Locomotion." *Science* 250 (4984): 1097–1103.

Biewener, A. A., C. T. Farley, T. J. Roberts, and M. Temaner. 2004. "Muscle Mechanical Advantage of Human Walking and Running: Implications for Energy Cost." *Journal of Applied Physiology* 97: 2266–74.

Biewener, A. A. 1989. "Scaling Body Support in Mammals: Limb Posture and Muscle Mechanics." *Science* 245 (4913): 45–48.

Biewener, A. A., W. R. Corning, and B. W. Tobalske. 1998. "In Vivo Pectoralis Muscle Force-

Length Behavior during Level Flight in Pigeons (*Columba Livia*)." *The Journal of Experimental Biology* 201: 3293–3307.

Biewener, A. A. 1992. *Biomechanics—Structures and Systems: A Practical Approach*. Oxford: Oxford University Press.

Biewener, A. A., D. D. Konieczynski, and R. V. Baudinette. 1998. "In Vivo Muscle Force-Length Behavior during Steady-Speed Hopping in Tammar Wallabies." *The Journal of Experimental Biology* 201: 1681–94.

Bilsborough, A., and B. A. Wood. 1988. "Cranial Morphometry of Early Hominids: Facial Region." *American Journal of Physical Anthropology* 76 (61–86).

Bock, W. J., and C. R. Shear. 1972. "A Staining Method for Gross Dissection of Vertebrate Muscles." *Anatomischer Anzeiger* 130: 222-227.

Boë, L. J., F. Berthommier, T. Legou, G. Captier, C. Kemp, T. R. Sawallis, Y. Becker, A. Rey, and J. Fagot. 2017. "Evidence of a Vocalic Proto-System in the Baboon (*Papio Papio*) Suggests Pre-Hominin Speech Precursors." *PLOS ONE* 12 (1): e0169321.

Borges, N. C., J. R. B. Nardotto, R. S. L. Oliveira, L. H. E. Rüncos, R. G. Ribeiro, and A. M. Bogoevich. 2017. "Anatomy Description of Cervical Region and Hyoid Apparatus in Living Giant Anteaters Myrmecophaga Tridactyla Linnaeus, 1758." *Pesquisa Veterinária Brasileira* 37 (11): 1345–51.

Bouillard, K., A. Nordez, and F. Hug. 2011. "Estimation of Individual Muscle Force Using Elastography." *PLOS ONE* 6 (12): e29261.

Bowie, J. D., and M. R. Clair. 1982. "Fetal Swallowing and Regurgitation: Observation of Normal and Abnormal Activity." *Radiology* 144(4): 877–78.

Brainerd, E. L., and E. Azizi. 2005. "Muscle Fiber Angle, Segment Bulging and Architectural Gear Ratio in Segmented Musculature." *The Journal of Experimental Biology* 208 (17): 3249–61.

Brainerd, E. L., D. B. Baier, S. M. Gatesy, T. L. Hedrick, K. A. Metzger, S. L. Gilbert, and J. J. Crisco. 2010. "X-Ray Reconstruction of Moving Morphology (XROMM): Precision, Accuracy and Applications in Comparative Biomechanics Research." *Journal of Experimental Zoology. Part A, Ecological Genetics and Physiology* 313 (5): 262–79.

Breik, O., K. Umapathysivam, D. Tivey, and P. Anderson. 2016. "Feeding and Reflux in Children after Mandibular Distraction Osteogenesis for Micrognathia: A Systematic Review." *International Journal of Pediatric Otorhinolaryngology* 85: 128–35.

Burkhead, L. M., C. M. Sapienza, and J. C. Rosenbek. 2007. "Strength-Training Exercise in

Dysphagia Rehabilitation: Principles, Procedures, and Directions for Future Research." *Dysphagia* 22 (3): 251–65.

Burkholder, T. J., and R. L. Lieber. 2001. "Sarcomere Length Operating Range of Vertebrate Muscles during Movement." *The Journal of Experimental Biology* 204 (9): 1529–36.

Butler, S. G., A. Stuart, L. Markley, C. Rees. 2009. "Penetration and Aspiration in Healthy Older Adults as Assessed During Endoscopic Evaluation of Swallowing." *Annals of Otology, Rhinology & Laryngology* 118 (3): 190–8.

Butler, S.G. A. Stuart, X. Leng, C. Rees, J. Williamson, S. B. Kritchevsky. 2010. "Factors Influencing Aspiration During Swallowing in Healthy Older Adults." *The Laryngoscope* 120: 2147–52.

Butterfield, T. A. 2005. "Differential Serial Sarcomere Number Adaptations in Knee Extensor Muscles of Rats Is Contraction Type Dependent." *Journal of Applied Physiology* 99 (4): 1352–58.

Butterfield, T. A., T. R. Leonard, and W. Herzog. 2005. "Differential Serial Sarcomere Number Adaptations in Knee Extensor Muscles of Rats Is Contraction Type Dependent." *Journal of Applied Physiology* 99 (4): 1352–58.

Camp, A. L., H. C. Astley, A. M. Horner, T. J. Roberts, and E. L. Brainerd. 2016. "Fluoromicrometry: A Method for Measuring Muscle Length Dynamics with Biplanar Videofluoroscopy." *Journal of Experimental Zoology Part A: Ecological Genetics and Physiology* 325 (7): 399–408.

Camp, A. L., and E. L. Brainerd. 2014. "Role of Axial Muscles in Powering Mouth Expansion during Suction Feeding in Largemouth Bass (Micropterus Salmoides)." *The Journal of Experimental Biology* 217 (December): 1333–45.

———. 2015. "Reevaluating Musculoskeletal Linkages in Suction-Feeding Fishes with X-Ray Reconstruction of Moving Morphology" *Integrative and Comparative Biology* 55 (1): 36–47.

Camp, A. L., T. J. Roberts, and E. L. Brainerd. 2015. "Swimming Muscles Power Suction Feeding in Largemouth Bass." *Proceedings of the National Academy of Sciences* 112 (28): 8690–95.

Carrier, D. R., C. S. Gregersen, and N. A. Silverton. 1998. "Dynamic Gearing in Running Dogs." *The Journal of Experimental Biology* 201 (23): 3185–95.

Carrier, D. R., N. C. Heglund, and K. D. Earls. 1994. "Variable Gearing during Locomotion in the Human Musculoskeletal System." *Science* 265 (5172): 651–53.

Casali, D. M., A. Perini. 2017. “The Evolution of Hyoid Apparatus in Xenarthra (Mammalia: Eutheria).” *Historical Biology* 29 (6): 777–88.

Cavagna, G. A., and G. Citterio. 1974. “Effect of Stretching on the Elastic Characteristics and the Contractile Component of Frog Striated Muscle.” *The Journal of Physiology* 239 (1): 1–14.

Cavagna, G. A., B. Dusman, and R. Margaria. 1968. “Positive Work Done by a Previously Stretched Muscle.” *Journal of Applied Physiology* 24 (1): 21–32.

Cavanagh, P. R., and P. V. Komi. 1979. “Electromechanical Delay in Human Skeletal Muscle under Concentric and Eccentric Contractions.” *European Journal of Applied Physiology and Occupational Physiology* 42 (3): 159–63.

Chapman, H. C. 1880. “On the Structure of the Orang Outang.” *Proceedings of the Academy of Natural Sciences of Philadelphia* 32: 160–75.

Charles, J. P., O. Cappellari, A. J. Spence, J. R. Hutchinson, and Dominic J. Wells. 2016. “Musculoskeletal Geometry, Muscle Architecture and Functional Specialisations of the Mouse Hindlimb.” *PLOS ONE* 11 (4): 1–22.

Charles, J. P., Ornella Cappellari, A. J. Spence, D. J. Wells, and J. R. Hutchinson. 2016. “Muscle Moment Arms and Sensitivity Analysis of a Mouse Hindlimb Musculoskeletal Model.” *Journal of Anatomy* 229 (4): 514–35.

Charlton, B. D, W. A. H. Ellis, A. J. McKinnon, G. J. Cowin, J. Brumm, K. Nilsson, and W. T. Fitch. 2011. “Cues to Body Size in the Formant Spacing of Male Koala (*Phascolarctos Cinereus*) Bellows: Honesty in an Exaggerated Trait,” *The Journal of Experimental Biology* 214: 3414–22.

Charlton, B. D., R. Frey, A. J, McKinnon, G. Fritsch, W. T. Fitch, and D. Reby. 2013. “Koalas Use a Novel Vocal Organ to Produce Unusually Low-Pitched Mating Calls.” *Current Biology* 23: R1035-6.

Chen, P. H., J. S. Golub, E. R. Hapner, and M. M. Johns. 2009. “Prevalence of Perceived Dysphagia and Quality-of-Life Impairment in a Geriatric Population.” *Dysphagia* 24 (1): 1–6.

Cheng, S., S. C. Gandevia, M. Green, R. Sinkus, and L. E. Bilston. 2011. “Viscoelastic Properties of the Tongue and Soft Palate Using MR Elastography.” *Journal of Biomechanics* 44 (3): 450–54.

Chi-Fishman, G., and B. C. Sonies. 2002. “Effects of Systematic Bolus Viscosity and Volume Changes on Hyoid Movement Kinematics.” *Dysphagia* 17 (4): 278–87.

Clarkson, P. M., and M. J. Hubal. 2002. “Exercise-Induced Muscle Damage in Humans.” *American Journal of Physical Medicine & Rehabilitation* 81 (11): S52–69.

Cook, I. J., W. J. Dodds, R. O. Dantas, B. Massey, M. K. Kern, I. M. Lang, J. G. Brasseur, and W. J. Hogan. 1989. “Opening Mechanisms of the Human Upper Esophageal Sphincter.” *The American Journal of Physiology-Gastrointestinal and Liver Physiology* 257 (5): G748-59.

Cox, P. G., and N. Jeffery. 2011. “Reviewing the Morphology of the Jaw-Closing Musculature in Squirrels, Rats, and Guinea Pigs with Contrast-Enhanced MicroCt.” *The Anatomical Record* 294 (6): 915–28.

Cox, P. G., and C. G. Faulkes. 2014. “Digital Dissection of the Masticatory Muscles of the Naked Mole-Rat, Heterocephalus Glaber (Mammalia, Rodentia).” *PeerJ* 2: e448.

Coyle, E. F., D. C. Feiring, T. C. Rotkis, R. W. Cote, F. B. Roby, W. Lee, and J. H. Wilmore. 1981. “Specificity of Power Improvements through Slow and Fast Isokinetic Training.” *Journal of Applied Physiology* 51 (6): 1437–42.

Crelin, ES. 1969. *Anatomy of the Newborn: An Atlas*. Philadelphia: Lea & Febiger.

———. 1973. *Functional Anatomy of the Newborn*. Yale University Press.

Crompton, A. W., R. Z. German, and A. J. Thexton. 1997. “Mechanisms of Swallowing and Airway Protection in Infant Mammals (*Sus domesticus* and *Macaca fascicularis*).” *Journal of Zoology* 241 (1): 89–102.

Currey, JD. 2013. *Bones: Structure and Mechanics*. Princeton University Press.

Daegling, D. J. 1993. “Functional Morphology of the Human Chin.” *Evolutionary Anthropology* 1 (5): 170–77.

———. 2001. “Biomechanical Scaling of the Hominoid Mandibular Symphysis.” *Journal of Morphology* 23: 12–23.

Daegling, D. J. 2012. “The Human Mandible and the Origins of Speech.” *Journal of Anthropology* 2012: 1–14.

Daggett, A., J. Logemann, A. Rademaker, B. Pauloski. 2006. “Laryngeal Penetration During Deglutition in Normal Subjects of Various Ages.” *Dysphagia* 21 (4): 270–4.

Dantas, R. O., W. J. Dodds, Benson T. M., R. Shaker, and I. J. Cook. 1990. “Manometric Characteristics of Glossopalatal Sphincter.” *Digestive Diseases and Sciences* 35 (2): 161–66.

Darwin, C. 1859. *On the Origin of Species by Means of Natural Selection, or the Preservation of Favoured Races in the Struggle for Life*. London: Murray.

Daegling, D. J. 2012. "The Human Mandible and the Origins of Speech". *Journal of Anthropology* 2012: 1-14.

Deban, S. M., J. C. O'Reilly, U. Dicke, and J. L. van Leeuwen. 2007. "Extremely High-Power Tongue Projection in Plethodontid Salamanders." *The Journal of Experimental Biology* 210 (4): 655–67.

De Brito Fontana, H., and W. Herzog. 2016. "Vastus Lateralis Maximum Force-Generating Potential Occurs at Optimal Fascicle Length regardless of Activation Level." *European Journal of Applied Physiology* 116 (6): 1267–77.

Dejaeger, E., W. Pelemans, E. Ponette, and E. Joosten. 1997. "Mechanisms Involved in Postdeglutition Retention in the Elderly." *Dysphagia* 12 (2): 63–67.

Demes, B., and N. Creel. 1988. "Bite Force, Diet, and Cranial Morphology of Fossil Hominids." *Journal of Human Evolution* 17 (7): 657–70.

Denny, M. 2016. *Ecological Mechanics: Principles of Life's Physical Interactions*. Princeton, NJ: Princeton University Press.

Deun, B. V., J. S. M. Hobbelen, B. Cagnie, B. Van Eetvelde, N. Van Den Noortgate, and D. Cambier. In press. "Reproducible Measurements of Muscle Characteristics Using the MyotonPRO Device." *Journal of Geriatric Physical Therapy*, in press.

Dick, T. J. M., A. A. Biewener, and J. M. Wakeling. 2017. "Comparison of Human Gastrocnemius Forces Predicted by Hill-Type Muscle Models and Estimated from Ultrasound Images." *The Journal of Experimental Biology* 220: 1643-1653.

Dick, T. J. M., A. S. Arnold, and J. M. Wakeling. 2016. "Quantifying Achilles Tendon Force *In Vivo* from Ultrasound Images." *Journal of Biomechanics* 49 (14): 3200–3207.

Dickinson, E., H. Stark, and K. Kupczik. 2018. "Non-Destructive Determination of Muscle Architectural Variables Through the Use of DiceCT." *The Anatomical Record* 301 (2): 363–77.

Dickinson, M. H., C. T. Farley, R. J. Full, M. A. R. Koehl, R. Kram, and S. Lehman. 2000. "How Animals Move: An Integrative View." *Science* 288 (5463): 100–106.

Diogo, R., J. M. Potau, J. F. Pastor, F. J. de Paz, E. M. Ferrero, G. Bello, M. Barbosa, B. A. Wood. 2011. *Photographic and Descriptive Musculoskeletal Atlas of Gorilla: With Notes on the Attachments, Variations, Innervation, Synonymy and Weight of the Muscles.* Enfield, NH: Science Publishers.

Diogo, R., J. M. Potau, J. F. Pastor, F. J. de Paz, E. M. Ferrero, G. Bello, M. Barbosa, M. A. Aziz, A. M. Burrows, J. Arias-Martorell, B. A. Wood. 2012. *Photographic and Descriptive Musculoskeletal Atlas of Gibbons and Siamangs (Hylobates): With Notes on the Attachments, Variations, Innervation, Synonymy and Weight of the Muscles.* Enfield, NH: Science Publishers.

Diogo, R., J. M. Potau, J. F. Pastor, F. J. de Paz, E. M. Ferrero, G. Bello, M. Barbosa, M. A. Aziz, A. M. Burrows, J. Arias-Martorell, B. A. Wood. 2013a. *Photographic and Descriptive Musculoskeletal Atlas of Chimpanzees: With Notes on the Attachments, Variations, Innervation, Function and Synonymy and Weight of the Muscles.* Boca Raton, FL: CRC Press.

Diogo, R., J. M. Potau, J. F. Pastor, F. J. de Paz, E. M. Ferrero, G. Bello, M. Barbosa, M. A. Aziz, J. Arias-Martorell, B. A. Wood. 2013b. *Photographic and Descriptive Musculoskeletal Atlas of Orangutans: With Notes on the Attachments, Variations, Innervation, Function and Synonymy and Weight of the Muscles.* Boca Raton, FL: CRC Press.

Dobson, S. D., and E. Trinkaus. 2002. "Cross-Sectional Geometry and Morphology of the Mandibular Symphysis in Middle and Late Pleistocene Homo." *Journal of Human Evolution* 43: 67–87.

Dodds, J., I. J. Cook, P. J. Kahrilas, E. T. Stewart, and M. K. Kern. 1988. "Influence of Bolus Volume on Swallow-Induced Hyoid Movement in Normal Subjects." *American Journal of Roentgenology*, 150: 1307–9.

Doeltgen, S. H., E. Ong, I. Scholten, C. Cock, and T. Omari. 2017. "Biomechanical Quantification of Mendelsohn Maneuver and Effortful Swallowing on Pharyngoesophageal Function." *Otolaryngology - Head and Neck Surgery* 157 (5): 816–23.

Doran, G. A., and H. Baggett. 1970. "The Vascular Stiffening Mechanism in the Tongue of the Echidna (*Tachyglossus aculeatus*)." *The Anatomical Record* 167 (2): 197–204.

Doran, A. G., and H. Baggett. 1971. "A Structural and Functional Classification of Mammalian Tongues." *Journal of Mammalogy* 52 (2): 427–29.

Doty, Robert W, and J. F Bosma. 1956. "An Electromyographic Analysis of Reflex Deglutition." *Journal of Neurophysiology* 19 (1): 44–60.

DuBrul, E. L., and H. Sicher. 1954. *The Adaptive Chin*. Springfield, IL: Charles C. Thomas.

Duchateau, J., and K. Hainaut. 1984. "Isometric or Dynamic Training: Differential Effects on Mechanical Properties of a Human Muscle." *Journal of Applied Physiology: Respiratory, Environmental and Exercise Physiology* 56 (2): 296–301.

Dunn, J. C., L. B. Halenar, T. G. Davies, J. Cristobal-Azkarate, D. Reby, D. Sykes, S. Dengg, W. T. Fitch, and L. A. Knapp. 2015. "Evolutionary Trade-off between Vocal Tract and Testes Dimensions in Howler Monkeys." *Current Biology* 25 (21): 2839–44.

Edgerton, V. R., J. L. Smith, and D. R. Simpson. 1975. "Muscle Fibre Type Populations of Human Leg Muscles." *The Histochemical Journal* 7 (3): 259–66.

Edman, K., C. Caputo, and F. Lou. 1993. "Depression of Tetanic Force Induced by Loaded Shortening of Frog Muscle Fibres." *Journal of Physiology* 466: 535–52.

Edman, K., G. Elzinga, and M. Noble. 1978. "Enhancement of Mechanical Performance by Stretch during Tetanic Contractions of Vertebrate Skeletal Muscle Fibres." *The Journal of Physiology* 281: 139–55.

Elder, Pliny the. 1855. *The Natural History, Book XI*. Edited by J Bostock and HT Riley. London, UK: Taylor & Francis.

Eng, C. M., S. R. Ward, C. J. Vinyard, and A. B. Taylor. 2009. "The Morphology of the Masticatory Apparatus Facilitates Muscle Force Production at Wide Jaw Gapes in Tree-Gouging Common Marmosets (*Callithrix jacchus*)." *Journal of Experimental Biology* 212 (24): 4040–55.

Eng, C. M., D. E. Lieberman, Katherine D. Zink, and Michael A. Peters. 2013. "Bite Force and Occlusal Stress Production in Hominin Evolution." *American Journal of Physical Anthropology* 151 (4): 544–57.

Falk, D. 1973. "Comparative Anatomy of the Larynx in Man and the Chimpanzee : Implications for Language in Neanderthal." *American Journal of Physical Anthropology* 43: 123–32.

Felder, A., S. R. Ward, and R. L. Lieber. 2005. "Sarcomere Length Measurement Permits High Resolution Normalization of Muscle Fiber Length in Architectural Studies." *The Journal of Experimental Biology* 208 (17): 3275–79.

Felton, S. M., T. A Gaige, T. G. Reese, V. J. Wedeen, and R. J. Gilbert. 2007. "Mechanical Basis for Lingual Deformation during the Propulsive Phase of Swallowing as Determined by Phase-Contrast Magnetic Resonance Imaging." *Journal of Applied Physiology* 103 (1): 255–65.

Feng, X., M. S. Cartwright, F. O. Walker, J. H. Bargoil, Y. Hu, and S. G. Butler. 2015. "Ultrasonographic Evaluation of Geniohyoid Muscle and Hyoid Bone during Swallowing in Young Adults." *Laryngoscope* 125 (8): 1886–91.

Finni, T., P. V. Komi, and J. Lukkariniemi. 1998. "Achilles Tendon Loading during Walking: Application of a Novel Optic Fiber Technique." *European Journal of Applied Physiology*

and Occupational Physiology 77 (3): 289–91.

Finni, T., P. V. Komi, and V. Lepola. 2000. "In Vivo Human Triceps Surae and Quadriceps Femoris Muscle Function in a Squat Jump and Counter Movement Jump." *European Journal of Applied Physiology* 83 (4–5): 416–26.

Fitch, W. T., B. De Boer, N. Mathur, and A. A. Ghazanfar. 2016. "Monkey Vocal Tracts Are Speech-Ready." *Science Advances* 2: e1600723.

Fitch, W. T., and D. Reby. 2001. "The Descended Larynx Is Not Uniquely Human." *Proceedings of the Royal Society B: Biological Sciences* 268: 1669–75.

Flores, T. C., B. G. Wood, L. Koegel, H. L. Levine, and H. M. Tucker. 1982. "Factors in Successful Deglutition Following Supraglottic Laryngeal Surgery." *Annals of Otology, Rhinology & Laryngology* 91 (6): 579–83.

Franks, H. A., R. Z. German, A. W. Crompton, and K. M. Hiiemae. 1985. "Mechanism of Intra-Oral Transport in a Herbivore, the Hyrax (*Procavia syriacus*)." *Archives of Oral Biology* 30 (7): 539–44.

Franks, H. A., A. W. Crompton, and R. Z. German. 1984. "Mechanism of Intraoral Transport in Macaques." *American Journal of Physical Anthropology* 65 (3): 275–82.

Franks, H. A., A. W. Crompton, and R. Z. German. 1984. "Mechanism of Intraoral Transport in Macaques." *American Journal of Physical Anthropology* 65 (3): 275–82.

Frey, R., A. Gebler, K. A. Olson, D. Odonkhuu, G. Fritsch, N. Batsaikhan, and I. W. Stuermer. 2008. "Mobile Larynx in Mongolian Gazelle: Retraction of the Larynx During Rutting Barks in Male Mongolian Gazelle (*Procapra gutturosa* PALLAS, 1777)." *Journal of Morphology* 269: 1223–37.

Fujiu, M., J. A. Logemann, and B. R. Pauloski. 1995. "Increased Postoperative Posterior Pharyngeal Wall Movement in Patients With Anterior Oral Cancer." *American Journal of Speech-Language Pathology* 4: 24–30.

Gans, C.. 1982. "Fiber Architecture and Muscle Function." *Exercise and Sport Sciences Reviews* 10 (1): 160–207.

Gans, C., and W. J. Bock. 1965. "The Functional Significance of Muscle Architecture – a Theoretical Analysis." *Ergebnisse Der Anatomie Und Entwicklungsgeschichte* 38: 115–42.

Gans, C., and A. S. Gaunt. 1991. "Muscle Architecture in Relation to Function." *Journal of Biomechanics* 24 (S1): 53–65.

Gans, C., and F. de Vree. 1987. "Functional Bases of Fiber Length and Angulation in Muscle."

Journal of Morphology 192 (1): 63–85.

García-Peris, P., L. Parón, C. Velasco, C. de la Cuerda, M. Camblor, I. Bretón, H. Herencia, J. Verdaguer, C. Navarro, and P. Clave. 2007. "Long-Term Prevalence of Oropharyngeal Dysphagia in Head and Neck Cancer Patients: Impact on Quality of Life." *Clinical Nutrition* 26 (6): 710–17.

Garland Jr., T. and Adolph, S. C., 1994. "Why not to do two-species comparative studies: limitations on inferring adaptation." *Physiological Zoology* 67 (4): 797–828.

Gasser, H. S., and A. V. Hill. 1924. "The Dynamics of Muscular Contraction." *Proceedings of the Royal Society B* 96 (678): 398–437.

Gassert, R. B., and W. G. Pearson Jr. 2016. "Evaluating Muscles Underlying Tongue Base Retraction in Deglutition Using Muscular Functional Magnetic Resonance Imaging (mfMRI)." *Magnetic Resonance Imaging* 34 (2): 204–8.

Genden, E. M., A. Ferlito, C. E. Silver, A. S. Jacobson, J. A. Werner, C. Suárez, C. René Leemans, P. J. Bradley, and A. Rinaldo. 2007. "Evolution of the Management of Laryngeal Cancer." *Oral Oncology* 43 (5): 431–39.

German, R. Z., A. W. Crompton, and A. J. Thexton. 1998. "The Coordination and Interaction between Respiration and Deglutition in Young Pigs." *Journal of Comparative Physiology A: Sensory, Neural, and Behavioral Physiology* 182 (4): 539–47.

German, R. Z., A. W. Crompton, L. C. Levitch, and A. J. Thexton. 1992. "The Mechanism of Suckling in Two Species of Infant Mammal: Miniature Pigs and Long-Tailed Macaques." *The Journal of Experimental Zoology* 261 (3): 322–30.

German, R. Z., S. A. Saxe, A. W. Crompton, and K. M. Hiiemae. 1989. "Food Transport through the Anterior Oral Cavity in Macaques." *American Journal of Physical Anthropology* 80: 369–77.

German, R. Z., R. Campbell-Malone, A. W. Crompton, P. Ding, S. Holman, N. Konow, and A. J. Thexton. 2011. "The Concept of Hyoid Posture." *Dysphagia* 26 (2): 97–98.

German, R. Z., A. W. Crompton, and A. J Thexton. 2009. "Integration of the Reflex Pharyngeal Swallow into Rhythmic Oral Activity in a Neurologically Intact Pig Model." *Journal of Neurophysiology* 102 (2): 1017–25.

Gewolb, I. H., and F. L. Vice. 2006. "Maturational Changes in the Rhythms, Patterning, and Coordination of Respiration and Swallow during Feeding in Preterm and Term Infants." *Developmental Medicine and Child Neurology* 48 (7): 589–94.

Gidmark, N. J., N. Konow, E. Lopresti, and E. L. Brainerd. 2013. "Bite Force Is Limited by the

Force-Length Relationship of Skeletal Muscle in Black Carp, *Mylopharyngodon piceus*." *Biology Letters* 9 (2): 20121181.

Gignac, P. M., and G. M. Erickson. 2017. "The Biomechanics Behind Extreme Osteophagy in Tyrannosaurus Rex." *Scientific Reports* 7 (1): 2012.

Gignac, P. M., and Nathan J. Kley. 2014. "Iodine-Enhanced Micro-CT Imaging: Methodological Refinements for the Study of the Soft-Tissue Anatomy of Post-Embryonic Vertebrates." *Journal of Experimental Zoology Part B: Molecular and Developmental Evolution* 322: 166–76.

Gignac, P. M., N. J. Kley, J. A. Clarke, M. W. Colbert, A. C. Morhardt, D. Cerio, I. N. Cost, P. G. Cox, J. D. Daza, C. M. Early, M. S. Echols, R. M. Henkelman, A. N. Herdina, C. M. Holliday, Z. Li, K. Mahlow, S. Merchant, J. Müller, C. P. Orsbon, D. J. Paluh, M. L. Thies, H. P. Tsai, L. M. Witmer. 2016. "Diffusible Iodine-Based Contrast-Enhanced Computed Tomography (diceCT): An Emerging Tool for Rapid, High-Resolution, 3-D Imaging of Metazoan Soft Tissues." *Journal of Anatomy* 228 (6): 889-909.

Gilbert, R. J., V. J. Napadow, T. A. Gaige, and V. J. Wedeen. 2007. "Anatomical Basis of Lingual Hydrostatic Deformation." *The Journal of Experimental Biology* 210 (23): 4069–82.

Godinho, R. M., L. C. Fitton, V. Toro-Ibacache, C. B. Stringer, R. S. Lacruz, T. G. Bromage, and P. O'Higgins. 2018. "The Biting Performance of Homo Sapiens and Homo Heidelbergensis." *Journal of Human Evolution* 118: 56–71.

Gonzalez, R. V., T. S. Buchanan, and S. L. Delp. 1997. "How Muscle Architecture and Moment Arms Affect Wrist Flexion-Extension Moments." *Journal of Biomechanics* 30 (7): 705–12.

Gordon, A. M., A. F. Huxley, and F. J. Julian. 1966. "The Variation in Isometric Tension with Sarcomere Length in Vertebrate Muscle Fibres." *The Journal of Physiology* 184 (1): 170–92.

Gordon, J. E. 1981. *Structures, or Why Things Don't Fall down*. New York, NY: Da Capo Press.

Gould, F. D. H., A. R. Lammers, J. Ohlemacher, A. Ballester, L. Fraley, A. Gross, R. Z. German. 2015. "The Physiologic Impact of Unilateral Recurrent Laryngeal Nerve (RLN) Lesion on Infant Oropharyngeal and Esophageal Performance." *Dysphagia* 30 (6): 714–22.

Gould, F. D. H., B. Yglesias, J. Ohlemacher, R. Z. German. 2016. "Pre-pharyngeal Swallow Effects of Recurrent Laryngeal Nerve Lesion on Bolus Shape and Airway Protection in an Infant Pig Model." *Dysphagia* 32 (3): 362–73.

Gregor, R. J., R. R. Roy, W. C. Whiting, R. G. Lovely, J. A. Hodgson, and V. R. Edgerton. 1988. "Mechanical Output of the Cat Soleus during Treadmill Locomotion: *In vivo* vs *in situ*

Characteristics." *Journal of Biomechanics* 21 (9): 721–32.

Groening, F., J. Liu, M. J. Fagan, and P. O'Higgins. 2011. "Why Do Humans Have Chins? Testing the Mechanical Significance of Modern Human Symphyseal Morphology with Finite Element Analysis." *American Journal of Physical Anthropology* 144 (4): 593–606.

Gross, A., J. Ohlemacher, R. Z. German, and F. Gould. 2018. "LVC Timing in Infant Pig Swallowing and the Effect of Safe Swallowing." *Dysphagia* 33 (1): 51–62.

Grosset, J. F., J. Piscione, D. Lambertz, and C. Pérot. 2009. "Paired Changes in Electromechanical Delay and Musculo-Tendinous Stiffness after Endurance or Plyometric Training." *European Journal of Applied Physiology* 105 (1): 131–39.

Guelfguat, M., N. Nurbhai, and N. Solounias. 2001. "Median Accessory Digastric Muscle: Radiological and Surgical Correlation." *Clinical Anatomy* 14 (1): 42–46.

Gür, H., N. Çakin, B. Akova, E. Okay, and S. Küçükoğlu. 2002. "Concentric versus Combined Concentric-Eccentric Isokinetic Training: Effects on Functional Capacity and Symptoms in Patients with Osteoarthrosis of the Knee." *Archives of Physical Medicine and Rehabilitation* 83 (3): 308–16.

Hamlet, S., R. Mathog, S. Fleming, L. Jones, and J. Muz. 1990. "Modification of compensatory swallowing in a supraglottic laryngectomy patient." *Head & Neck* 12: 131–36.

Hamlet, S., L. Jones, R. Patterson, G. Michou, and C. Cislo. 1991. "Swallowing Recovery Following Anterior Tongue and Floor of Mouth Surgery." *Head & Neck* 13 (4): 334–39.

Harper, C. J., S. M. Swartz, and E. L. Brainerd. 2013. "Specialized Bat Tongue Is a Hemodynamic Nectar Mop" *Proceedings of the National Academy of Sciences* 110 (22): 8852–7.

Hartstone-Rose, A., J. M. G. Perry, and C. J. Morrow. 2012. "Bite Force Estimation and the Fiber Architecture of Felid Masticatory Muscles." *Anatomical Record* 295 (8): 1336–51.

Heimlich, H. 1974. "Pop Goes the Cafe Coronary." *Emergency Medicine* 6 (6): 154–55.

———. 1975. "A Life-Saving Maneuver to Prevent Food-Choking." *Journal of the American Medical Association* 234 (4): 398–401.

Henneman, E., G. Somjen, and D. O. Carpenter. 1965. "Functional Significance of Cell Size in Spinal Motoneurons." *Journal of Neurophysiology*. 28 (3): 560–80.

Henry, H. T. 2005. "Performance of Guinea Fowl Numida Meleagris during Jumping Requires Storage and Release of Elastic Energy." *Journal of Experimental Biology* 208 (17): 3293–3302.

Herring, Susan W., and S. E. Herring. 1974. “The Superficial Masseter and Gape in Mammals.” *The American Naturalist* 108 (962): 561–76.

Herzog, W., and T. R. Leonard. 1997. “Depression of Cat Soleus Forces Following Isokinetic Shortening.” *Journal of Biomechanics* 30 (9): 865–72.

Herzog, W., K. Powers, K. Johnston, and M. Duvall. 2015. “A New Paradigm for Muscle Contraction.” *Frontiers in Physiology* 6: 1–11.

Herzog, W., and L. J. Read. 1993. “Lines of Action and Moment Arms of the Major Force-Carrying Structures Crossing the Human Knee Joint.” *Journal of Anatomy* 182 (2): 213–30.

Herzog, W., G. Schappacher, M. DuVall, T. R. Leonard, and J. A. Herzog. 2016. “Residual Force Enhancement Following Eccentric Contractions: A New Mechanism Involving Titin.” *Physiology* 31 (4): 300–312.

Higham, T. E., and A. A. Biewener. 2011. “Functional and Architectural Complexity within and between Muscles: Regional Variation and Intermuscular Force Transmission.” *Philosophical Transactions of the Royal Society of London B: Biological Sciences* 366: 1477–87.

Higham, T. E., A. A. Biewener, and J. M Wakeling. 2008. “Functional Diversification within and between Muscle Synergists during Locomotion.” *Biology Letters* 4 (1): 41–44.

Hiiemae, K. M., and J. B. Palmer. 2003. “Tongue Movements in Feeding and Speech.” *Critical Reviews in Oral Biology & Medicine* 14 (6): 413–29.

Hiiemae, K. M., and A. W. Crompton. 1985. “Mastication, Food Transport and Swallowing,” in *Functional Vertebrate Morphology*, edited by Mildebrand M., D. M. Bramble., K. F. Liem, D. B. Wake, 262–90.

Hiiemae, K. M., S. M. Hayenga, and A. Reese. 1995. “Patterns of Tongue and Jaw Movement in a Cinefluorographic Study of Feeding in the Macaque.” *Archives of Oral Biology* 40 (3): 229–46.

Hiiemae, K. M., and J. B. Palmer. 1999. “Food Transport and Bolus Formation during Complete Feeding Sequences on Foods of Different Initial Consistency.” *Dysphagia* 14 (1): 31–42.

Hiiemae, K. M., and J. B. Palmer. 2003. “Tongue Movements in Feeding and Speech .” *Critical Reviews in Oral Biology & Medicine* 14 (6): 413–29.

Hiiemae, K. M., A. Thexton, J. McGarrick, and A. W. Crompton. 1981. “The Movement of the Cat Hyoid during Feeding.” *Archives of Oral Biology* 26 (65–81).

Hill, A. V. 1949. “The Abrupt Transition from Rest to Activity in Muscle.” *Proceedings of the Royal Society B: Biological Sciences* 136 (884): 399–420.

Hill, AV. 1938. “The Heat of Shortening and the Dynamic Constants of Muscle.” *Proceedings of the Royal Society B: Biological Sciences* 126 (843): 136–95.

Hilloowala, R. A. 1975. “Comparative Anatomical Study of the Hyoid Apparatus in Selected Primates.” *American Journal of Anatomy* 142 (3): 367–84.

Hirano, M., M. Tateishi, S. Kurita, and H. Matsuoka. 1987. “Deglutition Following Supraglottic Horizontal Laryngectomy.” *Annals of Otology, Rhinology & Laryngology* 96 (1): 7–11.

Hoffman, M. R., C. A. Jones, Z. Geng, S. M. Abelhalim, C. C. Walczak, A. R. Mitchell, J. J. Jiang, and T. M. McCulloch. 2013. “Classification of High-Resolution Manometry Data according to Videofluoroscopic Parameters Using Pattern Recognition.” *Otolaryngology - Head and Neck Surgery* 149 (1): 126–33.

Holliday, C. M., H. P. Tsai, R. J. Skiljan, I. D. George, and S. Pathan. 2013. “A 3D Interactive Model and Atlas of the Jaw Musculature of Alligator Mississippiensis.” *PLOS ONE* 8 (6): e62806.

Holman, S. D., N. Konow, S. L. Lukasik, and R. Z. German. 2012. “Regional Variation in Geniohyoid Muscle Strain during Suckling in the Infant Pig.” *Journal of Experimental Zoology Part A: Ecological Genetics and Physiology* 317 (6): 359–70.

Holman, S. D., R. Campbell-Malone, P. Ding, E. M. Gierbolini-Norat, A. M. Griffioen, H. Inokuchi, S. L. Lukasik, R. Z. German. 2013. “Development, Reliability, and Validation of an Infant Mammalian Penetration–Aspiration Scale.” *Dysphagia* 28 (2): 178–87.

Holman, S. D., R. Campbell-Malone, P. Ding, E. M. Gierbolini-Norat, S. L. Lukasik, D. R. Waranch, R. Z. German. 2014. “Swallowing Kinematics and Airway Protection after Palatal Local Anesthesia in Infant Pigs.” *The Laryngoscope* 124 (2): 436–45.

Holt, N. C., and E. Azizi. 2016. “The Effect of Activation Level on Muscle Function during Locomotion: Are Optimal Lengths and Velocities Always Used?” *Proceedings of the Royal Society B: Biological Sciences* 283 (1823): 20152832.

Holt, N. C., T. J. Roberts, and G. N. Askew. 2014. “The Energetic Benefits of Tendon Springs in Running: Is the Reduction of Muscle Work Important?” *Journal of Experimental Biology* 217 (24): 4365–71.

Holt, N. C., and E. Azizi. 2014. “What Drives Activation-Dependent Shifts in the Force-Length Curve?” *Biology Letters* 10 (9): 20140651.

Holt, N. C., N. Danos, T. J. Roberts, and E. Azizi. 2016. “Stuck in Gear: Age-Related Loss of

Variable Gearing in Skeletal Muscle." *The Journal of Experimental Biology* 219 (7): 998–1003.

Hooper, S. L., C. Guschlbauer, M. Blumel, P. Rosenbaum, M. Gruhn, T. Akay, and A. Buschges. 2009. "Neural Control of Unloaded Leg Posture and of Leg Swing in Stick Insect, Cockroach, and Mouse Differs from That in Larger Animals." *Journal of Neuroscience* 29 (13): 4109–19.

Hooper, S. L. 2012. "Body Size and the Neural Control of Movement." *Current Biology* 22 (9): R318-22.

Hori, K., H. Taniguchi, H. Hayashi, J. Magara, Y. Minagi, Q. Li, T. Ono, and M. Inoue. 2013. "Role of Tongue Pressure Production in Oropharyngeal Swallow Biomechanics." *Physiological Reports* 1 (6): e00167.

Howell, A. B., and W. L. Straus. 1933. "The Muscular System," in *Anatomy of the Rhesus Monkey: Macaca Mulatta*, edited by C. G. Hartman and W. L. Straus. New York: Hafner Publicing Company.

Hoy, M. G., F. E. Zajac, and M. E. Gordon. 1990. "A Musculoskeletal Model of the Human Lower Extremity: The Effect of Muscle, Tendon, and Moment Arm on the Moment-Angle Relationship of Musculotendon Actuators at the Hip, Knee, and Ankle." *Journal of Biomechanics* 23 (2): 157–69.

Huang, C. S., H. Hiraba, G. M. Murray, and B. J. Sessle. 1989. "Topographical Distribution and Functional Properties of Cortically Induced Rhythmical Jaw Movements in the Monkey (*Macaca fascicularis*)." *Journal of Neurophysiology* 61 (3): 635–50.

Hubbard, I. J., M. W. Parsons, C. Neilson, and L. M. Carey. 2009. "The Role of Task-Specific Training in Rehabilitation Therapies." *Occupupational Therapy International* 16 (3–4): 175–89.

Huckabee, M. L., and C. M. Steele. 2006. "An Analysis of Lingual Contribution to Submental Surface Electromyographic Measures and Pharyngeal Pressure during Effortful Swallow." *Archives of Physical Medicine and Rehabilitation* 87 (8): 1067–72.

Huckabee, M. L., S. G. Butler, M. Barclay, and S. Jit. 2005. "Submental Surface Electromyographic Measurement and Pharyngeal Pressures during Normal and Effortful Swallowing." *Archives of Physical Medicine and Rehabilitation* 86 (11): 2144–49.

Huckabee, M. L., and P. Macrae. 2014. "Rethinking Rehab: Skill-Based Training for Swallowing Impairment." *SIG 13 Perspectives on Swallowing and Swallowing Disorders (Dysphagia)* 23: 46–53.

Humbert, I. A. and Vose, A., interview with with Leo Ferreira, Down the Hatch, podcast audio,

March 31, 2018. https://itunes.apple.com/us/podcast/down-the-hatch-the-swallowing-podcast/id1263588769?mt=2

Humbert, I. A., H. Christopherson, A. Lokhande, R. Z. German, M. Gonzalez-Fernandez, and P. Celnik. 2013. "Human Hyolaryngeal Movements Show Adaptive Motor Learning during Swallowing." *Dysphagia* 28: 139–45.

Humbert, I. A., A. Lokhande, H. Christopherson, R. Z. German, and A. Stone. 2012. "Adaptation of Swallowing Hyo-Laryngeal Kinematics Is Distinct in Oral vs. Pharyngeal Sensory Processing." *Journal of Applied Physiology* 112 (10): 1698–1705.

Humbert, I. A., and R. Z. German. 2013. "New Directions for Understanding Neural Control in Swallowing: The Potential and Promise of Motor Learning." *Dysphagia* 28 (1): 1–10.

Humbert, I. A., A. Lokhande, H. Christopherson, R. Z. German, and A. Stone. 2012. "Adaptation of Swallowing Hyo-Laryngeal Kinematics Is Distinct in Oral vs. Pharyngeal Sensory Processing." *Journal of Applied Physiology* 112 (10): 1698–1705.

Hutchinson, J. R., F. C. Anderson, S. S. Blemker, S. L. Delp, J. R. Hutchinson, F. C. Anderson, S. S. Blemker, and S. L. Delp. 2005. "Analysis of Hindlimb Muscle Moment Arms in Tyrannosaurus Rex Using a Three-Dimensional Musculoskeletal Computer Model: Implication for stance, gait, and speed." *Paleobiology* 31 (4): 676–701.

Hutchinson, J. R., J. W. Rankin, J. Rubenson, K. H. Rosenbluth, R. A. Siston, and S. L. Delp. 2015. "Musculoskeletal Modelling of an Ostrich (*Struthio camelus*) Pelvic Limb: Influence of Limb Orientation on Muscular Capacity during Locomotion." *PeerJ* 3: e1001.

Hylander, W. L., and K. R. Johnson. 1989. "The Relationship between Masseter Force and Masseter Electromyogram during Mastication in the Monkey *Macaca fascicularis*." *Archives of Oral Biology* 34 (9): 713–22.

Hylander, W.L., and A.W. Crompton. 1986. "Jaw Movements and Patterns of Mandibular Bone Strain during Mastication in the Monkey *Macaca fascicularis*." *Archives of Oral Biology* 31 (12): 841–48.

Hylander, W. L., K. R. Johnson, and A. W. Crompton. 1987. "Loading Patterns and Jaw Movements during Mastication in *Macaca fascicularis*: A Bone-Strain, Electromyographic, and Cineradiographic Analysis." *American Journal of Physical Anthropology* 72 (3): 287–314.

Hylander, W. L. 1984. "Stress and Strain in the Mandibular Symphysis of Primates : A Test of Competing Hypotheses" *American Journal of Physical Anthropology* 64 (1): 1-46.

Hylander, W. L. 2013. "Functional Links between Canine Height and Jaw Gape in Catarrhines with Special Reference to Early Hominins." *American Journal of Physical Anthropology*

150 (2): 247–59.

Hylander, W. L., and K. R. Johnson. 1993. “Modelling Relative Masseter Force from Surface Electromyograms during Mastication in Non-Human Primates.” *Archives of Oral Biology* 38 (3): 233–40.

Illingworth, R. S., and J. Lister. 1964. “The Critical or Sensitive Period, with Special Reference to Certain Feeding Problems in Infants and Children.” *The Journal of Pediatrics* 65 (6): 839–48.

Inamoto, Y., N. Fujii, E. Saitoh, M. Baba, S. Okada, K. Katada, Y. Ozeki, D. Kanamori, and J. B. Palmer. 2011. “Evaluation of Swallowing Using 320-Detector-Row Multislice CT Part II: Kinematic Analysis of Laryngeal Closure during Normal Swallowing.” *Dysphagia* 26 (3): 209–17.

Inokuchi, H., M. González-Fernández, K. Matsuo, M. B. Brodsky, M. Yoda, H. Taniguchi, H. Okazaki, T. Hiraoka, and J. B. Palmer. 2016. “Electromyography of Swallowing with Fine Wire Intramuscular Electrodes in Healthy Human: Amplitude Difference of Selected Hyoid Muscles.” *Dysphagia* 31 (1): 33–40.

———. 2014. “Electromyography of Swallowing with Fine Wire Intramuscular Electrodes in Healthy Human: Activation Sequence of Selected Hyoid Muscles.” *Dysphagia* 29 (6): 713–21.

Iriarte-Díaz, J., D. A. Reed, and C. F. Ross. 2011. “Sources of Variance in Temporal and Spatial Aspects of Jaw Kinematics in Two Species of Primates Feeding on Foods of Different Properties.” *Integrative and Comparative Biology* 51 (2): 307–19.

Iriarte-Diaz, J., D. K. Riskin, K. S. Breuer, and S. M. Swartz. 2012. “Kinematic Plasticity during Flight in Fruit Bats: Individual Variability in Response to Loading.” *PLOS ONE* 7 (5): 1–8.

Iriarte-Diaz, J., C. E. Terhune, A. B. Taylor, and C. F. Ross. 2017. “Functional Correlates of the Position of the Axis of Rotation of the Mandible during Chewing in Non-Human Primates.” *Zoology* 124: 106–18.

Jacob, P., P. J. Kahrilas, J. A. Logemann, V. Shah, and T. Ha. 1989. “Upper Esophageal Sphincter Opening and Modulation during Swallowing.” *Gastroenterology* 97 (6): 1469–78.

Jang, H. J., J. H. Leigh, H. G. Seo, T. R. Han, and B. M. Oh. 2015. “Effortful Swallow Enhances Vertical Hyolaryngeal Movement and Prolongs Duration after Maximal Excursion.” *Journal of Oral Rehabilitation* 42 (10): 765–73.

Jeffery, N. S., R. S. Stephenson, J. A. Gallagher, J. C. Jarvis, and P. G. Cox. 2011. “Micro-Computed Tomography with Iodine Staining Resolves the Arrangement of Muscle Fibres.” *Journal of Biomechanics* 44 (1): 189–92.

Joumaa, V., and W. Herzog. 2013. “Energy Cost of Force Production Is Reduced after Active Stretch in Skinned Muscle Fibres.” *Journal of Biomechanics* 46 (6). Elsevier: 1135–39.

Joumaa, V., D. E. Rassier, T. R. Leonard, and W. Herzog. 2008. “The Origin of Passive Force Enhancement in Skeletal Muscle.” *American Journal of Physiology* 294 (1): C74–78.

Kahrilas, P. J., J. A. Logemann, C. Krugler, and E. Flanagan. 1991. “Volitional Augmentation of Upper Esophageal Sphincter Opening during Swallowing.” *The American Journal of Physiology-Gastrointestinal and Liver Physiology* 260 (3): G450–56.

Kahrilas, P. J., Shezhang L., J. A. Logemann, G. A. Ergun, and F. Facchini. 1993. “Deglutitive Tongue Action: Volume Accommodation and Bolus Propulsion.” *Gastroenterology* 104 (1): 152–62.

Kajii, Y., T. Shingai, J. Kitagawa, Y. Takahashi, Y. Taguchi, T. Noda, and Y. Yamada. 2002. “Sour Taste Stimulation Facilitates Reflex Swallowing from the Pharynx and Larynx in the Rat.” *Physiology & Behavior* 77 (2–3): 321-325.

Kandel, E. R., J. H. Schwartz, T. M. Jessell, S. A. Siegelbaum, and A. J. Hudspeth. 2012. *Princples of Neural Science*. 5th ed. New York: McGraw-Hill Education / Medical.

Kargo, W. J., and L. C. Rome. 2002. “Functional Morphology of Proximal Hindlimb Muscles in the Frog *Rana pipiens*.” *The Journal of Experimental Biology* 205 (2002): 1987–2004.

Kawamata, S., J. Ozawa, M. Hashimoto, T. Kurose, and H. Shinohara. 2003. “Structure of the Rat Subcutaneous Connective Tissue in Relation to Its Sliding Mechanism.” *Archives of Histology and Cytology* 66 (3): 273–79.

Keefe, D. F., T. M. O’Brien, D. B. Baier, S. M. Gatesy, E. L. Brainerd, and D. H. Laidlaw. 2008. “Exploratory Visualization of Animal Kinematics Using Instantaneous Helical Axes.” *Computer Graphics Forum* 27 (3): 863–70.

Kembel, S. W., D. D. Ackerly, S. P. Blomberg, W. K. Cornwell, P. D. Cowan, M. R. Helmus, H. Morlon, and C. O. Webb. 2014. “Picante: R Tools for Integrating Phylogenies and Ecology, v1.6-2.” https://CRAN.R-project.org/package=picante

Kier, W. M. 2012. “The Diversity of Hydrostatic Skeletons.” *Journal of Experimental Biology* 215 (8): 1247–57.

Kier, W. M., and K. K. Smith. 1985. “Tongues, Tentacles and Trunks: The Biomechanics of Movement in Muscular-Hydrostats.” *Zoological Journal of the Linnean Society* 83 (4): 307–24.

Kim, Y., and G. H. McCullough. 2008. “Maximum Hyoid Displacement in Normal

Swallowing." *Dysphagia* 23 (3): 274–79.

King, S. N., N. E. Dunlap, P. A. Tennant, and T. Pitts. 2016. "Pathophysiology of Radiation-Induced Dysphagia in Head and Neck Cancer." *Dysphagia* 31 (3): 339–51.

Klahn, M. S., and A. L. Perlman. 1999. "Temporal and Durational Patterns Associating Respiration and Swallowing." *Dysphagia* 14 (3): 131–38.

Knörlein, B. J., D. B. Baier, S. M. Gatesy, J. D. Laurence-Chasen, and E. L. Brainerd. 2016. "Validation of XMALab Software for Marker-Based XROMM." *The Journal of Experimental Biology*, 219 (23): 3701–11.

Knigge, M., and S. Thibeault. 2016. "Relationship Between Tongue Base Region Pressures and Vallecular Clearance." *Dysphagia* 31 (3): 391–97.

Koh, T. J., and W. Herzog. 1998. "Increasing the Moment Arm of the Tibialis Anterior Induces Structural and Functional Adaptation: Implications for Tendon Transfer." *Journal of Biomechanics* 31 (7): 593–99.

Konow, N., E. Azizi, and T. J. Roberts. 2012. "Muscle Power Attenuation by Tendon during Energy Dissipation." *Proceedings of the Royal Society B: Biological Sciences* 279 (1731): 1108–13.

Konow, N., J. A. Cheney, T. J. Roberts, J. R. S. Waldman, and S. M. Swartz. 2015. "Spring or String: Does Tendon Elastic Action Influence Wing Muscle Mechanics in Bat Flight?" *Proceedings of the Royal Society B: Biological Sciences* 282 (1816): 1–7.

Konow, N., A. Thexton, A. W. Crompton, and R. Z. German. 2010. "Regional Differences in Length Change and Electromyographic Heterogeneity in Sternohyoid Muscle during Infant Mammalian Swallowing." *Journal of Applied Physiology* 109 (2): 439–48.

Kraaijenga, S. A. C., L. van der Molen, W. D. Heemsbergen, G. B. Remmerswaal, F. J. M. Hilgers, and M. W. M. van den Brekel. 2016. "Hyoid Bone Displacement as Parameter for Swallowing Impairment in Patients Treated for Advanced Head and Neck Cancer." *European Archives of Oto-Rhino-Laryngology* 274: 597–606.

Kupczik, K., H. Stark, R. Mundry, F. T. Neininger, T. Heidlauf, and O. Röhrle. 2015. "Reconstruction of Muscle Fascicle Architecture from Iodine-Enhanced microCT Images: A Combined Texture Mapping and Streamline Approach." *Journal of Theoretical Biology* 382: 34–43.

Lafarge, T., and B. Paterio-Lopz. 2017. "alphashape3d: Implementation of the 3D Alpha-Shape for the Reconstruction of 3D Sets from a Point Cloud." https://CRAN.R-project.org/package=alphashape3d

Laitman, J. T., E. S. Crelin, and G. J. Conlogue. 1977. “The Function of the Epiglottis in Monkey and Man.” *The Yale Journal of Biology and Medicine* 50 (1): 43–48.

van de Lande, L. S., C. J. J. M. Caron, B. I. Pluijmers, K. F. M. Joosten, M. Streppel, D. J. Dunaway, M. J. Koudstaal, and B. L. Padwa. "Evaluation of Swallow Function in Patients with Craniofacial Microsomia: A Retrospective Study." *Dysphagia* 33 (2): 234-242.

Lauder, G. V. 1981. “Form and Function: Structural Analysis in Evolutionary Morphology.” *Paleobiology* 7 (4): 430–42.

———. 1990. “Functional Morphology and Systematics: Studying Functional Patterns in an Historical Context.” *Annual Review of Ecology and Systematics* 21 (124): 317–40.

———. 1995. “On the Inference of Function from Structure”. *Functional Morphology in Vertebrate Paleontology*. Cambridge: Cambridge University Press.

———. 1996. “The Argument from Design.” In *Adaptation*. Cambridge: Cambridge University Press.

Lazarus, C. L., H. Husaini, D. Falciglia, M. Delacure, R. C. Branski, D. Kraus, N. Lee, M. Ho, C. Ganz, B. Smith, N. Sanfilippo. 2014. “Effects of Exercise on Swallowing and Tongue Strength in Patients with Oral and Oropharyngeal Cancer Treated with Primary Radiotherapy with or without Chemotherapy.” *International Journal of Oral and Maxillofacial Surgery* 43 (5): 523–30.

Lazarus, C., J. A. Logemann, C. W. Song, A. W. Rademaker, and P. J. Kahrilas. 2002. “Effects of Voluntary Maneurvers on Tongue Base Function for Swallowing.” *Folia Phoniatrica et Logopaedica* 54 (4): 171–76.

Lecker, D. N., S. Kumari, and A. Khan. 1997. “Iodine Binding Capacity and Iodine Binding Energy of Glycogen.” *Journal of Polymer Science, Part A: Polymer Chemistry* 35 (8): 1409–12.

Ledogar, J. A., P. C. Dechow, Q. Wang, P. H. Gharpure, A. D. Gordon, K. L. Baab, A. L. Smith, G. W. Weber, I. R. Grosse, C. F. Ross, B. G. Richmond, B. W. Wright, C. Byron, S. Wroe, D. S. Strait. 2016. “Human Feeding Biomechanics: Performance, Variation, and Functional Constraints.” *PeerJ* 4: e2242.

Lee, S. S. M., A. S. Arnold, M. de Boef Miara, A. A. Biewener, and J. M. Wakeling. 2013. “Accuracy of Gastrocnemius Muscles Forces in Walking and Running Goats Predicted by One-Element and Two-Element Hill-Type Models.” *Journal of Biomechanics* 46 (13). Elsevier: 2288–95.

Leonard, T. R., V. Joumaa, and W. Herzog. 2010. “An Activatable Molecular Spring Reduces Muscle Tearing during Extreme Stretching.” *Journal of Biomechanics* 43 (15): 3063–66.

Leonard, T. R., M. DuVall, and W. Herzog. 2010. “Force Enhancement Following Stretch in a Single Sarcomere.” *American Journal of Physiology - Cell Physiology* 299 (6): C1398–1401.

Lewin, J. S., K. A. Hutcheson, D. A. Barringer, A. H. May, D. B. Roberts, F. C. Holsinger, and E. M. Diaz. 2008. “Functional Analysis of Swallowing Outcomes after Supracricoid Partial Laryngectomy.” *Head and Neck* 30 (5): 559–66.

Lieber, R. L., and J. Fridén. 1993. “Muscle Damage Is Not a Function of Muscle Force but Active Muscle Strain.” *Journal of Applied Physiology (Bethesda, Md. : 1985)* 74 (2): 520–26.

Lieber, R. L., B. O. Ljung, and J. Fridén. 1997. “Intraoperative Sarcomere Length Measurements Reveal Differential Design of Human Wrist Extensor Muscles.” *The Journal of Experimental Biology* 200 (1): 19–25.

Lieber, R. L., T. M. Woodburn, and J. Fridén. 1991. “Muscle Damage Induced by Eccentric Contractions of 25% Strain.” *Journal of Applied Physiology* 70 (6): 2498–2507.

Lieber, R. L. 2009. *Skeletal Muscle Structure, Function, and Plasticity: The Physiological Basis of Rehabilitation*. 3rd ed. Baltimore, MD: Lippincott Williams & Wilkins.

Lieber, R. L., B. M. Fazeli, and M. J. Botte. 1990. “Architecture of Selected Wrist Flexor and Extensor Muscles.” *The Journal of Hand Surgery* 15 (2): 244–50.

Lieber, R. L, and J. Fridén. 2000. “Functional and Clinical Significance of Skeletal Muscle Architecture.” *Muscle & Nerve* 23: 1647–66.

Lieber, R. L., and S. R. Ward. 2011. “Skeletal Muscle Design to Meet Functional Demands.” *Philosophical Transactions of the Royal Society B: Biological Sciences* 366: 1466–76.

Lieberman, D. E., R. C. McCarthy, K. M. Hiiemae, and J. B. Palmer. 2001. “Ontogeny of Postnatal Hyoid and Larynx Descent in Humans.” *Archives of Oral Biology* 46: 117–28.

Lieberman, D. E.. 2011. *The Evolution of the Human Head*. Harvard University Press.

Lieberman, D. E. 1998. “Sphenoid Shortening and the Evolution of Modern Human Cranial Shape.” *Nature* 393: 158–62.

Lieberman, D. E., B. M. McBratney, and Gail Krovitz. 2002. “The Evolution and Development of Cranial Form in Homo Sapiens.” *Proceedings of the National Academy of Sciences* 99 (3): 1134–39.

Lieberman, P., E. S. Crelin, and D. H. Klatt. 1972. “Phonetic Ability and Related Anatomy of the

Newborn and Adult Human, Neanderthal Man, and the Chimpanzee." *American Anthropologist* 74 (3): 287–307.

Lieberman, P. 2012. "Vocal Tract Anatomy and the Neural Bases of Talking." *Journal of Phonetics* 40 (4): 608–22.

———. 2017. "Comment on 'Monkey Vocal Tracts are Speech-Ready'." *Science Advances* 3 (7): 1–4.

Lieberman, P., and E. S. Crelin. 1971. "On the Speech of Neanderthal Man." *Linguistic Inquiry* 2 (2): 203–22.

Lieberman, P., J. T. Laitman, J. S. Reidenberg, and P. J. Gannon. 1992. "The Anatomy, Physiology, Acoustics and Perception of Speech: Essential Elements in Analysis of Human Speech." *Journal of Human Evolution* 23: 447–68.

Lin, L. D., G. M. Murray, and B. J. Sessle. 1994. "Functional Properties of Single Neurons in the Primate Face Primary Somatosensory Cortex. I. Relations with Trained Orofacial Motor Behaviors." *Journal of Neurophysiology* 71 (6): 2377–90.

Liu, W., C.-Z. Jin, Y.-Q. Zhang, Y.-J. Cai, S. Xing, X.-J. Wu, H. Cheng, et al. 2010. "Human Remains from Zhirendong, South China, and Modern Human Emergence in East Asia." *Proceedings of the National Academy of Sciences* 107 (45): 19201–6.

Liu, Z. J., V. Shcherbatyy, M. Kayalioglu, and A. Seifi. 2009. "Internal Kinematics of the Tongue in Relation to Muscle Activity and Jaw Movement in the Pig." *Journal of Oral Rehabilitation* 36 (9): 660–74.

Liu, Z. J., B. Yamamura, V. Shcherbatyy, and J. R. Green. 2008. "Regional Volumetric Change of the Tongue during Mastication in Pigs." *Journal of Oral Rehabilitation* 35 (8): 604–12.

Loeb, G. E., and C. Gans. 1986. *Electromyography for Experimentalists*. Chicago, IL: University of Chicago Press.

Logemann, J. A., P. J. Kahrilas, J. Cheng, B. R. Pauloski, P. J. Gibbons, A. W. Rademaker, and S. Lin. 1992. "Closure Mechanisms of Laryngeal Vestibule during Swallow." *The American Journal of Physiology* 262 (2): G338-344.

Logemann, J. A., P. Gippons, A. W. Rademaker, B. R. Pauloski, P. J. Kahrilas, M. Bacon, J. Bowman, and E. McCracken. 1994. "Mechanisms of Recovery of Swallow after Supraglottic Laryngectomy." *Journal of Speech* 37 (5): 965–74.

Logemann, J. A., B. R. Pauloski, A. W. Rademaker, C. L. Lazarus, J. Gaziano, L. Stachowiak, L. Newman, E. MacCracken, D. Santa, and B. Mittal. 2008. "Swallowing Disorders in the First Year after Radiation and Chemoradiation." *Head and Neck* 30 (2): 148–58.

Logemann, J. A., A. W. Rademaker, B. R. Pauloski, C. L. Lazarus, B. B. Mittal, B. Brockstein, E. MacCracken, D. J. Haraf, E. E. Vokes, L. A. Newman, D. Liu. 2006. "Site of Disease and Treatment Protocol as Correlates of Swallowing Function in Patients with Head and Neck Cancer Treated with Chemoradiation." *Head & Neck* 28 (1): 64–73.

Lombard, R. E., and D. B Wake. 1977. "Tongue Evolution in the Lungless Salamanders, Family Plethodontidae. II. Function and Evolutionary Diversity." *Journal of Morphology* 153: 39–80.

Loren, G. J., S. D. Shoemaker, T. J. Burkholder, M. D. Jacobson, J. Fridén, and R. L Lieber. 1996. "Human Wrist Motors: Biomechanical Design and Application to Tendon Transfers." *Journal of Biomechanics* 29 (3): 331–42.

Lusted, L. 1971. "Signal Detectability." *Science* 171 (3977): 1217–19.

Maganaris, C. N., V. Baltzopoulos, and D. Tsaopoulos. 2006. "Muscle Fibre Length-to-Moment Arm Ratios in the Human Lower Limb Determined in Vivo." *Journal of Biomechanics* 39 (9): 1663–68.

Malas, F. Ü., L. Özçakar, B. Kaymak, A. Ulaşli, S. Güner, M. Kara, and A. Akinci. 2013. "Effects of Different Strength Training on Muscle Architecture: Clinical and Ultrasonographic Evaluation in Knee Osteoarthritis." *Physical Medicine and Rehabiliation* 5 (8): 655–62.

Marschner, S., and P. Shirley. 2015. *Fundamentals of Computer Graphics*. 4th ed. Boca Raton, FL: Taylor & Francis Group.

Martin-Harris, B., M. B. Brodsky, C. C. Price, Y. Michel, and B. Walters. 2003. "Temporal Coordination of Pharyngeal and Laryngeal Dynamics with Breathing during Swallowing: Single Liquid Swallows." *Journal of Applied Physiology* 94 (5): 1735–43.

Martin, R. E., P. Kemppainen, Y. Masuda, D. Yao, G. M. Murray, and B. J. Sessle. 1999. "Features of Cortically Evoked Swallowing in the Awake Primate (*Macaca fascicularis*)." *Journal of Neurophysiology* 82 (3): 1529–41.

Martin, R. E., G. M. Murray, P. Kemppainen, Y. Masuda, and B. J. Sessle. 1997. "Functional Properties of Neurons in the Primate Tongue Primary Motor Cortex During Swallowing." *Journal of Neurophysiology* 78 (3): 1516–30.

Martino, R., and T. McCulloch. 2016. "Therapeutic Intervention in Oropharnygeal Dysphagia." *Nature Reviews Gastroenterology & Hepatology*. 13 (11): 665–679.

Mason, S. J., G. Harris, and J. Blissett. 2005. "Tube Feeding in Infancy: Implications for the Development of Normal Eating and Drinking Skills." *Dysphagia* 20 (1): 46–61.

Matsubara, M., H. Tohara, K. Kara, H. Shinosaki, Y. Yamazaki, C. Susa, A. Nakane, Y. Wakasugi, and S. Minakuchi. 2018. “High-Speed Jaw-Opening Exercise in Training Suprahyoid Fast-Twitch Muscle Fibers.” *Clinical Interventions in Aging* 13: 125–31.

Matsuo, K., K. M. Hiiemae, M. Gonzalez-Fernandez, and J. B. Palmer. 2008. “Respiration during Feeding on Solid Food: Alterations in Breathing during Mastication, Pharyngeal Bolus Aggregation, and Swallowing.” *Journal of Applied Physiology* 104 (3): 674–81.

Matsuo, K., and J. B. Palmer. 2010. “Kinematic Linkage of the Tongue, Jaw, and Hyoid during Eating and Speech.” *Archives of Oral Biology* 55 (4): 325–31.

———. 2015. “Coordination of Oro-Pharyngeal Food Transport during Chewing and Respiratory Phase.” *Physiology & Behavior* 142 (January): 52–56.

McConnel, F. M. S., M. S. Mendelsohn, and J. A. Logemann. 1987. “Manofluorography of Deglutition after Supraglottic Laryngectomy.” *Head & Neck Surgery* 9 (3): 142–50.

McConnel, F. M. S. 1988. “Analysis of Pressure Generation and Bolus Transit during Pharyngeal Swallowing.” *The Laryngoscope* 98 (1): 71–78.

McConnel, F. M. S., M. S. Mendelsohn, and J. A. Logemann. 1986. “Examination of Swallowing after Total Laryngectomy Using Manofluorography.” *Head & Neck Surgery* 9 (1): 3–12.

McDonagh, M. J., and C. T. Davies. 1984. “Adaptive Response of Mammalian Skeletal Muscle to Exercise with High Loads.” *European Journal of Applied Physiology and Occupational Physiology* 52 (2): 139–55.

McFarland, D. H., and J. P. Lund. 1995. “Modification of Mastication and Respiration during Swallowing in the Adult Human.” *Journal of Neurophysiology* 74 (4): 1509–17.

Mendell, L. M. 2005. “The Size Principle: A Rule Describing the Recruitment of Motoneurons.” *Journal of Neurophysiology* 93 (6): 3024–26.

Menegaz, R. A., D. B. Baier, K. A. Metzger, S. W. Herring, and E. L. Brainerd. 2015. “XROMM Analysis of Tooth Occlusion and Temporomandibular Joint Kinematics during Feeding in Juvenile Miniature Pigs.” *Journal of Experimental Biology* 218 (16): 2573–84.

Metscher, B. D. 2009. “MicroCT for Comparative Morphology: Simple Staining Methods Allow High-Contrast 3D Imaging of Diverse Non-Mineralized Animal Tissues.” *BMC Physiology* 9: 11.

Meyer, R. A., and B. M. Prior. 2000. “Functional Magnetic Resonance Imaging of Muscle.” *Exercise and Sport Sciences Reviews* 28 (2): 89–92.

Millard, M., T. Uchida, A. Seth, and S. L. Delp. 2013. “Flexing Computational Muscle: Modeling and Simulation of Musculotendon Dynamics.” *Journal of Biomechanical Engineering* 135: 21005-1–21005-11.

Milner-Brown, H. S., R. B. Stein, and R. Yemm. 1973. “The Orderly Recruitment of Human Motor Units during Voluntary Isometric Contractions.” *The Journal of Physiology* 230 (2): 359–70.

Mittleman, R. E., and C. V. Wetli. 1982. “The Fatal Cafe Coronary: Foreign-Body Airway Obstruction.” *The Journal of the American Medical Association* 247 (9): 1285–88.

Molfenter, S. M., C. Y. Hsu, Y. Lu, and C. L. Lazarus. 2017. “Alterations to Swallowing Physiology as the Result of Effortful Swallowing in Healthy Seniors.” *Dysphagia*. In press.

Molfenter, S. M., and C. M. Steele. 2011. “Physiological Variability in the Deglutition Literature: Hyoid and Laryngeal Kinematics.” *Dysphagia* 26 (1): 67–74.

Monroy, J. A., K. L. Powers, C. M. Pace, T. Uyeno, and K. C. Nishikawa. 2016. “Effects of Activation on the Elastic Properties of Intact Soleus Muscles with a Deletion in Titin.” *The Journal of Experimental Biology* 220: 828-836.

Moo, E. K., R. Fortuna, S. C. Sibole, Z. Abusara, and W. Herzog. 2016. “In Vivo Sarcomere Lengths and Sarcomere Elongations Are Not Uniform across an Intact Muscle.” *Frontiers in Physiology* 7: 1–9.

Mooney, K., M. Warner, and M. Stokes. 2013. “Symmetry and within-Session Reliability of Mechanical Properties of Biceps Brachii Muscles in Healthy Young Adult Males Using the MyotonPRO Device.” *Working Papers in the Health Sciences* 1 (3): 1–11.

Mu, Liancai, and Ira Sanders. 2000. “Sensory Nerve Supply of the Human Oro- and Laryngopharynx: A Preliminary Study.” *The Anatomical Record* 258: 406–20.

Murray, G. M., L. D. Lin, E. M. Moustafa, and B. J. Sessle. 1991. “Effects of Reversible Inactivation by Cooling of the Primate Face Motor Cortex on the Performance of a Trained Tongue-Protrusion Task and a Trained Biting Task.” *Journal of Neurophysiology* 65 (3): 511–30.

Naganuma, K., M. Inoue, K. Yamamura, K. Hanada, and Y. Yamada. 2001. “Tongue and Jaw Muscle Activities during Chewing and Swallowing in Freely Behaving Rabbits.” *Brain Research* 915 (2): 185–94.

Nakamura, Y., J. Iriarte-Diaz, F. Arce-McShane, C. P. Orsbon, K. A. Brown, M. Eastment, L. Avivi-Arber, B. J. Sessle, M. Inoue, N. G. Hatsopoulos, C. F. Ross, K. Takahashi 2017. “Sagittal Plane Kinematics of the Jaw and Hyolingual Apparatus During Swallowing in

Macaca mulatta." *Dysphagia* 32 (5): 663-677.

Napadow, V. J., Q. Chen, V. J. Wedeen, and R. J. Gilbert. 1999. "Biomechanical Basis for Lingual Muscular Deformation during Swallowing." *The American Journal of Physiology* 277 (1): G695-701.

Napadow, V. J., Q. Chen, V. J. Wedeen, and R. J. Gilbert. 1999. "Intramural Mechanics of the Human Tongue in Association with Physiological Deformations." *Journal of Biomechanics* 32 (1): 1–12.

Napadow, V. J., Q. U. N. Chen, V. A. N. J. Wedeen, R. J. Gilbert, J. Vitaly, Q. Chen, and V. J. Wedeen. 1999. "Biomechanical Basis for Lingual Muscular Deformation during Swallowing." *American Journal of Phsyiology* 277 (3): 695–701.

Naples, V. L. 1999. "Morphology, Evolution and Function of Feeding in the Giant Anteater (*Myrmecophaga tridactyla*)." *Journal of Zoology* 249: 19–41.

National Safety Council. 2017. "Preventable Deaths: Odds of Dying." InjuryFacts.NSC.org. http://injuryfacts.nsc.org/all-injuries/preventable-death-overview/odds-of-dying/ (accessed May 8, 2018).

Negus, V. E. 1949. *The Comparative Anatomy and Physiology of the Larynx*. New York, NY: Hafner Pub. Company.

Nelson, F. E., and B. C. Jayne. 2001. "The Effects of Speed on the in Vivo Activity and Length of a Limb Muscle during the Locomotion of the Iguanian Lizard *Dipsosaurus dorsalis*." *The Journal of Experimental Biology* 204 (20): 3507–22.

Nishikawa, K. C., A. A. Biewener, P. Aerts, A. N. Ahn, H. J. Chiel, M. A. Daley, T. L. Daniel, R. J. Full, M. E. Hale, T. L. Hedrick, A. K. Lappin, T. R. Nichols, R. D. Quinn, R. A. Satterlie, B. Szymik. 2007. "Neuromechanics: An Integrative Approach for Understanding Motor Control." *Integrative and Comparative Biology* 47 (1): 16–54.

Nishikawa, K. C., J. A. Monroy, T. E. Uyeno, S. H. Yeo, D. K. Pai, and S. L. Lindstedt. 2012. "Is Titin a 'Winding Filament'? A New Twist on Muscle Contraction." *Proceedings of the Royal Society B: Biological Sciences* 279 (1730): 981–90.

Nishimura, T. 2003. "Comparative Morphology of the Hyo-Laryngeal Complex in Anthropoids: Two Steps in the Evolution of the Descent of the Larynx." *Primates* 44 (1): 41–49.

Nishimura, T., A. Mikami, J. Suzuki, and T. Matsuzawa. 2006. "Descent of the Hyoid in Chimpanzees: Evolution of Face Flattening and Speech." *Journal of Human Evolution* 51 (3): 244–54.

Nordez, A., and F. Hug. 2010. "Muscle Shear Elastic Modulus Measured Using Supersonic

Shear Imaging Is Highly Related to Muscle Activity Level." *Journal of Applied Physiology* 108 (5): 1389–94

Nordez, A., T. Gallot, S. Catheline, A. Gue, and C. Cornu. 2009. "Electromechanical Delay Revisited Using Very High Frame Rate Ultrasound" *Journal of Applied Physiology* 106: 1970–75.

Norman, R. W., and P. V. Komi. 1979. "Electromechanical Delay in Skeletal Muscle under Normal Movement Conditions." *Acta Physiologica Scandinavica* 160: 241–48.

O'Connell, D. A., J. Rieger, J. R. Harris, P. Dziegielewski, J. Zalmanowitz, A. Sytsanko, S. Li, J. Wolfaardt, R. D. Hart, and H. Seikaly. 2008. "Swallowing Function in Patients With Base of Tongue Cancers Treated With Primary Surgery and Reconstructed With a Modified Radial Forearm Free Flap." *Archives of Otolaryngology–Head & Neck Surgery* 134 (8): 857.

O'Connor, S. M., E. J. Cheng, K. W. Young, S. R. Ward, and R. L. Lieber. 2016. "Sarcomere Length Distribution Quantification in Whole Muscle Frozen Sections." *The Journal of Experimental Biology*, 219: 1432–36.

Obuchowski, N. A. 2003. "Receiver Operating Characteristic Curves and Their Use in Radiology." *Radiology* 229 (1): 3–8.

Ogura, J. H. 1979. "Hyoid Muscle Flap Reconstruction in Subtotal Supraglottic Laryngectomy A More Rapid Rehabilitation of Deglutition." *The Laryngoscope* 89: 1522–24.

Ogura, J. H., S. L. Saltzstein, and H. J. Spjut. 1961. "Experiences with Conservation Surgery in Laryngeal and Pharyngeal Carcinoma." *The Laryngoscope* 71 (3): 258–76.

Okada, T., Y. Aoyagi, Y. Inamoto, E. Saitoh, H. Kagaya, S. Shibata, K. Ota, and K. Ueda. 2013. "Dynamic Change in Hyoid Muscle Length Associated with Trajectory of Hyoid Bone during Swallowing: Analysis Using 320-Row Area Detector Computed Tomography." *Journal of Applied Physiology* 115 (8): 1138–45.

Olsen, A. M., and M. W. Westneat. 2016. "Linkage Mechanisms in the Vertebrate Skull: Structure and Function of Three-Dimensional, Parallel Transmission Systems." *Journal of Morphology* 277 (12): 1570–83.

Olsen, A. M. 2016. "linkR: 3D Lever and Linkage Mechanism Modeling. R Package Version 1.1.1."

Ono, T., K. Hori, K. I. Tamine, and Y. Maeda. 2009. "Evaluation of Tongue Motor Biomechanics during Swallowing-From Oral Feeding Models to Quantitative Sensing Methods." *Japanese Dental Science Review* 45: 65–74.

Organ, J. M., M. F. Teaford, and A. B. Taylor. 2009. “Functional Correlates of Fiber Architecture of the Lateral Caudal Musculature in Prehensile and Nonprehensile Tails of the Platyrrhini (Primates) and Procyonidae (Carnivora).” *The Anatomical Record* 292 (6): 827–41.

Orsbon, C.P., N.J. Gidmark, and C.F. Ross. 2018. “Dynamic Musculoskeletal Functional Morphology: Integrating diceCT and XROMM.” *The Anatomical Record* 301 (2): 378–406.

Osserman, R. 2002. *A Survey of Minimal Surfaces*. Mineola, NY: Dover Publications, Inc.

Otten, E. 1987. “Optimal Design of Vertebrate and Insect Sarcomeres.” *Journal of Morphology* 191: 49–62.

Ozgur, Z., F. Govsa, and S. Celik. 2010. “An Unreported Anatomical Finding: Unusual Insertions of the Stylohyoid and Digastric Muscles.” *Surgical and Radiologic Anatomy* 32: 513–17.

Pace, C. M., S. Mortimer, J. A. Monroy, and K. C. Nishikawa. 2017. “The Effects of a Skeletal Muscle Titin Mutation on Walking in Mice.” *Journal of Comparative Physiology A: Neuroethology, Sensory, Neural, and Behavioral Physiology* 203: 67–76.

Paik, N. J., S. J. Kim, H. J. Lee, J. Y. Jeon, J. Y. Lim, and T. R. Han. 2008. “Movement of the Hyoid Bone and the Epiglottis during Swallowing in Patients with Dysphagia from Different Etiologies.” *Journal of Electromyography and Kinesiology* 18 (2): 329–35.

Palmer, J. B. 1998. “Bolus Aggregation in the Oropharynx Does Not Depend on Gravity.” *Archives of Physical Medicine and Rehabilitation* 79 (6): 691–96.

Palmer, J. B., N. J. Rudin, G. Lara, and A. W. Crompton. 1992. “Coordination of Mastication and Swallowing.” *Dysphagia* 7 (4): 187–200.

Palmer, P. M., D. M. Jaffe, T. M. McCulloch, E. M. Finnegan, D. J. Van Daele, and E. S. Luschei. 2008. “Quantitative Contributions of the Muscles of the Tongue, Floor-of-Mouth, Jaw, and Velum to Tongue-to-Palate Pressure Generation.” *Journal of Speech Language and Hearing Research* 51: 828–35.

Pampush, J. D., and D. J. Daegling. 2016. “The Enduring Puzzle of the Human Chin.” *Evolutionary Anthropology* 25: 20–35.

Park, D., H. H. Lee, S. T. Lee, Y. Oh, J. C. Lee, K. W. Nam, and J. S. Ryu. 2017. “Normal Contractile Algorithm of Swallowing Related Muscles Revealed by Needle EMG and Its Comparison to Videofluoroscopic Swallowing Study and High Resolution Manometry Studies: A Preliminary Study.” *Journal of Electromyography and Kinesiology* 36: 81–89.

Patel, D. A., S. Krishnaswami, E. Steger, E. Conover, M. F. Vaezi, M. R. Ciucci, and D. O.

Francis. 2018. “Economic and Survival Burden of Dysphagia among Inpatients in the United States.” *Diseases of the Esophagus* 31 (1): 1–7.

Pauloski, B. R., and J. A. Logemann. 1995. “Biomechanical Analysis of the Pharyngeal Swallow in Postsurgical Patients with Anterior Tongue and Floor of Mouth Resection and Distal Flap Reconstruction.” *Journal of Speech & Hearing Research* 38 (1): 110-123.

Pearson Jr., W. G., B. K. Taylor, J. Blair, and B. Martin-Harris. 2016. “Computational Analysis of Swallowing Mechanics Underlying Impaired Epiglottic Inversion.” *Laryngoscope* 126 (8): 1854–58.

Pearson Jr., W. G., D. F. Hindson, S. E. Langmore, and A. C. Zumwalt. 2013. “Evaluating Swallowing Muscles Essential for Hyolaryngeal Elevation by Using Muscle Functional Magnetic Resonance Imaging.” *International Journal of Radiation Oncology, Biology, Physics* 85 (3): 735–40.

Pearson Jr., W. G, S. E. Langmore, L. B. Yu, and A. C. Zumwalt. 2012. “Structural Analysis of Muscles Elevating the Hyolaryngeal Complex.” *Dysphagia* 27 (4): 445–51.

Pearson Jr., W. G., S. E. Langmore, and A. C. Zumwalt. 2011. “Evaluating the Structural Properties of Suprahyoid Muscles and Their Potential for Moving the Hyoid.” *Dysphagia* 26 (4): 345–51.

Perez, L. M., N. Toledo, G. De Luliis, M. S. Bargo, and S. F. Vizcaino. 2010. “Morphology and Function of the Hyoid Apparatus of Fossil Xenarthrans (Mammalia).” *Journal of Morphology* 271 (9): 1119–33.

Perlman, A. L., D. J. VanDaele, and M. S. Otterbacher. 1995. “Quantitative Assessment of Hyoid Bone Displacement from Video Images during Swallowing.” *Journal of Speech, Language, and Hearing Research* 38 (3): 579–85.

Perreault, E. J., C. J. Heckman, and T. G. Sandercock. 2003. “Hill Muscle Model Errors during Movement Are Greatest within the Physiologically Relevant Range of Motor Unit Firing Rates.” *Journal of Biomechanics* 36 (2): 211–18.

Perry, J. M. G., A. Hartstone-Rose, and C. E. Wall. 2011. “The Jaw Adductors of Strepsirrhines in Relation to Body Size, Diet, and Ingested Food Size.” *The Anatomical Record* 294 (4): 712–28.

Peterson, G. E., and H. L. Barney. 1952. “Control Methods Used in a Study of the Vowels.” *The Journal of the Acoustical Society of America* 24 (2): 175–84.

Petrofsky, J. S. 2001. “The Use of Electromyogram Biofeedback to Reduce Trendelenburg Gait.” *European Journal of Applied Physiology* 85 (5): 491–95.

Porro, L. B., and C. T. Richards. 2017. “Digital Dissection of the Model Organism *Xenopus Laevis* Using Contrast-Enhanced Computed Tomography.” *Journal of Anatomy* 231 (2): 169-191.

Powell, P. L., R. R. Roy, P. Kanim, M. A. Bello, and V. R. Edgerton. 1984. “Predictability of Skeletal Muscle Tension from Architectural Determinations in Guinea Pig Hindlimbs.” *Journal of Applied Physiology* 57 (6): 1715–21.

Powers, K., K. Nishikawa, V. Joumaa, and W. Herzog. 2016. “Decreased Force Enhancement in Skeletal Muscle Sarcomeres with a Deletion in Titin.” *Journal of Experimental Biology* 219 (9): 1311–16.

Prilutsky, B. I., and V. M. Zatsiorsky. 2002. “Optimization-Based Models of Muscle Coordination.” *Exercise and Sport Sciences Reviews* 30 (1): 32–38.

Rabey, K. N., D. J. Green, A. B. Taylor, D. R. Begun, B. G. Richmond, and S. C. McFarlin. 2015. “Locomotor Activity Influences Muscle Architecture and Bone Growth but Not Muscle Attachment Site Morphology.” *Journal of Human Evolution* 78: 91–102.

Rack, P. M., and D. R. Westbury. 1969. “The Effects of Length and Stimulus Rate on Tension in the Isometric Cat Soleus Muscle.” *The Journal of Physiology* 204 (2): 443–60.

Ramsey, R. W. & Street, S. F. 1941. “The Isometric Length-Tension Diagram of Isolated Skeletal Muscle Fibers of the Frog.” *Protoplasma* 36 (1): 157–90.

Randhawa, A., M. E. Jackman, and J. M. Wakeling. 2013. “Muscle Gearing during Isotonic and Isokinetic Movements in the Ankle Plantarflexors.” *European Journal of Applied Physiology* 113 (2): 437–47.

Randhawa, A., and J. M Wakeling. 2013. “Clinical Biomechanics Associations between Muscle Structure and Contractile Performance in Seniors.” *Clinical Biomechanics* 28 (6): 705–11.

Reed, D. A., and C. F. Ross. 2010. “The Influence of Food Material Properties on Jaw Kinematics in the Primate, Cebus.” *Archives of Oral Biology* 55 (12): 946–62.

Reiss, K. Z. 1997. “Myology of the Feeding Apparatus of Myrmecophagid Anteaters (Xenarthra : Myrmecophagidae).” *Journal of Mammalian Evolution* 4 (2): 87–117.

Rice, M. J. 1973. “Supercontracting Striated Muscle in a Vertebrate.” *Nature* 243 (5404): 238–40.

Roberts, T. J. 2016. “Contribution of Elastic Tissues to the Mechanics and Energetics of Muscle Function during Movement.” *The Journal of Experimental Biology* 219 (2): 266–75.

Roberts, T. J., and A. M. Gabaldón. 2008. “Interpreting Muscle Function from EMG: Lessons

Learned from Direct Measurements of Muscle Force." *Integrative and Comparative Biology* 48 (2): 312–20.

Roberts, T. J., R. L. Marsh, P. G. Weyand, and C. R. Taylor. 1997. "Muscular Force in Running Turkeys: The Economy of Minimizing Work." *Science* 275 (5303): 1113–15.

Roberts, T. J, E. M. Abbott, and E. Azizi. 2011. "The Weak Link: Do Muscle Properties Determine Locomotor Performance in Frogs?" *Philosophical Transactions of the Royal Society of London B: Biological Sciences* 366 (1570): 1488–95.

Robbins, J., J. W. Hamilton, G. L. Lof, G. B. Kempster. 1992. "Oropharyngeal Swallowing in Normal Adults of Different Ages." *Gastroenterology* 103: 823–29.

Robinson, J. T. 1954. "Prehominid Dentition and Hominid Evolution." *Evolution* 8 (4): 324–34.

Rogus-Pulia, N., and N. P. Connor. 2016. "Muscle Strengthening Approaches to Dysphagia Rehabilitation." *Current Physical Medicine and Rehabilitation Reports* 4 (4): 277–86.

Ross, C. F. 1999. "How to Carry Out Functional Morphology Research." *Evolutionary Anthropology: Issues, News, and Reviews* 7 (6): 217–22.

Ross, C. F., R. Dharia, S. W. Herring, W. L. Hylander, Z.-J. Liu, K. L. Rafferty, M. J. Ravosa, and S. H. Williams. 2007. "Modulation of Mandibular Loading and Bite Force in Mammals during Mastication." *The Journal of Experimental Biology* 210 (6): 1046–63.

Ross, C. F., and M. Henneberg. 1995. "Basicranial Flexion, Relative Brain Size, and Facial Kyphosis in Homo Sapiens and Some Fossil Hominids." *American Journal of Physical Anthropology* 98 (4): 575–93.

Ross, C. F., and J. Iriarte-Diaz. 2014. "What Does Feeding System Morphology Tell Us about Feeding?" *Evolutionary Anthropology: Issues, News, and Reviews* 23 (3): 105–20.

Ross, C. F., J. Iriarte-Diaz, and C. L. Nunn. 2012. "Innovative Approaches to the Relationship Between Diet and Mandibular Morphology in Primates." *International Journal of Primatology* 33 (3): 632–60.

Ross, C. F., C. A. Lockwood, J. G. Fleagle, and W. L. Jungers. 2002. "Adaptation and Behavior in the Primate Fossil Record, " in *Reconstructing Behavior in the Primate Fossil Record* edited by J. M. Plavcan, R. F. Kay, W. L. Jungers, C. P. van Schaik, 1-41. New York: Kluwer Academic/Plenum Publishers.

Ross, C. F., B. A. Patel, D. E. Slice, D. S. Strait, P. C. Dechow, B. G. Richmond, and M. A. Spencer. 2005. "Modeling Masticatory Muscle Force in Finite Element Analysis: Sensitivity Analysis Using Principal Coordinates Analysis." *The Anatomical Record* 283 (2): 288–99.

Ross, C. F., D. A. Reed, R. L. Washington, A. Eckhardt, F. Anapol, and N. Shahnoor. 2009. "Scaling of Chew Cycle Duration in Primates." *American Journal of Physical Anthropology* 138 (1): 30–44.

Ross, C. F., and M. J. Ravosa. 1993. "Basicranial Flexion, Relative Brain Size, and Facial Kyphosis in Nonhuman Primates." *American Journal of Physical Anthropology* 91: 305–24.

Roszek, B., G. C. Baan, and P. A. Huijing. 1994. "Decreasing Stimulation Frequency-Dependent Length-Force Characteristics of Rat Muscle." *Journal of Applied Physiology* 77 (4): 2115–24.

Rupert, J. E., J. A. Rose, J. M. Organ, and M. T. Butcher. 2015. "Forelimb Muscle Architecture and Myosin Isoform Composition in the Groundhog (*Marmota monax*)." *The Journal of Experimental Biology* 218 (2): 194–205.

Sakai, T., T. Kitamura, T. Iwami, C. Nishiyama, K. Tanigawa-Sugihara, S. Hayashida, T. Nishiuchi, K. Kajino, T. Irisawa, T. Shiozaki, H. Ogura, O. Tasaki, Y. Kuwagata, A. Hiraide, T. Shimzau. 2014. "Effectiveness of Prehospital Magill Forceps Use for out-of-Hospital Cardiac Arrest due to Foreign Body Airway Obstruction in Osaka City." *Scandinavian Journal of Trauma, Resuscitation and Emergency Medicine* 22: 53.

Sanders, Ira, and Liancai Mu. 2013. "A Three-Dimensional Atlas of Human Tongue Muscles." *The Anatomical Record* 296 (7): 1102–14.

Sargon, M. F. 1994. "An Abnormal Digastric Muscle with Three Bellies." *Surgical and Radiologic Anatomy* 16: 215–16.

Sawicki, G. S., P. Sheppard, and T. J. Roberts. 2015. "Power Amplification in an Isolated Muscle-Tendon Unit Is Load Dependent." *Journal of Experimental Biology* 218 (22): 3700–3709.

Schlager, S., and G. Jefferis. 2017. "Morpho: Calculations and Visualisations Related to Geometric Morphometrics, v2.5.1." https://cran.r-project.org/package=Morpho.

Schmitt, E., and S. Wallace. 2014. "Shape Change and Variation in the Cranial Morphology of Wild Canids (*Canis lupus*, *Canis latrans*, *Canis rufus*) Compared to Domestic Dogs (*Canis familiaris*) Using Geometric Morphometrics." *International Journal of Osteoarchaeology* 24 (1): 42–50.

Sellers, K. C., K. M. Middleton, J. L. Davis, and C. M. Holliday. 2017. "Ontogeny of Bite Force in a Validated Biomechanical Model of the American Alligator." *The Journal of Experimental Biology* 220 (11): 2036–46.

Selley, W. G., F. C. Flack, R. E. Ellis, and W. A. Brooks. 1989. "Respiratory Patterns Associated

with Swallowing: Part 1. The Normal Adult Pattern and Changes with Age." *Age and Ageing* 18: 168–72.

Seo, H. G., B. M. Oh, and T. R. Han. 2016. "Swallowing Kinematics and Factors Associated with Laryngeal Penetration and Aspiration in Stroke Survivors with Dysphagia." *Dysphagia* 31 (2): 160–68.

Seo, H. G., B. M. Oh, J. H. Leigh, and T. R. Han. 2014. "Correlation Varies with Different Time Lags Between the Motions of the Hyoid Bone, Epiglottis, and Larynx during Swallowing." *Dysphagia* 29 (5): 591–602.

Sessle, B. J., K. Adachi, L. Avivi-Arber, J. Lee, H. Nishiura, D. Yao, and K. Yoshino. 2007. "Neuroplasticity of Face Primary Motor Cortex Control of Orofacial Movements." *Archives of Oral Biology* 52: 334–37.

Sessle, B. J., B. Yao, H. Nishiura, K. Yoshino, J. C. Lee, R. E. Martin, and G. M. Murray. 2005. "Properties and Plasticity of the Primate Somatosensory and Motor Cortex Related to Orofacial Sensorimotor Function." *Clinical and Experimental Pharmacology and Physiology* 32: 109–14.

Shaker, R., M. Kern, E. Bardan, A. Taylor, E. T. Stewart, R. G. Hoffmann, R. C. Arndorfer, C. Hofmann, and J. Bonnevier. 1997. "Augmentation of Deglutitive Upper Esophageal Sphincter Opening in the Elderly by Exercise." *The American Journal of Physiology* 272 (6): G1518–22.

Shaker, R., C. Easterling, M. Kern, T. Nitschke, B. Massey, S. Daniels, B. Grande, M. Kazandjian, and K. Dikeman. 2002. "Rehabilitation of Swallowing by Exercise in Tube-Fed Patients with Pharyngeal Dysphagia Secondary to Abnormal UES Opening." *Gastroenterology* 122 (5): 1314–21.

Sia, I., P. Carvajal, A. A. Lacy, G. D. Carnaby, and M. A. Crary. 2015. "Hyoid and Laryngeal Excursion Kinematics - Magnitude, Duration and Velocity - Changes Following Successful Exercise-Based Dysphagia Rehabilitation: MDTP." *Journal of Oral Rehabilitation* 42 (5): 331–39.

Slabaugh, G. G. 1999. "Computing Euler Angles from a Rotation Matrix." *Internal Report*.

Slovarp, L., L. King, C. Off, and J. Liss. 2016. "A Pilot Study of the Tongue Pull-Back Exercise for Improving Tongue-Base Retraction and Two Novel Methods to Add Resistance to the Tongue Pull-Back." *Dysphagia* 31: 416–423.

Smith, J., N. Wolkove, A. Colacone, and H. Kreisman. 1989. "Coordination of Eating, Drinking and Breathing in Adults." *Chest* 96 (3): 578–82.

Smith, J. M., and R. J. G. Savage. 1956. "Some Locomotory Adaptations in Mammals."

Zoological Journal of the Linnean Society 42: 603–22.

———. 1959. “The Mechanics of Mammalian Jaws.” *The School Science Review* 141: 289–301.

Smith, K. K. 1992. “The Evolution of the Mammalian Pharynx.” *Zoological Journal of the Linnean Society* 104 (4): 313–49.

Smith, K. K., and W. M. Kier. 1989. “Trunks, Tongues and Tentacles: Moving with Skeletons of Muscle.” *American Scientist* 77 (1): 28–35.

Sobol, S. M., and M. May. 1990. “Hyoid Preservation during Horizontal Supraglottic Laryngectomy: A Comparison of Techniques.” *Operative Techniques in Otolaryngology - Head and Neck Surgery* 1 (1): 52–55.

Sokoloff, A. J., and T. W. Deacon. 1992. “Musculotopic Organization of the Hypoglossal Nucleus in the Cynomolgus Monkey, *Macaca fascicularis*.” *Journal of Comparative Neurology* 324 (1): 81–93.

Sokoloff, A. J, B. Yang, H. Li, and T. J. Burkholder. 2007. “Immunohistochemical Characterization of Slow and Fast Myosin Heavy Chain Composition of Muscle Fibres in the Styloglossus Muscle of the Human and Macaque (*Macaca rhesus*).” *Archives of Oral Biology* 52 (6): 533–43.

Soman, A., T. L. Hedrick, and A. A. Biewener. 2005. “Regional Patterns of Pectoralis Fascicle Strain in the Pigeon *Columba livia* during Level Flight.” *The Journal of Experimental Biology* 208: 771–86.

Sonntag, CF. 1923. “On the Anatomy, Physiology, and Pathology of the Chimpanzee.” *Journal of Zoology* 92 (2): 323–429.

———. 1924. “On the Anatomy, Physiology, and Pathology of the Orang-Outan.” *Journal of Zoology* 24: 349–450.

Sorkine, O., D. Cohen-Or, Y. Lipman, M. Alexa, C. Rössl, and H.-P. Seidel. 2004. “Laplacian Surface Editing.” *Eurographics Symposium on Geometry Processing*, edited by R. Scopigno and D. Zorin.

Spector, S. A., P. F. Gardiner, R. F. Zernicke, R. R. Roy, and V. R. Edgerton. 1980. “Muscle Architecture and Force-Velocity Characteristics of Cat Soleus and Medial Gastrocnemius: Implications for Motor Control.” *Journal of Neurophysiology* 44 (5): 951–60.

Sprague, J. M. 1943. “The Hyoid Region of Placental Mammals with Especial Reference to the Bats.” *American Journal of Anatomy* 72 (3): 385–472.

———. 1944. “The Innervation of the Pharynx in the Rhesus Monkey, and the Formation of the

Pharyngeal Plexus in Primates." *The Anatomical Record* 90 (3): 197–208.

Spudich, J. A., and S. Watt. 1971. "The Regulation of Rabbit Skeletal Muscle Contraction." *Journal of Biological Chemistry* 246 (15): 4866–71.

Standring, Susan, ed. 2015. *Gray's Anatomy: The Anatomical Basis of Clinical Practice*. 41st ed. Elsevier Health Sciences.

Stathopoulos, E., and J. F. Ducchan. 2006. "History and Principles of Exercise-Based Therapy: How They Inform Our Current Treatment." *Seminars in Speech and Language* 27 (4): 227–35.

Steele, C. M., G. L. Bailey, T. Chau, S. M. Molfenter, M. Oshalla, A. A. Waito, and D. C. B. H. Zoratto. 2011. "The Relationship between Hyoid and Laryngeal Displacement and Swallowing Impairment." *Clinical Otolaryngology* 36 (1): 30–36.

Steele, C. M., and M. L. Huckabee. 2007. "The Influence of Orolingual Pressure on the Timing of Pharyngeal Pressure Events." *Dysphagia* 22 (1): 30–36.

Steele, C. M., and J. A. Y. Cichero. 2014. "Physiological Factors Related to Aspiration Risk: A Systematic Review." *Dysphagia* 29 (3): 295–304.

Steele, C. M., P. H. H. M. van Lieshout, and C. A. Pelletier. 2012. "The Influence of Stimulus Taste and Chemesthesis on Tongue Movement Timing in Swallowing." *Journal of Speech, Language, and Hearing Research* 55 (1): 262–75.

Stern, J. T. 1974. "Computer Modelling of Gross Muscle Dynamics." *Journal of Biomechanics* 7 (5): 411–28.

Stevens, H. C., and J. M. Snodgrass. 1932. "The Force-Velocity Curve of Striated Muscle." *Experimental Biology and Medicine* 30 (3): 373–75.

Stevens, K. N. 1989. "On the Quantal Nature of Speech." *Journal of Phonetics* 17: 3–45.

Stone, M. and A. Lundberg. 1996. "Three-Dimensional Tongue Surface Shapes of English Consonants and Vowels." *The Journal of the Acoustical Society of America* 99 (6): 3728–37.

Sulikowski, M. 1991. "The Role of the Hyoid Bone in the Act of Deglutition after Horizontal Epiglottic Laryngectomy." *Otolaryngologia Polska* 45 (5): 333–40.

Takahashi, K., M. D. Best, N. Huh, K. A. Brown, A. A. Tobaa, and N. G. Hatsopoulos. 2017. "Encoding of Both Reaching and Grasping Kinematics in Dorsal and Ventral Premotor Cortices." *The Journal of Neuroscience*, 1537–16.

Takasaki, K., H. Umeki, M. Hara, H. Kumagami, and H. Takahashi. 2011. “Influence of Effortful Swallow on Pharyngeal Pressure: Evaluation Using a High-Resolution Manometry.” *Otolaryngology - Head and Neck Surgery* 144 (1): 16–20.

Takemoto, H. 2001. “Morphological Analyses of the Human Tongue Musculature for Three-Dimensional Modeling.” *Journal of Speech, Language, and Hearing Research*, 95–107.

———. 2008. “Morphological Analyses and 3D Modeling of the Tongue Musculature of the Chimpanzee (*Pan troglodytes*).” *American Journal of Primatology* 70 (10): 966–75.

Taniguchi, H., T. Tsukada, S. Ootaki, Y. Yamada, and M. Inoue. 2008. “Correspondence between Food Consistency and Suprahyoid Muscle Activity, Tongue Pressure, and Bolus Transit Times during the Oropharyngeal Phase of Swallowing.” *Journal of Applied Physiology* 105 (3): 791–99.

Tate, J. J. and C. E Milner. 2010. “Real-Time Kinematic, Temporospatial, and Kinetic Biofeedback During Gait Retraining in Patients: A Systematic Review.” *Physical Therapy* 90 (8): 1123–34.

Taylor, A. B., Kelly E. Jones, Ravinder Kunwar, and Matthew J. Ravosa. 2006. “Dietary Consistency and Plasticity of Masseter Fiber Architecture in Postweaning Rabbits.” *The Anatomical Record* 288 (10): 1105–11.

Taylor, A. B., and C. J. Vinyard. 2004. “Comparative Analysis of Masseter Fiber Architecture in Tree-Gouging (*Callithrix jacchus*) and Nongouging (*Saguinus oedipus*) Callitrichids.” *Journal of Morphology* 261 (3): 276–85.

———. 2009. “Jaw-Muscle Fiber Architecture in Tufted Capuchins Favors Generating Relatively Large Muscle Forces without Compromising Jaw Gape.” *Journal of Human Evolution* 57 (6). Elsevier Ltd: 710–20.

———. 2013. “The Relationships among Jaw-Muscle Fiber Architecture, Jaw Morphology, and Feeding Behavior in Extant Apes and Modern Humans.” *American Journal of Physical Anthropology* 151 (1): 120–34.

Taylor, C. R. 1985. “Force Development during Sustained Locomotion: A Determinant of Gait, Speed and Metabolic Power.” *The Journal of Experimental Biology* 115: 253–62.

Terhune, C. E., J. Iriarte-Diaz, A. B. Taylor, and C. F. Ross. 2011. “The Instantaneous Center of Rotation of the Mandible in Nonhuman Primates.” *Integrative and Comparative Biology* 51 (2): 320–32.

Terhune, C. E., W. L. Hylander, C. J. Vinyard, and A. B. Taylor. 2015. “Jaw-Muscle Architecture and Mandibular Morphology Influence Relative Maximum Jaw Gapes in the Sexually Dimorphic *Macaca fascicularis*.” *Journal of Human Evolution* 82. Elsevier Ltd:

145–58.

Thexton, A. 1984. “Jaw, Tongue and Hyoid Movement—A Question of Synchrony? Discussion Paper.” *Journal of the Royal Society of Medicine* 77 (12): 1010–19.

Thexton, A. J., A. W. Crompton, and R. Z. German. 1998. “Transition from Suckling to Drinking at Weaning: A Kinematic and Electromyographic Study in Miniature Pigs.” *Journal of Experimental Zoology* 280: 327–43.

Thexton, A. J., A. W. Crompton, and R. Z. German. 2012. “EMG Activity in Hyoid Muscles during Pig Suckling.” *Journal of Applied Physiology* 112 (9): 1512–19.

Thexton, A. J., and J. D. McGarrick. 1988. “Tongue Movement of the Cat During Lapping.” *Archives of Oral Biology* 33 (5): 331–39.

Thorstensson, A., B. Hultén, W. von Döbeln, and J. Karlsson. 1976. “Effect of Strength Training on Enzyme Activities and Fibre Characteristics in Human Skeletal Muscle.” *Acta Physiologica Scandinavica* 96 (3): 392–98.

Todd, J. T., A. Stuart, C. R. Lintzenich, J. Wallin, K. Grace-Martin, S. G. Butler. 2013. “Stability of Aspiration Status in Healthy Adults.” *Annals of Otology, Rhinology & Laryngology* 122 (5): 289–93.

Trulsson, M., and G. K. Essick. 1997. “Low-Threshold Mechanorecptive Afferents in the Human Lingual Nerve.” *Journal of Neurophysiology* 77: 737–48.

Vandaele, D. J., A. L. Perlman, and M. D. Cassell. 1995. “Intrinsic Fibre Architecture and Attachments of the Human Epiglottis and Their Contributions to the Mechanism of Deglutition.” *Journal of Anatomy* 186: 1–15.

Van Eijden, T. M. G. J., J. A. M. Korfage, and P. Brugman. 1997. “Architecture of the Human Jaw-Closing and Jaw-Opening Muscles.” *The Anatomical Record* 248: 464–74.

Van Hooren, B., and J. Zolotarjova. 2017. “The Difference between Countermovement and Squat Jump Performances: A Review of Underlying Mechanisms with Practical Applications.” *Journals of Strength and Conditioning Research* 31 (7): 2011–20.

Veis, S., J. A. Logemann, and L. Colangelo. 2000. “Effects of Three Techniques on Maximum Posterior Movement of the Tongue Base.” *Dysphagia* 15 (3): 142–45.

Vickerton, P., J. Jarvis, and N. Jeffery. 2013. “Concentration-Dependent Specimen Shrinkage in Iodine-Enhanced microCT.” *Journal of Anatomy* 223 (2): 185–93

Vilke, G. M., A .M. Smith, L. U. Ray, P. J. Steen, P. A. Murrin, and T. C. Chan. 2004. “Airway Obstruction in Children Aged Less than 5 Years: The Prehospital Experience.” *Prehospital*

Emergency Care 8 (2): 196–99.

Vitti, M. and Basmajian, J. V. 1977. "Integrated actions of masticatory muscles: simultaneous EMG from eight intramuscular electrodes." *The Anatomical Record* 187 (2): 173–189.

Vogel, S. 2013. *Comparative Biomechanics: Life's Physical World*. 2nd ed. Princeton, NJ: Princeton University Press.

Wainwright, P. C., M. E. Alfaro, D. I. Bolnick, and C. D. Hulsey. 2005. "Many-to-One Mapping of Form to Function: A General Principle in Organismal Design?" *Integrative and Comparative Biology* 45 (2): 256–62.

Wakeling, J M., K. Uehli, and A. I. Rozitis. 2006. "Muscle Fibre Recruitment Can Respond to the Mechanics of the Muscle Contraction." *Journal of the Royal Society Interface* 3 (9): 533–44.

Wakeling, J. M., S. S. M. Lee, A. S. Arnold, M. De Boef Miara, and A. A. Biewener. 2012. "A Muscle's Force Depends on the Recruitment Patterns of Its Fibers." *Annals of Biomedical Engineering* 40 (8): 1708–20.

Wakeling, J. M., O. M. Blake, I. Wong, M. Rana, and S. S. M. Lee. 2011. "Movement Mechanics as a Determinate of Muscle Structure, Recruitment and Coordination." *Philosophical Transactions of the Royal Society of London B: Biological Sciences* 366 (1570): 1554–64.

Walker, S. M., and G. R. Schrodt. 1974. "I Segment Lengths and Thin Filament Periods in Skeletal Muscle Fibers of the Rhesus Monkey and the Human." *The Anatomical Record* 178 (1): 63–81.

Wall, C. E., S. G. Larson, and J. T. Stern. 1994. "EMG of the Digastric Muscle in Gibbon and Orangutan: Functional Consequences of the Loss of the Anterior Digastric in Orangutans." *American Journal of Physical Anthropology* 94 (4): 549–67.

Wall, C. E. 1999. "A Model of Temporomandibular Joint Function in Anthropoid Primates Based on Condylar Movements during Mastication." *American Journal of Physical Anthropology* 109 (1): 67–88.

Wallis, W. D. 1917. "The Development of the Human Chin." *The Anatomical Record* 12 (2): 315–28.

Wang, T. G., Y. C. Chang, W. S. Chen, P. H. Lin, and T. Y. Hsiao. 2010. "Reduction in Hyoid Bone Forward Movement in Irradiated Nasopharyngeal Carcinoma Patients With Dysphagia." *Archives of Physical Medicine and Rehabilitation* 91 (6): 926–31.

Wang, Y., C. Liu, J. Rohr, H. Liu, F. He, J. Yu, C. Sun, L. Li, S. Gu, and Y. Chen. 2011. "Tissue

Interaction Is Required for Glenoid Fossa Development during Temporomandibular Joint Formation." *Developmental Dynamics* 240 (11): 2466–73.

Ward, S. R., C. M. Eng, L. H. Smallwood, and R. L. Lieber. 2009. "Are Current Measurements of Lower Extremity Muscle Architecture Accurate?" *Clinical Orthopaedics and Related Research* 467 (4): 1074–82.

Weijs, W. A., J. A. Korfage, and G. J. Langenbach. 1989. "The Functional Significance of the Position of the Centre of Rotation for Jaw Opening and Closing in the Rabbit." *Journal of Anatomy* 162: 133–48.

Weissengruber, G. E., G. Forstenpointner, G. Peters, A. Kubber-Heiss, and W. T. Fitch. 2002. "Hyoid Apparatus and Pharynx in the Lion (*Panthera leo*), Jaguar (*Panthera onca*), Tiger (*Panthera tigris*), Cheetah (*Acinonyx jubatus*) and Domestic Cat (*Felis silvestris f. catus*)." *Journal of Anatomy* 201 (3): 195–209.

Wentzel, S. E., N. Konow, and R. Z. German. 2011. "Regional Differences in Hyoid Muscle Activity and Length Dynamics during Mammalian Head Shaking." *Journal of Experimental Zoology Part A: Ecological Genetics and Physiology* 315 A (3): 111–20.

Westneat, M. W. 2004. "Evolution of Levers and Linkages in the Feeding Mechanisms of Fishes." *Integrative and Comparative Biology* 44 (5): 378–89.

Westneat, M. W. 1990. "Feeding Mechanics of Teleost Fishes (Labridae; Perciformes): A Test of Four-bar Linkage Models." *Journal of Morphology* 205 (3): 269–95.

———. 2003. "A Biomechanical Model for Analysis of Muscle Force, Power Output and Lower Jaw Motion in Fishes." *Journal of Theoretical Biology* 223 (3): 269–81.

Williams, P. E., and G. Goldspink. 1973. "The Effect of Immobilization on the Longitudinal Growth of Striated Muscle Fibres." *Journal of Anatomy* 116 (Pt 1): 45–55.

Winkler, L. A. 1991. "Morphology and Variability of Masticatory Structures in the Orangutan." *International Journal of Primatology* 12 (1): 45–65.

Winters, T. M., M. Takahashi, R. L. Lieber, and S. R. Ward. 2011. "Whole Muscle Length-Tension Relationships Are Accurately Modeled as Scaled Sarcomeres in Rabbit Hindlimb Muscles." *Journal of Biomechanics* 44: 109–15.

Witte, U., M. L. Huckabee, S. H. Doeltgen, F. Gumbley, and M. Robb. 2008. "The Effect of Effortful Swallow on Pharyngeal Manometric Measurements During Saliva and Water Swallowing in Healthy Participants." *Archives of Physical Medicine and Rehabilitation* 89 (5): 822–28.

Wroe, S., T. L. Ferrara, C. R. McHenry, D. Curnoe, and U. Chamoli. 2010. "The

Craniomandibular Mechanics of Being Human." *Proceedings of the Royal Society B: Biological Sciences* 277 (1700): 3579–86.

Yamazaki, Y., H. Tohara, K. Hara, A. Nakane, Y. Wakasugi, K. Yamaguchi, and S. Minakuchi. 2017. "Excessive Anterior Cervical Muscle Tone Affects Hyoid Bone Kinetics during Swallowing in Healthy Individuals." *Clinical Interventions in Aging* 12: 1903–10.

Yao, D., K. Yamamura, N. Narita, R. E. Martin, G. M. Murray, and B. J Sessle. 2002. "Neuronal Activity Patterns in Primate Primary Motor Cortex Related to Trained or Semiautomatic Jaw and Tongue Movements." *Journal of Neurophysiology* 87 (5): 2531–41.

Yemm, R. 1977. "The Orderly Recruitment of Motor Units of the Masseter and Temporal Muscles during Voluntary Isometric Contraction in Man." *Journal of Physiology* 265 (1): 163–74.

Young, K. W., B. P. Kuo, S. M. O'Connor, S. Radic, and R. L. Lieber. 2017. "In Vivo Sarcomere Length Measurement in Whole Muscles during Passive Stretch and Twitch Contractions." *Biophysical Journal* 112 (4): 805–12.

Zajac, F. E. 1989. "Muscle and Tendon Properties, Models, Scaling, and Application to Biomechanics and Motor Control." *Critical Reviews in Biomedical Engineering* 17 (4): 359–410.

Zatsiorsky, V. M., and B. I. Prilutsky. 2012. *Biomechanics of Skeletal Muscles*. Champaign, IL: Human Kinetics.

Zollikofer, C. P. E., M. S. Ponce De León, D. E. Lieberman, F. Guy, D. Pilbeam, A. Likius, H. T. Mackaye, P. Vignaud, and M. Brunet. 2005. "Virtual Cranial Reconstruction of Sahelanthropus Tchadensis." *Nature* 434 (7034): 755–59.

Zumwalt, A. 2006. "The Effect of Endurance Exercise on the Morphology of Muscle Attachment Sites." *Journal of Experimental Biology* 209 (Pt 3): 444–54.